Universidade de Aveiro Departamento de Biologia
2011

Denisa Daud Mateus

Reconstrução molecular de uma alteração ao código genético

Molecular reconstruction of a genetic code alteration

Universidade de Aveiro Departamento de Biologia
2011

Denisa Daud Mateus

Reconstrução molecular de uma alteração ao código genético

Molecular reconstruction of a genetic code alteration

Dissertação apresentada à Universidade de Aveiro para cumprimento dos requisitos necessários à obtenção do grau de Doutor em Bioquímica, realizada sob a orientação científica do Doutor Manuel António da Silva Santos, Professor Associado do Departamento de Biologia da Universidade de Aveiro

Apoio financeiro da FCT e do POPH/FSE no âmbito do III Quadro Comunitário de Apoio.

o júri

presidente

Doutor Dinis Gomes de Magalhães dos Santos
Pofessor Catedrático da Universidade de Aveiro

Doutor António Carlos Matias Correia
Pofessor Catedrático da Universidade de Aveiro

Doutor Manuel António da Silva Santos
Professor Associado da Universidade de Aveiro

Doutora Carla Isabel Gonçalves de Oliveira
Investigadora Principal do IPATIMUP-Instituto de Patologia e Imunologia Molecular da Universidade do Porto

Doutor Jorge Manuel de Sousa Basto Vieira
Investigador Principal do IBMC-Instituto de Biologia Molecular e Celular da Universidade do Porto

Doutora Paula Maria Theriaga Mendes Bernardo Gonçalves
Professora Auxiliar da Faculdade de Ciências e Tecnologia da Universidade Nova de Lisboa

Doutora Gabriela Maria Ferreira Ribeiro de Moura
Investigadora Auxiliar do CESAM-Centro de Estudos do Ambiente e do Mar da Universidade de Aveiro

agradecimentos

First, I would like to express my sincere gratitude to my supervisor, Professor Manuel Santos, for giving me the opportunity to work in his laboratory and for the confidence in my work. Thanks for sharing your knowledge with me and helping me write this thesis.

I am deeply grateful to Professor Lluis Ribas de Pouplana, from the Gene Translation Lab of IRB – Barcelona. Thanks for your support, advices, for receiving me so well in your lab and for being available to discuss my work despite the distance.

I am sincerely thankful to Professor Paula Ludovico, from ICVS of University of Minho, for making me feel so welcoming in your lab, for all your advices, for the interest, commitment and dedication to this project. Your encouragement and enthusiasm gave me an extra motivation to continue.

I would like to thank to all my lab colleagues, past and present, but I specially thank the ones that contributed directly for this work, like Rita, Isabel and João Paredes. I also want to thank Laura, Raquel, Catarina, Patricia, João Simões and Tatiana for helping me with some experiments and to Ana and Francisca for all the fun moments. A special thank to Cristina, with whom I shared the good, the bad, the sad and the funny moments in the lab.

I warmly thank all the lab members of the Gene Translation Lab (IRB Barcelona), namely Yaiza, Tanit, Renaud, Noelia, Teresa and Manuel. Thanks for your help, support and fruitful discussions. A special thank to Yaiza for receiving me at her home and help me to find a place in Barcelona.

My warm thank to ICVS lab members, especially Xana for the help to finish my assays.

I gratefully acknowledged Fundação para a Ciência e Tecnologia (FCT) for the PhD grant (SFRH/BD/27867/2006) essential for carrying out this work.

I will always be grateful to all my friends, especially Ritinha and Joana for all your support, encourage and for listening me.

My loving thanks to my family for your love.

Last and most important, I am forever indebted to my parents and to Pedro. Sorry for not being always present and for the harsh mood. Without your love, support, incentive, understanding it would have been impossible to finish this work. Thanks to my mom for never stop believing.

palavras-chave

Alterações ao código genético, erros de tradução, redefinição do codão CUG, ambiguidade de codão, tRNA, CTG clade, estudos fenotípicos, expressão genética, evolução.

resumo

O código genético regula a correcta descodificação da informação contida nos genes durante a síntese de proteínas. Apresenta um elevado grau de conservação e estima-se que tenha sido originado há mais de 3.5 biliões de anos. Contudo, várias alterações ao código genético foram identificadas em procariotas e eucariotas, nomeadamente nos fungos denominados de "CTG clade", nos quais um tRNA de serina atípico ($tRNA_{CAG}^{Ser}$) descodifica o codão de leucina CUG como serina. Este $tRNA_{CAG}^{Ser}$ foi originado há 272±25 milhões de anos, pela inserção de uma adenosina no centro do anticodão do gene do $tRNA_{CGA}^{Ser}$ que alterou a sequência original do anticodão de 5´-CGA-3´ para 5´-CAG-3´. Esta alteração ao código genético promoveu a restruturação do proteoma das espécies denominadas de "CTG clade". Contudo, permanece por esclarecer o motivo que permitiu que esta alteração atípica fosse preservada no genome destes fungos.

Numa tentativa de clarificar os aspectos evolutivos desta alteração ao código genético, procedemos à reconstrução da via evolutiva, proposta para esta alteração, na levedura *Saccharomyces cerevisiae*. Para tal, induzimos a expressão do gene do $tRNA_{CGA}^{Ser}$ de *C. albicans*, nas versões mutantes e original, em *S. cerevisiae* e determinámos o impacto das mesmas no crescimento celular, bem como na estabilidade, eficiência na tradução e aminoacilação do tRNA. Os nossos dados, demonstram que as versões mutantes do tRNA, apesar de sua reduzida expressão, induzem a incorporação de serina nos codões CUG de leucina. Observámos ainda, através de uma estratégia de evolução forçada, que o $tRNA_{CAG}^{Ser}$ é facilmente inactivado por mutações naturais que impedem o seu reconhecimento pela seryl-tRNA synthetase. O nosso estudo demonstra que a repressão da expressão do $tRNA_{CAG}^{Ser}$, terá desempenhado um papel fundamental na evolução da redefinição do codão CUG de leucina para serina.

Com o intuito de compreender a evolução das alterações ao código genético, induzimos redefinições parciais em vários codões de levedura. Os nossos resultados confirmam que a ambiguidade no código genético afecta o crescimento, induz a produção de agregados proteicos, interfere no ciclo celular e promove alterações nucleares, morfológicas, instabilidade genómica e desregulação da expressão genética. Contudo, origina também variedade fenotípica e fenótipos vantajosos em determinadas condições ambientais. Este estudo demonstra o impacto do ambiente na evolução das alterações ao código genético.

keywords

Genetic code alterations, mistranslation, CUG codon reassignment, codon ambiguity, tRNA, CTG clade, phenomics, gene expression, evolution.

abstract

The genetic code establishes the rules that govern gene translation into proteins. It was established more than 3.5 billion years ago and it is one of the most conserved features of life. Despite this, several alterations to the standard genetic code have been discovered in both prokaryotes and eukaryotes, namely in the fungal CTG clade where a unique seryl transfer RNA ($tRNA_{CAG}^{Ser}$) decodes leucine CUG codons as serine. This $tRNA_{CAG}^{Ser}$ appeared 272±25 million years ago through insertion of an adenosine in the middle position of the anticodon of a $tRNA_{CGA}^{Ser}$ gene, which changed its anticodon from 5´-CGA-3´ to 5´-CAG-3´. This most dramatic genetic event re-structured the proteome of the CTG clade species, but it is not yet clear how and why such deleterious genetic event was selected and became fixed in those fungal genomes.

In this study we have attempted to shed new light on the evolution of this fungal genetic code alteration by reconstructing its evolutionary pathway *in vivo* in the yeast *Saccharomyces cerevisiae*. For this, we have expressed wild type and mutant versions of the *C. albicans* $tRNA_{CGA}^{Ser}$ gene into *S. cerevisiae* and evaluated the impact of the mutant $tRNA_{CGA}^{Ser}$ on fitness, tRNA stability, translation efficiency and aminoacylation kinetics. Our data demonstrate that these mutants are expressed and misincorporate Ser at CUGs, but their expression is repressed through an unknown molecular mechanism. We further demonstrate, using *in vivo* forced evolution methodologies, that the $tRNA_{CAG}^{Ser}$ can be easily inactivated through natural mutations that prevent its recognition by the seryl-tRNA synthetase. The overall data show that repression of expression of the mistranslating $tRNA_{CAG}^{Ser}$ played a critical role on the evolution of CUG reassignment from Leu to Ser.

In order to better understand the evolution of natural genetic code alterations, we have also engineered partial reassignment of various codons in yeast. The data confirmed that genetic code ambiguity affects fitness, induces protein aggregation, interferes with the cell cycle and results in nuclear and morphologic alterations, genome instability and gene expression deregulation. Interestingly, it also generates phenotypic variability and phenotypes that confer growth advantages in certain environmental conditions. This study provides strong evidence for direct and critical roles of the environment on the evolution of genetic code alterations.

List of Contents

Abbreviations

aaRS: *Aminoacyl tRNA synthetase*

aa-tRNA: *Aminoacyl-tRNA*

APS: *Ammonium persulphate*

ATP: *Adenosine 5'-triphosphate*

BCA: *Bicinchoninic acid*

β –gal: *β -galactosidase*

BSA: *Bovine serum albumin*

cDNA: *Complementary deoxyribonucleic*

CFU: *Colony forming units*

Cy3: *Cyanine 3*

Cy5: *Cyanine 5*

DAPI: *4,6-diamino-2-phenyl-indole dihydrochloride*

DEAE: *Diethylaminoethyl*

DIC: *Differential interference contrast*

DHE: *Dihydroethidium*

DHR1,2,3: *Dihydrorhodamine 123*

DMSO: *Dimethyl sulfoxide*

DNA: *Deoxyribonucleic acid*

dNTP: *Deoxyribonucleotide triphosphate*

DTT: *Dithiothreitol*

EDTA: *Ethylenediamine tetracetic acid*

ESR: *Environmental stress response*

GDP: *Guanosine diphosphate*

GFP: *Green fluorescent protein*

GST-B-gal: *Glutathione S-transferase*

HEPES: *4-(2-hydroxyethyl)-1-piperazineethanesulfonic acid*

HSP: *Heat shock protein*

LB: *Lysogeny broth*

LeuRS: *LeucyltRNA synthetase*

MM: *Minimal medium*

mRNA: *Messenger RNA*

OD: *Optical density*

ONPG: *Ortho-Nitrophenyl-β-galactoside*

PBS: *Phosphate buffered saline*

PCIA: *Phenol/chloroform/isoamyl alcohol*

PCR: *Polymerase chain reaction*

PI: *Propidium iodide*

PMSF: *Phenylmethanesulfonylfluoride*

RNA: *Ribonucleic acid*

ROS: *Reactive oxygen species*

rRNA: *Ribosomal RNA*

SDM: *Site directed mutagenesis*

SDS: *Sodium dodecyl sulfate*

SDS-PAGE: *Sodium dodecyl sulfate polyacrylamide gel electrophoresis*

SerRS: *Seryl tRNA synthetase*

Suc-LLVY-MCA: *Succinyl-Leu-Leu-Val-Tyr-4-methylcoumaryl-7-amide*

TCA: *Trichloroacetic acid*

TEMED: *Tetramethylethylenediamine*

tRNA: *Transfer RNA*

TUNEL: *Terminal deoxynucleotidyl transferase*

UPS: *Ubiquitin proteasome system*

YPD: *Rich medium*

List of figures

List of tables

Thesis outline

Alterations to the standard genetic code have been found in various eukaryotes, namely in the CTG clade species where the leucine (Leu) CUG codon is decoded as serine (Ser) by a mutant serine $tRNA_{CAG}^{Ser}$. However, we do not yet fully understand the molecular and evolutionary mechanisms of genetic code alterations. It seems that the CTG clade genetic code alteration was possible due to the appearance of a mutant Ser tRNA ($tRNA^{Ser}$) in the ancestor of yeasts approximately 272±25 million years ago. This tRNA originated through various mutations in the anticodon loop of a $tRNA_{CGA}^{Ser}$ gene, namely insertion of an adenosine at position 35, $A_{37}\rightarrow G_{37}$ and $U_{33}\rightarrow G_{33}$ transitions. Such mutations raise fundamental questions that we have attempted to solve in this thesis, namely how did the anticodon-loop of the $tRNA_{CGA}^{Ser}$ accommodate those mutations? Did those mutations destabilize the $tRNA_{CGA}^{Ser}$? Was the mutant $tRNA_{CGA}^{Ser}$ an efficient and accurate decoder? In order to answer these questions we have reconstructed *in vivo* the evolutionary pathway of this sense-to-sense codon reassignment. The $tRNA_{CAG}^{Ser}$ is the only known tRNA which is recognized by two aminoacyl-tRNA synthetases (aaRS), namely the Seryl and Leucyl, which aminoacylate it with Ser and Leu, respectively. This dual aaRSs recognition, which is responsible for natural genetic code ambiguity existent in the CTG clade species, indicates that the $tRNA_{CAG}^{Ser}$ must contain identity elements for both aaRSs. This raises the questions of wether the identity elements for SerRS are located in the variable arm and discriminator base, as in the case of other $tRNA^{Ser}$? And, whether the identity elements for the LeuRS are located in the anticodon loop, as is expected for $tRNA^{Leu}$? In this thesis we have tried to answer these questions *in vivo* using a forced evolution strategy.

Previous studies performed in our laboratory showed that Leu-for-Ser misincorporation at CUG codons, induced by expression of the mutant *C. albicans* $tRNA_{CAG}^{Ser}$ into *S. cerevisiae* cells, alters cell and colony morphologies, reduces mating, locks yeast in a diploid state, remodels gene expression and induces stress cross-protection, creating adaptive advantages under environmental stress conditions. However, we do not know if this is a general response to mistranslation or if it is specific of Leu-for-Ser misincorporation. In here we addressed the question of wether other types of mistranslation (involving other amino acids substitutions) produce similar phenotypic outcomes. For this, we have compared cells misincorporating different amino acids at

various codons and correlated the phenotypes with those of the well studied Leu-for-Ser mistranslation. These data provides new clues on how to engineer the genetic code.

This thesis is organized in 5 chapters. Chapter 1 is a general introduction centred on genetic code alterations, namely in the CTG clade Leu-for-Ser reassignment and on the biology of aminoacyl-tRNA synthetases and tRNAs. A brief summary of mistranslation is also presented. Chapter 2, focus on the *in vivo* molecular reconstruction of the CUG codon reassignment in *S. cerevisiae*. This was achieved by transforming yeast cells with a series of *C. albicans* $tRNA_{CGA}^{Ser}$ genes containing single or multiple mutations (A_{35}, $A_{37}\rightarrow G_{37}$ and $U_{33}\rightarrow G_{33}$). The impact of each mutation on the $tRNA_{CGA}^{Ser}$ was evaluated by measuring the stability, translation efficiency, aminoacylation kinetics and yeast growth rate. We will also discuss results obtained using an *in vivo* forced evolution methodology which we used to identify the identity elements of the $tRNA_{CAG}^{Ser}$.

Chapter 3 is dedicated to the characterization of the phenotypic response of yeast cells harbouring partial genetic code alterations generated by inducing mistranslation at different codons. For this, we have constructed eight different mutant $tRNA^{Ser}$ containing anticodons that could decode codons belonging to 8 distinct amino acids. We have carried out an extensive phenotypic characterization of our Wt and mistranslating strains, focusing on fitness, cell viability, oxidative stress, nuclear, morphologic and organelle alterations, protein aggregation and protein synthesis rate. The data shows that the CTG clade CUG reassignment from Leu-to-Ser was a highly unlikely event as it is much more toxic than other types of codon reassignments. However, Ser-CUG misincorporation is advantageous in specific ecological niches suggesting that the evolution of genetic code alterations can only be understood in the context of environmental adaptation. In chapter 4, we go one step deeper into the characterization of codon misreading by studying the molecular response to amino acids misincorporation. For this, we profiled the transcriptome of yeast clones misincorporating various amino acids at non-cognate codons. The differences in the stress response activated by these mistranslations are explored in detail.

Chapter 5 is a general discussion of the results presented in this thesis, where we discuss the evolution of the CUG reassignment and postulate the existence of a new pathway/mechanism involved in regulation of mistranslating tRNAs, and discuss the difficulties posed by the toxic effects of amino acid misincorporation induced by engeering genetic code alterations.

Chapter 1

INTRODUCTION

1.1. The standard genetic code

In the late 60's, during a symposium in Cold Spring Harbor on the gene coding problem, the first genetic code table was shown to the scientific community. Those studies demonstrated that the genetic code was common, or nearly so, to all the organisms examined, including bacteria, yeasts, plants and animals, and for this reason it was named the "Universal Genetic Code" (Crick, 1966b). This genetic code translates 61 nucleotide codons into 20 canonical amino acids and contains 3 codons for translation termination (figure 1.1). A detailed analysis of the genetic code table shows that the same amino acid can be codified by more than one codon. For example, leucine (Leu) and serine (Ser) are codified by 6 different codons. These codons are called "synonymous codons" and tend to differ only in the third letter of the triplet, except in case of Leu, Ser and Arg (Jones & Nirenberg, 1966; Nirenberg et al., 1965). Later on, two additional amino acids were discovered, namely selenocysteine (Bock et al., 1991) and pyrrolisine (Hao et al., 2002) and the 2011 genetic code contains 22 rather than the original 20 amino acids.

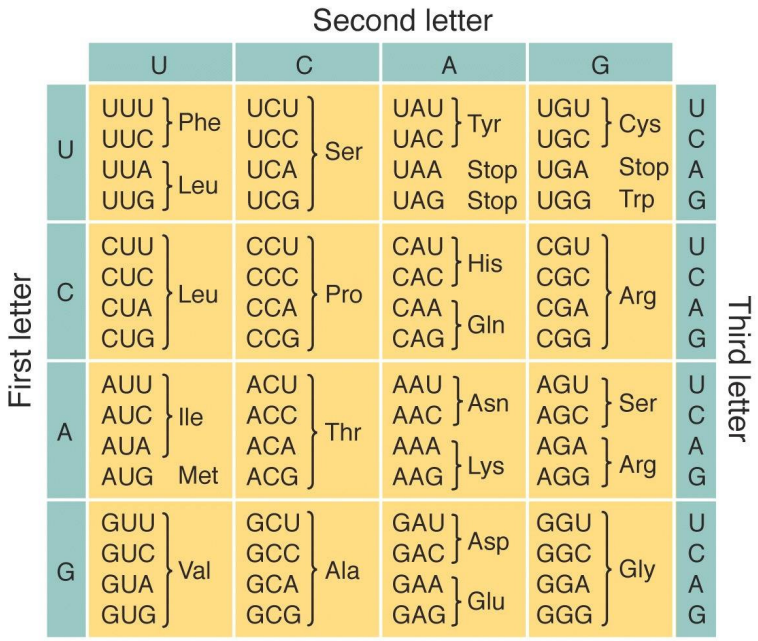

Figure 1.1: The standard genetic code table. The standard genetic code contains 64 codons of which 61 codify 20 different amino acids and 3 codify stop codons.

It is still unclear how the genetic code evolved, but previous studies have show a correlation between the three codon bases with the amino acid chemical properties. Usually, codons with U in second position codify for hydrophobic amino acids, namely leucine, isoleucine, valine, methionine and phenylalanine, while codons with A in the second position codify hydrophilic amino acids, although tyrosine is an exception (Taylor & Coates, 1989). Furthermore, the number of synonyms codons coding for an amino acid is linked to the relative frequency of the amino acid in the genome of Archaea, Bacteria and Eukarya (Gilis et al., 2001), but have a negative correlation with the molecular weight of the amino acid (Hasegawa & Miyata, 1980). A connexion between codons and aaRS classes has also been uncovered, showing that XCX codons code for amino acids handled by class II aaRS, whereas XUX codons, with the exception of phenylalanine, code for amino acids handled by class I aaRS (Wetzel, 1995).

1.2 Control of translation fidelity

1.2.1. mRNA translation

Gene expression involves two fundamental steps, namely the transcription of a DNA sequence into the complementary mRNA, and the translation of the mRNA into protein (Daviter et al., 2006). In eukaryotes, the pre-mRNA transcript undergoes several modifications including capping of 5' terminus, intron splicing, cleavage, polyadenylation and a quality control before export from the nucleus to the cytoplasm. Once in the cytoplasm the mRNAs are normally available for translation of its encoded message into a polypeptide chain or, alternatively, they may remain silent or be degraded. The regulation of this processes is controlled by proteins, the RNA-binding proteins (RBP), and/or small regulatory RNAs, like small interfering RNAs or microRNAs (reviewed in Mata et al., 2005; McKee & Silver, 2007; Quesne et al., 2010).

The mRNA message is translated into proteins by the ribosome, whose structure is formed by a small and a large ribonucleoprotein complex. The small subunit (in eukaryotes 40S) contains the decoding site where the tRNA anticodons interact with mRNA codons, while the large subunit (in eukaryotes 60S) contains the active site where the peptidyl transfer and hydrolysis reactions occur. Both subunits contain three tRNA binding sites: the amino-acyl (A) site, where the aminoacyl-tRNAs transporting the amino

acid to be incorporated into the polypeptide chain bind, the peptidyl (P) site, where the peptidyl-tRNA is positioned and the exit (E) site, where deacylated tRNAs are placed before exit from the ribosome (reviewed in Lackner & Bahler, 2008; Steitz, 2008).

The translation process is divided in three steps: initiation, elongation and termination. In order to initiate translation the ribosomal 40S and 60S subunits must be dissociated, which is controlled by the eukaryotic initiation factors (eIFs) eIF3, eIF1, eIF1A and eIF6. The first step in the initiation phase is the assembly of a ternary complex formed by eIF2, GTP and methionyl-initiator tRNA (Met-tRNA$_i^{met}$). This step is regulated by eIF2B. The ternary complex binds to the 40S ribosomal subunit to form the 43S preinitiation complex in the presence of eIF1, eIF1A and eIF3, in mammalian cells, or in the presence of eIF1, eIF3 and eIF5 in yeast cells (figure 1.2). Then, the 43S preinitiation complex assembles and scans the 5' UTR of the mRNA until it finds the AUG start codon, in a process regulated by the eIF4 factor and PAPB. Specific codon-anticodon interactions between Met-tRNA$_i^{met}$ of the 43S preinitiation complex and the AUG start codon at the P site of the ribosome permit the formation of a stable complex, known as 48S initiation complex. Then, the GTP complexed to the eIF2 is hydrolyzed by eIF5, with a consequent release of eIF2-GDP and the other initiation factors from the 40S subunit. Finally, eIF5B-GTP stimulates the assembly of the 60S subunit to the 48S initiation complex to form the 80S ribosome, with the hydrolysis of GTP and consequent release of eIF5B-GDP (figure 1.2) (reviewed in Lackner & Bahler, 2008; Preiss & Hentze, 2003).

The translation elongation phase involves the movement of tRNA through the three tRNA-binding sites (A→P→E) on the ribosome. In eukaryotic cells, the first step of elongation is the formation of a ternary complex between the aminoacyl-tRNA (aa-tRNA), the elongation factor eEF1A and GTP, which is brought to the A-site of the ribosome. Correct mRNA codon and tRNA anticodon interaction activates the GTPase activity of the ribosome inducing GTP hydrolysis and release of the aminoacyl end of the tRNA from eEF1A. The peptidyl-tRNA, located at the P-site, and the aminoacyl-tRNA, at the A-site, suffer conformational changes which promote the transfer of the polypeptide chain from the tRNA in the P to that in the A-site. Next, the peptidyl-tRNA and the deacylated tRNA retranslocate respectively from the A- and P-sites into the P- and E-sites. These reactions are catalyzed by the elongation factor eEF-2 with the consumption of energy produced by GTP hydrolysis. These movements free the A-site to receive a new aa-tRNA and shift the ribosome in the 3' mRNA direction to decode the next codon and continue the elongation cycle (figure 1.3).

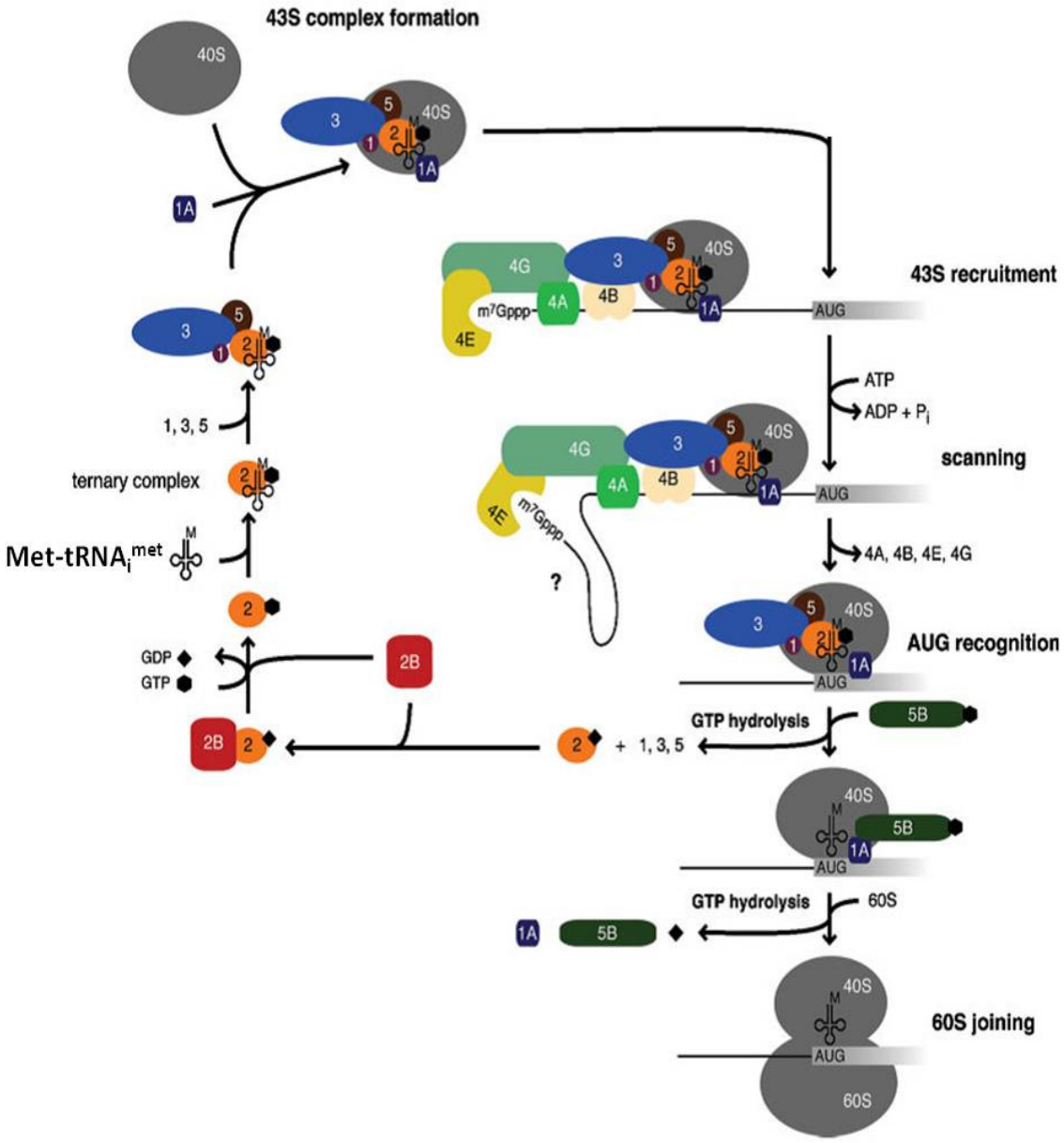

Figure 1.2: Eukaryotic mRNA translation initiation steps. Translation initiation begins with the binding of eIF2 (2), GTP and Met-tRNA$_i^{met}$, in the presence of eIF2B (2B) to form the ternary complex. This complex assemble with the 40S ribosomal small subunit to form the 43S preinitiation complex in the presence of the eIF1 (1), eIF3 (3) and eIF5 (5). The 43S complex is next recruited to the mRNA where it scans the molecule until it finds the AUG start codon, in the presence of the eIF4 factor. This will lead to the formation of a complex between the AUG codon and the 43S preinitiation complex known as 48S initiation complex. Finally, after recognition of the AUG codon, two distinct GTP hydrolysis steps occur and the 60S large ribosomal subunit associates with the 48S complex to form the 80S ribosome. Adapted and modified from (Preiss & Hentze, 2003).

The arrival of an mRNA stop codon into the A-site activates the termination of protein synthesis. The release factor eRF1 binds to the ribosome and hydrolyzes the peptidyl-tRNA bond, releasing the polypeptide chain in the presence of eRF3 and GTP consumption. The two ribosomal subunits separate and all the other factors are recycled for another translation (reviewed in Sohmen et al., 2009; Steitz, 2008; Zaher & Green, 2009).

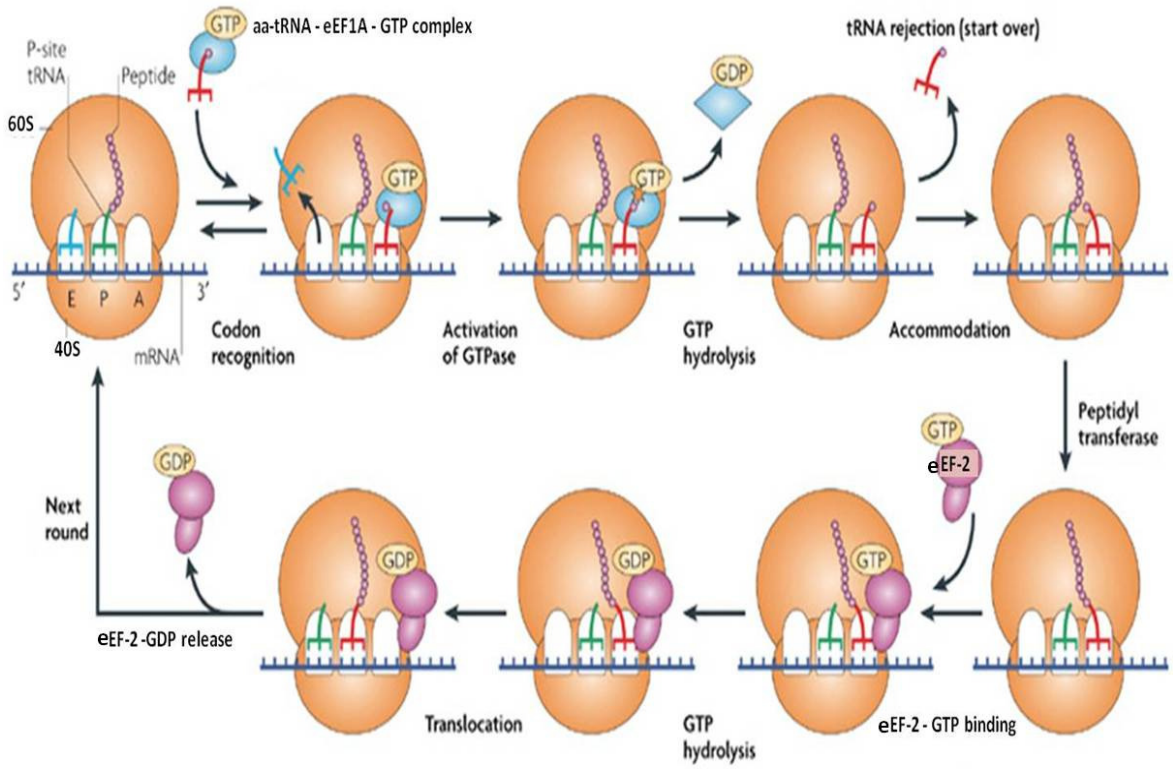

Figure 1.3: mRNA translation elongation steps. The translation elongation phase is initiated with the binding of a complex formed by the aminoacyl-tRNA (aa-tRNA), the elongation factor eEF1A and GTP into the A-site of the ribosome. When correct codon-anticodon pairing interactions are formed the GTPase activity of the ribosome is activated and the GTP hydrolysis releases the aminoacyl end of the tRNA from eEF1A. The polypeptide chain is then transferred from the tRNA at the P-site to the aa-tRNA at the A-site. Finally, the deacylated tRNA and the peptidyl-tRNA are translocated respectively from A- and P-site to the P- and E-site, by the eEF-2 with consumption of GTP. The ribosome is then ready to receive a new aa-tRNA in the A-site to continue translation elongation. Adapted and modified from (Steitz, 2008).

DNA replication, transcription and translation evolved over billions of years and occur with high efficiency and accuracy, but errors do happen. Indeed, the estimated error rates during DNA replication are around 10^{-8} in bacteria and 10^{-10} in eukaryotes (Kunkel & Bebenek, 2000) and 10^{-5} during bacterial mRNA transcription (Blank et al., 1986). Error rates of translation are higher when compared to DNA replication and transcription, and are estimated at $10^{-3} – 10^{-4}$ *in vivo* in *E. coli* (Ogle & Ramakrishnan, 2005; Rosenberger & Hilton, 1983). The translational errors can occur in part due to the high speed of protein synthesis. Indeed, the average of amino acid incorporation rate into growing peptide chain in the ribosome is 10 amino acids per second and, therefore, protein synthesis is a compromise between speed and accuracy (Daviter et al., 2006; Thompson & Karim, 1982).

Translational errors can be due to incorrect tRNA aminoacylation or can occur during mRNA decoding by the ribosome. mRNA decoding errors can be of three types: 1) missence errors, which result in the incorporation of an incorrect amino acid at a sense codon; 2) frameshifting errors, which alter the mRNA reading frame producing out-of-frame truncated proteins; 3) processivity errors, which involve readthrough of nonsense codons and lead to production of proteins with extended C-termini, or premature termination of translation leading to truncated proteins. Missense errors occur with a frequency of $5x10^{-4}$ errors/codon decoded. The third codon nucleotide is misread more often followed by the first codon nucleotide, whereas the second codon base is not misread with detectable frequency. Since errors in reading the third codon nucleotide usually lead to incorporation of the same amino acid or to one with similar chemical properties, only 1 in 400 missense errors completely inactivate protein activity. Frameshifting errors can be to the +1 or -1 frames and have the same effect as the insertion or deletion of one nucleotide. Proteins produced have a dramatically different sequence and can be shorter or longer than wild type proteins, depending on the proximity of the nearest stop codon. The frequency of this type of errors is in the order of $3x10^{-5}$ and likely result from incorporation of an incorrect tRNA in the ribosome A-site, which may slip to an overlapping triplet to the left or to the right of the correct reading frame. The frequency of processivity errors is around $4x10^{-4}$ and is estimated to use 3% of energy in dividing cells (Moura et al., 2009; Nierhaus, 2001). It is known that stress conditions, namely carbon and amino acid starvation increase translation errors due to reduction in the pool of charged tRNAs (Fredriksson et al., 2007). Also, aminoglycosilic antibiotics, which inhibit specific steps of translation can introduce errors (Daviter et al., 2006; Moura et al., 2009; Ogle & Ramakrishnan, 2005).

Translation steps are closely scrutinized by proofreading and quality control pathways to minimize errors. These control steps occur during synthesis of aminoacyl-tRNAs by cognate aminoacyl-tRNA synthetases (aaRS) and during interaction of tRNA anticodon with mRNA codons in the ribosome. These aspects are discussed in detailed below.

1.2.2. Aminoacyl-tRNA synthetases

1.2.2.1. Kinetic mechanism

The aminoacyl-tRNA synthetases (aaRS) are a class of enzymes that catalyze the aminoacylation of tRNAs, that is, they match amino acids with cognate tRNAs in a two-step reaction. The first step includes the activation of the cognate amino acid into an aminoacyl adenylate, with the release of pyrophosphate (equation I). The second corresponds to the transfer of the activated amino acid to a cognate tRNA, as represented in equation II. Because these two steps involve specific recognition of amino acids and tRNAs that bring specificity to the overall reaction (reviewed in Francklyn, 2008; Meinnel et al., 1995).

(I) Activation: $aa + ATP{:}Mg^{2+} + aaRS \rightarrow aaRS{:}aa \approx AMP + PPi{:}Mg^{2+}$

(II) Transfer: $aaRS{:}aa \approx AMP + tRNA \rightarrow aa\text{-}tRNA + AMP + aaRS$

Aminoacylation is a highly accurate process. The specific recognition of tRNAs by aaRS is not a major problem in the aminoacylation process because tRNAs are large enough to provide a wide range of specific interactions with the corresponding synthetase. In fact, the error rate in tRNA selection is 10^{-6} or lower. However, the discrimination of the cognate amino acid by aaRSs is more difficult compared to tRNA selection, and the error rate is much higher, around 10^{-4} 10^{-5} (reviewed in Jakubowski & Goldman, 1992). This happens because amino acids are smaller and share very similar structures and chemical properties (Bacher et al., 2005; Reynolds et al., 2010; Sankaranarayanan & Moras, 2001). Several aaRSs use proofreading mechanisms to correct the misactivation of non-cognate amino acids. If the proofreading mechanism occurs before transfer of the amino acid to the tRNA it is called pre-transfer editing. If it occurs after amino acid transfer to tRNA it is called post-transfer editing (figure 1.4).

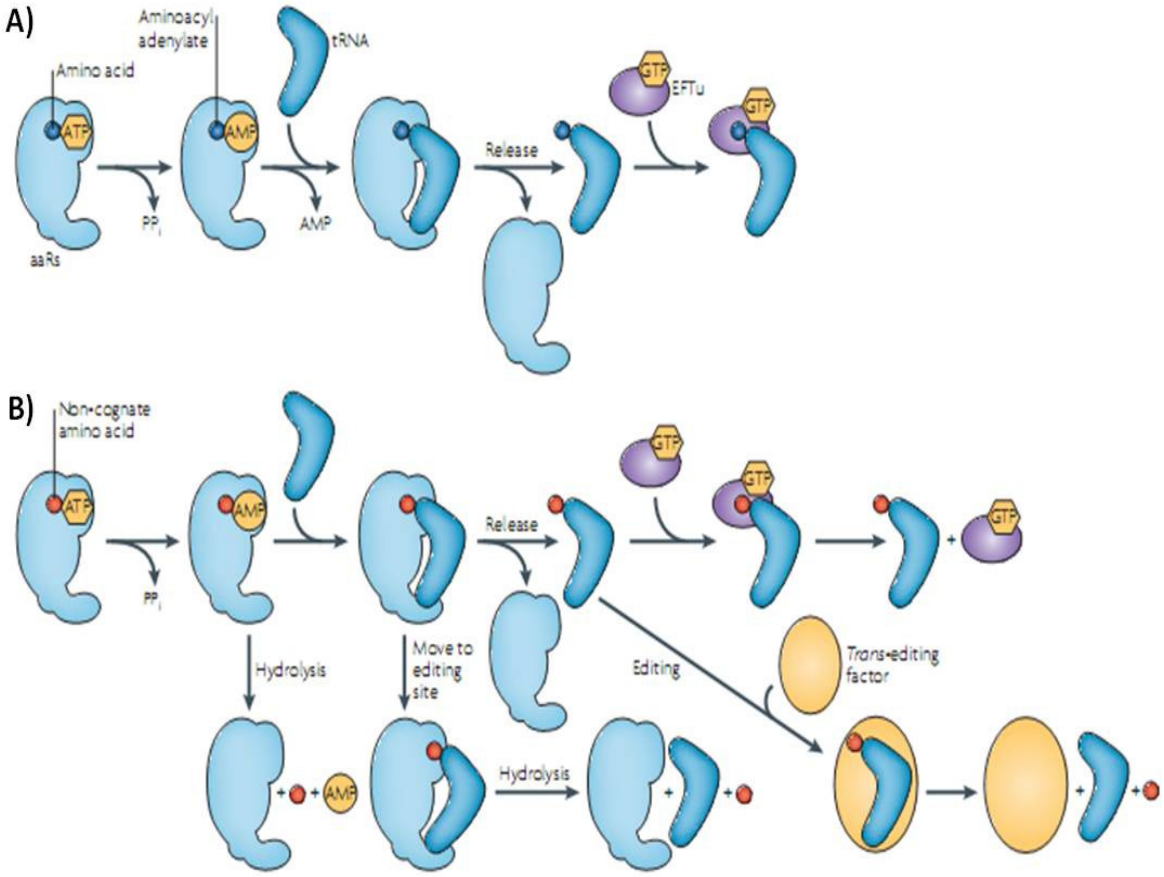

Figure 1.4: aaRS editing mechanisms. A) Recognition of cognate amino acid and tRNA. The cognate amino acid (blue) is activated in the aminoacyl-tRNA synthetase (aaRS) active site in the presence of ATP, to form the aminoacyl-adenylate with release of PPi. Next, the cognate tRNA binds to the aaRS, and the amino acid attach to the 3′ end of the tRNA, with AMP release. The aminoacyl-tRNA (aa-tRNA) is recognized by the elongation factor and both form a ternary complex with GTP to be release in the ribosome during translation. B) Editing mechanism of aaRS. After the activation of a non-cognate amino acid (red), the aminoacyl adenylate may be hydrolysed and released (pre-transfer editing), or can be attached to a non-cognate tRNA. In this case, the editing activity in the aaRS is called post-transfer editing and implicates the hydrolysis of the amino acid – tRNA ester linkage. If the mischarged aa-tRNA is formed and released, it can be hydrolyzed by specific proteins named trans-editing factors. Finally, the elongation factor can also discriminate misacylated tRNA, by binding it too weakly for efficient delivery in the ribosome. Adapted from (Reynolds et al., 2010).

Pre-transfer editing can occur in the presence or absence of tRNA and involves specific mechanisms that promote the hydrolysis of the non-cognate aminoacyl adenylate with the release of non-cognate amino acid, AMP and PPi. Post-transfer editing involves

the tRNA–amino acid ester linkage hydrolysis, with release of tRNA and amino acid (reviewed in Martinis & Boniecki, 2010; Reynolds et al., 2010). The post-transfer editing activity is not exclusive of the aaRSs. There are proteins, named trans-acting factors, with editing domains which are able to hydrolyze efficiently the misacylated tRNAs. These trans-acting factors are very similar to the editing domains and/or parts of aaRSs, suggesting an evolutionary related link to aaRSs (Ahel et al., 2003). Besides the pre-transfer and the post-transfer editing, elongation factors can have an important role in translation accuracy, as they bind weakly to misacylated tRNAs during the formation of the ternary complex for translation. This fragile interaction promotes the release of the mysacylated tRNAs which became available to rebind to the aaRSs (Ling et al., 2009).

1.2.2.2. The one-to-one correspondence

In most organisms each of the 20 canonical amino acids is recognized by a cognate aaRS. However, several exceptions exist. For example, the majority of bacteria, Archaea and chloroplasts do not encode the enzyme glutaminyl-tRNA synthetase (GlnRS) and glutamine-tRNA^{Gln} (Gln-tRNA^{Gln}) is synthesized in a two step indirect pathway (Tumbula et al., 2000). In these organisms the glutamine-tRNA (tRNA^{Gln}) is first misaminoacylated with glutamic acid (Glu), originating the glutamyl-tRNA (Glu-tRNA^{Gln}), in a reaction catalyzed by a non-discriminating glutamyl-tRNA synthetase (ND-GluRS). The Glu residue on the Glu-tRNA^{Gln} is then transamidated by a glutamyl-tRNA^{Gln} amidotransferase (Glu-AdT) in the presence of ATP and an amide donor to form the Gln-tRNA^{Gln} (reviewed in RajBhandary, 1997; Sheppard et al., 2008). Yeast and mammalian mitochondrial genomes also lack GlnRS and synthesize Gln-tRNA^{Gln} using an indirect pathway. In human mitochondria the ND-GluRS role is catalyzed by mitochondrial glutamyl-tRNA synthetase (GluRS) (Nagao et al., 2009), while in yeast mitochondria is catalyzed by cytoplasmatic GluRS which is imported into the mitochondria where it glutaminates mitochondrial tRNA^{Gln} originating Glu-tRNA^{Gln} (Frechin et al., 2009).

Furthermore, prokaryotes lacking the asparaginyl-tRNA synthetase (AsnRS) produce asparagine-tRNA^{Asn} (Asn-tRNA^{Ans}) using an indirect two step reaction. In these organisms, a non-descriminating aspartyl-tRNA synthetase (ND-AspRS) mischarges the asparagine tRNA (tRNA^{Ans}) with aspartic acid (Asp) originating Asp-tRNA^{Ans}. The Asp moiety is then transaminated by an aspartyl-tRNA^{Asn} amidotransferase (Asp-AdT) to produce the Asn-tRNA^{Ans}, in the presence of ATP and an amide donor. Also, some

methanogenic archeae lack the cysteinyl-tRNA synthetase (CysRS). In these organisms the cysteine tRNA ($tRNA^{Cys}$) is aminoacylated with O-phosphoserine (Sep) by O-phosphoseryl-tRNA synthetase (SepRS) to form Sep-$tRNA^{Cys}$. The Sep residue is then converted to Cys by Sep-tRNA:Cys-tRNA synthetase (SepCysS), in the presence of a sulfur donor, to form Cys-$tRNA^{Cys}$ (reviewed in Sheppard et al., 2008).

Another exception to the one-to-one amino acid-aaRS correspondence occurs in some eukaryotic cells, where a single protein has two distinct functional domains containing glutamyl-tRNA synthetase (GluRS) and prolyl-tRNA synthetase (ProRS) activity (Cerini et al., 1991). Finally, in other cases, the same amino acid can be recognized by two distinct synthetases. For example, *E. coli* has two isoforms of lysyl-tRNA synthetase (LysRS) and *Bacillus subtilis* has two isoforms of tyrosyl-tRNA synthetase (TyrRS) and threonyl-tRNA synthetase (ThrRS) (reviewed in Meinnel et al., 1995).

1.2.2.3. Two aminoacyl-tRNA synthetases classes

The 20 aaRS are divided into two classes (classes I and II), which originated from an primordial distinct single-domain protein (Ribas de Pouplana & Schimmel, 2001; Schimmel et al., 1993). The 11 class I enzymes have an active site domain containing a Rossmann nucleotide-binding fold composed of alternating β strands and α helices. The class I enzymes are divided in three sub-classes, Ia, Ib and Ic, and the enzymes of each subclass have a preference to recognize chemically related amino acids (figure 1.5). For example, subclass Ia enzymes recognize the branched chain hydrophobic amino acids isoleucine (Ile), leucine (Leu) and valine (Val), the sulphur-containing residues methionine (Met) and cysteine (Cys), and also arginine (Arg). Subclass Ib recognize the charged amino acids, namely glutamic acid (Glu) and lysine (Lys) and the derivative glutamine (Gln). Subclass Ic recognize aromatic tyrosine (Tyr) and tryptophan (Trp). The 10 class II enzymes contain a six-stranded β sheet with flanking α helices in the active site. This class is also divided in three subclasses, IIa, IIb and IIc, which recognize chemical related residues, as in the case of the class I enzymes (figure 1.5). Therefore, subclass IIa enzymes recognize alanine (Ala), glycine (Gly) and the polar amino acids serine (Ser), threonine (Thr), proline (Pro) and histidine (His). The subclass IIb enzymes recognize the charged residues aspartic acid (Asp) and Lys, and the derivative asparagine (Asn), while

subclass IIc recognizes the aromatic phenylalanine (Phe) (reviewed in Giege & Eriani, 2002; Ribas de Pouplana & Schimmel, 2001).

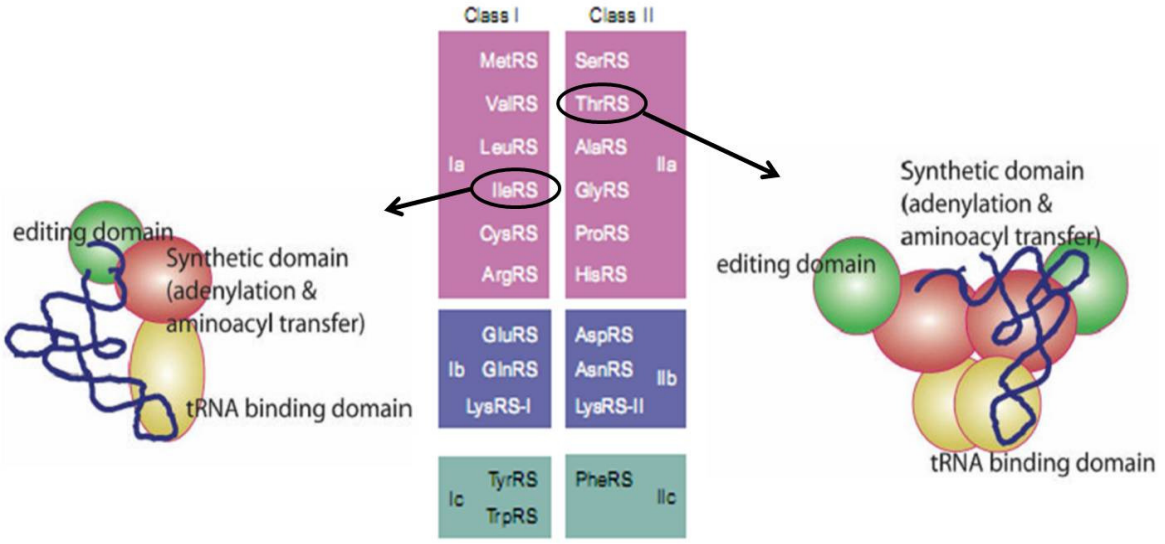

Figure 1.5: The two classes of aminoacyl-tRNA synthetases. The different subclasses from each aaRS class are shown. The two schematic representations on each side of the table correspond to the class I monomer enzyme isoleucyl-tRNA synthetase (IleRS) on the left side, and to the class II dimer enzyme threonyl-tRNA synthetase (ThrRS) on the right side. Adapted and modified from (Francklyn, 2008; Ribas de Pouplana & Schimmel, 2001).

The differences between class I and II enzymes are resumed in table 1.1. Besides the differences in the catalytic domain, class I enzymes are generally monomers whereas the class II exist as dimers. In class I the conserved peptidic motifs HIGH and KMSKS are responsible for the interaction with subtracts, while in class II the motif 1 is responsible for subunits interaction to form the dimer, and motifs 2 and 3 are involved in interaction with subtracts. The ATP binding domains is also different between two classes. In class I the ATP adopts a conformation similar to the one found in other protein containing Rossmann fold. In class II the ATP exhibits a bent conformation, where the γ-phosphate folds back over the adenine. Relatively to amino acid charging of tRNA, the difference seems to be only the site where the amino acid attaches, which can be explained in part by the mode of entry of the tRNA into the active site of the enzyme. In class I the amino acid attachment occurs in the 2' hydroxyl site of the last ribose of the tRNA, while in class II occurs in the 3' hydroxyl. The tRNA entry into the active site of both class enzymes is also different. Crystal structures of GlnRS and AspRS of *E. coli* show that class I enzymes bind

the acceptor stem of tRNA through the minor groove side, while class II bind it through the major groove side. As a consequence the variable region of tRNA is exposed to the solvent in class I enzymes, and faced to the protein side in class II enzymes, while the D loop has the opposite orientation (reviewed in Giege & Eriani, 2002; Ribas de Pouplana & Schimmel, 2001; Sankaranarayanan & Moras, 2001).

Table 1.1: Structural and functional features that define the two classes of aaRS. Adapted from (Giege & Eriani, 2002).

	Class I	Class II
Catalytic domain		
Architectural organization	**Rossmann fold-like Parallel β sheet Monomeric**	**Six stranded Antiparallel β sheet Dimeric**
Consensus peptidic motifs	**HiGh kmSKs**	**gϕxxϕxxP (motif 1) fRxr (motif 2) Gxgxgfd/eR (motif 3)**
ATP binding conformation	**Extended**	**Bent**
Amino acid attachment on the last ribose	**2' hydroxyl**	**3' hydroxyl**
tRNA approach		
Acceptor stem	**Minor groove side**	**Major groove side**
Variable arm	**Exposed to solvent**	**Faces the protein**
D-loop side	**Faces the protein**	**Exposed to solvent**

1.2.3. Transfer RNA

1.2.3.1. tRNA structure

tRNAs constitute around 10-15% of total RNA in cells. Each tRNA has a relative molecular weight of 25 kDa and a chain length of 75 to 95 nucleotides. They can be divided in 20 families corresponding to 20 cognate amino acids. For example, in *E. coli*, the Trp family contains only one tRNA isoaceptor, while the Leu family contains five different isoaceptors. Each family of tRNA isoaceptors is recognized by a single cognate aaRS (Goldman, 2002). The main cellular role of aminoacylated tRNAs is to serve as an adaptor that brings amino acids to the growing polypeptide chain in the ribosome (Allen et al., 1959). Although, tRNA molecules can also participate in other cellular processes, namely amino acid transformation, e.g., conversion of serine into selenocysteine and

porphyrin biosynthesis (RajBhandary & Soll, 1995). In bacteria, tRNAs also play an important role in cell wall biosynthesis (Giannouli et al., 2009).

All tRNAs have a secondary cloverleaf type structure (figure 1.6 a). This structure consists of four domains, namely the acceptor stem, the D-arm, the anticodon arm, the TψC-arm, and a variable loop, which are stabilized by tertiary hydrogen bounds formed between them. The acceptor stem contains seven base pairs, followed by an unpaired nucleotide at position 73 and the CCA terminal sequence where amino acids attach. The D-arm, or left arm, usually contains 3-4 base pairs and a D-loop of 8-11 bases. The TψC-arm, present on the right side of the cloverleaf structure, is formed by a 5 base pairs stem and a loop of 7 unpaired nucleotides (TψC-loop). The variable arm contains a variable number of nucleotides, and its length differentiates two families of tRNAs. Class I tRNAs have a short variable sequence of 4-5 nucleotides, while class II tRNAs have a variable arm of 10-24 nucleotides. The anticodon arm contains a stem of 5 base pairs and a loop of 7 unpaired bases. The anticodon is located between positions 34-36 in the centre of the anticodon loop. The tertiary structure of tRNA, determined by X-ray crystallography, corresponds to an L-shaped molecule formed by tertiary interactions between the arms (figure 1.6 b).

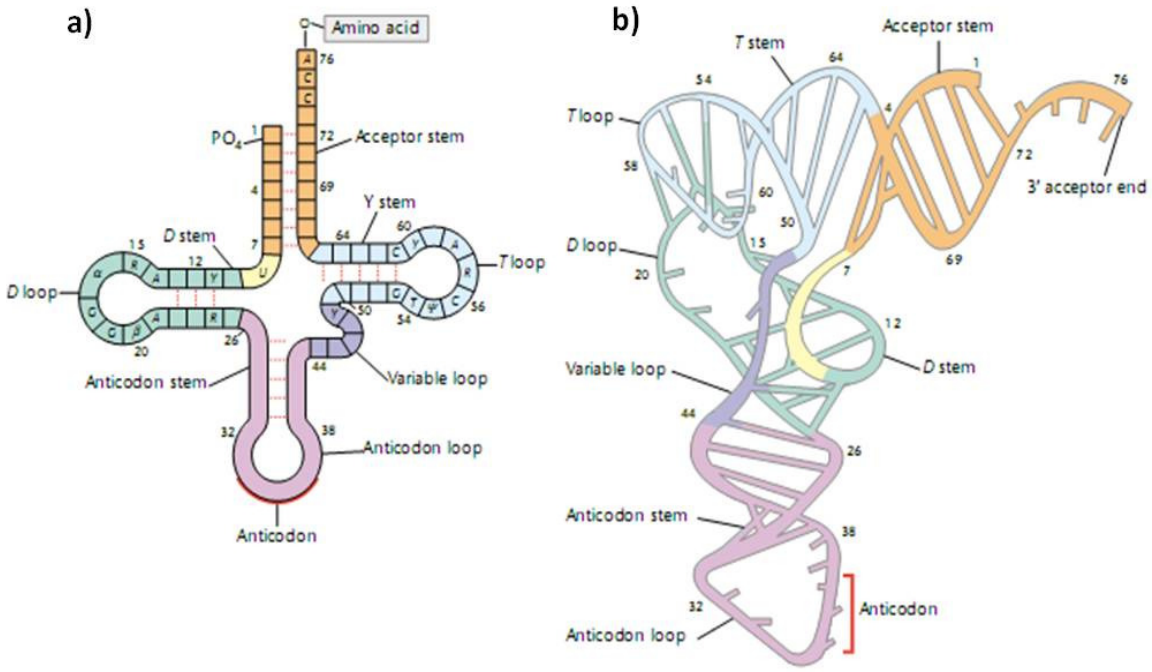

Figure 1.6: Representation of tRNA 2D and 3D structures. A) Secondary structure of tRNA cloverleaf model. B) The L-shapped 3D structure of the tRNA showing the anticodon and the acceptor ends. Adapted from (Goldman, 2002; Rich & Kim, 1978).

The acceptor stem and the TψC-arm stack onto each other to form a continuous A-helix, while the D-arm and the anticodon arm stack to form another continuous helix. The two RNA double helices form a 90º angle to produce the characteristic tertiary L-structure. This interaction is stabilized by two conserved residues of the D- and TψC-loops, namely the G19:C56 pair. At one of the two ends of the L-shaped molecule is the anticodon, which interacts with the codon, while at the other end is the amino acid attachment site, at the end of the 3' CCA terminal sequence (reviewed in Dirheimer et al., 1995; Goldman, 2002).

1.2.3.2. tRNA processing

Transcription of all tRNA genes in eukaryotes is performed by RNA polymerase III. This enzyme requires short conserved cis-elements called A and B Boxes. Box-A is located in the D-arm, nucleotides 8–19, while Box-B is located in the TψC arm, nucleotides 52–62 of mature tRNAs. These two boxes are essential for binding of transcription factors and to initiate transcription. In addition, the 5' and 3' flanking regions contain elements that influence transcriptional efficiency (reviewed in Goldman, 2002; Ueda & Watanabe, 2001).

The primary transcript (pre-tRNA) is longer than the final tRNA molecule due to 5' and 3' extension sequences (figure 1.7). The 5' leader sequence is removed by endonucleolytic cleavage by ribonuclease P (RNAse P), which is present in all organisms. Processing of the 3' sequence is more complicated and involves different enzymes. The endonuleases Rnase E and Rnase III cleave the middle of the 3' extension sequence, followed by an exonucleolytic cleavage promoted by exonucleases RNase II, RNase PH, RNase BN/RNase Z (reviewed in Nakanishi & Nureki, 2005).

In eubacteria the CCA 3' terminal sequence is encoded in tRNA genes, while in eukaryotes the CCA is added post-transcriptionally to the tRNA by the enzyme ATP(CTP):tRNA nucleotidyl transferase, using CTP and ATP as subtracts. This enzyme also checks the status of the tRNA 3' end, and reconstructs the CCA sequence if necessary. This is important because the CCA end is subject to nuclease degradation, as it is not base paired and sticks out from tRNA structure turning it susceptible to nuclease attack. This enzyme can be divided into two classes, class I is present in archeae, and class II is present in eukaryotes. Both enzymes have a L-shape catalytic pocket where the terminal of the tRNA is inserted to stack the nucleotides (Deutscher, 1995; Nakanishi &

Nureki, 2005). Interestingly, tRNAs of yeasts growing under amino acid starvation conditions lack the CCA sequence, which is removed by a specific nuclease. This prevents abortive aminoacylation of tRNAs and saves ATP (Ueda & Watanabe, 2001).

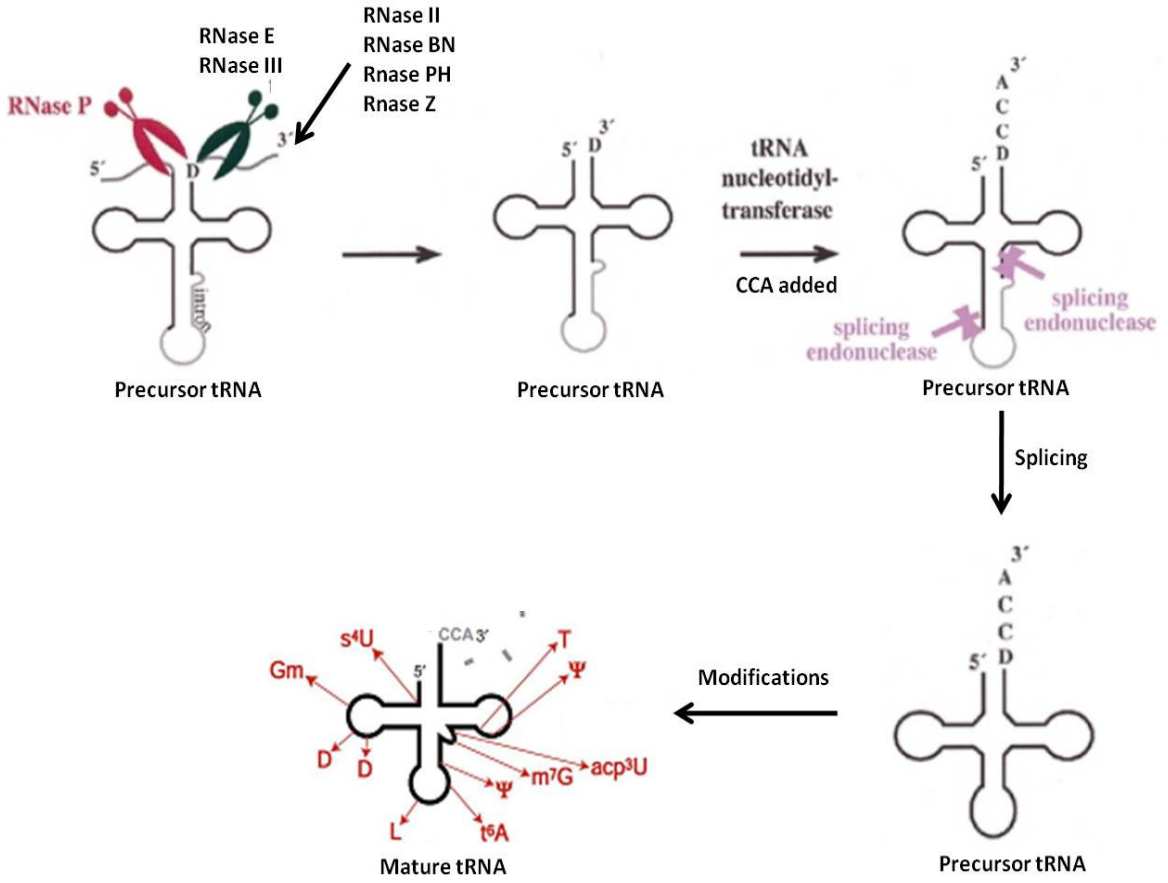

Figure 1.7: tRNA processing in eukaryotes. The 5' trailer of the precursor tRNA is removed by RNase P, while 3' is removed first by endonucleolytic and then by exonucleolytic cleavage by various RNases. The terminal CCA sequence is added by tRNA nucleotidyl transferase and the introns are removed by splicing enzymes, tRNA ligase and phosphor-transferase enzymes. The precursor tRNA is finally modified to originate the mature tRNA. Adapted and modified from (Morl & Marchfelder, 2001; Nakanishi & Nureki, 2005).

Some eukaryotic, chloroplast, plant mitochondrial and bacterial tRNAs contain an intron in the anticodon loop region. The intron is removed by specific endonucleases and the two tRNA halfs are joined by a RNA ligase. In eukaryotes, more or less 20% of tRNA precursors contain an intron which is cleaved by a heterotetrameric tRNA splicing

endonuclease formed by the subunits, Sen54p, Sen2p, Sen34p, and Sen15p. During splicing the Sen2p and Sen34p subunits cleave the 5'-exon-intron junction and the intron-3'-exon junction, respectively. The 2',3'-cyclic phosphate, at the 3' of the 5' half is converted to 2' phosphate by a cyclic phosphodiesterase. Then, the 5' hydroxy of the 3' tRNA half fragment is phosphorylated, by a polynucleotide kinase, and an adenylated tRNA ligase transfers its AMP to the same residue. Finally, the two fragments are ligated by a tRNA ligase with the release of AMP (Shawk et al., 1995; Ueda & Watanabe, 2001). Splicing was originally thought to be restricted to the nucleus, but recent data show that it can also occur in the cytoplasm (Yoshihisa et al., 2003; Yoshihisa et al., 2007).

tRNAs contain various modified ribonucleotides derived from the normal ribonucleotides adenosine (A), guanosine (G), cytosine (C) and uridine (U), which are added postranscriptionally, with the exception of queuosine (Q). tRNAs with fewer modified nucleotides (2–6 per tRNA molecule) are found in mitochondria and Mycoplasma, whereas cytoplasmatic tRNAs from high eukaryotes can contain up to 22 modified nucleotides per molecule (Grosjean et al., 2007). At least 120 different nucleotide modifications are known today, from which 100 are present in tRNA molecules (Czerwoniec et al., 2009). Interestingly, some of these modifications are shared between Archaea, Bacteria and Eukarya, while others are specific of each phylogenetic domain, suggesting that some modified nucleotides have evolved after the separation between prokaryotes and eukaryotes (Bjork, 1995).

Usually, the modifications located in the tRNA core region, between D- and TψC-loops, contribute to the L-shaped tertiary structure stabilization, while modifications in the anticodon loop are important for codon-anticodon interaction and accurate recognition of tRNAs by aaRSs (Nakanishi & Nureki, 2005). Surprisingly, tRNAs can lose their modified nucleotides in some stress conditions, namely in the presence of hydrogen peroxide, arsenite and hypochloride, due to decreased expression of modifying enzymes (Chan et al., 2010).

Most of the modified nucleotides are found in positions 34 and 37 of mature tRNAs, where they play a role in codon-anticodon interactions. The interaction of the first base pair of the anticodon with the third base pair of the codon is known as the wobble interaction which has specific base pairing rules which were first mentioned by Crick and were latter modified by Agris and colleagues (Agris et al., 2007; Crick, 1966a). According to these rules the codon-anticodon paring follows the traditional base paring rules for the first two nucleotides of the triplets, namely C pairs with G and A pairs with U, while the

third base can pair with more than one nucleotide (table 1.2). The wobble base permits anticodon degeneracy which means that certain tRNA anticodons can recognize more than one codon.

Table 1.2: The wobble anticodon hypothesis. Adapted and modified from (Agris et al., 2007).

Wobble hypothesis		Modified wobble hypothesis	
Anticodon N34	Codon N3	Anticodon N34	Codon N3
G	C,U	G	C,U
C	G	C	G
I	U,C,A	I	U,C,A
U	A,G	Xm5U	G
		S2U	A,G
		Xo5U	A,G,U, (C)

On the other hand, i^6A_{37} is found in tRNAs decoding codons starting with 5'-U and t^6A_{37} is present in tRNAs decoding codons starting with 5'-A (Goldman, 2002). The modified bases at position 34 can also be important for correct aminoacylation of tRNA. For example, $mnm^5s^2U_{34}$ is important for $tRNA^{Glu}$, $tRNA^{Gln}$ and $tRNA^{Lys}$ identity; Q_{34} is important for $tRNA^{Asp}$ and $tRNA^{Tyr}$ identity. By contrast, some modified nucleotides have no effect on tRNA aminoacylation, namely ac^4C_{34} in $tRNA^{Met}$ and Q_{34} in $tRNA^{His}$. In other cases, the same modification can have an opposite role. For example, m^1G_{37} is important for $tRNA^{Leu}$ recognition by leucyl-tRNA synthetase (LeuRS) and acts as an identity antideterminant for $tRNA^{Asp}$ (reviewed in Bjork, 1995; Goldman, 2002)

1.2.3.3. tRNA discrimination by aaRS

The specificity of tRNA in translation depends on codon-anticodon interactions, while the specificity in aminoacylation depends on tRNA interaction with cognate aaRSs. The discrimination of tRNAs by aaRS is complex because they have a similar 3D L-shaped structure, with a terminal CCA sequence. Even though tRNA comprises at least 76 nucleotides, only a small number is involved in tRNA identity determination. These elements, which contribute to tRNA recognition by cognate aaRS, are named tRNA identity elements. They can be of two types, positive elements, also known as identity

determinates, which contribute to specific recognition and aminoacylation of tRNA by cognate aaRS, and negative elements or antideterminants, which inhibit aminoacylation by non-cognate aaRSs (McClain, 1993; Normanly et al., 1986).

An *in silico* analysis of 67 *E. coli* tRNA sequences predicted that tRNA identity elements locate predominantly in the anticodon and acceptor end (including nucleotide 73), and, although some deviations to this rule exist, experimental data confirmed that prediction and re-inforced the role of the anticodon and acceptor stem (figure 1.8.) (McClain, 1993).

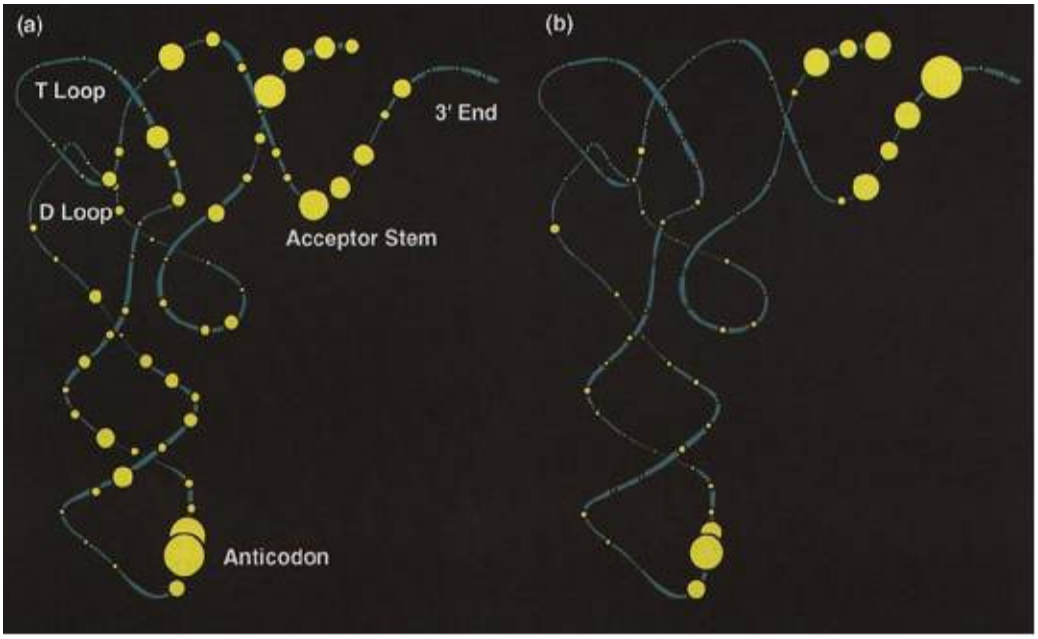

Figure 1.8: Comparison between predicted (a) and observed (b) tRNA identity elements in *E. coli*. The tRNA chain is represented by the blue line and the tRNA identity elements by the yellow circles. *In silico* studies predicted that tRNA identity elements localized mainly in the anticodon and acceptor stem. The diameter of the circle is proportional to the frequency of prediction. Adapted from (McClain, 1993).

To study tRNA identity elements and identify the bases that affect tRNA recognition by cognate aaRSs, both *in vitro* and *in vivo* strategies have been used. The main limitation of *in vitro* studies resides in the fact that many *in vitro* synthesized tRNAs have incorrect or altered structure, either due to synthesis error or due to the absence of base modifications. The other limitation is related to the fact that this strategy does not

reproduce the *in vivo* competition between tRNAs and aaRSs. This approach can however determine correctly the effects of specific mutations on tRNA charging, namely the kinetic parameters of the aminoacylation reaction (Kcat and Km). *In vivo* studies can overcome the above limitations, however the efficiency of *in vivo* assays does not represent the efficiency of recognition of tRNA by aaRS only, it also represents the efficiency of a tRNA synthesis, processing, base modification, and interaction with translational machinery. In other words, both assays are complementary (Giege & Eriani, 2002; Pallanck et al., 1995).

The data available shows that tRNA identity elements change between tRNA families of the same organism, and between the same tRNA family of different organisms. For example, in *E. coli* the anticodon of 16 tRNA isoacceptor families contain identity elements for cognate aaRSs (Ardell, 2010; Giege et al., 1998). The tRNAs most affected by mutations in the anticodon region are $tRNA^{Val}$ and $tRNA^{Met}$, because their cognate aaRSs recognize mainly the tRNA anticodon (Schulman & Pelka, 1988). By opposition, only 3 tRNA families lack identity elements in the anticodon, namely the $tRNA^{Ser}$, $tRNA^{Leu}$ and $tRNA^{Ala}$. This is likely related to the high degeneracy of the anticodon sequences of these tRNAs, which decode 6 Ser and Leu codons and 4 Ala codons (Giege & Eriani, 2002; Hou & Schimmel, 1988). Another interesting example is the *E. coli* $tRNA^{His}$, which is the only *E. coli* tRNA with 8 base-pairs in the acceptor stem. In this case, the discriminatory base (nucleotide 73) pairs with the G1:C73 base pair, which functions as a tRNA identity element (Himeno et al., 1989).

The identity of tRNAs is determined by both the presence of positive identity elements and the presence of negative elements. Some of the tRNA determinants for cognate aaRS may act as antideterminants for other aaRSs, as is the case of A_{73}, which is a determinate for LeuRS, and an antideterminant for SerRS in human cells (Breitchopf & Gross, 1996). Some examples of other known antideterminants are listed in table 1.3.

Table 1.3: A few examples of tRNA antideterminants. Adapted from (Giege et al., 1998).

Antideterminant	tRNA	Against aaRS
G3:U70	$tRNA^{Ala}$ (yeast)	ThrRS
U30:G40	$tRNA^{Ile}$ (yeast)	GlnRS/LysRS
U34	$tRNA^{Ile}$ (yeast)	MetRS
L34	$tRNA^{Ile}$ (*E. coli*)	MetRS
A36	$tRNA^{Arg}$ (*E. coli*)	TrpRS
G37	$tRNA^{Ser}$ (yeast)	LeuRS
m1G37	$tRNA^{Asp}$ (yeast)	ArgRS
A73	$tRNA^{Leu}$ (human)	SerRS

1.3. Alterations to the standard genetic code

The genetic code was thought to be immutable and universal, but the discovery in 1979 that the UGA codon is decoded as Trp and is not used to terminate mRNA translation, and that the AUA is decoded as Met instead of Ile in human mitochondria invalidated the universality hypothesis (Barrell et al., 1979). Since then, several alterations were found in mitochondria and cytoplasm of various organisms, namely bacteria, yeast, ciliated protozoa and algae. The alterations to the standard genetic code include the discovery of the 21st and 22nd amino acids and the reassignment of sense and non-sense codons (Knight et al., 2001; Osawa et al., 1992). In mitochondria both sense and nonsense codons can change identity, but in cytoplasmic translation only stop codons are normally involved in genetic code changes. The exception is the leucine CUG codon which is decoded as serine in the CTG clade species *(Butler & et al, 2009; Ohama et al., 1993; Santos & Tuite, 1995; Sugita & Nakase, 1999)*.

1.3.1. Evolutionary theories of genetic code alterations

Alterations to the standard genetic code are explained by the “codon capture theory” and the “ambiguous intermediate theory” (figure 1.9).

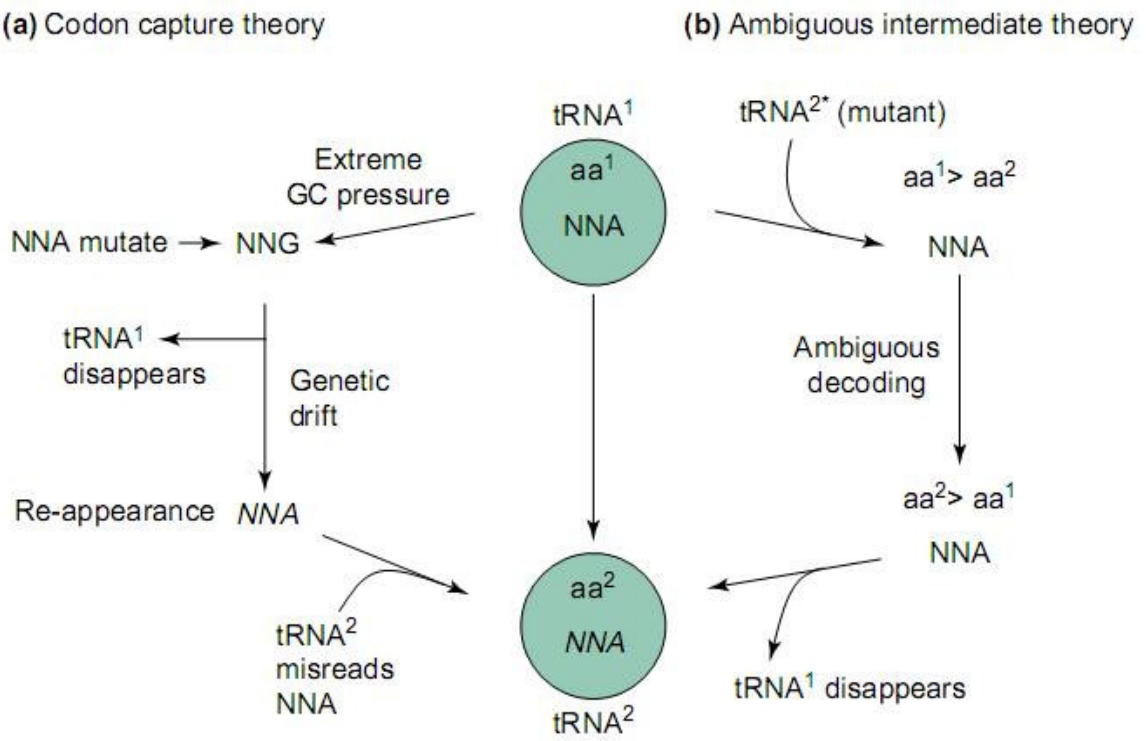

Figure 1.9: Molecular mechanisms of evolution of genetic code alterations. A) The "codon capture theory" postulates that high GC pressure may eliminate A or U ending codons. If an NNA codon reappears by genetic drift it can be decoded by a non-cognate tRNA, thus changing the identity of the codon. B) The "ambiguous intermediate theory" postulates that a misreading tRNA (tRNA2*) competes with cognates tRNA (tRNA1) for decoding NNA codon, creating ambiguity. The disappearance of the cognate tRNA (tRNA1) allows for reassignment of NNA codon. Adapted from (Santos et al., 2004).

The "codon capture theory" (Osawa et al., 1992; Osawa & Jukes, 1989; Osawa & Jukes, 1995) postulates that genetic code alterations arise from fluctuations of genome GC/AT content. In organisms with a high GC or AT content, selective pressure leads to elimination of AT or GC rich codons, respectively. Genes encoding the tRNAs that decode vanished codons are also erased from the genome. This creates unassigned codons that can be re-introduced in the genome at a later stage with a new meaning. Re-introduction of unassigned codons is mainly due to GC fluctuations over time. Since the re-introduced codons can be decoded by non-cognate tRNAs they become reassigned to new amino acids families. This theory is supported by disappearance of the CGG codon in *Mycoplasma capricolum*, whose genome only has 25% GC (Oba et al., 1991), and also by the unassignment of AGA and AUA codons in *Micrococus luteus* whose genome has 75%

GC (Kano et al., 1991; Ohama et al., 1990). However, the reassignment of codons in cases where GC or AT enrichment are not observed raise questions about the validity of the "codon capture theory" (Miranda et al., 2006; Santos & Tuite, 2004).

The "ambiguous intermediate theory" suggests that misreading tRNAs drive genetic code changes through codon ambiguity. Initial low level codon ambiguity is essential for gradual codon reassignment. Ambiguity can then increase gradually leading to loss of the cognate tRNA that decodes the codon accurately. This hypothesis does not require codon disappearance prior to reassignment, however it suggests that rare codons are more easily reassigned than frequently used ones. Since codon misreading leads to amino acid misincorporation, proteins become altered and the proteome is destabilized. This proteotoxic stress may be energetically costly and may even cause cell death, eliminating the codon identity alteration (Schultz & Yarus, 1994). However, the discovery of CUG reassignment from Leu to Ser in the CTG clade species support this hypothesis (Massey et al., 2003; Santos et al., 2004).

1.3.2. Expansion of the genetic code

With few exceptions the same genetic code is used in all organisms. Although, various post-translational amino acid modifications have been identified in natural proteins expanding the natural amino acid repertoire (Uy & Wold, 1977; Wang et al., 2009b). Two additional amino acids also joined the "exclusive club" of the genetically encoded amino acids that are incorporated into proteins, namely selenocysteine (Bock et al., 1991) and pyrrolysine (Srinivasan et al., 2002). The discovery of these two new amino acids, which are encoded by nonsense codons, re-opened the discussion of the evolution of the genetic code (Yoshizawa & Bock, 2009).

Selenocysteine and pyrrolysine, the 21st and 22nd amino acids, are inserted into polypeptides during translation, in response to the stop codons UGA and UAG, respectively. The insertion of both amino acids uses different mechanisms. Selenocysteine (Sec) is synthesized from the selenium and is usually found in the active centre of a small number of selenoproteins (Bock et al., 1991). The human genome encodes 25 selenoproteins involved in a variety of cellular processes (Kryukov et al., 2003). Perturbations of selenoprotein biosynthesis is implicated in a variety of diseases,

including muscle and cardiovascular disorders, immune dysfunction, cancer, neurological disorders and endocrine function (Bellinger et al., 2009). As Sec is used in all three domains of life, its appearance is likely ancestral, before the divergence of Bacteria, Archaea and Eukarya. The mechanism of synthesis and incorporation of Sec is very complex but has been studied in detail. The decoding of the UGA codon in the mRNA of selenoproteins requires the formation of a quaternary complex between GTP, a unique Sec-tRNA^{Sec}, a specific translation factor (SelB) and an unsual mRNA secondary structure (SECIS). An unique helical secondary structure after the UGA_{Sec} codon in the mRNA of selenoproteins, termed SECIS (selenocysteine insertion element), works as a cis-regulatory element for Sec incorporation. During translation, Sec-tRNA^{Sec} is delivered to the ribosome by a specific translation elongation factor, SelB, which has the particularity to interact both with the Sec-tRNA^{Sec} and the mRNA coding for selenoproteins (SECIS). Besides these elements, Sec incorporation requires a unique tRNA, the tRNA^{Sec}, containing a UCA anticodon. This unusual tRNA has eight base-pairs in the acceptor stem and five in the TψC-stem in bacteria, and nine base-pairs in the acceptor stem and 4 in the TψC-stem in eukaryotes. Canonical tRNAs have 7 base-pairs in the acceptor stem and 5 in the TψC-stem (reviewed in Yoshizawa & Bock, 2009; Yuan et al., 2010). The synthesis of Sec on the unique tRNA^{Sec} is different in Bacteria and Archaea/Eukarya (Figure 1.10) (Lobanov et al., 2006; Yuan et al., 2010). In bacteria, eukaryotes and archaea there is not a selenocysteinyl-tRNA^{Sec} synthetase (SecRS), and for this reason the tRNA^{Sec} is recognized by the canonical SerRS. The first step in Sec biosynthesis, identical in Bacteria, Eukarya and Archaea, involves the serylation of tRNA^{Sec} with serine by SerRS. In bacteria a selenocysteine synthase (SelA) converts the Ser-tRNA^{Sec} into Sec-tRNA^{Sec}, in the presence of selenophosphate as a selenium donor. The Sec-tRNA^{Sec} is then transferred to the ribosome by the elongation factor SelB, when the helical secondary structure present in the mRNAs of selenoproteins is recognized (Ehrenreich et al., 1992). In Archaea and Eukarya the Sec biosynthesis occurs in a two step reaction because there is no analogue of the SelA bacterial enzyme. Ser-tRNA^{Sec} is converted into o-phosphoseryl-tRNA^{Sec} (Sep-tRNA^{Sec}) by O-phosphoseryl-tRNA kinase (PSTK). The PSTK transfers the γ-phosphate of the ATP to the Ser residue linked to tRNA^{Sec} in the presence of magnesium. The resulting Sep-tRNA^{Sec} is then transformed into Sec-tRNA^{Sec} by Sep-tRNA:Sec-tRNA synthase (SepSecS), using selenophosphate as selenium donor (Araiso et al., 2008).

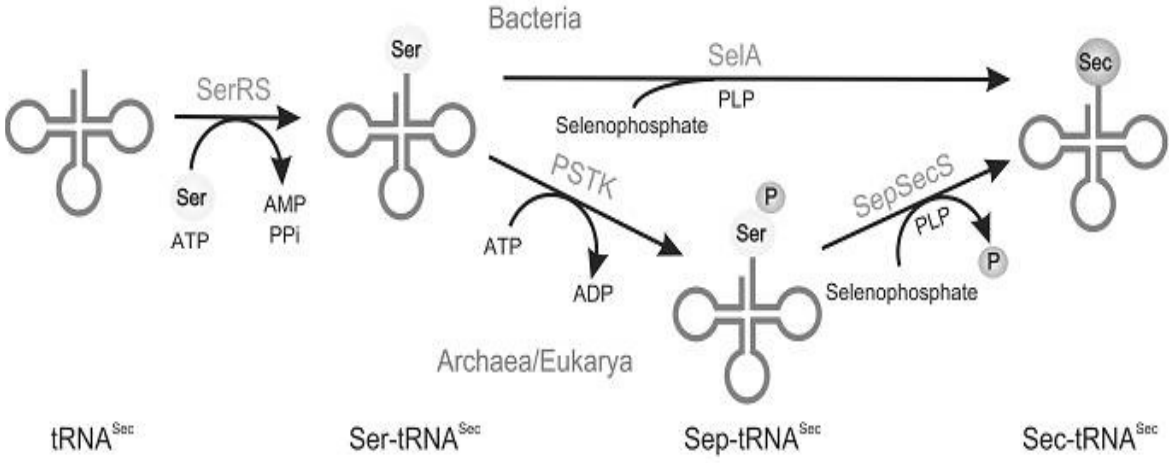

Figure 1.10: Biosynthesis of Sec-tRNA^{Sec}. In all organisms the first step consists in the aminoacylation of tRNA^{Sec} by SerRS to form Ser-tRNA^{Sec}. In bacteria, the Ser bound to the tRNA is converted to Sec by SelA, in the presence of selenophosphate, to form Sec-tRNA^{Sec}. In Eukarya and Archaea the serine loaded on the tRNA^{Sec} is first phosphorylated by PSTK to form Sep-tRNA^{Sec}, which is then converted to Sec-tRNA^{Sec} by SepSecS, in the presence of selenophosphate. Adapted from (Sheppard et al., 2008).

Pyrrolysine (Pyl) was discovered in 2002, and is known as the 22nd amino acid (Hao et al., 2002; Srinivasan et al., 2002). It is a rare amino acid that occurs in methanogenic Archaea. Pyl is a lysine derivate, containing an N$^{\varepsilon}$ linkage to a pyrroline ring. It is incorporated in response to the UAG stop codon and requires a specific tRNA with a CTA anticodon (Blight et al., 2004). The incorporation of Pyl into proteins is not fully understood, but the mechanism seems less complex than that of Sec. In this case, a pyrrolysyl-tRNA synthetase (PylRS) ligates pyrrolysine to the tRNA^{Pyl} (Zhang et al., 2005). This tRNA and its cognate aaRS co-evolved in a distinct way relatively to other tRNA-aaRS systems. The crystal structure of tRNA^{Pyl} demonstrated that tRNA^{Pyl} is different from the canonical tRNAs: the anticodon stem has 6 base-pairs instead of 5, the variable loop only has 3 bases, a single base separates the acceptor and D-stems, the D-loop only has 5 bases, the conserved G18 and G19 residues in the D-loop and the TψC sequence in the TψC-loop are absent, and it contains a small number of post-transcriptional base modifications. These features result in a tRNA with an atypical structure that deviates from the L-shaped structure of all tRNAs (Polycarpo et al., 2004; Yuan et al., 2010). Crystalographic studies suggest that PylRS is very similar to class II synthetases (Kavran et al., 2007).

1.3.3. Mitochondrial and cytoplasmic genetic code alterations

Tables 1.4 and 1.5 summarize the genetic code alterations found in mitochondria and cytoplasm of various organisms.

In mitochondria of yeasts, vertebrates and some invertebrates the Ile AUA codon is decoded as Met, while in the mitochondria of several organisms the UGA stop codon is reassigned to Trp. In the mitochondria of yeast the Leu CUU, CUG, CUA and CUC codons are decoded as Thr (Walker & Weller, 1994) by a new mutant $tRNA_{UAG}^{Thr}$ with an enlarged 8bp anticodon loop that evolved from a $tRNA_{GUG}^{His}$ (Su et al., 2011), while the Lys AAA codon is assigned to Asn in echinoderm (Castresana et al., 1998) and Platyhelminths. In the mitochondria of green plants the UAG stop codon is assigned to both Leu and Ala depending on the specie (Ishimaru et al., 1996; Szymanski & Barciszewski, 2007) (table 1.4).

Table 1.4: Variations in mitochondrial genetic codes. Adapted from (Watanabe & Ueda, 2001).

Organism	UGA Stop	AUA Ile	AAA Lys	AGR Arg	CUN Leu	UAA Stop	UAG Stop	Example
Vertebrates	Trp	Met		Stop				Human, bovine, frog
Tunicates	Trp	Met		Gly				*Halocynthia roretzi*
Echinoderms	Trp		Asn	Ser				Starfish, sea urchin
Arthropods	Trp	Met		Ser				*Drosophila spp.*, mosquito, honeybee
Molluscs	Trp	Met		Ser				Squid, *Mytilus edulis*
Nematodes	Trp	Met		Ser				*Caenorhabditis elegans, Ascaris suum*
Platyhelminths	Trp		Asn	Ser		Tyr		*Fasciola hepatica, planaria*
Coelenterates	Trp	ND	ND		ND	ND		Hydra, *Metridium senile*
Yeasts	Trp	Met			Thr			*S. cerevisiae, Torulopsis glabrata*
Green algae	Trp Trp						Ala Leu	*H. reticulatum* *C. Microporum*
Euascomycetes	Trp							*A. nidulans, N. crassa*
Protozoa	Trp							*Paramecium spp.*

The cytoplasmic genetic code alterations (table 1.5) include reassignment of the nonsense codons UGA and UAR (where R means A or G) to Gln, Cys or Trp, and the assignment of the CUG Leu codon to Ser (Osawa et al., 1992).

Table 1.5: Variations in cytoplasmic genetic codes. Adapted from (Watanabe & Ueda, 2001).

Organism	UGA Stop	UAR Stop	CUN Leu	Example
Mollicutes (Eubacteria)	Trp Trp			*Mycoplasma* *Spiroplasma*
Hemiascomycetes			Ser	*Candida spp.*
Holotrichous ciliates		Gln		*Tetrahymena spp., Paramecium spp.*
Hypotrichous ciliates	 Cys	Gln		*Stylonicia sp., Oxytricha spp.* *Euplotes sp.*
Unicellular green algae		Gln		*Acetabularia spp.*

1.4. The fungal CTG clade genetic code alteration

To date the only sense to sense codon reassignment identified in a nuclear genetic code occurs in species of the so called CTG clade (*C. albicans, C. dubliniensis, C. tropicalis, C. parapsilosis, L. elongisporus, C. guillermondi, D. hansenii, C. lusitaniae*) (Butler & et al, 2009), where the Leu CUG codon was reassigned to Ser through a mutant serine tRNA ($tRNA_{CAG}^{Ser}$). This $tRNA_{CAG}^{Ser}$ is a hybrid molecule containing the body of a $tRNA^{Ser}$ and a Leu 5'-CAG-3' anticodon which can decode the Leu CUG codons. Interestingly, this is the only known tRNA recognized by two aaRS, namely the seryl-tRNA synthetase (SerRS) and the leucyl-tRNA synthetase (LeuRS), which can charge it with Ser and Leu with different efficiencies. Differences in LeuRS and SerRS interaction with this mutant tRNA are responsible for different CUG reassignment status in species expressing the mutant $tRNA_{CAG}^{Ser}$. Previous studies have demonstrated that these differences are related to the tRNA anticodon arm sequence and structure (Ohama et al., 1993; Santos et al., 1993; Suzuki et al., 1994; Suzuki et al., 1997; Tuite & Santos, 1996).

1.4.1. The mutant $tRNA_{CAG}^{Ser}$

As mentioned before the mutant $tRNA_{CAG}^{Ser}$ is the only known tRNA that is recognized by two different aaRSs, indicating that this tRNA has identity elements for both SerRS and LeuRS. Both synthetases recognize class II tRNAs, which are characterized by having long variable arms. In eukaryotes, Leu and Ser tRNAs are the only class-II tRNAs. The SerRS does not recognize the anticodon of Ser tRNAs and interacts mainly with the variable arm and the discriminator base, while the LeuRS recognizes mainly the

A_{35} and m^1G_{37} in the anticodon of Leu tRNAs (Lincecum & Martinis, 2005; Weygand-Durasevic & Cusack, 2005). *In silico* studies suggest that Ser identity elements of the $tRNA_{CAG}^{Ser}$ are the discriminator base (G_{73}) and three GC base pairs located in the variable arm, while the Leu identity elements are the A_{35} and m^1G_{37} bases in the anticodon (Figure 1.11) (Miranda et al., 2006).

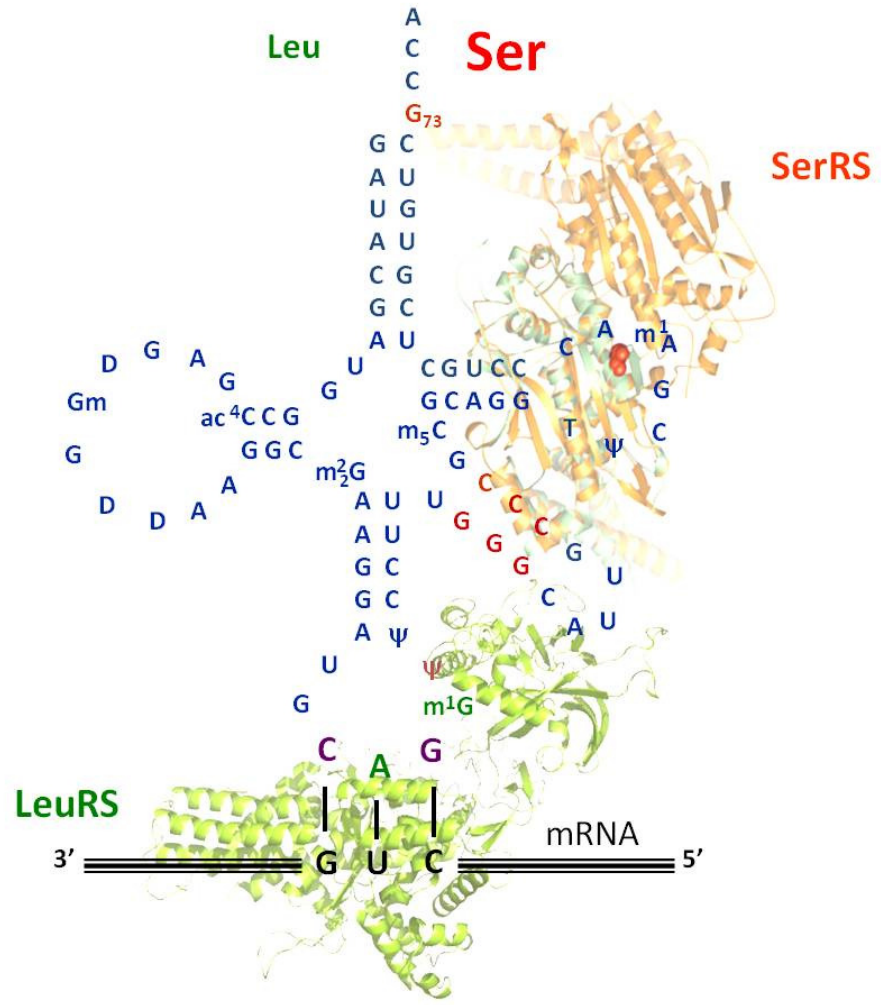

Figure 1.11: Secondary structure of *Candida albicans* $tRNA_{CAG}^{Ser}$. The $tRNA_{CAG}^{Ser}$ is a hybrid molecule with a body of serine tRNAs and an anticodon of leucine tRNAs. This tRNA contains identity elements for the SerRS (G_{73} and 3 GC base pairs of variable arm) and the LeuRS (A_{35} and m^1G_{37}). Adapted and modified from (Miranda et al., 2006).

There is sequence variability between $tRNA_{CAG}^{Ser}$ genes which influence CUG decoding. In most CTG clade species the $tRNA_{CAG}^{Ser}$ contains a methyl group in the nucleotide 37 (m^1G_{37}) and, in the case of *C. albicans* an insertion of ~3% of Leu and

~97% of Ser was measured at CUG codons (Gomes et al., 2007). The *Candida cylindracea* $tRNA_{CAG}^{Ser}$ contains A_{37} and inserts 100% of Ser at CUGs codons. These evidences are sustained by previous studies showing that the m^1G_{37} is directly recognized by the LeuRS (Suzuki et al., 1997). One of the most remarkable structural features of the $tRNA_{CAG}^{Ser}$ is the presence of a guanosine at position 33 (G_{33}) instead of the well conserved uridine (U_{33}) (Ohama et al., 1993; Santos et al., 1993). U_{33} is necessary for the U-turn structure of the anticodon loop and for stacking of the codon-anticodon bases in all tRNAs (Ahsen et al., 1997; Ashraf et al., 1999). The function of G_{33} is apparently linked to its leucylation as it distorts the anticodon-stem and prevents efficient recognition by the LeuRS. In other words, G_{33} is a negative modulator of $tRNA_{CAG}^{Ser}$ leucylation, preventing excessive Leu misincorporation at CUG codons *in vivo* (Figure 1.12) (Suzuki et al., 1997).

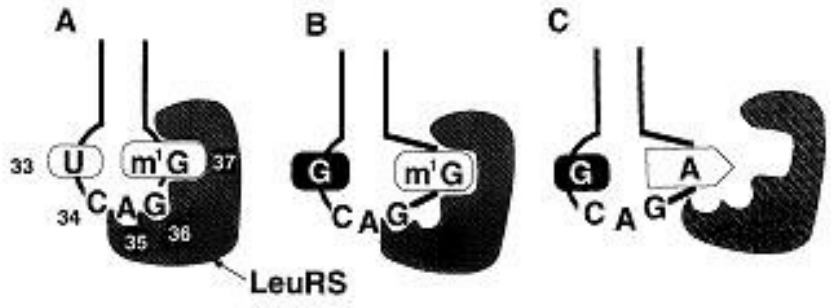

Figure 1.12: Interaction of LeuRS with the anticodon of tRNAs. A) Model of the interaction of LeuRS with the anticodon loop of a standard $tRNA_{CAG}^{Leu}$. B) Interaction of LeuRS with CTG clade $tRNA_{CAG}^{Ser}$. The G_{33} destabilizes the anticodon structure of the tRNA and prevents efficient recognition by LeuRS, while the methyl group of G_{37} (m^1G_{37}) facilitates the recognition of this tRNA by LeuRS. C) Model explaining the inability of the *C.cylindracea* $tRNA_{CAG}^{Ser}$ to interact with its LeuRS. The presence of A_{37} and G_{33} inhibit the leucylation of the tRNA. Adapted from (Suzuki et al., 1997).

1.4.2. Evolutionary mechanism of CUG reassignment in *Candida albicans*

The CUG reassignment from Leu to Ser started 272±25 million years (My) ago, by the mutant $tRNA_{CAG}^{Ser}$. This mutant tRNA originated from a Ser $tRNA_{CGA}^{Ser}$ which underwent several mutations in the anticodon arm that changed its decoding properties. During the initial stages of CUG reassignment, the $tRNA_{CGA}^{Ser}$ competed with the endogenous $tRNA_{CAG}^{Leu}$ for CUG codons, introducing CUG ambiguity in the yeast

ancestor. This ambiguity lasted for over 100 My and erased CUGs from the genome of the fungal ancestor. This lead to deletion of $tRNA_{CAG}^{Leu}$ gene from ancestor genome, but the mutant $tRNA_{CAG}^{Ser}$ was retained in the genome (figure 1.13).

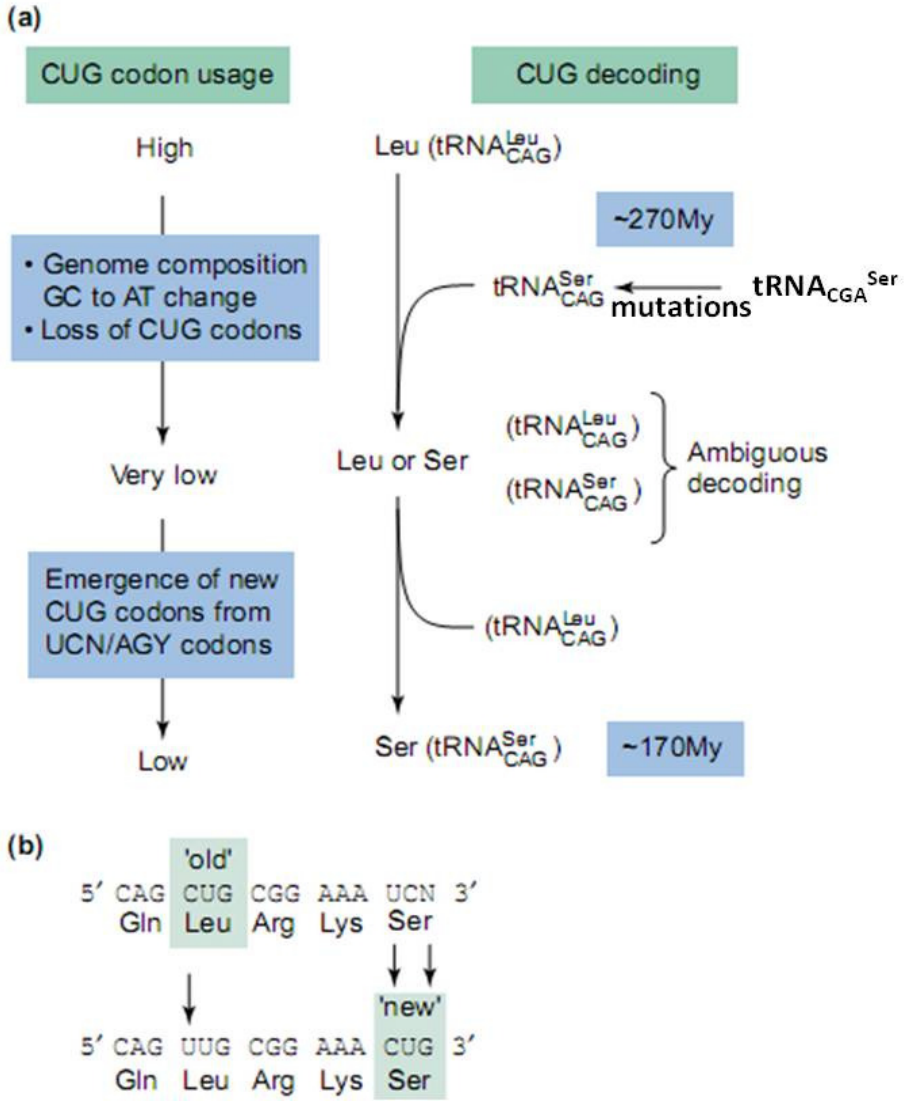

Figure 1.13: The evolutionary mechanism of CUG reassignment in *Candida albicans*. A) Mutation in $tRNA_{CGA}^{Ser}$ (272 My) created the novel $tRNA_{CAG}^{Ser}$. This mutant tRNA competed with the endogenous $tRNA_{CAG}^{Leu}$ for CUG decoding, creating ambiguity in the ancestor's cells. With the disappearance of the $tRNA_{CAG}^{Leu}$ the reassignment of CUG codons from Leu to Ser was accomplished. B) The ambiguity introduced forced the replacement of Leu CUG codons, while the presence of the mutant $tRNA_{CAG}^{Ser}$ created a positive pressure that enable the re-introduction of new CUG codons, by mutation of serine UCN codons. Adapted from (Santos et al., 2004).

The ~26000 CUG codons that exist in the genome of extant *C. albicans* evolved from Ser codons and are mainly located in positions were Ser is conserved in orthologous genes (Massey et al., 2003; Santos et al., 2004).

It is not yet clear how the CUG codon changed identity, but previous studies carried out in our laboratory, which reconstructed the early stages of CUG reassignment in *S. cerevisiae* cells, have shown that CUG ambiguity decreases growth rate, probably due to the synthesis of aberrant proteins that increase proteotoxic stress. This triggers the stress response, which is characterized by increased expression of molecular chaperons and other stress genes. Activation of the stress response creates stress cross protection which is advantageous under environmental stress. This suggests that the disadvantage that resulted from CUG ambiguity could be beneficial for adaption to new ecological niches (Santos et al., 1999).

1.5. General effects of mistranslation

Protein synthesis fidelity is fundamental to maintain cellular homeostasis. To minimize the deleterious effects of errors cells developed quality control mechanisms, namely aaRSs editing, discrimination against misacylated aa-tRNAs by elongation factor and ribosome proofreading. Despite this, protein synthesis errors can occur, leading to incorporation of wrong amino acids and formation of mistranslated proteins. During the last few years a connection between neurodegenerative disorders and mistranslation was uncovered highlighting a role of the latter in human diseases. Studies connecting mutations in the editing domain of aaRS and neurodegenerative disorders have been carried out by the Schimmel's group, which demonstrated that mice expressing a mutant form of alanyl-tRNA synthetase (AlaRS), where the alanine residue 734 is mutated to a glutamate (A734E), have cerebellar Purkinje cell loss and ataxia (Lee et al., 2006). This is a well known conserved residue in the editing domain of AlaRS, which is essential for proofreading activity of the enzyme (Beebe et al., 2003). Cells expressing this mutation have an AlaRS editing efficiency that decreases deacylation of the Ser-tRNA^{Ala}. In other words, these cells accumulate misacylated Ser-tRNA^{Ala} which in turn leads to Ser mistranslation with consequent accumulation of misfolded proteins and apoptotic cell death (Lee et al., 2006). Moreover, inducible expression of an editing-defective ValRS, in cultured NIH/3T3 mouse fibroblast cell line, induces mistranslation due to inability to hydrolyse misacylated Thr-tRNA^{Val}. These cells show disruption of morphology,

membrane blebbing and caspase-3 activation, characteristic events of apoptosis induction. These phenotypes are exacerbated by addition of the non canonical amino acid, similar to Thr, L-a-aminobutyric acid [a-Abu] (Nangle et al., 2006).

A link between ROS induced toxicity and mistranslation has also been observed in *E. coli*. Hydrogen peroxide oxidizes cysteine182, a critical residue for editing activity of threonyl-tRNA synthetase (ThrRS). This increases formation of misacylated Ser-tRNA^{Thr}, which induces protein mistranslation and growth rate reduction (Ling & Soll, 2010). Another study, induced misincorporation of Ser at different codon families in human cells demonstrated that mistranslation activates the unfolded protein response (UPR) and the expression of several miRNA involved in apoptosis induction (Geslain et al., 2009).

Interestingly, mistranslation can be advantageous in unicellular organisms. For example, *C. albicans* which normally decodes CUG codons as Ser (97%) and Leu (3%), can tolerate levels of Leu incorporation up to 28% (Gomes et al., 2007; Miranda et al., 2007). Also, *E. coli* mutants expressing misacylated Cys-tRNA^{Pro}, Ser-tRNA^{Thr}, Glu-tRNA^{Gln} and Asp-tRNA^{Asn} can tolerate 10% of mistranslation without any visible effect on growth rate (Ruan et al., 2008). Moreover, bacteria expressing a defective IleRS, which produces misacylated Val-tRNA^{Ile}, have lower growth rate in normal medium or in medium with high concentrations of Val but, surprisingly, have a growth advantage in Ile limiting conditions (Pezo et al., 2004). A similar study, with *Acinetobacter baylyi*, showed that a mutation in the IleRS confer a growth rate advantage under limited availability of Ile (Bacher et al., 2007). The tolerance and advantage of mistranslation, in some situations, may be associated with protein plasticity, since many positions in a protein molecule, except catalytic active centres, permit amino acid substitutions (Rennell et al., 1991). In line with this, Met-misacylation, in mammalian cells increases up to 10-fold upon exposure to oxidative stress, a mistranslation event which apparently protects cells against oxidative stress (Netzer et al., 2009).

1.6. Principal objectives of this thesis

Alterations to the standard genetic code have been found in various eukaryotes, but the molecular and evolutionary mechanisms mediating these alterations are still unclear. In the CTG clade species a mutant $tRNA_{CAG}^{Ser}$ mediated the reassignment of Leu CUG codons to Ser. *In silico* data suggest that this mutant $tRNA_{CAG}^{Ser}$ appeared through mutations in the anticodon of a $tRNA_{CGA}^{Ser}$ gene, namely an A_{35} insertion and $A_{37}\rightarrow G_{37}$ and $U_{33}\rightarrow G_{33}$ transitions. Moreover, the $tRNA_{CAG}^{Ser}$ contains identity elements for two aaRSs, the SerRS and the LeuRS, which aminoacylate it with Ser and Leu, respectively. Previous studies have also show that the expression of *C. albicans* $tRNA_{CAG}^{Ser}$ in *S. cerevisiae*, which induces Leu-for-Ser misincorporation, produces severe proteome and transcriptome alterations causing growth rate decrease, morphological alterations and genome instability. Besides the negative impact, the Leu-for-Ser misincorporation induced cross resistance to environmental stressors (Santos et al., 1996; Santos et al., 1999; Silva et al., 2007).

This thesis was planned to reconstruct *in vivo* the CTG clade genetic code alteration and to elucidate the consequences of engineering genetic code alterations. The specific objectives of this thesis are to:

1. Characterize the various mutations acquired by the $tRNA_{CGA}^{Ser}$ during evolution of the $tRNA_{CAG}^{Ser}$.
2. Identify the identity elements of the $tRNA_{CAG}^{Ser}$ and clarify its dual identity.
3. Engineer new genetic code alterations in yeast using new codon-to-amino acid assignments.
4. Characterize yeast strains harbouring partial genetic code alterations.

Chapter 2

MOLECULAR RECONSTRUCTION OF THE CTG CLADE GENETIC CODE ALTERATION

2.1. Introduction

The reassignment of Leu CUG codons to Ser in the so called CTG clade, namely *C. albicans, C. dubliniensis, C. tropicalis, C. parapsilosis, L. elongisporus, C. guillermondi, D. hansenii, C. lusitaniae* (Butler & et al, 2009), is mediated by a mutant $tRNA^{Ser}$ with a Leu 5'-CAG-3' anticodon ($tRNA_{CAG}^{Ser}$) (Ohama *et al.*, 1993; Santos *et al.*, 1996; Suzuki *et al.*, 1997). This mutant tRNA appeared 272±25 million years (My) ago in the Saccharomycotina sub-phyla ancestor, before the separation of the *Candida* and *Sacharomyces* genera (Massey et al., 2003). *In silico* studies suggest that this tRNA originated from a serine tRNA ($tRNA_{CGA}^{Ser}$) that decoded the Ser-UCG codon, through the insertion of an adenosine in the middle position of the anticodon (Figure 2.1, step 1). This insertion changed the original 5'-CGA-3' anticodon to 5'-CAG-3', originating an hybrid molecule with a $tRNA^{Ser}$ body and a 5'-CAG-3' Leu anticodon (Massey *et al.*, 2003). The insertion of A_{35} in the anticodon of the $tRNA_{CAG}^{Ser}$ (5'-U_{33}-C_{34}-A_{35}-G_{36}-A_{37}-3') likely disrupted decoding accuracy and efficiency of the mutant $tRNA_{CAG}^{Ser}$ because this base was placed in an incorrect anticodon arm context (Miranda et al., 2006). In order to restore decoding accuracy, an efficiency additional mutations were required, namely $A_{37} \rightarrow G_{37}$ at the 3'-of the CAG anticodon (Figure 2.1, step 2). In most $tRNA_{CAG}^{Ser}$ from the CTG clade species the position 37 is occupied by 1-methyl guanosine (m^1G), but *C. cylindracea* $tRNA_{CAG}^{Ser}$ contains A_{37} and it is unclear how this tRNA decodes CUG codons (Suzuki *et al.*, 1997). Insertion of A_{35} and m^1G_{37} in the $tRNA_{CAG}^{Se}$ permitted its recognition by the leucyl-tRNA synthetase (LeuRS) (Miranda et al., 2006; Soma et al., 1996) and did not perturbe its recognition by the seryl-tRNA-synthetase (SerRS), as this enzyme recognizes three GC base pairs located in the extra arm and the tRNA discriminator base (G_{73}). The interaction of this tRNA with two synthetases, LeuRS and SerRS, created ambiguity during CUG decoding which has been preserved in most species expressing this mutant $tRNA_{CAG}^{Ser}$ (Butler & et al, 2009).

One most remarkable structural feature of the $tRNA_{CAG}^{Ser}$ is the presence of G_{33}, instead of the conserved U_{33} residue, present in most tRNAs. The G_{33} induces a distortion of the $tRNA_{CAG}^{Ser}$ anticodon stem, which prevents efficient recognition of the $tRNA_{CAG}^{Ser}$ by the LeuRS (Perreau et al., 1999; Suzuki et al., 1997). So, the ambiguity of the CUG codon created by LeuRS recognition of $tRNA_{CAG}^{Ser}$ was lowered by the replacement of U_{33} by G_{33} (Figure 2.1, step 3). This lower toxicity of the $tRNA_{CAG}^{Ser}$ due to G_{33} may have allowed CUG reassignment to proceed to near completion (Miranda *et al.*, 2006).

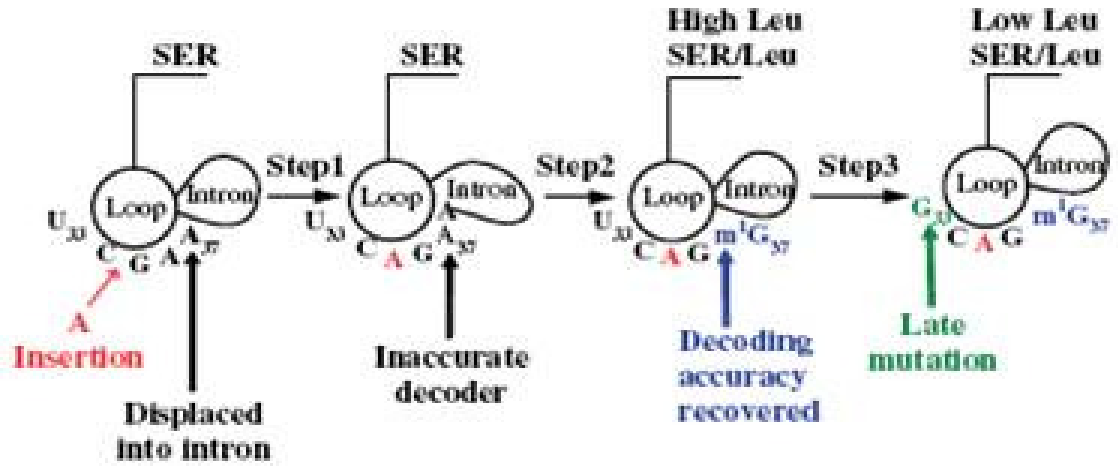

Figure 2.1: Putative evolutionary pathway of *Candida albicans* $tRNA_{CAG}^{Ser}$. *In silico* studies suggest that insertion of an adenosine in the middle position of the anticodon of a $tRNA_{CGA}^{Ser}$ gene transformed the 5'-CGA-3' into a 5'-CAG-3' anticodon (step 1), creating a mutant $tRNA_{CAG}^{Ser}$ capable of decoding Leu CUG codons as Ser. To maintain decoding accuracy two other mutations were introduced, A_{37} was replaced by G_{37} (step 2) and the conserved U_{33} was replaced by G_{33} (step 3). The second mutation permitted the recognition of the $tRNA_{CAG}^{Ser}$ by the LeuRS in addition to its cognate SerRS, which introduced ambiguity at CUG codons, while the third mutation lowered leucylation efficiency of the $tRNA_{CAG}^{Ser}$. Adapted from (Miranda et al., 2006).

In our laboratory the evolutionary reconstruction of the *C. albicans* $tRNA_{CAG}^{Ser}$ pathway has been studied in *S. cerevisiae* using the $tRNA_{CAG}^{Ser}$. These studies focused on the cellular impact of $tRNA_{CAG}^{Ser}$ toxicity in *S. cerevisiae*. Two versions of the *C. albicans* $tRNA_{CAG}^{Ser}$ were investigated in these studies, namely the wild-type tRNA ($tRNA_{CAG}^{Ser}$, G_{33}) and a mutant version containing uridine at position 33 ($tRNA_{CAG}^{Ser}$, U_{33}). As most tRNAs have uridine at position 33 it was postulated that G_{33} played an important role in CUG reassignment. Indeed, *S. cerevisiae* haploid cells could not be transformed with plasmids caring the *C. albicans* $tRNA_{CAG}^{Ser}$ containing U_{33}, suggesting that it is lethal, however yeast transformation with the $tRNA_{CAG}^{Ser}$ G_{33} yielded viable clones, indicating that G_{33} lowers decoding efficiency and consequently the toxicity of the $tRNA_{CAG}^{Ser}$ (Santos et al., 1996). Additional studies showed that yeast spores carrying the $tRNA_{CAG}^{Ser}$ U_{33} had frequent mutations in the $tRNA_{CAG}^{Ser}$ gene, re-inforcing the hypothesis that the $tRNA_{CAG}^{Ser}$ U_{33} was too toxic to the CTG ancestor (Silva et al., 2007). Interestingly, yeast diploid strains tolerate both forms of the $tRNA_{CAG}^{Ser}$ (U_{33} and G_{33}), demonstrating that the $tRNA_{CAG}^{Ser}$ is not lethal in higher ploidy cells. However, growth rate, sporulation and

mating efficiency were affected. More importantly, yeast diploid cells expressing the $tRNA_{CAG}^{Ser}$ were locked in a tetraploide state, with significant alterations in gene expression. For example, molecular chaperons, cell wall, membrane proteins and proteasome activity were up-regulated and cells accumulated glycogen and trehalose (Santos et al., 1996; Silva et al., 2007).

In the present study we extend the previous studies on the molecular evolution of CUG reassignment and we reconstruct *in vivo* the first steps of CUG reassignment following the evolutionary pathway outlined in figure 2.1. We also develop a strategy to identify *in vivo* the identity elements of this mutant tRNA.

In order to achieve those objectives we have expressed the wild-type *C. albicans* $tRNA_{CGA}^{Ser}$ in diploid yeast strains (step 1 Figure 2.1). We then created yeast clones expressing each one of the mutants in the evolutionary pathway outlined in figure 2.1 and evaluated their impact on fitness. Our results demonstrate that the mutant Ser tRNAs are expressed, mistranslate *in vivo* and have a negative impact on growth rate. We demonstrate that CUG reassignment was not lethal and eliminated by natural selection because yeast represses dramatically the expression of mistranslating tRNAs, through yet unknown mechanisms. This repression in the expression of misreading tRNAs allowed for gradual adaptation of CTG clade ancestor to the toxic effects of CUG mistranslation and permitted CUG reassignment, or at least may have prevented its elimination by natural selection.

Our second objective is the identification of the identity elements of the $tRNA_{CAG}^{Ser}$. In most $tRNA^{Ser}$ the SerRS recognizes the long variable arm and the discriminator base G_{73} (Aschel & Gross, 1993; Chimnaronk et al., 2005; Himeno et al., 1997). Indeed, previous bioinformatics studies from our laboratory indicate that *C. albicans* $tRNA_{CAG}^{Ser}$ recognition by SerRS is mediated by the discriminator base (G_{73}) and by 3 GC base pairs present in the extra-arm of the tRNAs, while its recognition by the LeuRS is mediated by m^1G_{37} and A_{35} which are localized in the anticodon loop (figure 1.11) (Miranda *et al.*, 2005 e Suzuki, *et al.*, 1997). In order to confirm these *in silico* predictions we have used an *in vivo* forced evolution methodology (J. Paredes, unpublished), which was based on the integration of the *C. albicans* $tRNA_{CAG}^{Ser}$ U_{33} in diploid yeast cells, which were then sporulated and the spores dissected. As this $tRNA_{CAG}^{Ser}$ U_{33} is lethal in haploid cells, haploid spores that survived were expected to contain mutations in the $tRNA_{CAG}^{Ser}$ gene. Sequencing of the tRNA gene amplified from viable spores confirmed this hypothesis and identified mutations in the $tRNA_{CAG}^{Ser}$ gene. These mutations are mostly located in the

tRNA variable arm and acceptor stem, which contain the identity elements of other Ser tRNAs.

2.2. Material and Methods

2.2.1. Strains and growth conditions

Escherichia coli strains JM109 (e14–(McrA–) *recA1 endA1 gyrA96 thi-1 hsdR17* (r_K– m_K+) *supE44 relA1* Δ(*lac-proAB*) [F´ *traD36 proAB lacI*q*Z*Δ*M15*]) and DH5α (F-φ80*lac*ZΔM15 Δ(*lac*ZYA-*arg*F) U169 *deo*R *rec*A1 *end*A1 *hsd*R17(rk-, mk+) *pho*A *sup*E44 *thi*-1 *gyr*A96 *rel*A1 λ-) were grown at 37ºC in LB broth medium or in LB 2% agar (Formedium) supplemented with ampicilin 50 µg/ml (Sigma-Aldrich). *E. coli* wt and transformed strains were preserved at -80ºC in LB + 20% glycerol.

S. cerevisiae strains used were W303–BMA64 (MATa/MATa; ura3-52/ura3-52; trp1D2/trp1D2; leu2-3_112/leu2-3_112; his3-11/his3-11; ade2-1/ade2-1; can1-100/can1-100), CEN-PK2 (MATa/MATα ura3-52/ura3-52; trp1-289/trp1-289; leu2-3,112/leu2-3,112; his3Δ 1/his3Δ 1; MAL2-8C/MAL2-8C; SUC2/SUC2´), BY4743 (MATa/MATα his3Δ 0/his3Δ 0; leu2Δ /leu2Δ 0; met15Δ 0/MET15; LYS2/lys2Δ 0; ura3Δ 0/ura3Δ 0) and respective BY4743 knockouts for RNY1, XRN1, TRF4, TRF5, MET22, AIR2 and RRP6 (Euroscarf, Germany). All yeast strains were grown at 30ºC in YPD + 2% agar (Formedium) or minimal medium (0.67% yeast nitrogen base without amino acids, 100 µg/ml of each of the required amino acids, 2% glucose, 2% agar) (Formedium). In the case of yeast expressing the integrative tRNA, YPD medium was supplemented with 200 mg/l of geneticin (Formedium). All strains were preserved at -80ºC in YPD/MM + 40% glycerol.

Candida albicans CAI4 strain (ura3D::imm434/ura3::imm434) was grown at 30ºC in YPD medium. This strain was preserved at -80ºC in YPD + 40% glycerol.

2.2.2. Expression of *C. albicans* $tRNA^{Ser}$ in yeast

Oligonucleotides were purchased from IDT (Integrated DNA Technologies, Belgium) and were ressuspended in ultra-pure milliQ water to a final concentration of 100 µM. Oligonucleotide sequences used in this work are described in the tables bellow with respective Tm. List and description of plasmids constructed are described in the tables bellow, and maps of plasmids and respective sequences are described in annexes I.

2.2.2.1. Expression of the *C. albicans* $tRNA_{CGA}^{Ser}$ in yeast

For heterologous expression of the *C. albicans* $tRNA_{CGA}^{Ser}$ gene in yeast, a genomic DNA fragment of 150 bp encoding the *C. albicans* $tRNA_{CGA}^{Ser}$ gene (annexe I), was amplified by PCR using the oligonucleotides oUA2177 and oUA2178 (Table 2.2). PCR reactions were performed with 50 ng of template DNA, 1x Taq DNA polymerase buffer, 2.5 mM $MgCl_2$, 20 pmol of each specific oligonucleotide, 200 µM of each dNTP and 2 units of Taq DNA polymerase (Fermentas) in a final volume of 50 µl. PCR reactions were carried out in a thermal cycler (Eppendorf or BioRad) using a standard program of 95ºC 2 min followed by 30 cycles (95ºC 30 sec, Tm 30 sec, 72ºC 2 min) and a final extension of 72ºC for 5 min. PCR products were purified using QIAquick PCR purification kits (QIAGEN) according to the manufacturer instructions, and 3 µg of product were digested with BamHI and SalI restriction enzymes (Fermentas). The multicopy and single-copy vectors pRS425 and pRS315, respectively, were also digested with BamHI and SalI and dephosporilated with SAP (shrimp alkaline phosphatase) (Promega). Next, the tRNA gene was ligated to 100 ng of dephosphorilated pRS315 and pRS425 using T4 DNA ligase (Fermentas) in appropriate buffer. Ligation efficiency was evaluated using agarose gel electrophoresis. Efficient ligations were transformed in *E. coli* DH5α competent cells according to a transformation protocol already described (Sambrook et al., 2008). Positive clones were selected in LB + ampicilin (50 mg/l). Plasmid DNA was extracted using plasmid mini prep kit (QIAGEN) and sequenced. The plasmid containing the $tRNA_{CGA}^{Ser}$ gene cloned in pRS315 was named pUA211 and the tRNA gene cloned in pRS425 was named pUA212 (table 2.1).

The mutations described in the evolutionary pathway, A_{35} insertion, $A_{37}\rightarrow G_{37}$ transition and $U_{33}\rightarrow G_{33}$ transversion in the $tRNA_{CGA}^{Ser}$ were inserted by site directed

mutagenesis (SDM) in its gene. SDM were performed with 50 ng of plasmid template DNA, 1x Pfu DNA polymerase buffer, 2 mM $MgSO_4$, 20 pmol of each specific oligonucleotide (table 2.2), 200 µM of each dNTP and 2.5 units of Pfu DNA polymerase (Fermentas) in a final volume of 50 µl. PCR reactions were carried out in a thermal cycler (Eppendorf or BioRad) using a standard program of 95ºC 30 sec followed by 18 cycles (95ºC 30 sec, 55ºC 1 min, 68ºC 7 min). SDM products were digested at 37ºC during 2 hours with 20 unit of DpnI (Fermentas) and next transformed in DH5 α competent cells. Plasmids were extracted using minipreparation kits and sequenced.

The pUA211 and pUA212 plasmids were used to insert an adenosine by SDM into the middle position of the anticodon (position 35) of the $tRNA_{CGA}^{Ser}$ gene. This was carried out using the oligonucleotides oUA2105 and oUA2106 (Table 2.2). The resulting plasmids were named pUA213 (A_{35}-pRS315) and pUA214 (A_{35}-pRS425) (table 2.1). $A_{37}\rightarrow G_{37}$ mutation was then inserted into the mutant $tRNA_{CGA}^{Ser}$ by SDM using the plasmids pUA213 and pUA214 and the primers oUA2107 and oUA2108 (Table 2.2). These new plasmids were named pUA215 (A_{35}+G_{37}-pRS315) and pUA216 (A_{35}+G_{37}-pRS425) (table 2.1). The transversion of $U_{33}\rightarrow G_{33}$ was introduced in the $tRNA_{CGA}^{Ser}$ gene containing the A_{35} and G_{37} mutations by SDM of the plasmid pUA215 and pUA216, using the primers oUA2109 and oUA2110 (Table 2.2). The resulting plasmids were named pUA217 (A_{35}+G_{37}+G_{33}-pRS315) and pUA218 (A_{35}+G_{37}+G_{33}-pRS425) (table2.1). The pUA219 and pUA220 plasmids (table 2.1) containing the $G_{73}\rightarrow A_{73}$ mutation, were constructed by mutagenising the pUA217 and pUA218 plasmids, respectively, using oligonucleotides oUA2111 and oUA2112 (table 2.2). The insertion of a U in the intron of the $tRNA_{CGA}^{Ser}$ (A_{35}) gene was carried out by SDM in pUA213 with oligonucleotides oUA2401 and oUA2402 (table 2.2), originating the plasmid pUA241 (table 2.1).

Table 2.1: Description of the plasmids constructed to reconstruct the evolutionary pathway

Name	Description
pUA211	pRS315 plasmid containing one copy of *C. albicans* $tRNA_{CGA}^{Ser}$ cloned into BamHI and SalI restriction sites
pUA212	pRS425 plasmid containing one copy of *C. albicans* $tRNA_{CGA}^{Ser}$ cloned into BamHI and SalI restriction sites
pUA213	Variant of pUA211 with the insertion of A_{35} in the middle of the anticodon of

	$tRNA_{CGA}^{Ser}$ gene
pUA214	Variant of pUA212 with the insertion of A_{35} in the middle of the anticodon of $tRNA_{CGA}^{Ser}$ gene
pUA215	Variant of pUA213 with the mutation $A_{37} \rightarrow G_{37}$ in $tRNA_{CGA}^{Ser}$ (A_{35}) gene, ($tRNA_{CGA}^{Ser}$ with A_{35}+G_{37})
pUA216	Variant of pUA214 with the mutation $A_{37} \rightarrow G_{37}$ in $tRNA_{CGA}^{Ser}$ (A_{35}) gene, ($tRNA_{CGA}^{Ser}$ with A_{35}+G_{37})
pUA217	Variant of pUA215 with the mutation $U_{33} \rightarrow G_{33}$ in $tRNA_{CGA}^{Ser}$ (A_{35}+G_{37}) gene, ($tRNA_{CGA}^{Ser}$ with A_{35}+G_{37}+G_{33})
pUA218	Variant of pUA216 with the mutation $U_{33} \rightarrow G_{33}$ in $tRNA_{CGA}^{Ser}$ (A_{35}+G_{37}) gene, ($tRNA_{CGA}^{Ser}$ with A_{35}+G_{37}+G_{33})
pUA219	Variant of pUA217 with the mutation $G_{73} \rightarrow A_{73}$ in $tRNA_{CGA}^{Ser}$ (A_{35}+G_{37}+G_{33}) gene, ($tRNA_{CGA}^{Ser}$ with A_{35}+G_{37}+G_{33}+A_{73})
pUA220	Variant of pUA218 with the mutation $G_{73} \rightarrow A_{73}$ in $tRNA_{CGA}^{Ser}$ (A_{35}+G_{37}+G_{33}) gene, ($tRNA_{CGA}^{Ser}$ with A_{35}+G_{37}+G_{33}+A_{73})
pUA241	Variant of pUA213 with the insertion of U in position IX of the intron of the $tRNA_{CGA}^{Ser}$ (A_{35}), ($tRNA_{CGA}^{Ser}$ with A_{35}+Uix)

Table 2.2: Oligonucleotides used to construct the plasmids used for the reconstruction of the evolutionary pathway

Oligo	Tm (ºC)	Sequence 5'-3'
Integration of $tRNA_{CGA}^{Ser}$ in pRS315 and pRS425		
oUA2177	60ºC	CGCGTCGACAAATTTGACAGTGTGGCCGAGC
oUA2178	60ºC	CGCGGATCCGTGGGAAAAAAATATTCAAGAAAC
SDM of $tRNA_{CGA}^{Ser}$ for A_{35} insertion		
oUA2105	55ºC	GTTAAGGCGTCTGACTCAGAATCTTATTCGCG
oUA2106	55ºC	CGCGAATAAGATTCTGAGTCAGACGCCTTAAC

SDM of $tRNA_{CGA}^{Ser}$ (A_{35}) for A_{37}→G_{37} transition		
oUA2107	55ºC	GTTAAGGCGTCTGACTCAGGATCTTATTCGCGTTATCAG
oUA2108	55ºC	CTGATAACGCGAATAAGATCCTGAGTCAGACGCCTTAAC
SDM of $tRNA_{CGA}^{Ser}$ (A_{35}+G_{37}) for U_{33}→G_{33} transversion		
oUA2109	55ºC	GTTAAGGCGTCTGACGCAGGATCTTATTCGCGTTATCAG
oUA2110	55ºC	CTGATAACGCGAATAAGA TCCTGCGTCAGACGCCTTAAC
SDM of $tRNA_{CGA}^{Ser}$ (A_{35}+G_{37}+G_{33}) for G_{73}→A_{73} transition		
oUA2111	55ºC	GCGCAGGTTCGAATCCTACTGCTGTCGTCATAAG
oUA2112	55ºC	CTTATGACGACAGCAGTAGGATTCGAACCTGCGC
SDM of $tRNA_{CGA}^{Ser}$ (A_{35}) for U_{IX} insertion in the intron		
oUA2401	55ºC	GACTCAGAATCTTATTCTGCGTTATCAGTTGGGC
oUA2402	55ºC	GCCCAACTGATAACGCAGAATAAGATTCTGAGTC

S. cerevisiae BMA64 cells were transformed using the lithium acetate method (Gietz & Woods, 1994), with the empty plasmids, pRS315 and pRS425, and Wt and mutant $tRNA_{CGA}^{Ser}$ expressed from single-copy and multicopy plasmids. Transformants were selected in minimal medium without leucine. The tRNA gene was amplified from grown clones using PCR and was sequenced using oligonucleotides oUA2177 and oUA2178 (table 2.2).

2.2.2.2. Forced evolution strategy

The *Candida albicans* Ser-$tRNA_{CAG}^{Ser}$ gene fused with the KanMX4 gene was amplified by PCR from the plasmid pUA69 (Silva et al., 2007), using oligonucleotides oUA243 and oUA244 (table 2.3), which contain tails with homology to the Leu2 locus. The KanMX4 was amplified from the plasmid pUA707 (Silva et al., 2007), using the oligonucleotides oUA611 and oUA243 (table 2.3). PCR products were then purified with QIAquick PCR purification kit (QIAGEN) according to the manufacturer protocol. 500 ng of PCR product were transformed, using the lithium acetate method (Gietz & Woods, 1994), in *S. cerevisiae* CEN-PK2. Cells were selected in YPD + geneticin (200 mg/l). The tRNA gene was amplified by PCR directly from colonies, purified and sequenced using oUA219

and oUA222 oligonucleotides (table 2.3). The KanMX4 gene integration was checked by PCR using oligonucleotides oUA622 and oUA623 (table 2.3).

Selected clones containing the $tRNA_{CAG}^{Ser}$ gene integrated into the genome were grown at 30ºC, 180 rpm, overnight in YPD+geneticine and then collected, washed and transferred to sporulation medium (1% potassium acetate, 0.1% yeast extract and 0.05% glucose) at 30ºC, 180 rpm until sporulate. Spores were then treated with zymolyase 20 mg/ml for 10 min at room temperature, digested asci were spread on thin YPD + geneticin plates and dissected with a MSM System Series 300 micromanipulator (Singer). From grown spores, DNA was extracted using the Wizard genomic DNA purification kit (Promega) and $tRNA_{CAG}^{Ser}$ gene was amplified by PCR and sequenced using oUA219 and oUA222 oligonucleotides.

Table 2.3: Oligonucleotides used in the forced evolution strategy

Oligo	Tm (ºC)	Sequence 5'-3'
KanMX4-$tRNA_{CAG}^{Ser}$ integration in the Leu2 locus		
oUA243	59ºC	CTTGACCGCAGTTAACTGTGGGAATACTCAGGTATCGTAAGA TGCAAGAGTTCGCCGGGTTAATTAAGGCGCGC
oUA244	59ºC	GGGGCAGACATTAGAATGGTATATCCTTGAAATATATATATAT ATATTGCTGTAGTTGAAACACCAAACAAAAGATG
$tRNA_{CAG}^{Ser}$ integration confirmation		
oUA219	47ºC	CTCAATCTCGAGCCCACAGATGATTGAC
oUA222	47ºC	AATTTACCGCGGACTAGTTGAAACACC
KanMx4 integration in the Leu2 locus		
oUA611	59ºC	GGGGCAGACATTAGAATGGTATATCCTTGAAATATATATATAT ATATTGCTGGCATGTAATAAAGTCAATCATCTG
KanMX4 integration confirmation		
oUA622	59ºC	CCG GGT TAA TTA AGG CGC GC
oUA623	59ºC	GCA TGT AAT AAA GTC AAT CAT CTG

2.2.2.3. Overexpression of *C. albicans* mutant $tRNA_{CAG}^{Ser}$ in yeast using multicopy plasmids

The mutated versions of the $tRNA_{CAG}^{Ser}$ were cloned into the pRS425 multicopy plasmid (U_{33} and G_{33} versions) (table 2.4), using the strategy described in section 2.2.2.1. For that, mutated tRNA genes obtained through the forced evolution strategy outlined above (section 2.2.2.2) were amplified by PCR using the oligos pUA643 and oUA645 (table 2.5), purified, restricted with BamHI and SalI and ligated into digested plasmid. Plasmid sequences were confirmed by PCR and DNA sequencing. Mutant tRNAs containing G_{33} were obtained by SDM using previous plasmids harbouring $U_{33}\rightarrow G_{33}$ mutation introduced by SDM using the oligos oUA2129 and oUA2130 (table 2.5), except in the case of $C_{41}\rightarrow G_{41}$ and $G_{47}\rightarrow A_{47}$, where the oligos oUA2191 and oUA2192, oUA2131 and oUA2132 (table 2.7) were used. The plasmids contructed were expressed in the diploid *S. cerevisiae* BMA-64.

Table 2.4: Description of the plasmids constructed to express the mutant $tRNA_{CAG}^{Ser}$ from multicopy plasmids

Name	Description
pUA200	pRS425 plasmid containing one copy of *C. albicans* $tRNA_{CAG}^{Ser}$ U_{33} cloned into BamHI and SalI restriction sites
pUA201	Variant of pUA200 with the mutation $C_5\rightarrow U_5$ in tRNA gene
pUA202	Variant of pUA200 with the mutation $G_{73}\rightarrow A_{73}$ in tRNA gene
pUA203	Variant of pUA200 with the mutation $G_1\rightarrow A_1$ in tRNA gene
pUA204	Variant of pUA200 with the mutation $C_{65}\rightarrow A_{65}$ in tRNA gene
pUA205	Variant of pUA200 with the mutation C_{56} deletion in tRNA gene
pUA206	Variant of pUA200 with the mutation $G_{47E}\rightarrow U_{47E}$ in tRNA gene
pUA207	Variant of pUA200 with the mutation $G_{47}\rightarrow A_{47}$ in tRNA gene
pUA208	Variant of pUA200 with the mutation $C_{41}\rightarrow G_{41}$ in tRNA gene

pUA209	Variant of pUA200 with the mutation $C_{47F} \rightarrow U_{47F}$ in tRNA gene
pUA210	Variant of pUA200 with the mutation $C_{47H} \rightarrow A_{47H}$ in tRNA gene
pUA242	pRS425 plasmid containing one copy of *C. albicans* $tRNA_{CAG}^{Ser}$ with G_{33} between BamHI and SalI restriction sites with mutation $G_1 \rightarrow A_1$
pUA243	pRS425 plasmid containing one copy of *C. albicans* $tRNA_{CAG}^{Ser}$ with G_{33} between BamHI and SalI restriction sites with mutation $C_5 \rightarrow U_5$
pUA244	pRS425 plasmid containing one copy of *C. albicans* $tRNA_{CAG}^{Ser}$ with G_{33} between BamHI and SalI restriction sites with mutation $C_{41} \rightarrow G_{41}$
pUA245	pRS425 plasmid containing one copy of *C. albicans* $tRNA_{CAG}^{Ser}$ with G_{33} between BamHI and SalI restriction sites with mutation $G_{47} \rightarrow A_{47}$
pUA246	pRS425 plasmid containing one copy of *C. albicans* $tRNA_{CAG}^{Ser}$ with G_{33} between BamHI and SalI restriction sites with mutation $G_{47E} \rightarrow U_{47E}$
pUA247	pRS425 plasmid containing one copy of *C. albicans* $tRNA_{CAG}^{Ser}$ with G_{33} between BamHI and SalI restriction sites with mutation $C_{47F} \rightarrow U_{47F}$
pUA248	pRS425 plasmid containing one copy of *C. albicans* $tRNA_{CAG}^{Ser}$ with G_{33} between BamHI and SalI restriction sites with mutation $C_{47H} \rightarrow A_{47H}$
pUA249	pRS425 plasmid containing one copy of *C. albicans* $tRNA_{CAG}^{Ser}$ with G_{33} between BamHI and SalI restriction sites with mutation C_{56} deletion
pUA250	pRS425 plasmid containing one copy of *C. albicans* $tRNA_{CAG}^{Ser}$ with G_{33} between BamHI and SalI restriction sites with mutation $C_{65} \rightarrow A_{65}$
pUA251	pRS425 plasmid containing one copy of *C. albicans* $tRNA_{CAG}^{Ser}$ with G_{33} between BamHI and SalI restriction sites with mutation $G_{73} \rightarrow A_{73}$

Table 2.5: Oligonucleotides used to construct the plasmids for expression of the mutant $tRNA_{CAG}^{Ser}$ from multicopy plasmids

Oligo	Tm (ºC)	Sequence 5'-3'
Mutant $tRNA_{CAG}^{Ser}$ integration in pRS425 plasmid		
oUA643	52ºC	ATTACAGTCGACAACACCAAACAAAAGATGC
oUA645	52ºC	AACTTAGGATCCTGATTGACTTTATTACATGC
SDM of U_{33}-G_{33} of mutant $tRNA_{CAG}^{Ser}$ cloned in pRS425		
oUA2129	55ºC	GTTAAGGCGAAGGATGCAGGTTCCTTTGGGC
oUA2130	55ºC	GCCCAAAGGAACCTGCATCCTTCGCCTTAAC

2.2.3. *In vitro* tRNA synthesis

In order to clone Wt *C. albicans* $tRNA_{CGA}^{Ser}$ for *in vitro* transcription 6 oligonucleotides, namely oUA2165, oUA2166, oUA2167, oUA2168, oUA2169, oUA2170 (Table 2.7) were used. Oligonucleotides (400 µM) were phosphorylated with 1x T4 polynucleotide kinase buffer, 100 µM ATP, 8 units of T4 polynucleotide kinase (Takara) in 50 µl reaction at 37ºC 1h. 2 µl of each reaction of phosphorylation of the oligonucleotides were taken and mixed with $MgCl_2$ 200 mM and Tris-Cl 1 mM pH 7.6. Oligonucleotides were heated at 95ºC in a water bath and cooled to room temperature for self annealing. The oligonucleotides annealed were then ligated between HindIII and BamHI restriction sites of plasmid pUC19, previously digested with the same enzymes and dephosphorylated, as explained in section 2.2.2.1, the resulting plasmid was named pUA237 (table 2.6). A_{35} insertion and A_{37} deletion from the tRNA gene were performed by SDM of plasmid pUA237 using the primers oUA2171 and oUA2172 (table 2.7). This produced the plasmid pUA238 (table 2.6). A_{37} was then replaced by G_{37} (using the plasmid pUA238) using the primers oUA2173 and oUA2174 (table 2.7), creating the plasmid pUA239 (table 2.6). The U_{33} was replaced by G_{33} (in plasmid pUA239) using the primers oUA2175 and oUA2176 (table 2.7), creating the plasmid pUA240 (table 2.6).

Mutant $tRNA_{CAG}^{Ser}$ genes for *in vitro* transcription were prepared by SDM using the plasmids pUKC1304 ($tRNA_{CAG}^{Ser}$ G_{33}) and pUKC1302 ($tRNA_{CAG}^{Ser}$ U_{33}) constructed in a previous work (Perreau et al., 1999). Both, pUKC1304 and pUKC1302 contain the $tRNA_{CAG}^{Ser}$ cloned into the plasmid pUC18 for *in vitro* transcription. The primers used for

SDM of pUKC1304 and pUKC1302, to insert mutations in the $tRNA_{CAG}^{Ser}$ (G_{33} and U_{33} version) are listed in table 2.7.

Table 2.6: Description of the plasmids constructed for *in vitro* transcription of the mutant $tRNA^{Ser}$

Name	Description
pUA237	pUC19 containing C. albicans $tRNA_{CGA}^{Ser}$ inserted between BamHI and HindIII for in vitro transcription of tRNA
pUA238	Variant of pUA237 containing the insertion of A_{35} and replacement of A_{37} of tRNA gene sequence, ($tRNA_{CGA}^{Ser}$ with A_{35})
pUA239	Variant of pUA238 containing the mutation $A_{37}\rightarrow G_{37}$ in tRNA gene, ($tRNA_{CGA}^{Ser}$ with A_{35}+G_{37})
pUA240	Variant of pUA239 containing the mutation $U_{33}\rightarrow G_{33}$ in tRNA gene, ($tRNA_{CGA}^{Ser}$ with A_{35}+G_{37}+G_{33})
pUA221	Variant of pUK1302: plasmid containing the $tRNA_{CAG}^{Ser}$ gene with U_{33} for in vitro transcription, plus the mutation $C_{41}\rightarrow A_{41}$ in tRNA gene.
pUA222	Variant of pUK1302: plasmid containing the $tRNA_{CAG}^{Ser}$ gene with U_{33} for in vitro transcription, plus the mutation $C_{5}\rightarrow U_{5}$ in tRNA gene.
pUA223	Variant of pUK1302: plasmid containing the $tRNA_{CAG}^{Ser}$ gene with U_{33} for in vitro transcription, plus the mutation $G_{47}\rightarrow A_{47}$ in tRNA gene.
pUA224	Variant of pUK1302: plasmid containing the $tRNA_{CAG}^{Ser}$ gene with U_{33} for in vitro transcription, plus the mutation $G_{47E}\rightarrow U_{47E}$ in tRNA gene.
pUA225	Variant of pUK1302: plasmid containing the $tRNA_{CAG}^{Ser}$ gene with U_{33} for "in vitro" transcription, plus the mutation $C_{47F}\rightarrow U_{47F}$ in tRNA gene.
pUA226	Variant of pUK1302: plasmid containing the $tRNA_{CAG}^{Ser}$ gene with U_{33} for in vitro transcription, plus the mutation $C_{47H}\rightarrow A_{47H}$ in tRNA gene.
pUA227	Variant of pUK1302: plasmid containing the $tRNA_{CAG}^{Ser}$ gene with U_{33} for in vitro transcription, plus the mutation $C_{65}\rightarrow A_{65}$ in tRNA gene.

pUA228	Variant of pUK1302: plasmid containing the $tRNA_{CAG}^{Ser}$ gene U_{33} for in vitro transcription, plus the mutation $G_{73}\rightarrow A_{73}$ in tRNA gene.
pUA229	Variant of pUK1304: plasmid containing the $tRNA_{CAG}^{Ser}$ gene with G_{33} for in vitro transcription, plus the mutation $C_5\rightarrow U_5$ in tRNA gene.
pUA230	Variant of pUK1304: plasmid containing the $tRNA_{CAG}^{Ser}$ gene with G_{33} for in vitro transcription, plus the mutation $C_{41}\rightarrow G_{41}$ in tRNA gene.
pUA231	Variant of pUK1304: plasmid containing the $tRNA_{CAG}^{Ser}$ gene with G_{33} for in vitro transcription, plus the mutation $G_{47}\rightarrow A_{47}$ in tRNA gene.
pUA232	Variant of pUK1304: plasmid containing the $tRNA_{CAG}^{Ser}$ gene with G_{33} for in vitro transcription, plus the mutation $G_{47E}\rightarrow U_{47E}$ in tRNA gene.
pUA233	Variant of pUK1304: plasmid containing the $tRNA_{CAG}^{Ser}$ gene with G_{33} for in vitro transcription, plus the mutation $C_{47F}\rightarrow U_{47F}$ in tRNA gene.
pUA234	Variant of pUK1304: plasmid containing the $tRNA_{CAG}^{Ser}$ gene with G_{33} for in vitro transcription, plus the mutation $C_{47H}\rightarrow A_{47H}$ in tRNA gene.
pUA235	Variant of pUK1304: plasmid containing the $tRNA_{CAG}^{Ser}$ gene with G_{33} for in vitro transcription, plus the mutation $C_{65}\rightarrow$A in tRNA gene.
pUA236	Variant of pUK1304: plasmid containing the $tRNA_{CAG}^{Ser}$ gene with G_{33} for in vitro transcription, plus the mutation $G_{73}\rightarrow A_{73}$ in tRNA gene.

Table 2.7: Oligonucleotides used to construct the mutant $tRNA^{Ser}$ for *in vitro* transcription

Oligo	Tm (ºC)	Sequence 5'-3'
Cloning of $tRNA_{CGA}^{Ser}$ in pUC19		
oUA2165		AGCTTAATACGACTCACTATAGACAGTGTGGCCGAG-
oUA2166		CGGTTAAGGCGTCTGACTCGAAATCAGTTGGGCTTTG
oUA2167		CCCGCGCA GGTTCGAATCCTGCTGCTGTCGCCAGGG
oUA2168		TTAACCGCTCGGCCACACTGTCTATAGTGAGTCGTATTA
oUA2169		GCGCGGGCAAAGCCCAACTGATTTCGAGTCAGACGCC
oUA2170		GATCCCCTGGCGACAGCAGCAGGATTCGAACCT

SDM of $tRNA_{CGA}^{Ser}$ gene cloned in pUC19 for A_{35} insertion

oUA2171 55ºC CGGTTAAGGCGTCTGACTCAGAATCAGTTGGGCTTTG

oUA2172 55ºC CAAAGCCCAACTGATTCTGAGTCAGACGCCTTAACCG

SDM of $tRNA_{CGA}^{Ser}$ (A_{35}) gene cloned in pUC19 for A_{37}→G_{37} transition

oUA2173 55ºC CGGTTAAGGCGTCTGACTCAGGATCAGTTGGGCTTTG

oUA2174 55ºC CAAAGCCCAACTGATCCTGAGTCAGACGCCTTAACCG

SDM of $tRNA_{CGA}^{Ser}$ (A_{35}+G_{37}) cloned in pUC19 for U_{33}→G_{33} transversion

oUA2175 55ºC CGGTTAAGGCGTCTGACGCAGGATCAGTTGGGCTTTG

oUA2176 55ºC CAAAGCCCAACTGATCCTGCGTCAGACGCCTTAACCG

SDM of pUK1302 and pUK1304 for C_5→U_5 transition

oUA2127 55ºC CTCACTATAGATAUGATGGCCGAGTGG

oUA2128 55ºC CCACTCGGCCATCATATCTATAGTGAG

SDM of pUK1302 for C_{41}→G_{41} transition

oUA2185 55ºC GAAGGATTCAGGTTCGTTTGGGCATTGCC

oUA2186 55ºC GGCAATGCCCAAACGAACCTGAATCCTTC

SDM of pUK1304 for C_{41}→G_{41} transition

oUA2191 55ºC GAAGGATGCAGGTTCGTTTGGGCATTGCC

oUA2192 55ºC GGCAATGCCCAAACGAACCTGCATCCTTC

SDM of pUK1302 for G_{47}→A_{47} transition

oUA2115 55ºC GATTCAGGTTCCTTTGGACATTGCCCGCGCAGG

oUA2116 55ºC CCTGCGCGGGCAATGTCCAAAGGAACCTGAATC

SDM of pUK1304 for G_{47}→A_{47} transition

oUA2131 55ºC GATGCAGGTTCCTTTGGACATTGCCCGCGCAGG

oUA2132 55ºC CCTGCGCGGGCAATGTCCAAAGGAACCTGCATC

SDM of pUK1304 and pUK1302 for G_{47E}→U_{47E} transition

oUA2187 55ºC GTTCCTTTGGGCATTTCCCGCGCAGGTTC

oUA2188 55ºC GAACCTGCGCGGGAAATGCCCAAAGGAAC

SDM of pUK1304 and pUK1302 for C_{47F}→U_{47F} transition

oUA2119 55ºC GGTTCCTTTGGGCATTGTCCGCGCAGGTTCGAACC

oUA2120 55ºC GGTTCGAACCTGCGCGGACAATGCCCAAAGGAACC

SDM of pUK1304 and pUK1302 for C_{47H}→A_{47H} transition

oUA2121	55ºC	CCTTTGGGCATTGCCAGCGCAGGTTCGAACCC
oUA2122	55ºC	GGGTTCGAACCTGCGCTGGCAATGCCCAAAGG
SDM of pUK1304 and pUK1302 for C_{65}→U_{65} transition		
oUA2123	55ºC	CGCAGGTTCGAACCCTGATCGTGTCGCCAGGCC
oUA2124	55ºC	GGCCTGGCGACACGATCAGGGTTCGAACCTGCG
SDM of pUK1304 and pUK1302 for G_{73}→A_{73} transition		
oUA2125	55ºC	CTGCTCGTGTCACCAGGCCC
oUA2126	55ºC	GGGCCTGGTGACACGAGCAG

In vitro transcription using T7 RNA polymerase was performed according to standard protocols (Sampson & Uhlenbeck, 1988), where the *C. albicans* $tRNA^{Ser}$ were transcribed using BstNI-linearized plasmids. Transcripts were fractioned on 8% polyacrilamide-8 M urea gels and were eluted from the gels using a dialysis membrane (Dialysis tubing, high retention seamless cellulose tubing, Sigma), in 0.5x TBE, 150 V, 2 h. Prior to use, tRNAs were refolded by heating at 80ºC followed by gradual reduction of the temperature in presence of 15 mM magnesium chloride/15 mM potassium chloride/100 mM Hepes pH= 7.6.

2.2.4. Aminoacylation assays and thermal stability

Aminoacylation of tRNA was performed at 30ºC in 100 mM HEPES-KOH pH=7.6, 20 µM L-[^{3}H] serine (500 Ci/mol) (*Perkin Elmer*), 15 mM magnesium chloride, 4 mM DTT, 2 mM ATP, 15 mM potassium chloride, 0.1mg/ml BSA, 5 µM tRNA transcripts and 50 nM of purified SerRS (Rocha et al., 2011). Aliquots (13 µl) of the reaction mixture were transferred onto pieces of Whatman 3MM paper which was previously washed with 5% trichloroacetic acid (TCA). [^{3}H]-Amino acid not bound to tRNA was removed by three washes of 10 min in 5% TCA, at room temperature, and one wash of 10 seconds with room temperature ethanol. Radiolabelled aminoacyl-tRNA was then quantified using a liquid scintillation counter (Beckman Coulter).

Determination of thermal stability of mutant *in vitro* synthesized tRNAs was carried out according to the procedure already described (Hao et al., 2004). Approximately 0.5

µM of *in vitro* synthesized and annealed tRNA was prepared in 50 mM HEPES buffer pH 7.6, 15 mM potassium chloride and 15 mM of magnesium chloride. tRNAs were subjected to thermal denaturation from 20 to 95ºC, at a rate of 1ºC/min and UV absorbance was monitored 3 times per minute at 260 nm using a Jasco 630 spectrophotometer.

2.2.5. Growth curves

Yeast cells transformed with Wt and mutant tRNAs were grown at 30ºC, 180 rpm until late stationary phase. Growth curves were obtained by inoculating yeasts to an initial OD_{600} of 0.02 in 100 ml Erlenmeyer flasks. At various time points aliquots of the culture were removed and OD_{600} was measured. Growth rate corresponds to growth of yeast cells in exponential phase and was calculated for cells expressing the mutant tRNA relative to control cells.

2.2.6. β-Galactosidase assays

Yeast cells expressing the empty plasmid (lacking tRNA genes), Wt and mutant tRNAs, either in single-copy or multicopy versions, were co-transformed with the multicopy vector pGL-C1. This vector contains the β-Galactosidase (β-gal) gene under the control of the GPD promoter and is fused with the glutathione S-transferase (GST-β-gal). Yeast cells expressing both vectors were selected on minimal medium lacking Leu and Trp. The resulting double transformants were named Gal-pRS315 (pGL-C1/pRS315), Gal-wt (pGL-C1/pUA211), Gal-A_{35} (pGL-C1/ pUA213), Gal-A_{35}+G_{37} (pGL-C1/pUA215) and Gal-A_{35}+G_{37}+G_{33} (pGL-C1/pUA217). The same double transformation was introduced in yeast expressing the tRNA gene from a multicopy plasmid.

β-gal thermoinactivation was monitored directly in yeast cells as described previously (Burke et al., 2000; Santos et al., 1996). For this, 3.5 ml of exponentially growing yeast cells transformed both with pGL-C1 and each on of the plasmids expressing the mutant tRNAs were harvested, washed and ressuspended in 5.6 ml of Z buffer (60 mM sodium phosphate, 40 mM sodium dihydrogen phosphate, 10 mM potassium chloride, 1 mM magnesium sulfate hepta, 50 mM 2-mercaptoetanol, pH 7.0), 140 µl 0.1% sodium dodecyl sulphate and 350 µl chloroform. Cell suspension was

vortexed for 30s and equally divided into seven o-ring microfuge tubes, which were incubated at 47ºC for different time periods, from T0' up to T15' with intervals of 2.5'. After incubation tubes were placed on ice for 30 min. Cell suspensions were then transferred to 30ºC for 5 min and 200 µl of o-nitrophenyl-β-D-galactopyranoside (ONPG) (*Calbiochem*) were then added to each tube. Reactions were allowed to proceed for 2 min and then stopped by addition of 400 µl of 1 M disodium carbonate. Cell suspensions were centrifuged at 13000 rpm 10 min and OD_{420} was measured. Relative β-Gal thermoinactivation was calculated as the % of variation of β-gal activity at each time point, relative to cells that were not incubated at 47ºC.

β-gal activity was determined as described in (Sambrook et al., 2008) with small modifications. Briefly, 5 ml of yeast cells in mid exponential phase were collected, washed, ressuspended in 250 µl of breaking buffer (100 mM Tris-Cl pH 8, 1 mM DTT and 20% Glycerol) and frozen at -30ºC. To the thawed pellet 12.5 µl of PMSF (40 mM in 100% isopropanol) and 150 µl of glass beads were added. Cells were disrupted with three cycles (5000 rpm 10 sec followed of 2 min on ice) in a Precellys system (Omni international). Cells suspensions were centrifuged at 2300Xg 15 min and 990 µl of Z buffer were added to 10 µl of cell extracts. To the cell extracts previously incubated at 30ºC for 5 min 200 µl of ONPG (4mg/ml in Z buffer) were added and reactions were allowed to proceed until a pale yellow color appeared. Reactions were inactivated with 500 µl of 1 M disodium carbonate and sample OD was measured at 420 nm. Protein concentration of cell extracts was evaluated using the BCA protein quantification kit (Pierce). Activity of β-gal was calculated as follows: Activity= (OD420 X 1.7)/ (protein concentration (mg/ml) X volume extract (ml) X time (min)). β-gal activity of each mutant was calculated relative to the activity of control cells expressing the empty plasmid (Gal-pRS315 or Gal-pRS425).

For quantification of β-gal expression by western blot 10 ml of exponentially growing yeast (OD_{600} 0.8) double transformed with β-gal and tRNA plasmids, were collected and washed with cold PBS 1X. Cells were ressuspended in 300 µl of lysis buffer (50 mM PBS 1x, pH= 7, 1 mM EDTA, 5% Glycerol, 1 mM PMSF) and 200 µl of glass beads. Cells were disrupted in three cycles (5000 rpm 10 sec followed of 2 min on ice) in a Precellys system. Extracts were centrifuged at 600X g for 5 min and total lysates were quantified using the BCA protein quantification kit. About 20 µg of protein extracts were separated on 12% resolving acrylamide gels with 4% stacking gel. Prior to loading of gels,

samples were diluted with 6x sample buffer (30 % glycerol, 10 % SDS, 0.6 M DTT and 0.012 % bromophenol blue in 0.5 M Tris-Cl / 0.4 % SDS, pH 6.8) and were denatured for 5 min at 95ºC. Gels were run for 2 hours at 100-150 V on a Bio-Rad mini-gel system in electrophoresis buffer (25 mM Tris, 192 mM Glycine and 0.2 % SDS). After electrophoresis, gels were stained with Coomassie Blue (0.25 % Brilliant Blue R in 50 % methanol and 10 % acetic acid) for 5 to 10 minutes with slow agitation. After staining, gels were distained for 1 hour in 25 % methanol and 5 % acetic acid with slow agitation and washed overnight in distilled water. For western bloting, electrophoresed proteins were transferred from the acrylamide gels to nitrocellulose membranes (Hybond ECL, *Amersham*), pre-hydrated in TGM buffer (0.025 M Tris, 0.192 M glycine pH= 8.3). Protein transfer was performed using a semi-dry blotter (Bio-Rad) at 0.8 mA/cm^2 of membrane for 20 min. Membranes were washed during 15 min in TBS buffer (0.5M Tris Base, 9% sodium chloride pH= 7.6) and were blocked during 1 hour in blocking solution of TBS-T 1x (10x TBS-Tween 20: 0.5M Tris Base, 9% sodium chloride, 0.5% Tween 20, pH= 7.6) + 3% dry nonfat milk. Incubation was performed overnight at 4ºC in blocking buffer with 1:5000 anti-β-gal rabbit IgG antibody (invitrogen). Membranes were washed 2 times 15 min in TBS-T buffer and blocked during 15 min in blocking solution. Membranes were next incubated for 2 hours with 1:10000 dilution of secondary goat-anti-rabbit antibody (IFRDye680 Li-cor antibody, *Odyssey*) in blocking solution. Finally membranes were washed 3 times for 10 min in TBS-T buffer and were visualized using the Odyssey system (*Li-Cor Biosciences*). Quantification of each band was carried out with photoshop CS3. First the image adjustment was set to invert and then with the lasso tool the gel bands were selected and the mean and pixel intensity were quantified. β-gal expression was calculated in cells expressing the mutant tRNAs relative to control cells expressing the empty plasmid (Gal-pRS315 or Gal-pRS425).

2.2.7. tRNA detection by northern blot analysis

2.2.7.1. RNA preparation

For total RNA extractions 250 ml cultures grown until early stationary phase (OD_{600} of 1.2) or early exponential phase (OD_{600} of 0.4) were harvested and cell pellets were frozen overnight at -80ºC. Cells were ressuspended in 12 ml lysis buffer (10 mM Tris pH 7.5, 10 mM EDTA, 0.5% SDS) and 12 ml of acid phenol chloroform 5:1 pH 4.7 (Sigma),

and heated at 65ºC. Cells suspension was vigorously shaken for 30 seconds and incubated at 65ºC for 1h with agitation every 10 min. The aqueous phase containing RNAs was separated from the phenolic phase by centrifugation at 8000xg for 30 min at 4ºC, and re-extracted with same volume of fresh phenol at 7000xg for 20 min at 4ºC. Aqueous phases were re-extracted with the same volume of Chloroform Isoamyl Alcohol 24:1 (Fluka), by centrifugation at 7000xg for 20 min at 4ºC. RNA was precipitated overnight at -30ºC with 3 volumes of ethanol 100% and 0.1 volumes of 3M sodium acetate pH 5.2. RNAs were harvest by centrifugation at 7000xg for 30 min at 4ºC and ressuspended in 2 ml of 0.1M sodium acetate pH 4.5. tRNAs were isolated on a 50 ml DEAE-cellulose column equilibrated with the RNA ressuspension buffer. Samples were washed with 10 volumes of 0.1 M sodium acetate/0.3 M sodium chloride, and tRNAs were eluted with 2 volumes of 0.1 M sodium acetate/1 M sodium chloride. tRNAs precipitated with 2.5 volumes of ethanol overnight were harvested by centrifugation and finally ressuspended in 10 mM sodium acetate pH 4.5/1 mM EDTA and stored a -80ºC. Deacylated tRNAs were obtained through incubation at 37ºC, 1h in 1M Tris pH 8.0/1M EDTA buffer.

2.2.7.2. Northern blots

For northern blots, 50 µg of total tRNA was fractionated at room temperature in 12-15% polyacrylamide (40% Acril:Bis) gels containing 8 M urea (30 cm long, 0.8 mm thick), buffered with 1x TBE pH 8.0. The gels were electrophoresed at 550 V for 15 hours. Fractionated tRNAs were stained with ethidium bromide, visualized by UV shadowing and the portion of the gel containing the tRNAs was transferred to nitrocellulose membranes (Hybond N, Amersham) using a Semy-Dry Trans Blot (Bio-Rad). This transfer was performed using a semi-dry blotter (Bio-Rad) at 0.8 mA/cm^2 of membrane for 35-45 min. Membranes were pre-hybridized at 55ºC during 2h in hybridization solution containing 6x SSPE (20x SSPE = 3M sodium chloride, 0.2M sodium phosphate, 0.02M NA_2EDTA)/5x Denhardt's solution (50x Denhardt's solution = 0.02% bovine, serum albumin, 0.02% polyvinylpyrrolidone and 0.02% Ficoll) and 0.05% sodium dodecyl sulfate. Probes were prepared using 10 pmol of dephosphorilated oligonucleotide and 4 µl of γ-^{32}P-ATP (5000Ci/mmol) (*Perkin Elmer*) in 1x T4 kinase buffer, 10 mM spermidine and 16 units of T4 kinase (Takara). Phosphorylation reactions were incubated for 1h at 37ºC and

extracted with 100 µl phenol:chlorophom:isolamyl alcohol (PCIA). Membrane hybridization was performed overnight in 10 ml of hybridization solution with 50 µl of PCIA extracted ɣ-^{32}P-ATP labeled probe (Y. Espanõl, unpublished). Membranes were washed 4 times for 3 min each time at hybridization temperature, in 2x SSPE/0.5% sodium dodecyl sulfate, wrapped in saran wrap and exposed 24 hours to a K-screen and visualized using a Molecular Imager FX (*Biorad*).

In order to determine whether tRNAs were aminoacylated 200 µg of total tRNA were resuspended in 100 µl of Tris 1 M pH 8.0/1 mM EDTA and were incubated at 37°C for 1 h, followed by overnight precipitation and were finally resuspended in 20 µl of 10 mM sodium acetate pH 4.5/1 mM EDTA and stored at -20°C. Acid denaturing polyacryamide gels were prepared with 6.5% polyacrylamide (40% Acril:Bis) and 8M urea buffered with 0.1M sodium acetate (pH=4.5). 50 µg of total tRNAs acylated and deacylated, obtained previously, were fractioned on the acid denaturing polyacrylamide gels in 10 mM sodium acetate (pH= 4.5) buffer at 4ºC, 36 h at 250 V (Santos et al., 1996). Fractionated tRNAs were stained with ethidium bromide, visualized by UV shadowing and the portion of the gel containing the tRNAs was transferred onto nitrocellulose membranes (Hybond N, Amersham) using a Semy-Dry Trans Blot (Bio-Rad) at 0.8 mA/cm^2 of membrane for 35-45 min. Northern blot was performed as described above. All probes used for northern blot analysis are listed in table 2.8.

Table 2.8: Oligonucleotides used for northern blot analysis

Oligo	Tm (ºC)	Sequence 5'-3'
$tRNA_{CCC}^{Gly}$ detection by northern blot		
oUA2195	52-55ºC	GCGGAAGCCGGGAATCGAAC
$tRNA_{CAG}^{Ser}$ detection by northern blot		
oUA2193	55ºC	GCGACACGAGCAGGGTTC
$tRNA_{CGA}^{Ser}$ detection by northern blot		
oUA2194	55ºC	GCGACAGCAGCAGGATTCG
oUA2196	60ºC	GCCCAACTGATTTCGAGTCAG
oUA2197	60ºC	GCCCAACTGATTCTGAGTCAG
oUA2198	62ºC	GCCCAACTGATTTCTGAGTCAG

2.3. Results

2.3.1. Reconstruction of the CUG reassignment pathway in yeast

In silico studies suggested that the $tRNA_{CAG}^{Ser}$ is derived from an intron-containing $tRNA^{Ser}$, namely the $tRNA_{CGA}^{Ser}$, which underwent important alterations, in particular in the anticodon arm, since it appeared at 272±25 MY ago (Massey *et al.*, 2003; Ohama *et al.*, 1993; Suzuki *et al.*, 1994) (figure 2.2).

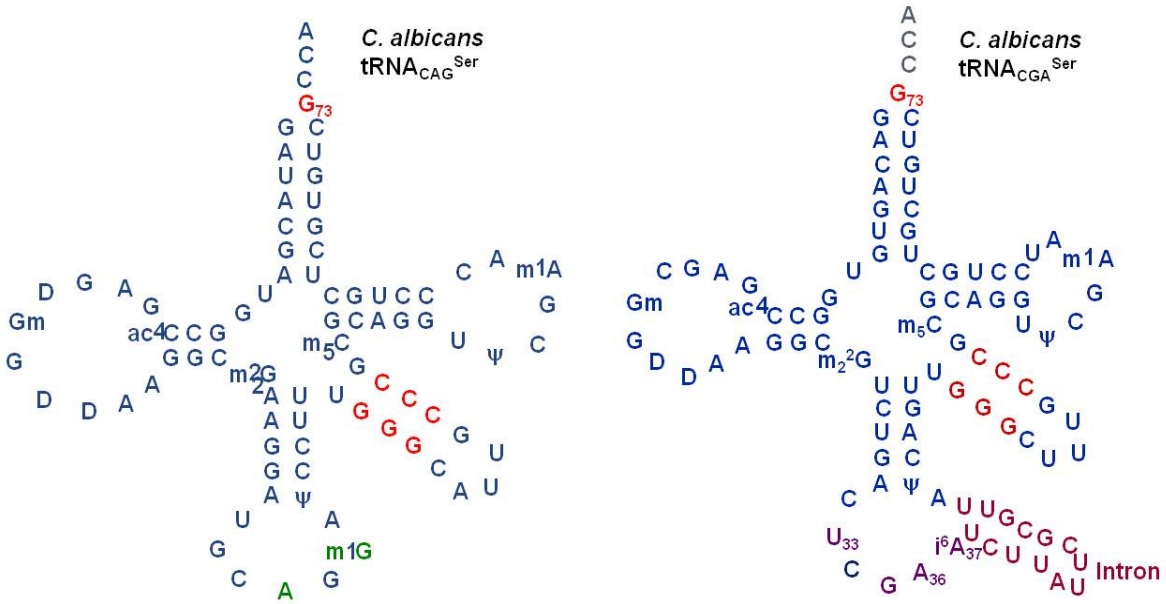

Figure 2.2: Comparison of the *C. albicans* $tRNA_{CAG}^{Ser}$ and $tRNA_{CGA}^{Ser}$. *In silico* studies suggest that the 3 GC base pairs in the extra-arm and the discriminator base (G_{73}), shown in red are the identity elements for SerRS in both tRNAs, while A_{35} and G_{37} of the $tRNA_{CAG}^{Ser}$ (shown in green) are the bases recognized directly by the LeuRS in $tRNA_{CAG}^{Ser}$. The nucleotides in purple in $tRNA_{CGA}^{Ser}$ are those that were mutated to reconstruct the evolutionary pathway.

In order to confirm that mutations in the anticodon loop did not destabilize or inhibit serylation of our model $tRNA_{CGA}^{Ser}$, we have aminoacylated *in vitro* synthesized tRNAs using purified recombinant SerRS from *Candida albicans.* For this, we have cloned the wild type sequence of the $tRNA_{CGA}^{Ser}$, without the intron, between BamHI-HindIII restriction sites of the pUC19 plasmid (pUA237) (section 2.2.3). The T7 phage promoter sequence was inserted immediately upstream of the $tRNA_{CGA}^{Ser}$ gene. Then, the three

mutant tRNAs proposed as intermediates for the evolutionary pathway of CUG reassignment were constructed by site directed mutagenesis (SDM) (figure 2.3), as explained in section 2.2.3. Briefly, two mutations were introduced in pUA237 to create pUA238 ($tRNA_{CGA}^{Ser}+A_{35}$), namely the A_{35} insertion in the middle position of the anticodon of the tRNA gene and deletion of A_{37} which was necessary to maintain the anticodon loop size (figure 2.3 A). Then, the $A_{37}\rightarrow G_{37}$ mutation was inserted by SDM in pUA238, originating pUA239 ($tRNA_{CGA}^{Ser}+A_{35}+G_{37}$) (figure 2.3 B). Finally, the $U_{33}\rightarrow G_{33}$ transversion was created in pUA239 originating the plasmid pUA240 ($tRNA_{CGA}^{Ser}+A_{35}+G_{37}+G_{33}$) (figure 2.3 C).

The aminoacylation of mutant and wt $tRNA_{CGA}^{Ser}$ (figure 2.4) showed similar kinetics confirming that mutations in the anticodon loop of $tRNA_{CGA}^{Ser}$ did not affect serylation. Previous data showed that the anticodon loop of nuclear encoded $tRNA^{Ser}$ from methanogenic archaea (Korencic et al., 2004), bacteria (Normanly et al., 1992), yeasts (Gruic-sovulj et al., 2002; Himeno et al., 1997; Lenhard et al., 1999; Soma et al., 1996), humans (Achsel & Gross, 1993; Breitchopf & Gross, 1994; Wu & Gross, 1993) and mammalian mitochondrial $tRNA^{Ser}$ (Chimnaronk et al., 2005) are not recognized by the respective SerRSs, supporting our data. This allowed us to reconstruct the CUG reassignment pathway *in vivo*.

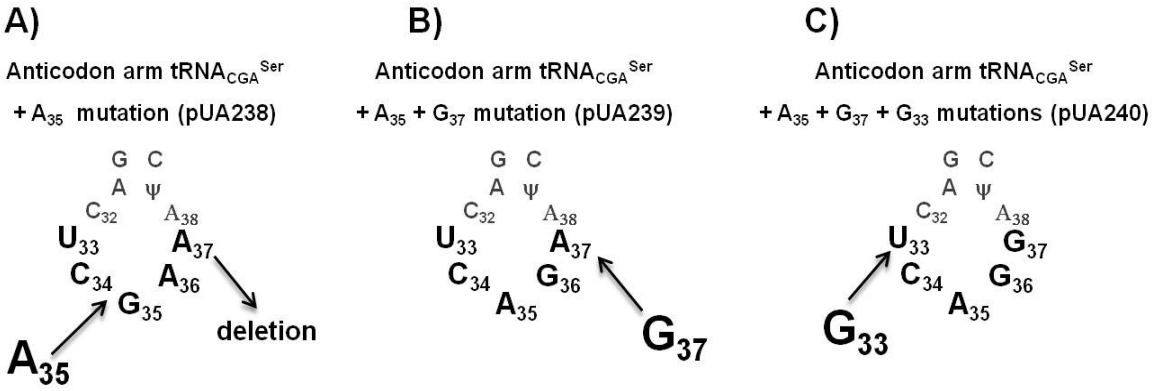

Figure 2.3: Mutant $tRNA_{CGA}^{Ser}$ constructed for tRNA *in vitro* transcription. The CUG reassignment pathway was reconstructed by introducing a series of mutations in the *C. albicans* $tRNA_{CGA}^{Ser}$ gene cloned in pUC19 (pUA237), namely A_{35} insertion and A_{37} deletion by SDM, originating the plasmid pUA238 ($tRNA_{CGA}^{Ser}+A_{35}$) (A). In pUA238, the $A_{37}\rightarrow G_{37}$ transition was introduced by SDM creating the plasmid pUA239 ($tRNA_{CGA}^{Ser}+A_{35}+G_{37}$) (B). Finally, in pUA239 was inserted the $U_{33}\rightarrow G_{33}$ transversion, creating the plasmid pUA240 ($tRNA_{CGA}^{Ser}+A_{35}+G_{37}+G_{33}$) (C).

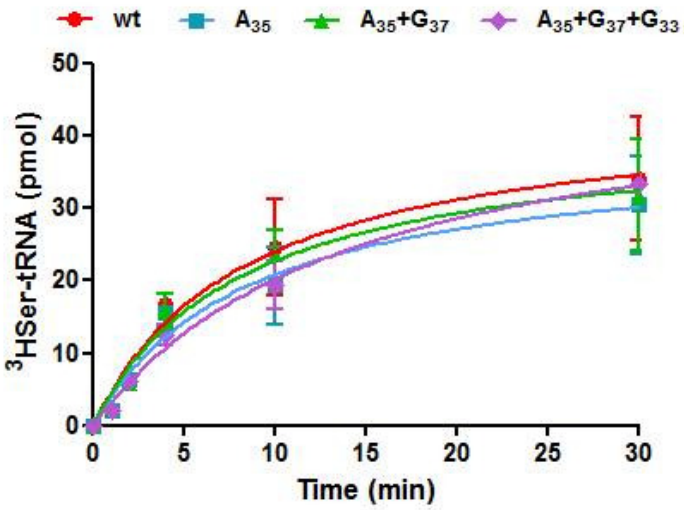

Figure 2.4: Mutations in the anticodon loop of the $tRNA_{CAG}^{Ser}$ do not affect serylation. *In vitro* aminoacylation assays were carried out with *in vitro* synthesized wild-type (Wt) and mutant $tRNA_{CGA}^{Ser}$, mutations are indicated as A_{35} ($tRNA_{CGA}^{Ser}$+A_{35}), A_{35}+G_{37} ($tRNA_{CGA}^{Ser}$+A_{35}+G_{37}) and A_{35}+G_{37}+G_{33} ($tRNA_{CGA}^{Ser}$+A_{35}+G_{37}+G_{33}). Aminoacylation reactions were carried out using purified *C. albicans* SerRS overexpressed in *E. coli* (section 2.2.4). Data represent the mean ± s.e.m. of 3 independent experiments.

In order to reconstruct *in vivo* the evolutionary pathway of the *C. albicans* CUG reassignment we have expressed the Wt $tRNA_{CGA}^{Ser}$ and its mutant versions in *S. cerevisiae* BMA-64 strain. For this the *C. albicans* $tRNA_{CGA}^{Ser}$ gene was cloned into the single copy vector pRS315 originating the plasmid pUA211 (Wt). Then, A_{35} was inserted in the middle position of the anticodon of the $tRNA_{CGA}^{Ser}$ gene (figure 2.5 A), changing the 5'-CGA-3' anticodon into the 5'-CAG-3' anticodon creating the plasmid pUA213 ($tRNA_{CGA}^{Ser}$+A_{35}). The *in silico* reconstruction of the evolutionary pathway suggested that A_{37} was displaced into the intron by the A_{35} insertion, maintaining the correct tRNA anticodon loop structure (figure 2.5 B). Then, A_{37} was replaced by G_{37} (figure 2.5 B), originating the plasmid pUA215 ($tRNA_{CGA}^{Ser}$+A_{35}+G_{37}). The last mutation was the U_{33}→G_{33} transversion (figure 2.5 C) which originated the plasmid pUA217 ($tRNA_{CGA}^{Ser}$+A_{35}+G_{37}+G_{33}). These mutations created the 5'-CAG-3' anticodon of the $tRNA_{CAG}^{Ser}$ (figure 2.5 D).

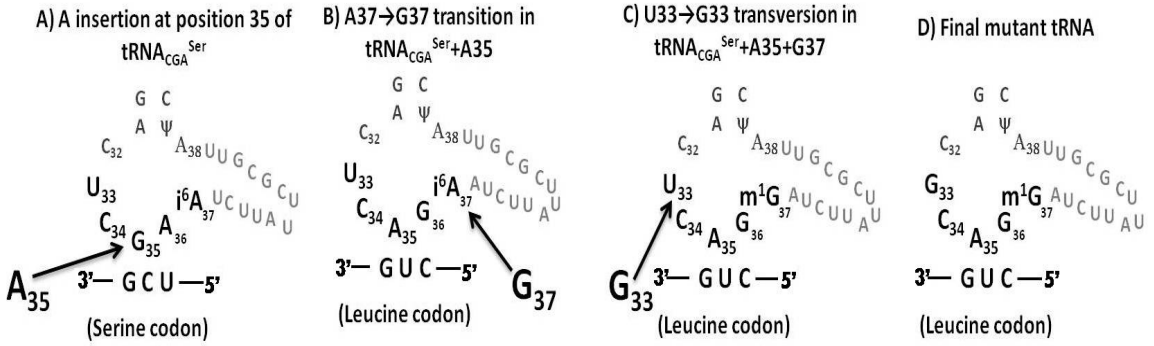

Figure 2.5: Evolutionary pathway of the CTG clade tRNA$_{CAG}^{Ser}$. In order to reconstruct the evolutionary pathway of the CUG reassignment the Wt tRNA$_{CGA}^{Ser}$ gene was mutagenised in a stepwise manner in order to recreate the intermediate steps of the evolution of the tRNA$_{CAG}^{Ser}$. Firstly, an adenosine was inserted in the middle position of the anticodon (A_{35}) (A). The A_{35} insertion changed the 5'-CGA-3' anticodon to the 5'-CAG-3' anticodon. Then, A_{37} was replaced by G_{37} generating the tRNA$_{CGA}^{Ser}$+A_{35}+G_{37} (B). Finally, U_{33} was replaced by G_{33} (C) creating the triple mutant tRNA$_{CGA}^{Ser}$+A_{35}+G_{37}+G_{33} (D).

Yeast expressing the Wt *C. albicans* tRNA$_{CGA}^{Ser}$ (Wt) showed identical growth rate to that of control (pRS315) cells (figure 2.6 A and B). This was expected because this tRNA decodes UCG Ser codons in a canonical way as Ser. Conversely, expression of the mutant versions of the tRNA$_{CGA}^{Ser}$ had a significant negative impact on yeast growth rate (Figure 2.5 A and B), suggesting that they are inserting Ser at CUG codons. In other words, they are expressed and are functional. The tRNA$_{CGA}^{Ser}$+A_{35}+G_{37}+G_{33} was the most toxic tRNA followed by tRNA$_{CGA}^{Ser}$+A_{35}, while the least toxic tRNA was the tRNA$_{CGA}^{Ser}$+A_{35}+G_{37} mutant. Indeed, the growth rate decrease for the tRNA$_{CGA}^{Ser}$+A_{35} and tRNA$_{CGA}^{Ser}$+A_{35}+G_{37}+G_{33} mutants was ≈30% and ≈46%, respectively, while the tRNA$_{CGA}^{Ser}$+A_{35}+G_{37} mutant reduced it by ≈23% relative to control pRS315 cells. The lower toxicity of the latter may be explained by the fact that G_{37} is an identity element of the LeuRS (Suzuki et al., 1997) and, consequently, the mutant tRNA$_{CGA}^{Ser}$ was likely charged with both Ser and Leu. In other words, two isoforms of the mutant tRNA$_{CGA}^{Ser}$ existed in those cells, namely the Ser-tRNA$_{CGA}^{Ser}$, which is toxic due to Ser insertion at CUGs, and the Leu-tRNA$_{CGA}^{Ser}$ which is not toxic because it inserts Leu at CUGs (Miranda *et al.*, 2006). The higher toxicity of the tRNA$_{CGA}^{Ser}$+A_{35}+G_{37}+G_{33} mutant likely resulted from a distortion of the anticodon stem of the RNA helix, created by the U_{33}→G_{33} transversion, which decreases tRNA leucylation (Miranda et al., 2006; Perreau et al., 1999; Suzuki et

al., 1997). The $tRNA_{CGA}^{Ser}$+A_{35} mutant is likely an inefficient tRNA decoder, because its anticodon context, i.e., bases around the 5'-CAG-3' anticodon, is typical of Ser anticodons rather than Leu anticodons. In particular, this tRNA has A_{37} which does not exist in tRNAs containing the 5'-CAG-3' anticodon (Miranda *et al.*, 2006).

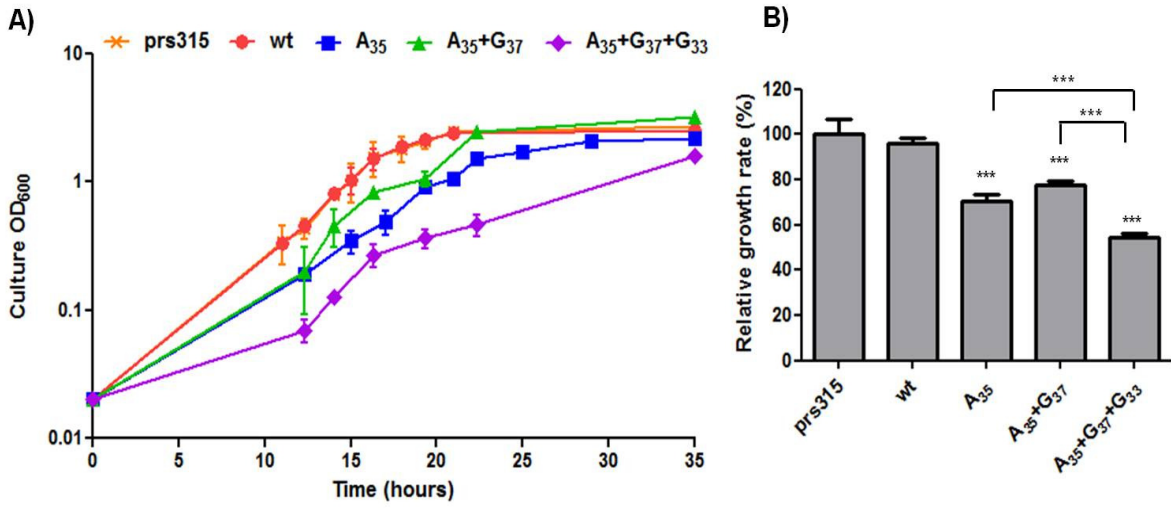

Figure 2.6: CUG reassignment has a strong negative impact on yeast growth rate. A) Growth of yeast cells transformed with the Wt and mutant *C. albicans* $tRNA_{CGA}^{Ser}$, which represent critical intermediate steps of the CUG reassignment pathway. Yeast cultures were inoculated at an initial OD_{600} of 0.02 and were grown in selective medium at 30ºC, 180rpm, until they reached stationary phase. B) The relative growth rate of cells transformed with Wt and mutant serine $tRNA_{CGA}^{Ser}$ was determined using exponential growth phase values, relative to the control cells. Data represent the mean ± s.e.m. of duplicates of 3 independent clones. (***p < 0.001 one-way Anova post Bonferroni's multiple comparison test with CI 95%, relative to pRS315).

2.3.2. Decoding efficiency of the mutant $tRNA_{CGA}^{Ser}$

In order to quantify CUG decoding efficiency of each mutant $tRNA_{CGA}^{Ser}$ and confirm that the growth inhibition observed was caused by Ser CUG decoding and not by other secondary effects, we have used a β-galactosidase (β-gal) thermostability assay developed previously (Santos *et al.*, 1996) to monitor Ser misincorporation at CUGs. Sense codon misreading affects the thermostability of β-gal and the rate of thermoinactivation gives a relative measure of amino acid misincorporation. Since the *E. coli* β-gal gene contains 54 CUG codons, misincorporation of Ser at these positions

reduces β-gal thermostability and its thermoinactivation rate allows for measuring mistranslation *in vivo* (Santos et al., 1996). For this, yeast cells transformed with the mutant $tRNA^{Ser}$ were co-transformed with the pGL-C1 plasmid, which allows for expression of chimeric glutathione S-transferase β-gal reporter genes (GST-β-gal). β-gal thermoinactivation profiles were determined directly in yeast cells by denaturing the protein at 47ºC for up to 15 min (see section 2.2.6). The percentage of β-gal activity at each time point was determined relatively to non denatured protein for each strain. Our results show that β-gal synthesized in presence of the Wt $tRNA_{CGA}^{Ser}$ (Gal-wt) and in control cells (Gal-pRS315) had similar thermostability (figure 2.7 A). But, β-gal synthesized in presence of mutant Ser tRNAs, $tRNA_{CGA}^{Ser}+A_{35}$ (Gal-A_{35}), $tRNA_{CGA}^{Ser}+A_{35}+G_{37}$ (Gal-$A_{35}+G_{37}$) and $tRNA_{CGA}^{Ser}+A_{35}+G_{37}+G_{33}$ ($A_{35}+G_{37}+G_{33}$), was less stable than that produced in the control non-mistranslating cells.

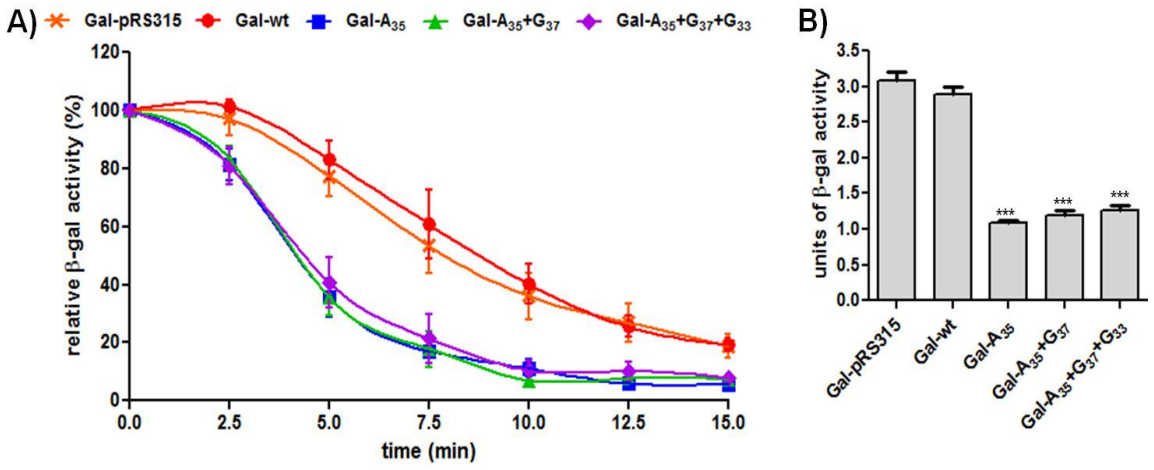

Figure 2.7: Mutant $tRNA_{CGA}^{Ser}$ decreases β-galactosidase stability in yeast. A) *E. coli* β-gal was co-expressed with Wt and mutant $tRNA_{CGA}^{Ser}$ in yeast cells. β-gal themoinactivation profiles were determined by measuring its activity after incubating cells at 47ºC, to denature the protein. The β-gal activity that remained functional after thermal inactivation was determined by incubating cells at 30ºC for 2 minutes with ONPG. β-gal activity at each time point corresponds to the % of activity relative to total activity measured in cells prior to denaturation (section 2.2.6). Data represent the mean ± s.e.m. of triplicates of 3 independent clones. B) β-gal activity was quantified after incubating total cell protein extracts at 30ºC with ONPG until a pale yellow colour appeared. Reactions were stopped with addition of 1M sodium carbonate. Data represent the mean ± s.e.m. of triplicates of 3 independent clones. (***$p < 0.001$ for one-way Anova post Bonferroni's multiple comparison test with CI 95%, relative to pRS315).

The thermostability was similar for the three mutant $tRNA_{CGA}^{Ser}$ at each time point. Total β-gal activity (non-denatured) was also similar in cells expressing the three $tRNA_{CGA}^{Ser}$ mutants and was lower than that of the control cells (Figure 2.7 B), suggesting that Ser insertion at CUG positions destabilizes the protein. In order to further clarify the misreading phenotype, total protein extracts were prepared from the transformed cells (see section 2.2.6), fractionated on SDS-PAGE and the β-gal reporter was quantified by Western blot (Figure 2.8 A). The cellular concentration of β-gal was reduced in cells transformed with the mutant tRNAs relatively to the control cells (Gal-pRS315). This reduction was approximately 40% for the $tRNA_{CGA}^{Ser}+A_{35}$ mutant and 50% for the $tRNA_{CGA}^{Ser}+A_{35}+G_{37}$ and $tRNA_{CGA}^{Ser}+A_{35}+G_{37}+G_{33}$ mutants. Therefore, Ser misincorporation at Leu CUG positions reduced both the β-gal thermostability and its cellular concentration confirming that the mutant tRNAs were fully functional.

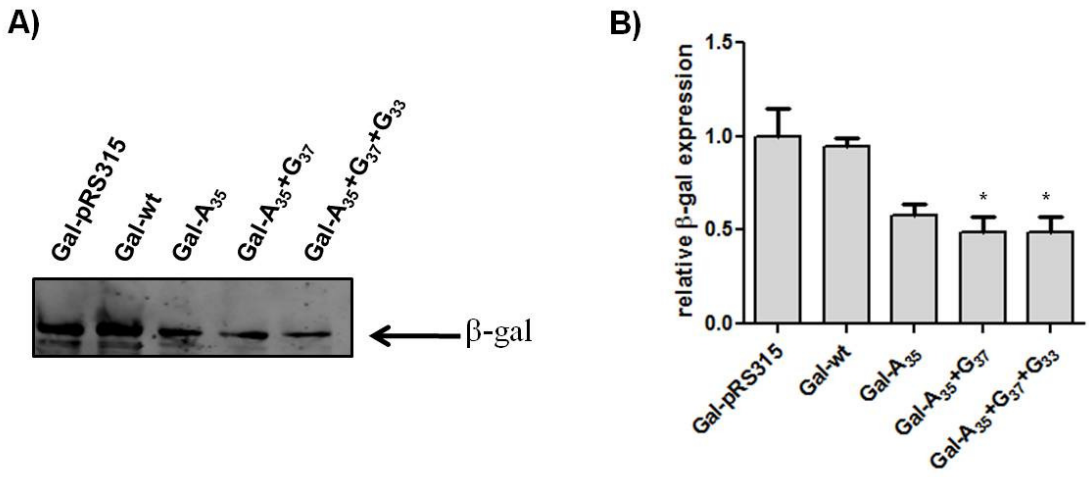

Figure 2.8: Mutant $tRNA_{CGA}^{Ser}$ decreases total β-galactosidase abundance in yeast. A) β-gal expression was quantified by western blot using an anti-β-gal rabbit IgG antibody and a secondary goat-anti-rabbit antibody (section 2.2.6). B) Relative β-gal expression was quantified for each mutant tRNA relative to control cells. Data represent the mean ± s.e.m. of duplicates of three independent clones. (*$p < 0.05$ for one-way Anova post Bonferroni's multiple comparison test with CI 95% relative to pRS315).

2.3.3. Expression and stability of the mutant $tRNA_{CGA}^{Ser}$

The tRNA decoding efficiency results from a combination of tRNA stability, expression level, aminoacylation kinetics and ribosome binding efficiency. In order to

determine whether these parameters were affected by the mutations introduced in the $tRNA_{CGA}^{Ser}$, northern blot analysis was performed, as described previously (Santos *et al.*, 1996). For this, tRNAs were extracted and purified from early stationary phase yeast cells and were fractionated on denaturing 15% poliacrylamyde gels containing 8M urea (section 2.2.7). The Wt $tRNA_{CGA}^{Ser}$ showed high level of expression, but the abundance of the mutant tRNAs was significantly reduced (figure 2.9).

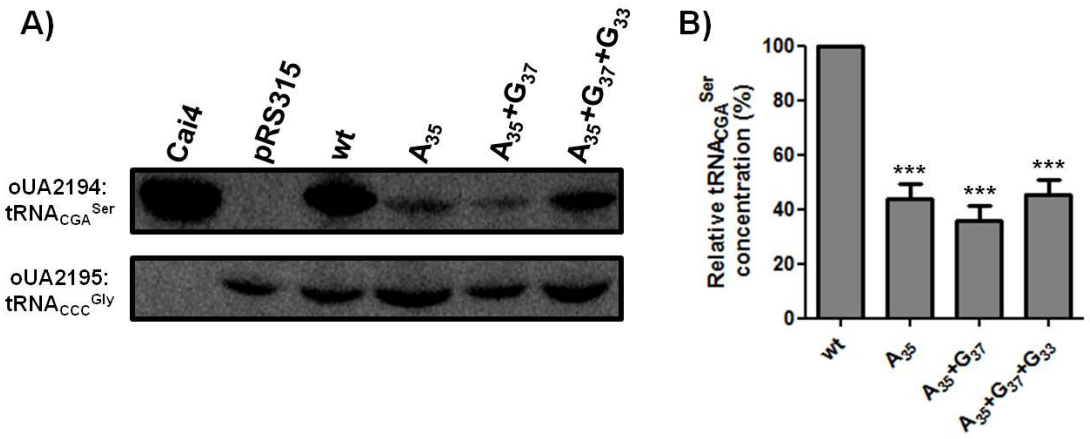

Figure 2.9: The mutant $tRNA_{CGA}^{Ser}$ are expressed at low level in yeast cells. 50 µg of total tRNA, extracted and purified under acidic conditions, were fractionated on 15% polyacrylamide gels containing 8M urea at room temperature. $tRNA_{CGA}^{Ser}$ and $tRNA_{CCC}^{Gly}$ were detected using γ-^{32}P-ATP-$tRNA_{CGA}^{Ser}$ and γ-^{32}P-ATP-$tRNA_{CCC}^{Gly}$ probes. Cai4 corresponds to total tRNA purified from *C. albicans*. Membranes were exposed for 24 hours to a K-screen and were visualized using a Bio-Rad Molecular Imager FX. B) Quantification of expression of the mutant tRNAs relative to the Wt tRNA. Data represent the mean ± s.e.m. of 3 independent clones (***$p < 0.001$, one-way Anova post Bonferroni's test with CI 95% relative to Wt $tRNA_{CGA}^{Ser}$).

In order to evaluate whether the mutations affected aminoacylation *in vivo*, the tRNAs were fractionated using acidic PAGE electrophoresis followed by northern blot analysis (section 2.2.7). Our data demonstrate that both the Wt and mutant tRNAs were aminoacylated in yeast cells (figure 2.10).

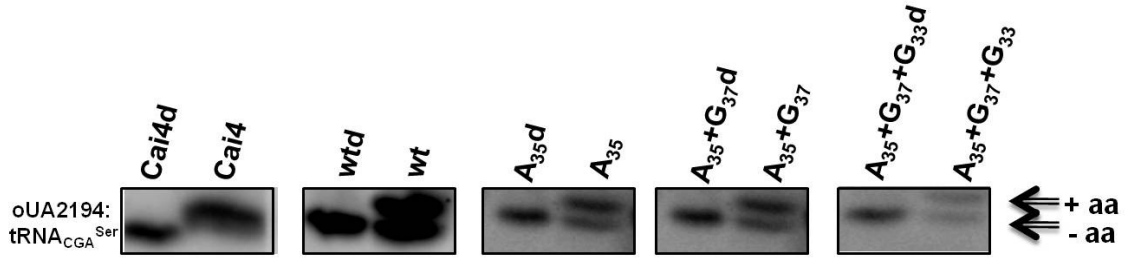

Figure 2.10: *In vivo* aminoacylation of the Wt and mutant $tRNA_{CGA}^{Ser}$ in yeast. *In vivo* aminoacylation of Wt and mutant $tRNA_{CGA}^{Ser}$ was evaluated using acidic northern blot analysis. *In vitro* deacylated and *in vivo* acylated tRNAs were fractionated on 6.5% polyacrylamide gels containing 8M urea at 4ºC, using 10 mM sodium acetate (pH= 4.5) buffer. The $tRNA_{CGA}^{Ser}$ was detected using γ-^{32}P-ATP-$tRNA_{CGA}^{Ser}$ probe. Cai4 corresponds to tRNA extracted from *C. albicans*. Membranes were exposed for 24 hours to a K-screen and were visualized using the Bio-Rad Molecular Imager FX.

In order to confirm that the A_{35} insertion in the $tRNA_{CGA}^{Ser}$ did not affect tRNA anticodon structure *in vivo*, as is hypothesized for the evolutionary pathway (Figure 2.1), northern blot analysis of the tRNAs was carried out using anticodon specific probes. The first hybridization was carried out with the oUA2196 probe, which is fully complementary to the Wt $tRNA_{CGA}^{Ser}$ anticodon sequence. A second hybridization was carried out with the probe oUA2197, which is fully complementary to the anticodon sequence of $tRNA_{CGA}^{Ser}$ containing A_{35} and the original A_{37} displaced into the intron (Figure 2.11 B). A third hybridization was carried out using the oUA2198 probe, which is fully complementary to the anticodon sequence of the $tRNA_{CGA}^{Ser}$ containing A_{35} and A_{37} in the anticodon-loop. As the first and second membranes had positive signal while the third did not (figure 2.11), it is likely that the A_{35} insertion displaced A_{37} to the intron as proposed by our model. In other words, the A_{35} insertion did not disrupted the structure of the anticodon loop of the $tRNA_{CGA}^{Ser}$.

Our northern blot results showed that the mutant $tRNA_{CGA}^{Ser}$ were expressed at low level (significantly lower than the Wt tRNA) in yeast cells, conversely to the Wt $tRNA_{CGA}^{Ser}$ which was expressed at high level. This could be due to low tRNA transcription by RNA polymerase III or to specific tRNA degradation. Since the level of the control $tRNA_{CCC}^{Gly}$ was not affected, the lower expression of the mutant tRNAs was not a general phenomenon that affected all tRNAs, rather it was a specific feature of those tRNAs. In

order to check whether the low level of the mutant tRNAs was related to their expression from single-copy plasmids, we expressed them using multicopy plasmids.

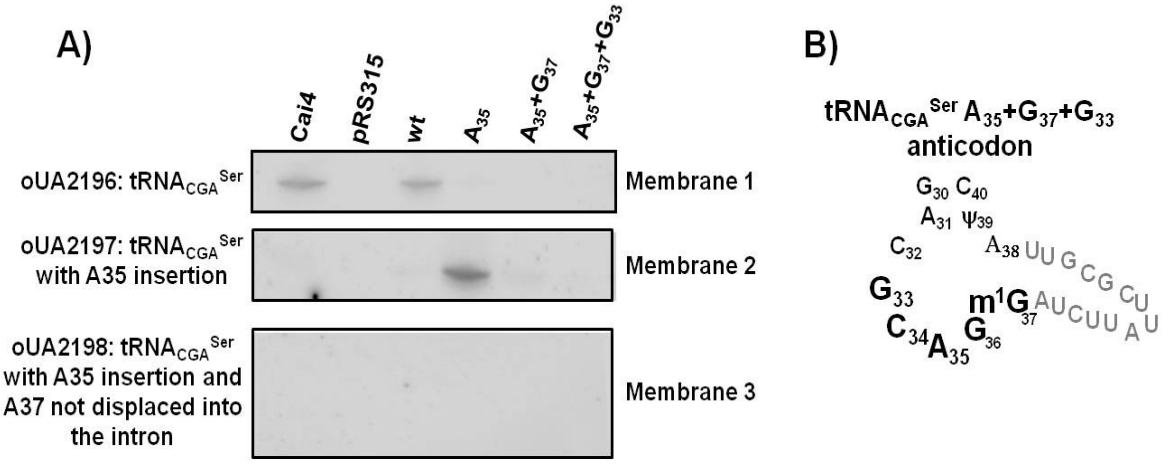

Figure 2.11: The A_{35} insertion did not disrupt the anticodon loop of the $tRNA_{CGA}^{Ser}$. A) 50 µg of total tRNA extracted and purified under acidic conditions were fractionated on 15% polyacrylamide gels containing 8M urea at room temperature. Northern blot hybridizations were carried out at high temperature (60-62ºC) with three different probes. One was complementary to the sequence of the Wt anticodon of the $tRNA_{CGA}^{Ser}$ (oUA2196), the other was complementary to the anticodon containing the A_{35} and A_{37} displaced to the intron (oUA2197) and the third one was complementary to the anticodon containing the A_{35} and the A_{37} not displaced into the intron (oUA2198). Northern blot hybridizations were carried with γ-^{32}P-ATP-$tRNA_{CGA}^{Ser}$ and γ-^{32}P-ATP-$tRNA_{CGA}^{Ser}$+A_{35} and γ-^{32}P-ATP-$tRNA_{CGA}^{Ser}$+$A_{35+}A_{37}$. Membranes were exposed for 24 hours to a K-screen and were visualized using a Bio-Rad Molecular Imager FX. B) Anticodon loop structure of the $tRNA_{CGA}^{Ser}$ triple mutant with A_{37} displaced to the intron as postulated by our evolutionary pathway model.

2.3.4. Multicopy expression of the mutant $tRNA_{CGA}^{Ser}$

For multicopy expression, the Wt and mutant Ser tRNAs were cloned into the plasmid pRS425 following the same experimental strategy used for single-copy expression (section 2.2.2.1). Four different plasmids were prepared, namely the Wt $tRNA_{CGA}^{Ser}$ (pUA212) and the mutant $tRNA_{CGA}^{Ser}$+A_{35} (pUA214), $tRNA_{CGA}^{Ser}$+A_{35}+G_{37} (pUA216) and $tRNA_{CGA}^{Ser}$+A_{35}+G_{37}+G_{33} (pUA218).

Our results (figure 2.12), show that the mutant tRNAs expressed from multicopy plasmids had a strong negative impact on yeast growth. The growth reduction was lower for the $tRNA_{CGA}^{Ser}+A_{35}+G_{37}$ mutant, but was stronger for $tRNA_{CGA}^{Ser}+A_{35}+G_{37}+G_{33}$, as observed before when the tRNAs were expressed from single-copy plasmids. In the case of the multicopy plasmids the growth rate reduction was higher relative to the single copy plasmids. For example, the $tRNA_{CGA}^{Ser}+A_{35}$ reduced growth rate by 45% in multicopy and 30% when expressed in single-copy. For the $tRNA_{CGA}^{Ser}+A_{35}+G_{37}$ the growth decrease in multicopy was 30% while in single copy was 23% and the $tRNA_{CGA}^{Ser}+A_{35}+G_{37}+G_{33}$ reduced growth rate by 68% in multicopy and 46% in single-copy. This higher toxicity observed in multicopy expression was expected since tRNA expression is dependent on tRNA gene copy number (Murphy & Baralle, 1983; Paolella et al., 1983).

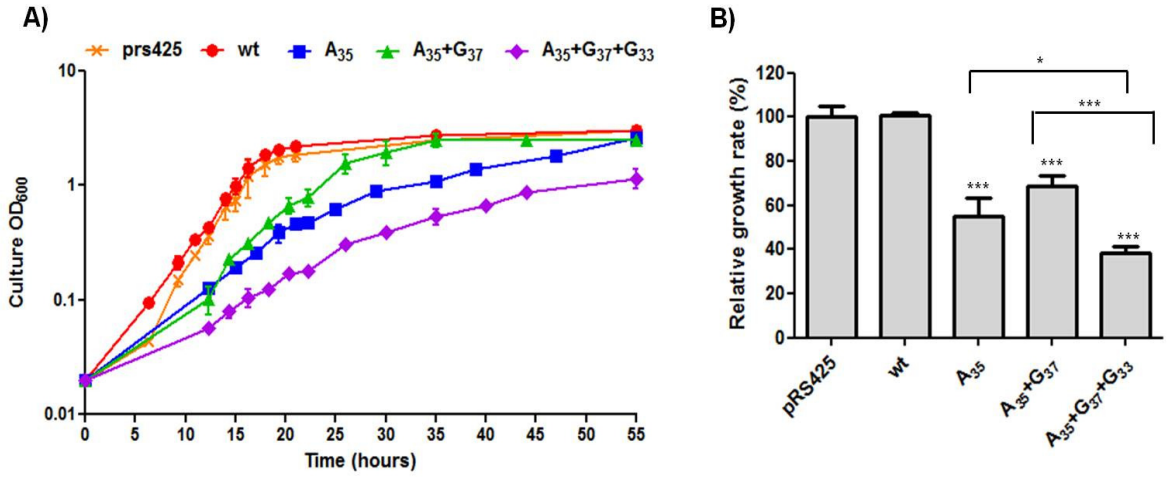

Figure 2.12: Multicopy expression of the mutant $tRNA_{CGA}^{Ser}$ decreases yeast growth rate. A) Growth of yeast cells transformed with the Wt and mutant $tRNA_{CGA}^{Ser}$ expressed from multicopy plasmids. Cultures were inoculated at an initial OD_{600} of 0.02 and were grown in selective medium, at 30ºC, 180rpm, until stationary phase. B) The relative growth rate of cells transformed with Wt and mutant $tRNA_{CGA}^{Ser}$ was determined using exponential growth phase values, relative to the control cells. Data represent the mean ± s.e.m. of duplicates of 3 independent clones. (***$p < 0.001$, *$p < 0.05$ one-way Anova post Bonferroni's test with CI 95% relative to pRS425).

The β-gal reporter system was then used to evaluate the toxic effects of CUG misreading *in vivo* in yeast cells. As before, the mutant tRNAs decreased the thermostability of β-gal (figure 2.13 A) and β-gal total activity (figure 2.13 B) although,

unexpectedly, the β-gal thermostability and activity reduction was lower in multicopy than in single-copy expression (figure 2.7 A and B).

β-gal abundance was also quantified by western blot. A reduction in total β-gal abundance was observed (figure 2.14), but it was lower than the reduction observed in the single-copy tRNA expression experiments (figure 2.8).

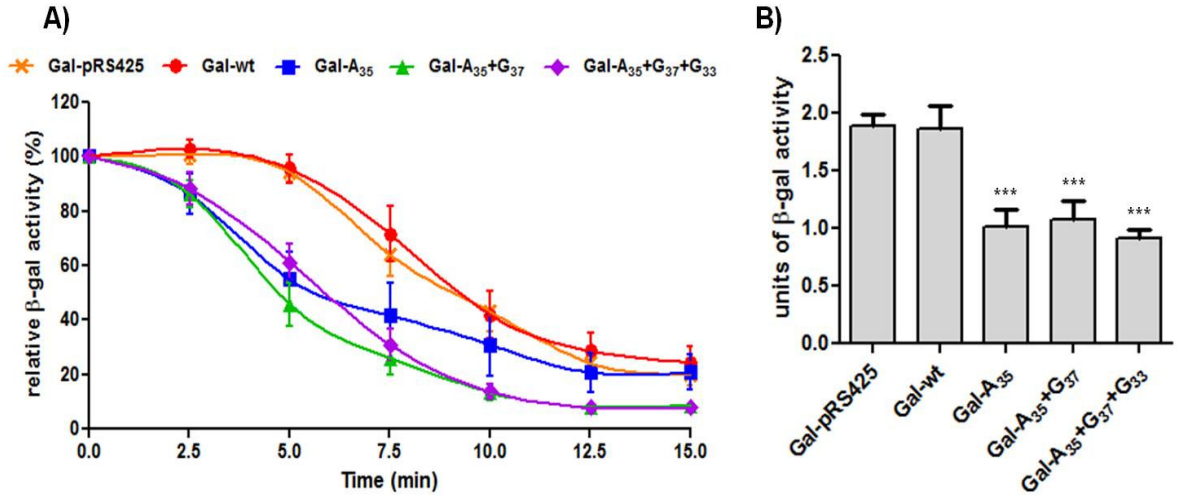

Figure 2.13: Multicopy expression of mutant $tRNA_{CGA}^{Ser}$ destabilizes β-galactosidase in yeast. *E. coli* β-gal was co-expressed with Wt and mutant $tRNA_{CGA}^{Ser}$ in yeast cells. A) β-gal thermostability profiles were determined as described in section 2.2.6. β-gal activity at each time point corresponds to the relative percentage of decreased activity relative to total activity measured in cells prior to denaturation. Data represent the mean ± s.e.m. of triplicates of 3 independent clones B) The β-gal activity was quantified after incubating cell extracts at 30ºC with ONPG until a pale yellow colour appeared (section 2.2.6). Data represent the mean ± s.e.m. of triplicates of 3 independent clones. (***p < 0.001 for 1way Anova post Bonferroni's test with CI95% relative to pRS425).

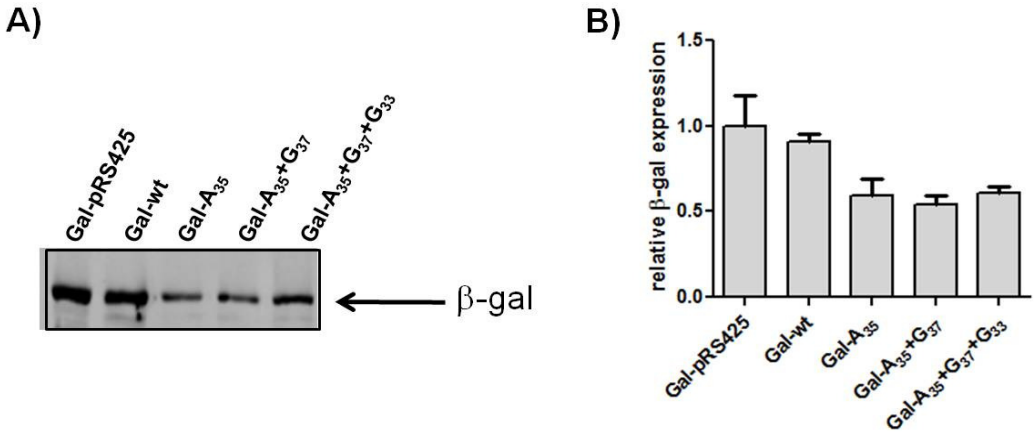

Figure 2.14: Multicopy expression of the mutant $tRNA_{CGA}^{Ser}$ decreases β-galactosidase expression in yeast. A) β-gal abundance was quantified by western blot using an anti-β-gal rabbit IgG antibody and a secondary goat-anti-rabbit antibody (section 2.2.6). B) Relative β-gal abundance of each tRNA sample relative to control cells (Gal-pRS425). Data represent the mean ± s.e.m. of duplicates of three independent clones (one-way Anova post Bonferroni's multiple comparison test with CI 95%, relative to pRS425).

This surprising result showing similar toxicity of the mutant $tRNA_{CGA}^{Ser}$ expressed from single-copy and multicopy vectors, prompted us to quantify by northern blot the multicopy expression of the mutant tRNAs. Interestingly, the level of the mutant $tRNA_{CGA}^{Ser}$ showed stronger decrease, relative to the Wt $tRNA_{CGA}^{Ser}$, than the single-copy expression (figure 2.15). In other words, the level of the mutant tRNAs was not related to gene copy number, which contradicts the generalized idea that tRNA gene copy number determines the level of tRNA expression in eukaryotes. Indeed, in eukaryotes tRNA genes have intragenic promoters (box A and box B) indicating that tRNA abundance is exclusively regulated by tRNA gene copy number (Murphy & Baralle, 1983; Paolella et al., 1983).

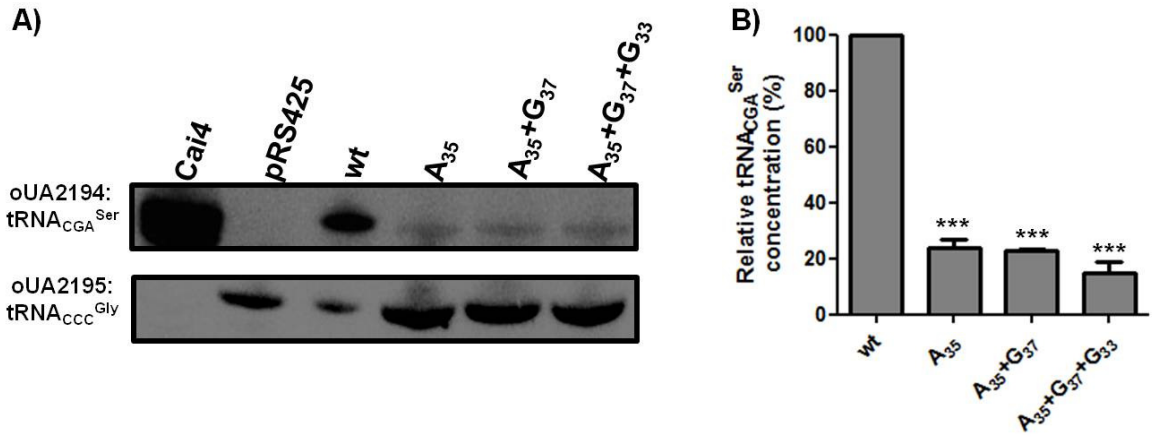

Figure 2.15: Multicopy expression of the mutant $tRNA_{CGA}^{Ser}$ does not increase tRNA abundance. A) 50 µg of total tRNA extracted and purified under acidic conditions were fractionated on 15% polyacrylamide gels containing 8M urea at room temperature. Detection of $tRNA_{CGA}^{Ser}$ and $tRNA_{CCC}^{Gly}$ was carried out with γ-^{32}P-ATP-$tRNA_{CGA}^{Ser}$ and γ-^{32}P-ATP-$tRNA_{CCC}^{Gly}$ probes. Cai4 corresponds to total *C. albicans* tRNA. Membranes were exposed 24 hours to a K-screen and were visualized using Bio-Rad Molecular Imager FX. B) Quantification of mutant $tRNA_{CGA}^{Ser}$ expression relative to Wt tRNA. Data represent the mean ± s.e.m. of three independent clones (***$p < 0.001$, 1 way Anova post Bonferroni's test with CI 95% relative to Wt $tRNA_{CGA}^{Ser}$).

2.3.5. Mechanism of repression of the mutant misreading $tRNA_{CGA}^{Ser}$

If one considers that tRNA transcription is mainly regulated by tRNA gene copy number, then the low abundance of the misreading $tRNA_{CGA}^{Ser}$ is likely due to specific degradation by ribonucleases. Some of the proteins involved in tRNA degradation are: Rny1p, which is involved in stress induced cleavage (Thompson, 2009a; Thompson, 2009b); Rrp6p and the TRAMP complex, which contains the poly(A) polymerases Trf4p or Trf5p, the RNA-binding proteins Air1p or Air2p and the RNA helicase Mtr4p in the case of nuclear degradation (Kadaba et al., 2004; Kadaba et al., 2006; Vanacova et al., 2005) (Doma & Parker, 2007); and finally the 5' to 3' exonucleases Rat1p or Xrn1p and Met22p in the case of cytoplasmic degradation (Chernyakov *et al.*, 2008).

In order to determine whether our mutant serine tRNAs were degraded in yeast by one of the above mentioned pathways, we have expressed them from single-copy plasmids in yeast strains harboring knock-outs of the RNY1, XRN1, TRF4, TRF5, MET22, AIR2 and RRP6 genes.

The northern blots showed that the abundance of the misreading $tRNA_{CGA}^{Ser}$ was not restored in the knock-out strains tested (figure 2.16), suggesting that deregulation of the mutant $tRNA_{CGA}^{Ser}$ was not mediated by known tRNA degradation pathways. This suggests the existence of new tRNA degradation pathway, or the existence of other regulatory processes, namely transcriptional repression of tRNA expression.

In order to further clarify the above expression phenotype, a mutation was introduced in the intron of the $tRNA_{CGA}^{Ser}$ gene. The introns interact with the anticodon loop of tRNAs and the structure formed by them is recognized by the introns splicing enzymes (Abelson et al., 1998; Negri et al., 1997). In other words, if the intron of the $tRNA_{CGA}^{Ser}$ gene interacts with the anticodon bases, the insertion of A_{35} in the middle position of the anticodon could disrupt this putative intron/anticodon interaction (figure 2.17A). Since this perturbation in the intron structure could interfere with its recognition by the splicing machinery, it could inhibit intron removal and consequently tRNA processing. With the aim of testing this hypothesis a U was inserted in position IX of the intron. This U_{IX} is expected to interact with A_{35} (figure 2.17 B) and restore the helical structure of the anticodon-intron domain of the pre-tRNA. This mutation was introduced in the $tRNA_{CGA}^{Ser}$ gene cloned in the single-copy plasmid containing the mutant $tRNA_{CGA}^{Ser}+A_{35}$.

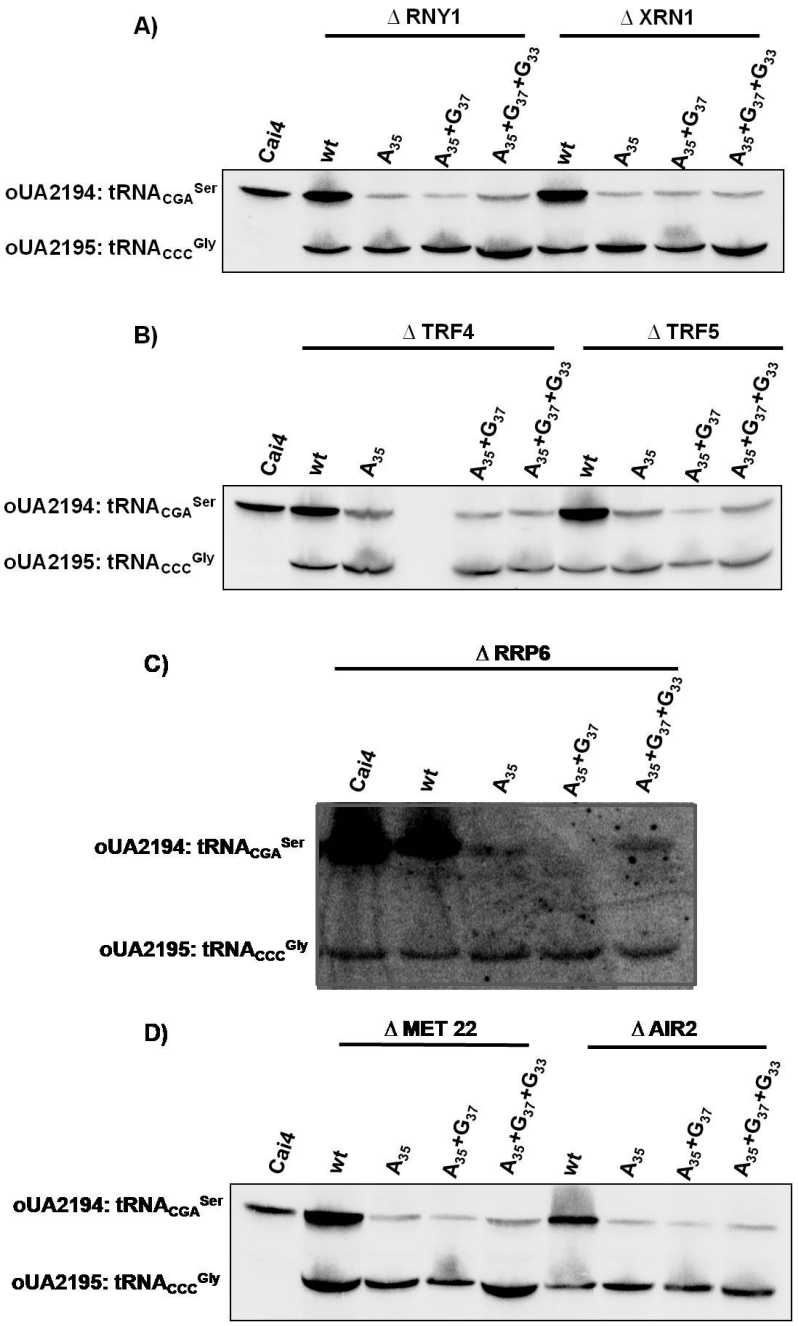

Figure 2.16: Putative degradation of the mutant $tRNA_{CGA}^{Ser}$ is not mediated by knwon tRNA degradation pathways. In order to restore the levels of mutant tRNAs, Wt and mutant $tRNA_{CGA}^{Ser}$ were expressed in yeast strains deleted in the RNY1, XRN1, TRF4, TRF5, RRP6, MET22 and AIR2 genes, respectively, which encode proteins involved in tRNA degradation. 50 µg of total tRNA extracted and purified under acidic conditions were fractionated on 15% polyacrylamide gels containing 8M urea at room temperature. Detection of $tRNA_{CGA}^{Ser}$ and $tRNA_{CCC}^{Gly}$ was carried out with γ-^{32}P-ATP-$tRNA_{CGA}^{Ser}$ and γ-^{32}P-ATP-$tRNA_{CCC}^{Gly}$ probes. Membranes were exposed 24 hours to a K-screen and were visualized using Bio-Rad Molecular Imager FX.

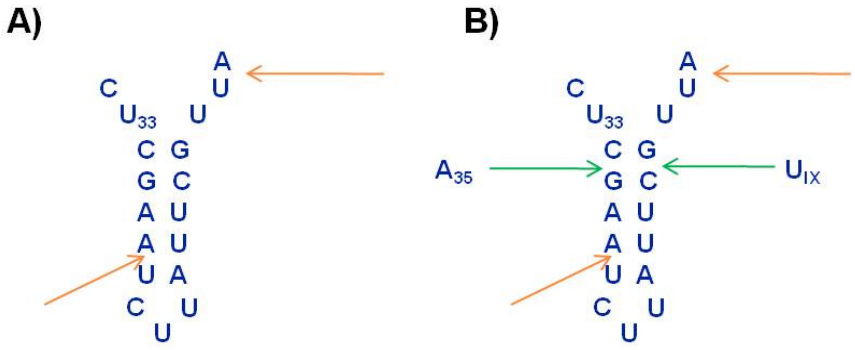

Figure 2.17: Putative interaction of the intron and anticodon loop nucleotides of the $tRNA_{CGA}^{Ser}$. A) Represents the interaction between the anticodon loop of the $tRNA_{CGA}^{Ser}$ and the intron located between the arrows. B) The uridine inserted at position IX (U_{IX}) in the intron is expected to compensate and maintain the intron structure after A_{35} insertion.

Unfortunatly, northern blot analysis did not confirm our hypothesis (figure 2.18), as U_{IX} insertion did not alter the abundance of the mutant $tRNA_{CGA}^{Ser}$.

The previous negative results prompted us to test whether the repression of the misreading $tRNA_{CGA}^{Ser}$ was related to the toxicity of Leu-for-Ser mistranslation and not to altered stability of the tRNA induced by those mutations. In order to test this alternative hypothesis, we have reduced the toxicity of the mutant $tRNA_{CGA}^{Ser}$ by altering its identity through introduction of additional mutations in the acceptor-stem of the tRNA. For that, the G_{73} discriminator base was changed to the Leu A_{73} discriminator base in the mutant $tRNA_{CGA}^{Ser}$+A_{35}+G_{37}+G_{33}. This $G_{73} \rightarrow A_{73}$ mutation alters the identity of $tRNA^{Ser}$ converting it into a Leu $tRNA^{Leu}$ (Breitchopf & Gross, 1996). This should have no impact on tRNA stability because the nucleotide at position 73 is a non-paired base located at 3'-end of the $tRNA^{Ser}$ (figure 2.2). We were expecting that this mutation abolished toxicity and restored the expected level of expression of the mutant $tRNA_{CGA}^{Ser}$. Unexpectedly, this mutation did not restored tRNA levels as demonstrated by northern blot analysis (figure 2.18).

Finally, the level of the mutant $tRNA_{CGA}^{Ser}$ was evaluated at different growth time points. For that, the level of the mutant $tRNA_{CGA}^{Ser}$ was determined in cells during early exponential and stationary growth phases. Our results (figure 2.19 A and B) show no significant difference in the abundance of the mutant $tRNA_{CGA}^{Ser}$ in these two growth time points. However, a significant increase in the expression of Wt $tRNA_{CGA}^{Ser}$ was observed in stationary phase, but the expression of the mutant $tRNA_{CGA}^{Ser}$ and the control $tRNA_{CCC}^{Gly}$ showed no alteration. This interesting observation suggests that some tRNAs

are indeed regulated at transcriptional or post-transcriptional levels in eukaryotes, but unfortunately our data are not enough to understand the mechanism involved in the regulation of mutant $tRNA_{CGA}^{Ser}$ expression.

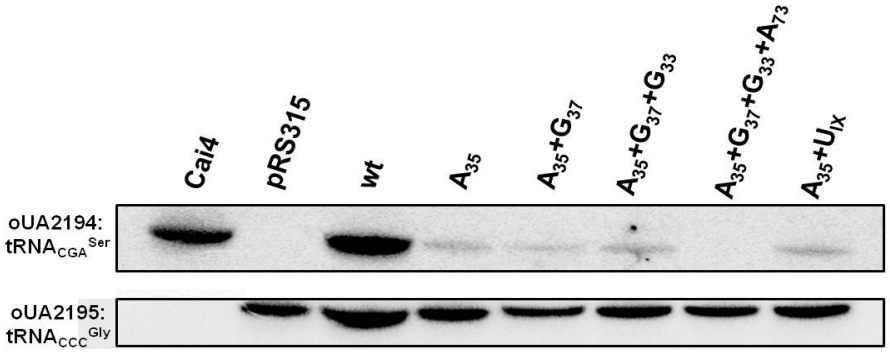

Figure 2.18: The abundance of the mutant $tRNA_{CGA}^{Ser}$ is not restored by mutations that abolish their toxicity. 50 µg of total tRNA extracted and purified under acidic conditions were fractionated on 15% polyacrylamide gels containing 8M urea at room temperature. Detection of $tRNA_{CGA}^{Ser}$ and $tRNA_{CCC}^{Gly}$ was carried out with γ-^{32}P-ATP-$tRNA_{CGA}^{Ser}$ and γ-^{32}P-ATP-$tRNA_{CCC}^{Gly}$ probes. Cai4 corresponds to total *C. albicans* tRNA. Membranes were exposed during 24 hours to a K-screen and were visualized using the Bio-Rad Molecular Imager FX.

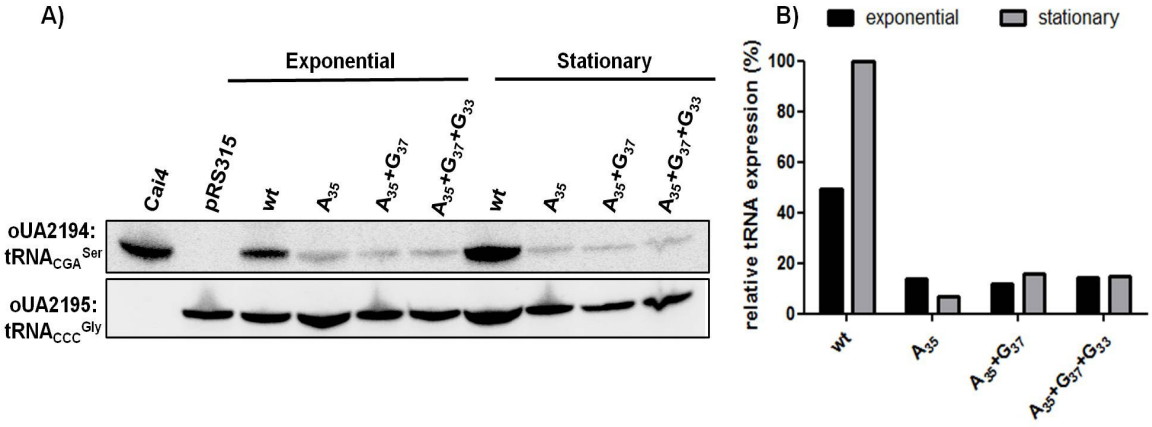

Figure 2.19: Expression of $tRNA_{CGA}^{Ser}$ in exponential and stationary phase. A) 50 µg of total tRNA extracted and purified under acidic conditions were fractionated on 15% polyacrylamide gel containing 8M urea at room temperature. Detection of $tRNA_{CGA}^{Ser}$ and $tRNA_{CCC}^{Gly}$ was carried out with γ-^{32}P-ATP-$tRNA_{CGA}^{Ser}$ and γ-^{32}P-ATP-$tRNA_{CCC}^{Gly}$ probes. Membranes were exposed during 24 hours to a K-screen and were visualized using Bio-Rad Molecular Imager FX. B) Quantity of Wt and mutant $tRNA_{CGA}^{Ser}$ in early exponential and stationary phases relative to Wt $tRNA_{CGA}^{Ser}$ expressed in stationary phase.

2.3.6. *In vivo* forced evolution approach for identification of the $tRNA_{CAG}^{Ser}$ identity elements

The systematic failure to restore expression of the mutant $tRNA_{CGA}^{Ser}$ to Wt levels prompted us to develop an *in vivo* forced evolution strategy, which could help identify the $tRNA_{CAG}^{Ser}$ identity determinats, i.e., mutations that would repress or abolish serylation of the mutant $tRNA_{CGA}^{Ser}$. For this, we have taken advantage of a previous observation which showed that the $tRNA_{CAG}^{Ser}$ containing U at position 33 (U_{33}) is highly detrimental or even lethal in haploid yeast cells, but is mildly detrimental in diploid cells (Santos et al., 1996). We have hypothesized that expressing the $tRNA_{CAG}^{Ser}$ in diploid cells and then sporulating them would allow us to identify haploid cells where expression or identity of the $tRNA_{CAG}^{Ser}$ changed significantly or completely, thus abolishing $tRNA_{CAG}^{Ser}$ misreading of CUGs. For this, the $tRNA_{CAG}^{Ser}$ U_{33} gene sequence fused to the KanMX4 gene (resistance to the antibiotic geneticine) was cloned into the single-copy vector pRS315 (Silva et al., 2007). This chimeric cassette was then amplified by PCR using long 5' and 3' oligonucleotides containing homologous extensions for integration into the yeast LEU2 locus (section 2.2.2.2). Only one copy of the fusion cassette $tRNA_{CAG}^{Ser}$-KanMx4 could integrate into the LEU2 locus of yeast (CEN.PK2) cells because two copies of the $tRNA_{CAG}^{Ser}$ are lethal (Silva et al., 2007). The $tRNA_{CAG}^{Ser}$ gene integrated into the genome was then sequenced from diploid yeast clones that could grow in YPD+geneticine. Clones containing the authentic tRNA sequence were then selected for downstream screening. For this, cells were grown overnight in YPD+geneticine and then collected, washed and transferred to a sporulation medium during 4-8 days (section 2.2.2.2). The asci were then dissected using a micromanipulator and were grown in YPD+geneticine plates. Viable spores containing the $tRNA_{CAG}^{Ser}$ gene were then used for PCR amplification of the $tRNA_{CAG}^{Ser}$ and subsequently DNA sequencing. Sequenced $tRNA_{CAG}^{Ser}$ genes had at least one mutation (figure 2.20).

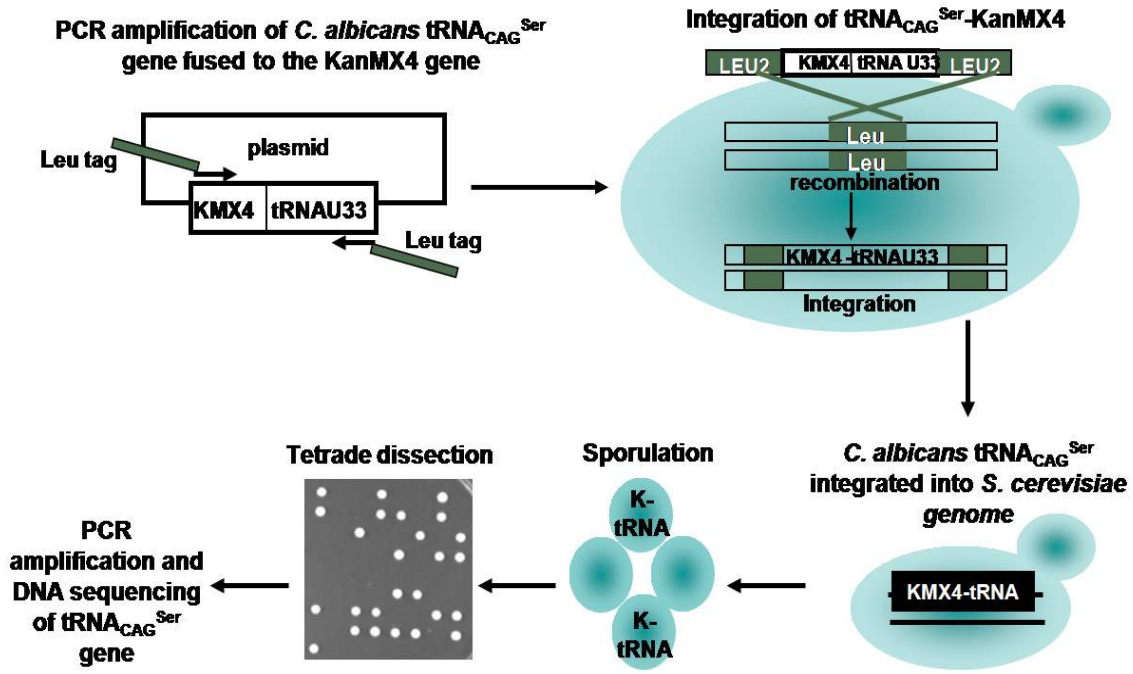

Figure 2.20: Forced *in vivo* evolution methodology. The experimental *in vivo* forced evolution methodology was used to screen for mutations that affect *C. albicans* $tRNA_{CAG}^{Ser}$ stability and identity. This method was based on PCR amplification of the cassette containing the $tRNA_{CAG}^{Ser}$ fused to the KanMx4 gene and subsequent integration by homologous recombination into the LEU2 locus of diploid yeast cells. Yeast with $tRNA_{CAG}^{Ser}$ gene integrated were sporulated and tetrades dissected using a micromanipulator. The $tRNA_{CAG}^{Ser}$ gene was amplified from viable spores by PCR and the amplified DNA was sequenced.

The mutations identified in the $tRNA_{CAG}^{Ser}$, using our *in vivo* methodologies (figure 2.21 A), are mostly localized in the acceptor stem and variable arm of the $tRNA_{CAG}^{Ser}$ gene. The variable arm contains four of the ten mutations identified, namely the $G_{47}\rightarrow A_{47}$, $G_{47E}\rightarrow U_{47E}$, $C_{47F}\rightarrow U_{47F}$, $C_{47H}\rightarrow A_{47H}$, which correspond to nucleotides located in the three conserved GC base pairs, which were identified as possible identity elements of $tRNA_{CAG}^{Ser}$ (Miranda et al., 2006). Two mutations were identified in the acceptor stem, the $G_1\rightarrow A_1$ and $C_5\rightarrow U_5$. The $G_1\rightarrow A_1$ may disrupt folding of the $tRNA_{CAG}^{Ser}$ acceptor helix and may open the acceptor stem. Previous, structural studies showed that decreasing the stability of the G_1-C_{72} base pair, due to replacement of $A_{73}\rightarrow G_{73}$, affects human LeuRS recognition of $tRNA^{Leu}$ (Metzger et al., 1997). The impact of $C_5\rightarrow U_5$ may be less negative. Two additional mutations were identified in the TψC arm, namely a C_{56} deletion and

C_{65}→A_{65}. Tertiary interactions between the TψC and D arms are important for tRNA structure, i.e., in the crystal structure of $tRNA^{Phe}$, G_{18} and G_{19} base-pair through tertiary interactions with the bases 55 and 56 of the TψC arm to form the L-shaped structure (Kim et al., 1974). This suggests that the mutant $tRNA_{CAG}^{Ser}$ with a deletion of C_{56} lacks the tRNA tertiary interaction between D and TψC arms and probably will not form a correct 3D structure. Similarly, the C_{65}→A_{65} mutation may prevent the formation of a correct TψC arm structure. The only mutation identified in the anticodon stem was C_{41}→G_{41}. The anticodon stem of $tRNA^{Ser}$ is not recognized by the SerRS which suggests that this mutation may not affect serylation of $tRNA_{CAG}^{Ser}$, but it may destabilize the anticodon region and could probably affect codon-anticodon interaction due to the G_{29}-G_{41} mismatch. Finally, the last mutation screened was located in the discriminator base, the G_{73}→A_{73}. In *E. coli*, SerRS does not recognize the anticodon nor the discriminator base G_{73} of $tRNAs^{Ser}$, instead it recognizes the length and the structure of the variable arm in a sequence independent way (Asahara et al., 1994; Himeno et al., 1990; Lenhard et al., 1999). Conversely, yeast SerRS recognizes the sequence and structure of the variable arm (Himeno et al., 1990) and the discriminator base G_{73} of $tRNAs^{Ser}$. Indeed, in yeast cells G_{73} acts as an anti-determinant for the LeuRS and is a determinant for the SerRS (Soma et al., 1996). In humans $tRNAs^{Ser}$ recognition by SerRS involves the discriminator base G_{73} and the long extra-arm. The exchange of the short extra arm of $tRNA^{Val}$ for the long extra arm of $tRNAs^{Ser}$ and the replacement of A_{73}→G_{73} in $tRNAs^{Val}$ converts it into a Ser acceptor (Aschel & Gross, 1993). More importantly, human $tRNA^{Leu}$ can be converted into a Ser acceptor by changing A_{73}→G_{73} only, because the long extra-arm of both tRNAs is similar in length and structure (not in sequence) (Breitchopf et al., 1995; Breitchopf & Gross, 1994; Breitchopf & Gross, 1996). The most frequent mutation was the C_{56} deletion which appeared in 43% of the spores while the least common were C_{47F}→U_{47F} and C_{47H}→A_{47H} which appeared in only 1% of the spores (figure 2.21 B).

A comparison of the conserved nucleotides in the CTG clade $tRNA_{CAG}^{Ser}$ (figure 2.22) showed that most of the mutations screened with this work correspond to conserved positions of the $tRNA_{CAG}^{Ser}$, namely G_1, C_{56}, G_{73}, G_{47E}, C_{47F} and C_{47H}. On the other hand, C_{41} is conserved in all species of the CTG clade except in one, the C_5 is conserved in all except two species and C_{65} is conserved in all except three species. Therefore, the mutations identified in our screen may correspond to identity elements of $tRNA_{CAG}^{Ser}$, suggesting that the mutation may alter $tRNA_{CAG}^{Ser}$ identity or block tRNA serylation, thus reducing tRNA toxicity and permitting spore viability.

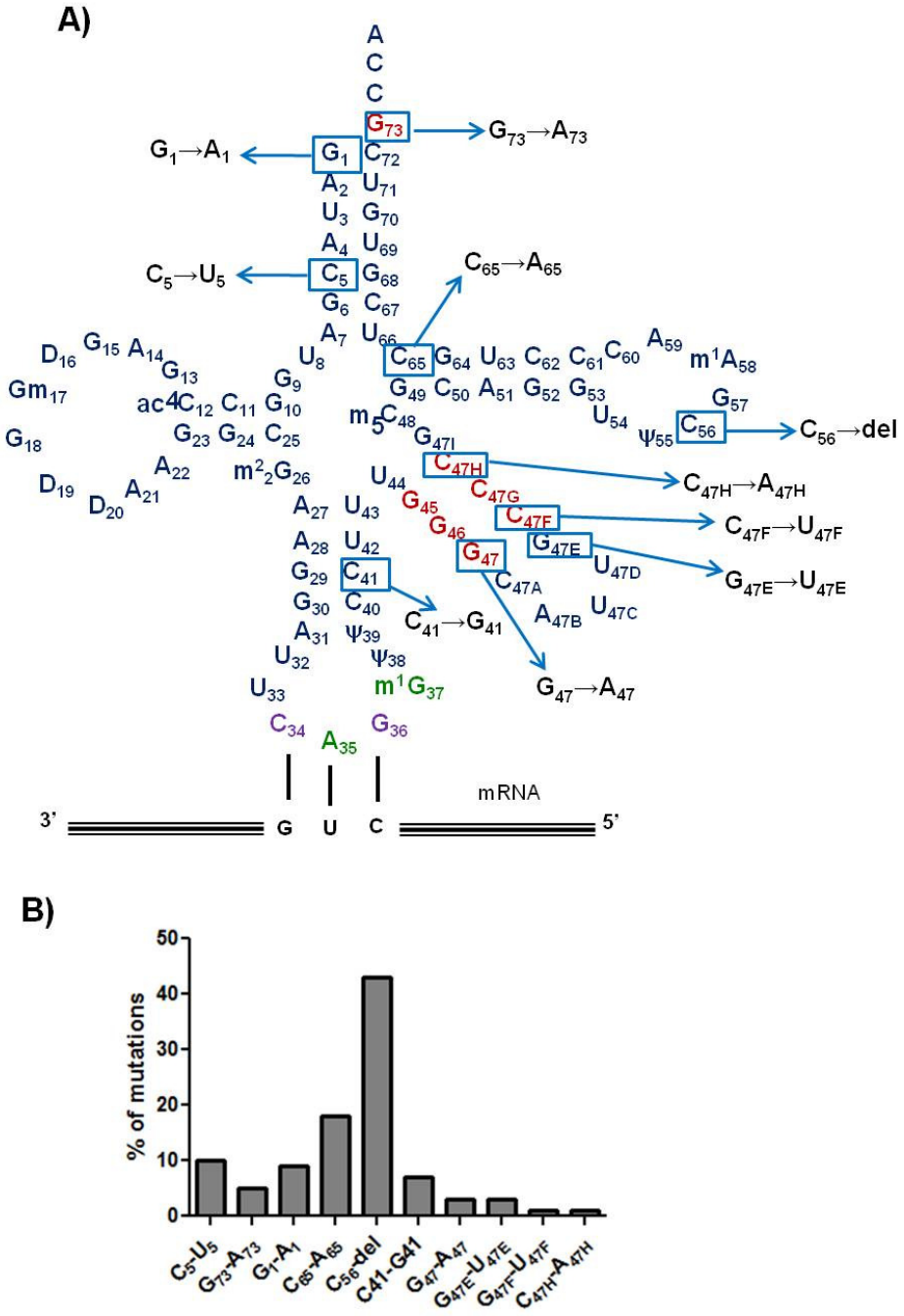

Figure 2.21: Mutations identified using our *in vivo* forced evolutionary strategy. A) *In vivo* forced evolution strategy using the $tRNA_{CAG}^{Ser}$ gene expressed in yeast cells identified 10 different mutations. Most mutations localized in the acceptor stem and variable arm, and 3 of these appeared in the TψC-arm and anticodon stem. B) The frequency of each mutation is represented as the percentage of each mutation scored relative to total number of spores sequenced.

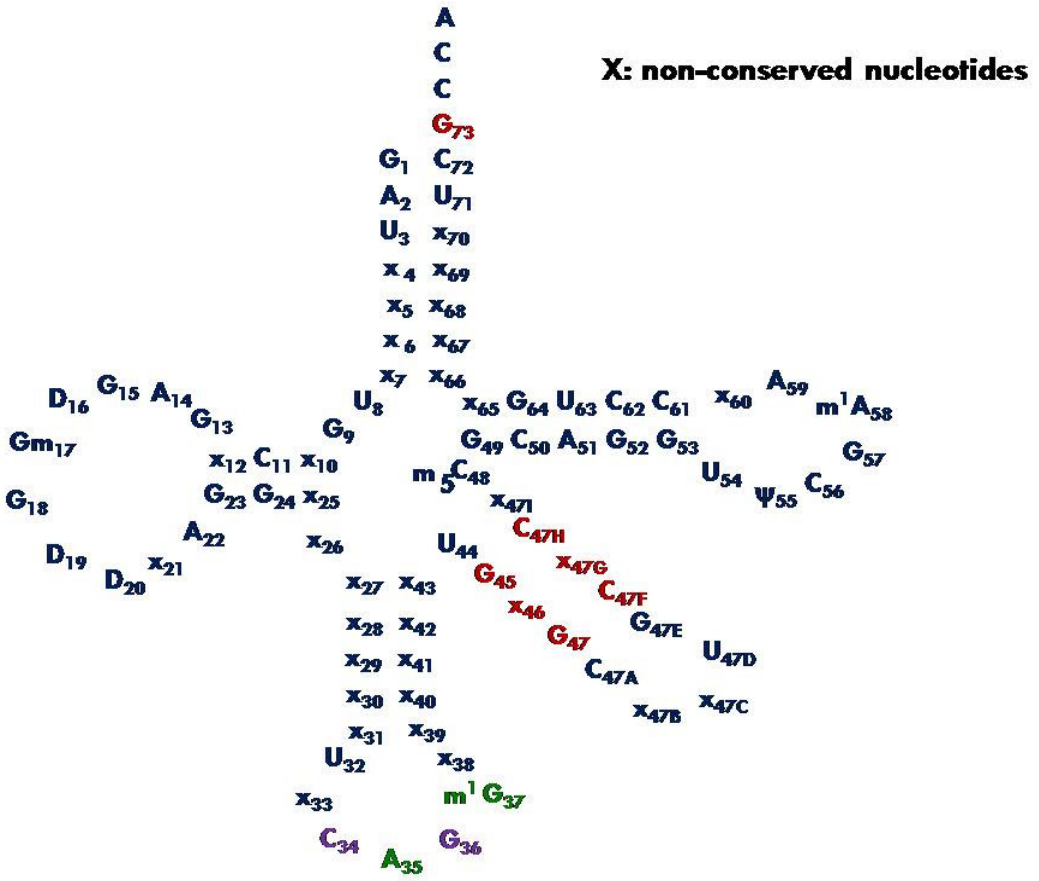

Figure 2.22: Cloverleaf representation of composite structure of $tRNA_{CAG}^{Ser}$ of the CTG clade. The sequence alignment of $tRNA_{CAG}^{Ser}$ from all CTG clade species (*C. albicans, C. dubliniensis, C. tropicalis, C. parapsilosis, L. elongisporus, C. guillermondi, D. hansenii, C. lusitaniae*) were used in compilation. The indicated nucleotides correspond to the ones conserved between all species, while X corresponds to non-conserved nucleotides. Sequences were adapted from (Wang et al., 2009a).

2.3.7. Expression and stability of mutant $tRNA_{CAG}^{Ser}$

As mentioned above, the *C. albicans* $tRNA_{CAG}^{Ser}$ is lethal when expressed in haploid yeast cells, but our screen showed that the mutations identified allow for survival of haploid yeast cells (figure 2.23). Surprisingly, growth rate of control cells (integrated KanMX4 gene only) was similar to that of cells expressing the mutant $tRNA_{CAG}^{Ser}$, with the exceptions of mutant $tRNA_{CAG}^{Ser}$ $C_{41}\rightarrow G_{41}$ and $C_{47F}\rightarrow U_{47F}$, where relative growth rate was 76% and 65%, respectively. In conclusion, the lower toxicity of our mutant $tRNA_{CAG}^{Ser}$

suggests that the mutant tRNAs were unstable, or were only charged with Leu or were not charged at all.

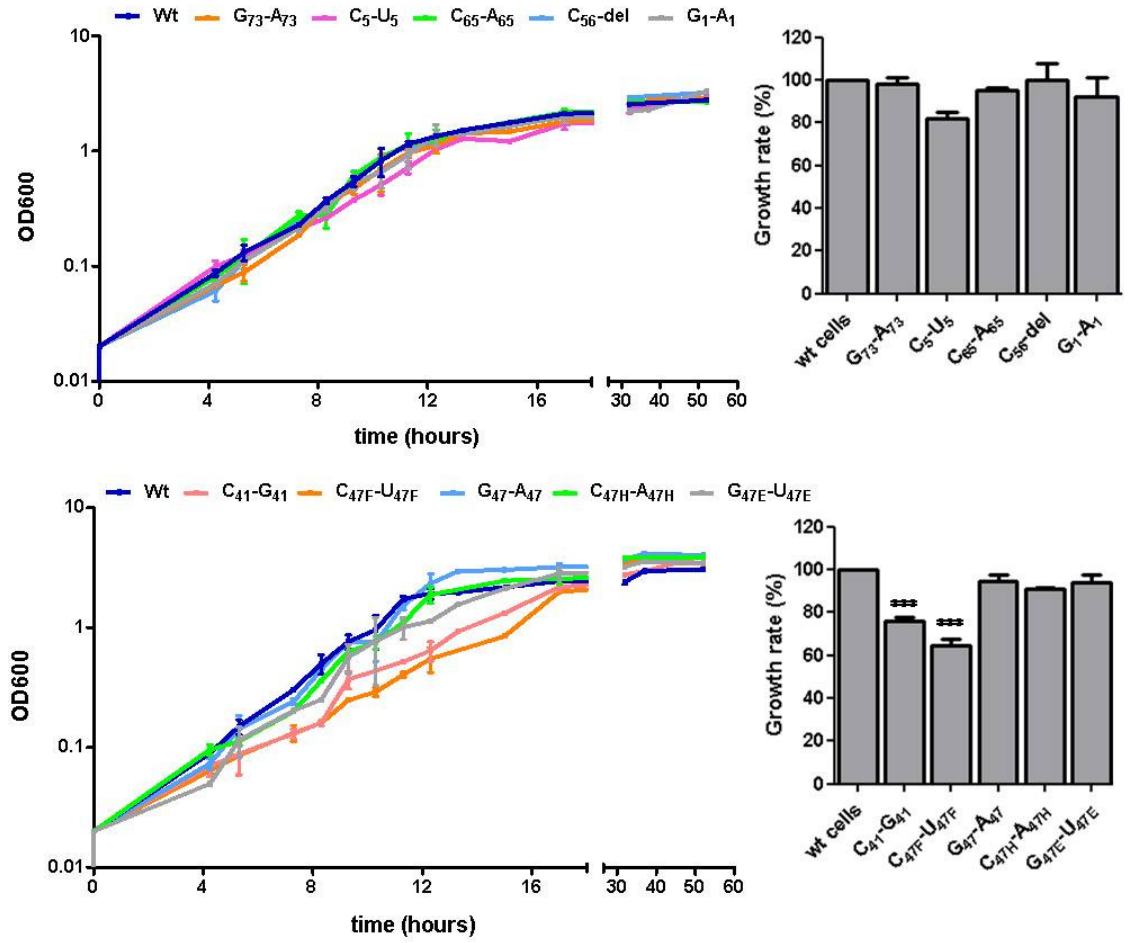

Figure 2.23: Mutations in *C. albicans* $tRNA_{CAG}^{Ser}$ restore yeast growth. Yeast cultures were inoculated at an initial OD of 0.02 and were grown at 30ºC in 100 ml culture flasks in YPD+geneticine until late stationary phase. Wt correspond to cells containing KanMX4 cassette only. The relative growth rate of cells transformed with mutant $tRNA_{CAG}^{Ser}$ was determined using exponential growth phase values, relative to the control cells (Wt). Data represent the mean ± s.e.m. of 3-5 independent experiments. (***p < 0.001 one-way Anova post Bonferroni's multiple comparison test with CI of 95%, relative to the Wt control cells).

The abundance of the Wt and mutant $tRNA_{CAG}^{Ser}$ was then checked by northern blot analysis (section 2.2.7). The Wt $tRNA_{CAG}^{Ser}$ integrated into the genome of diploid yeast cells was expressed at low level (figure 2.24), but none of the mutant $tRNA_{CAG}^{Ser}$

was detected by northern blot analysis (figure 2.25), while the control $tRNA_{CCC}^{Gly}$ was expressed as expected.

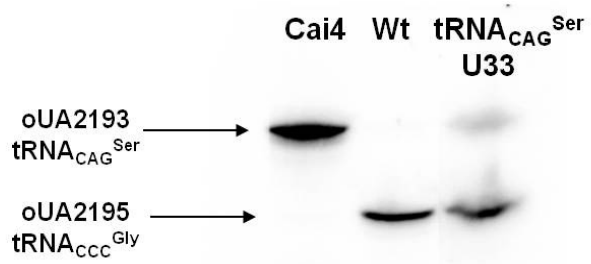

Figure 2.24: Northern blot analysis of *C. albicans* $tRNA_{CAG}^{Ser}$ expressed in diploid yeast. 50 µg of tRNAs extracted and purified under acidic conditions were fractionated on 12% polyacrylamide gels containing 8M urea at room temperature. Detection of $tRNA_{CAG}^{Ser}$ and $tRNA_{CCC}^{Gly}$ was carried out using γ-^{32}P-ATP-$tRNA_{CAG}^{Ser}$ and γ-^{32}P-ATP-$tRNA_{CCC}^{Gly}$ probes. Cai4 corresponds to $tRNA_{CAG}^{Ser}$ extracted from *C. albicans*, Wt corresponds to tRNAs extracted from *S. cerevisiae* cells containing the KanMX4 cassette only or the $tRNA_{CAG}^{Ser}$ U_{33} integrated into the LEU2 locus. Membranes were exposed for 24 hours to a K-screen and were visualized using Bio-Rad Molecular Imager FX.

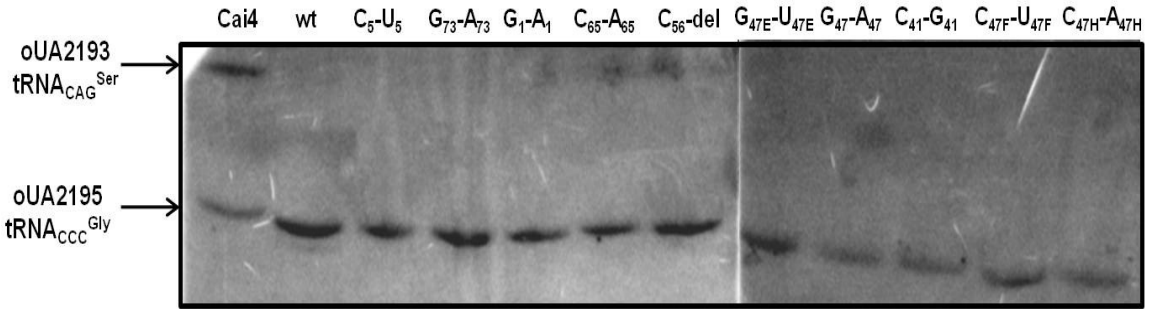

Figure 2.25: Northern blot analysis of mutant *C. albicans* $tRNA_{CAG}^{Ser}$ expressed in yeast haploid cells. 50 µg of tRNAs extracted from viable haploid spores that grew in liquid culture were purified under acidic conditions and fractionated on 12% polyacrylamide gel containing 8M urea at room temperature. Detection of $tRNA_{CAG}^{Ser}$ and $tRNA_{CCC}^{Gly}$ was carried out using γ-^{32}P-ATP-$tRNA_{CAG}^{Ser}$ and γ-^{32}P-ATP-$tRNA_{CCC}^{Gly}$ probes. Cai4 corresponds to *C. albicans* total tRNA extract and wt corresponds to tRNAs extracted from *S. cerevisiae* cells containing KanMx4 cassette only. Membranes were exposed for 24 hours to a K-screen and were visualized using Bio-Rad Molecular Imager FX.

2.4.8. Multicopy expression of mutant $tRNA_{CAG}^{Ser}$

In order to clarify whether the mutant $tRNA_{CAG}^{Ser}$ could be detected we expressed it from a multicopy plasmid (pRS425). For this, mutant $tRNA_{CAG}^{Ser}$ genes were subcloned into pRS425 vector and were expressed in diploid yeast cells (BMA-64 strain) (section 2.2.2.3). No transformants were obtained for the $tRNA_{CAG}^{Ser}$ U_{33} suggesting that it is lethal when expressed from multicopy plasmids. Growth curves were obtained as before for the $tRNA_{CAG}^{Ser}$ mutant genes (figure 2.26).

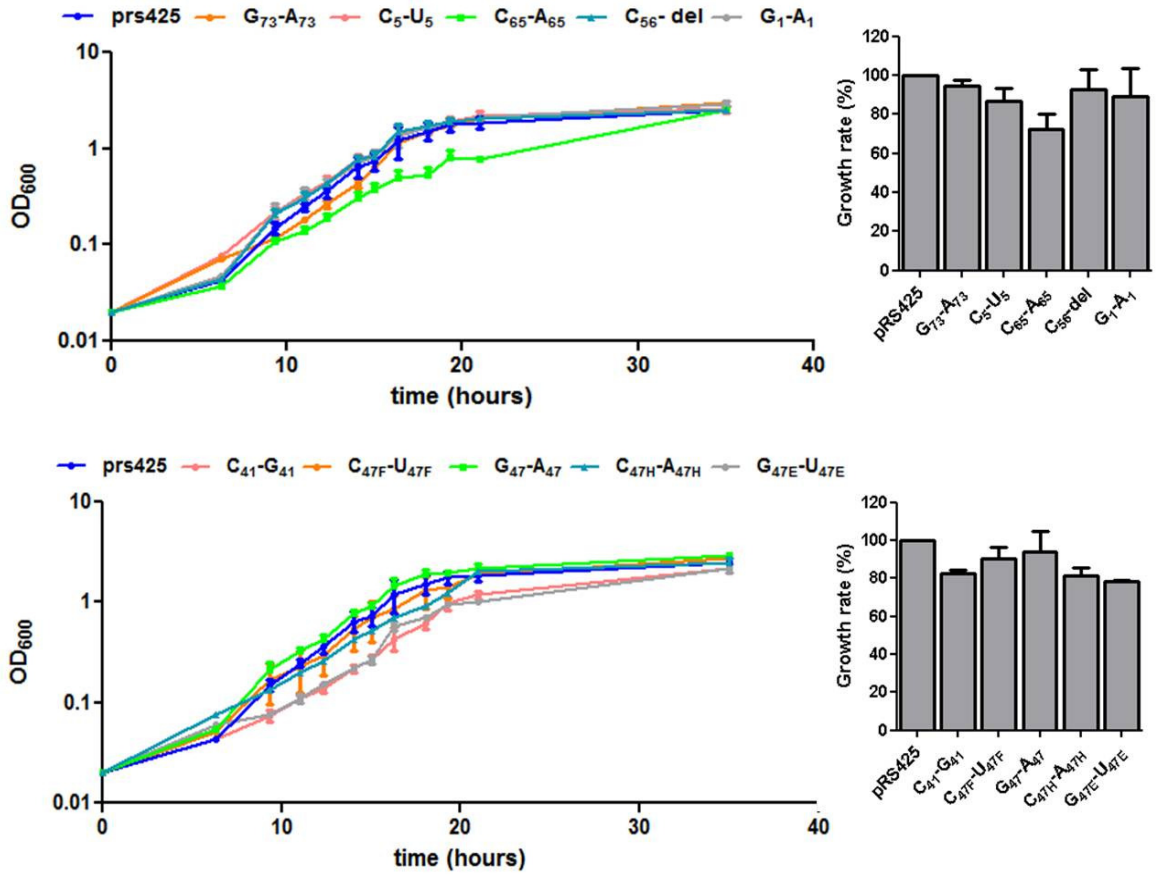

Figure 2.26: Mutant $tRNA_{CAG}^{Ser}$ expressed from multicopy plasmids do not affect yeast growth. Yeast cultures were inoculated at an initial OD of 0.02 and were grown at 30ºC in 100 ml culture flasks in minimal medium without Leu until late stationary phase. pRS425 correspond to control cells transformed with the empty plasmid. The relative growth rate of cells transformed with mutant $tRNA_{CAG}^{Ser}$ was determined using exponential growth phase values, relative to the control cells (pRS425). Data represent the mean ± s.e.m. of 3-5 independent experiments (one-way Anova post Bonferroni's multiple comparison test with CI of 95%, relative to the pRS425 control cells).

All mutant $tRNA_{CAG}^{Ser}$ decreased growth rate slightly relative to cells transformed with the empty plasmid (100% growth rate). In other words, the mutant $tRNA_{CAG}^{Ser}$ expressed from single-copy genes integrated into the yeast genome or from multicopy plasmids had similar impact on growth rate.

The level of each mutant $tRNA_{CAG}^{Ser}$ expressed from the multicopy plasmids was then checked by northern blot analysis (figure 2.27). As for the mutant $tRNA_{CAG}^{Ser}$ integrated into the yeast genome, the diploid cells expressing them from multicopy plasmids did not show detectable level of $tRNA_{CAG}^{Ser}$. The only exceptions were $C_{41}\rightarrow G_{41}$ and $G_{73}\rightarrow A_{73}$ mutants, which produced faint bands in the northern blots, indicating that the mutations affect $tRNA_{CAG}^{Ser}$ stability or may block transcription.

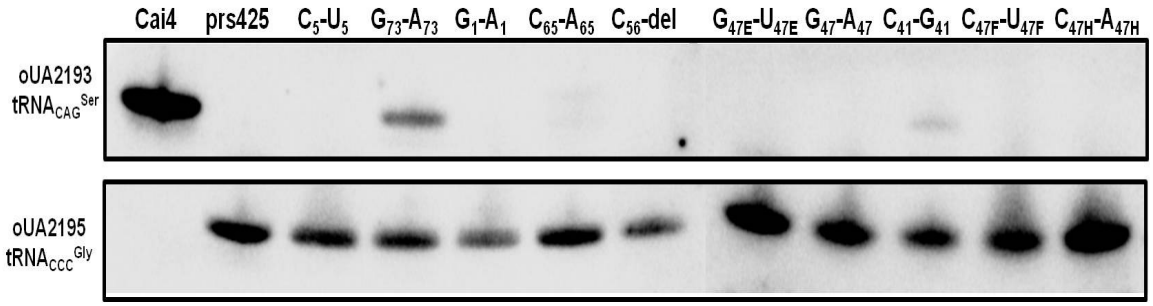

Figure 2.27: Northern blot analysis of *C. albicans* mutant $tRNA_{CAG}^{Ser}$ expressed from multicopy plasmids in diploid yeast cells. 50 µg of tRNAs extracted and purified under acidic conditions were fractionated on 12% polyacrylamide gels containing 8M urea at room temperature. Detection of $tRNA_{CAG}^{Ser}$ and $tRNA_{CCC}^{Gly}$ was carried out using γ-^{32}P-ATP-$tRNA_{CAG}^{Ser}$ and γ-^{32}P-ATP-$tRNA_{CCC}^{Gly}$ probes. Cai4 corresponds to *C. albicans* total tRNA extract and wt corresponds to tRNAs extracted from yeast cells transformed with the empty plasmid pRS425. Membranes were exposed for 24 hours to a K-screen and were visualized using Bio-Rad Molecular Imager FX.

.

2.3.9. Stability and serylation of the mutant $tRNA_{CAG}^{Ser}$ synthesized *in vitro*

Since most of the mutants $tRNA_{CAG}^{Ser}$ were not detected by northern blot analysis we decided to check their serylation efficiency. For this, the mutants $tRNA_{CAG}^{Ser}$ genes were subcloned into the plasmid pUKC1304 (containing $tRNA_{CAG}^{Ser}$ U_{33} for *in vitro* transcription) (Perreau et al., 1999) for *in vitro* transcription (section 2.2.3). The $G_1\rightarrow A_1$

and C_{56}-deletion mutant $tRNA_{CAG}^{Ser}$ were excluded from *in vitro* characterization because we had strong evidences that these tRNAs did not fold correctly and were non-functional.

The serylation efficiency of the mutant $tRNA_{CAG}^{Ser}$ showed accentuated decrease in mutant tRNAs relative to Wt $tRNA_{CAG}^{Ser}$ (figure 2.28). Mutants $G_{73}\rightarrow A_{73}$, $G_{47E}\rightarrow A_{47E}$ and $C_{47F}\rightarrow U_{47F}$ showed the highest serylation efficiencies, although the values were three times lower than those of the Wt $tRNA_{CAG}^{Ser}$. The $C_{41}\rightarrow G_{41}$ mutant was not serylated and the other mutants exhibited low serylation levels, suggesting that the lack of toxicity of the mutant tRNAs may be related to aminoacylation deficiency likely due to decreased $tRNA_{CAG}^{Ser}$ affinity for the SerRS.

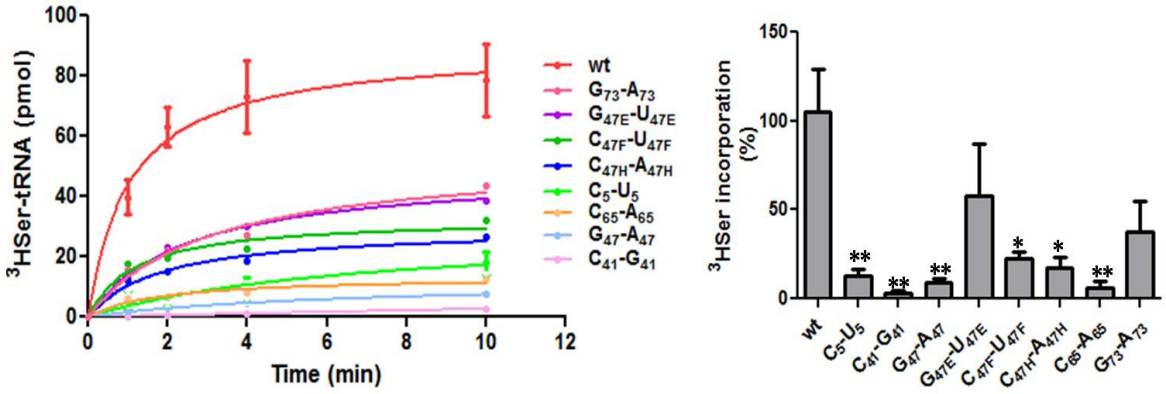

Figure 2.28: Serylation of *C. albicans* Wt and mutant $tRNA_{CAG}^{Ser}$ with *C. albicans* SerRS. ^{3}H-Serine acceptance of *in vitro* synthesized wt and mutant $tRNA_{CAG}^{Ser}$ with recombinant purified *C. albicans* SerRS was determined at 30ºC *in vitro*. The graph represents the incorporation of 3H-Ser of each tRNA. Data represent the mean ± s.e.m. of 3 independent experiments (*p < 0.05, **p < 0.01 one-way Anova post Bonferroni's multiple comparison test wit CI 95%, relatively to wt tRNA).

In order to determine whether the mutations affected the $tRNA_{CAG}^{Ser}$ folding and stability they were thermally denatured and the melting profiles were compared to those of Wt $tRNA_{CAG}^{Ser}$ (section 2.2.4). The thermal denaturation curves of the mutant and Wt $tRNA_{CAG}^{Ser}$ were very similar (figure 2.29), only $C_{41}\rightarrow G_{41}$ showed a slight difference in the melting profile. However, we have observed atypical thermal denaturation curves for the mutant $tRNA_{CAG}^{Ser}$ lacking the shape profile, which prevented determination of the melting temperature of each mutant tRNA (Hao et al., 2004; Jones et al., 2008; Yarian et al., 1999). This suggests that the folding *in vitro* may not be as expected, but we cannot

exclude a technical problem because the denaturation profile of the Wt transcript was also atypical (figure 2.28).

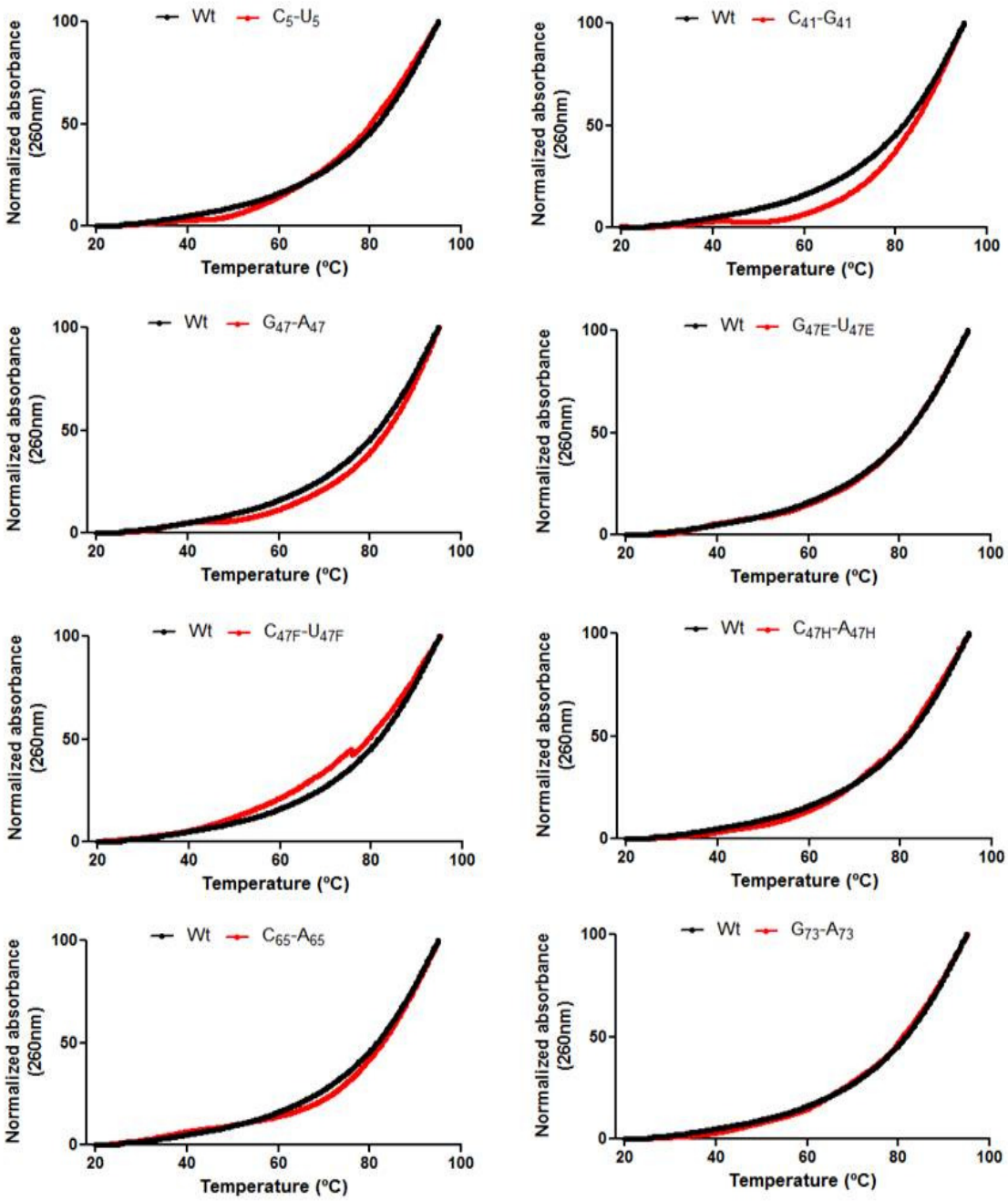

Figure 2.29: Thermal denaturation of the mutant $tRNA_{CAG}^{Ser}$. *In vitro* synthesized tRNAs were subjected to thermal denaturation from 20 to 95ºC at a rate of 1ºC/min. UV absorbance was recorded 3 times per minute at 260 nm using a Jasco 630 spectrophotometer (section 2.2.4). Wt correspond to non-mutated $tRNA_{CAG}^{Ser}$ containing G_{33}. The absorbance was normalized to 100% for each data set.

2.4.10. U_{33} affects the expression of $tRNA_{CAG}^{Ser}$ *in vivo*

97% of the 2716 tRNA genes sequenced to date have a uridine at position 33 (U_{33}), which makes this one of the most conserved nucleotide positions in tRNAs (Sprinzl et al., 1998). The only exception to this rule is found in plant, vertebrate and cytoplasmatic initiator $tRNAi^{Met}$ which have C_{33} and in the $tRNA_{CAG}^{Ser}$ from the CTG clade which have G_{33} (Dirheimer et al., 1995). Crystal structures of yeast $tRNA^{Phe}$ and $tRNA^{Asp}$ showed that U_{33} in the anticodon loop and the ψ of TψC-loop are involved in sharp turns of the phosphodiester backbone (Ahsen et al., 1997; Ashraf et al., 1999). The U_{33} is required for the turn of the anticodon loop, known as the anticodon U-turn, which exposes the anticodon bases to the solvent to facilitate codon-anticodon interaction. Previous *in vitro* studies showed that G_{33} distorts the anticodon arm of the $tRNA_{CAG}^{Ser}$ and reduces decoding efficiency (Perreau et al., 1999), but the impact of this nucleotide was never evaluated *in vivo*. Surprisingly, the replacement of U_{33} with G_{33} in the mutant $G_{73}\rightarrow A_{73}$ $tRNA_{CAG}^{Ser}$ gene increased expression of this mutant tRNA sharply (figure 2.30), suggesting that G_{33} stabilizes this tRNA, despite its negative effect on the anticodon stem structure (Ahsen et al., 1997; Ashraf et al., 1999).

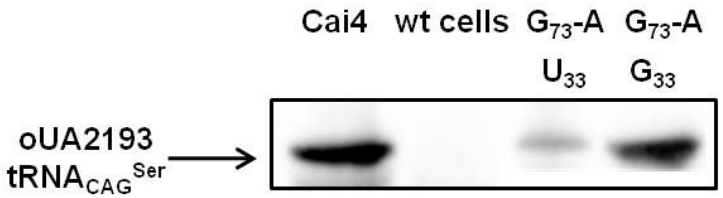

Figure 2.30.: Northern blot analysis of the *C. albicans* mutant $G_{73}\rightarrow A_{73}$ tRNA. 50 µg of tRNAs extracted and purified under acidic conditions were fractionated on 12% polyacrylamide gels containing 8M urea at room temperature. Detection of $tRNA_{CAG}^{Ser}$ was carried out using γ-^{32}P-ATP-$tRNA_{CAG}^{Ser}$ probe. Cai4 corresponds to *C. albicans* total tRNA extract and wt corresponds to tRNAs extracted from yeast cells transformed with the empty plasmid pRS425. Membranes were exposed for 24 hours to a K-screen and were visualized using Bio-Rad Molecular Imager FX.

This unexpected stabilization of the mutant $tRNA_{CAG}^{Ser}$ G_{33} prompted us to determine whether the same was happening with the other mutant $tRNA_{CAG}^{Ser}$. In order to test this hypothesis the U_{33} was replaced by G_{33} in all mutant $tRNA_{CAG}^{Ser}$ that were cloned

into multicopy plasmids. Our northern blot results (figure 2.31) confirmed that G_{33} stabilizes the $tRNA_{CAG}^{Ser}$. The mutant $tRNA_{CAG}^{Ser}$ U_{33} $C_{41}\rightarrow G_{41}$ which was expressed at low level (figure 2.27) had high expression with G_{33} (figure 2.31). A similar result was obtained for the mutant $tRNA_{CAG}^{Ser}$ $G_{73}\rightarrow A_{73}$, thus confirming that G_{33} is needed to stabilize the mutant $tRNA_{CAG}^{Ser}$ *in vivo*.

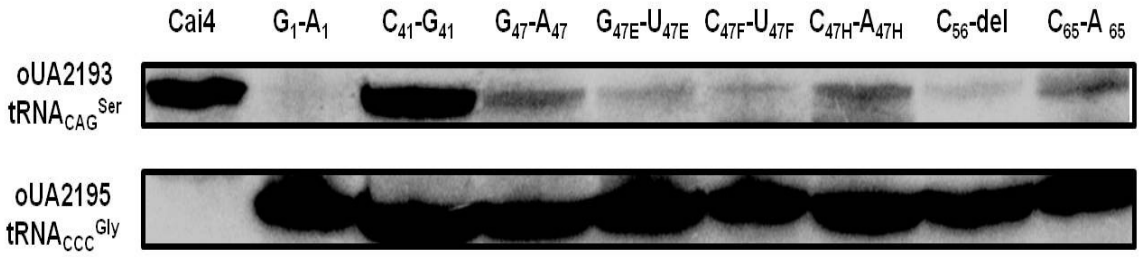

Figure 2.31.: Northern blot analysis of the *C. albicans* mutant $tRNA_{CAG}^{Ser}$ containing G_{33}. 50 µg of tRNAs extracted and purified under acidic conditions were fractionated on 12% polyacrylamide gels containing 8M urea at room temperature. Detection of $tRNA_{CAG}^{Ser}$ and $tRNA_{CCC}^{Gly}$ was carried out using γ-^{32}P-ATP-$tRNA_{CAG}^{Ser}$ and γ-^{32}P-ATP-$tRNA_{CCC}^{Gly}$ probes. Cai4 corresponds to *C. albicans* total tRNA extract. Membranes were exposed for 24 hours to a K-screen and were visualized using Bio-Rad Molecular Imager FX.

Unexpectedly, *in vitro* synthesized $tRNA_{CAG}^{Ser}$ with G_{33} and U_{33} showed no stability differences between them (figure 2.32 A). Although, the *in vitro* aminoacylation of the A_{33}, G_{33}, C_{33} and U_{33} $tRNA_{CAG}^{Ser}$ with *C. albicans* SerRS showed that the $tRNA_{CAG}^{Ser}$ G_{33} and A_{33} versions had higher serylation efficiency than C_{33} and U_{33} (figure 2.32 B). Previous results obtained with yeast cells expressing *C. albicans* mutant $tRNA_{CAG}^{Ser}$ with G_{33}, C_{33} and A_{33} showed that the $tRNA_{CAG}^{Ser}$ C_{33} was expressed at low level and decreased slightly yeast growth, while A_{33} and G_{33} versions were expressed at higher level and decreased yeast growth more sharply (Santos et al., 1996).

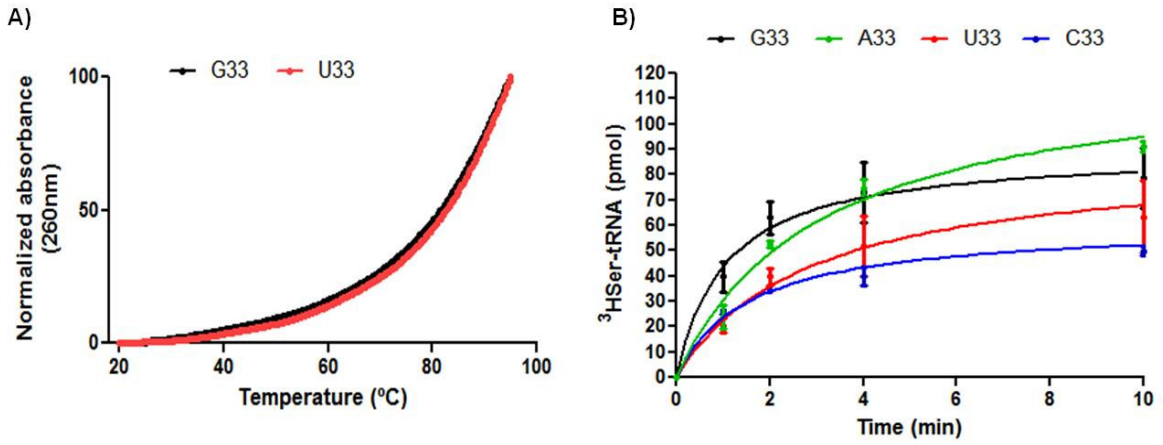

Figure 2.32.: Stability and serylation of the *C. albicans* mutant $tRNA_{CAG}^{Ser}$ transcripts containing A_{33}, G_{33}, C_{33} and U_{33}. A) $tRNA_{CAG}^{Ser}$ transcripts containing G_{33} and U_{33} were subjected to thermal denaturation from 20 to 95ºC at a rate of 1ºC/min. UV absorbance was monitored 3 times per minute at 260 nm using a Jasco 630 spectrophotometer (section 2.2.4). B) ^{3}H-Serine acceptance of $tRNA_{CAG}^{Ser}$ transcripts containing A_{33}, G_{33}, C_{33} and U_{33} using purified SerRS from *C. albicans*.

2.4. Discussion

We have reconstructed *in vivo* the evolutionary pathway of the *C. albicans* CUG reassignment in the close relative *S. cerevisiae*. Our results demonstrate that *C. albicans* Wt $tRNA_{CGA}^{Ser}$ does not affect yeast growth rate, is not toxic and is stably expressed and aminoacylated. Conversely, expression of the three mutant $tRNA_{CGA}^{Ser}$ representing intermediate steps of the CUG reassignment pathway had a strong negative impact on yeast growth rate, due to mistranslation of the Leu CUG codon as Ser, as demonstrated by our β-gal assays. The level of toxicity was dependent upon tRNA decoding efficiency. We have also demonstrated that the mutant tRNAs were expressed at low level in yeast cells, but our data is insufficient to clarify the molecular mechanism that regulates the cellular abundance (expression) of the mutant $tRNA_{CGA}^{Ser}$. These data strongly suggest that this genetic code alteration was not eliminated by natural selection, because repression of the expression of the new mistranslating $tRNA_{CGA}^{Ser}$ reduced its toxicity and consequently the initial impact of Ser-mistranslation on fitness was also low. Therefore, unraveling this putative novel tRNA turnover pathway is essential to further understand

tRNA metabolism in general and to further clarify the reassignment pathway of CUG codons from Leu-to-Ser.

The $tRNA_{CAG}^{Ser}$ mutations identified *in vivo* through our forced evolution methodology provide further evidence for a critical role of $tRNA_{CAG}^{Ser}$ stability in the evolution of CUG reassignment. Indeed, the identified mutations affected aminoacylation efficiency, but the most stricking phenotype was again the low expression level of these tRNAs.

Interestingly, the $tRNA_{CAG}^{Ser}$ $G_{73}\rightarrow A_{73}$ and $C_{41}\rightarrow G_{41}$, which were the most highly expressed mutant $tRNA_{CAG}^{Ser}$ in the *in vivo* multicopy system, were also those with the highest and lowest serylation efficiency *in vitro*, respectively. The absence of tRNA modifications likely interferes with tRNA secondary and tertiary structures, folding and thus tRNA function (Gustilo et al., 2008), as has been demonstrated for other tRNAs, and interpretation of our results needs to take this fact into consideration. Indeed, in yeast $tRNA^{Phe}$ the conserved modifications m^5C49, rT54 and ψ55 are important for tRNA D and TψC arm interaction (Helm, 2006; Nobles et al., 2002) and some tRNA modifications can affect aminoacyl charging and codon recognition (Engelke & Hopper, 2006). This complicates direct comparisons and extrapolations between our *in vivo* and *in vitro* results. Nevertheless our overall data strongly suggests that $tRNA_{CAG}^{Ser}$ stability and aminoacylation efficiency were critical in the evolution of CUG reassignment.

A surprising result was the stabilization of the mutant $tRNA_{CAG}^{Ser}$ by the G_{33} instead of the U_{33} mutation. Although, previous studies from our laboratory showed that the $tRNA_{CAG}^{Ser}$ containing U_{33} is a more efficient decoder and is more toxic than $tRNA_{CAG}^{Ser}$ G_{33}. Indeed, $tRNA_{CAG}^{Ser}$ U_{33} misincorporates 2.31% of Ser while $tRNA_{CAG}^{Ser}$ G_{33} misincorporates 1.40% Ser (Silva et al., 2007). Therefore, our data suggest that $tRNA_{CAG}^{Ser}$ stability was likely the critical factor in the reassignment of CUG identity from Leu-to-Ser.

Chapter 3

Strategies and cellular consequences of engineering the yeast genetic code

3.1. Introduction

The genetic code was established in the 60' and consists of 3 stop codons and 61 codons that codify 20 canonical amino acids. The discovery of two additional amino acids, selenocysteine (Bock et al., 1991) and pyrrolysine (Srinivasan et al., 2002), the existance of post-transcriptionally modifications of the amino acids incorporated in proteins (Uy & Wold, 1977) and codon reassignments discovered in mitochondrial and cytoplasmic codes (Knight et al., 2001) demystified the theory that genetic code was universal and frozen.

The interest of altering the standard genetic code started in the 50's, with the incorporation of ethionine in rat cells (Levine & Tarver, 1951). The increased interest in expanding the code to incorporate unnatural amino acids into proteins prompted the creation of a new research area called genetic code engineering, whose main goal is to change standard genetic code rules and reprogram protein translation, creating organisms with novel genetic codes (Budisa, 2006).

In the last 20 years, various groups developed methodologies to expand the standard genetic code in bacteria, yeast and mammalian cells (Wang & Schultz, 2005). In the first study, reported by the Schultz group, non-sense suppressor tRNAs (tRNAs that read stop codons) chemically acylated with non-canonical amino acids were mixed with *E. coli* cell extracts, containing all factors required for transcription and translation, and a plasmid DNA containing the gene of interest with a nonsense codon. Successful incorporation of p-nitrophenylalanine, p-fluorophenylalanine and homophenylalanine at residue Phe66 of the β-lactamase gene was then achieved (Noren et al., 1989). Although, relatively small quantities of recombinant protein were obtained, various different amino acids and analogues were successfully incorporated into proteins using this *in vitro* approach (Ellman et al., 1991). Further improvements on chemical acylation of tRNAs allowed microinjection of these tRNAs into *Xenopus* oocytes expressing a mutant version of the nicotinic acetylcholine receptor gene. The translational machinery of the oocyte inserted efficiently phenylalanine derivatives at UAG positions, but protein yield was again low due to rapid exhaustion of the acylated suppressor tRNA during translation. Lack of acylated tRNA regeneration was the main limitation of this method (Nowak et al., 1995).

The obvious limitations of the *in vitro* system prompted the development of methodologies to incorporate unnatural amino acids directly into proteins *in vivo*. This improved the yield of mutant protein produced and increased the potential to study

proteins in cells or in multicellular organisms. This strategy required the development of a unique tRNA, containing an anticodon to could read nonsense codons, which was not recognized by endogenous aaRSs, and the development of a unique aaRS, which did not recognize other endogenous tRNAs and was able to incorporate unnatural amino acids supplemented in the culture medium (figure 3.1).

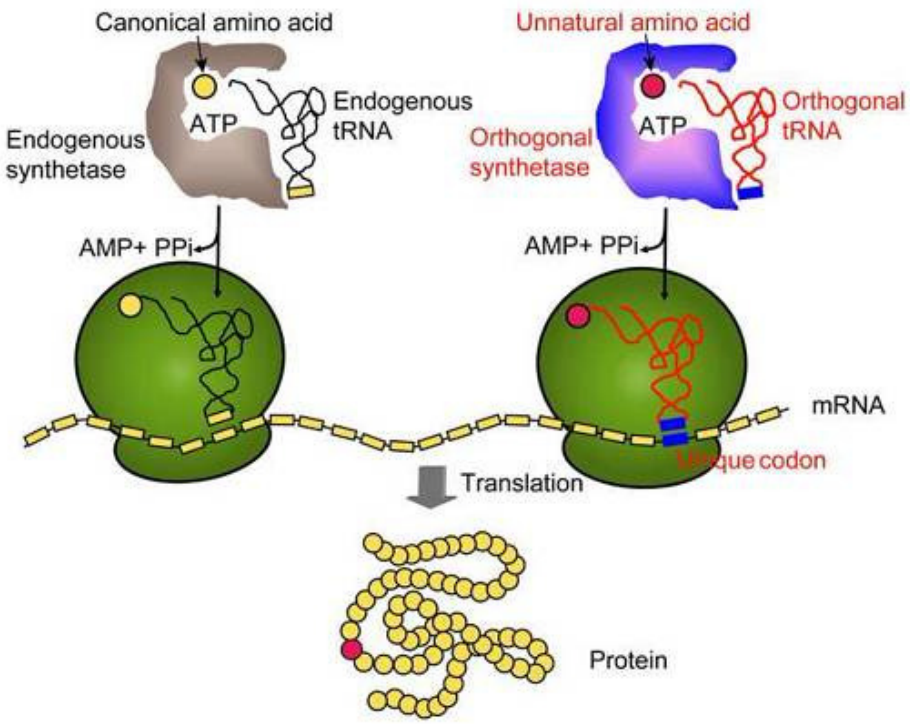

Figure 3.1: A general method to genetically encode unnatural amino acids in living cells. An engineered pair aaRS/tRNA/unnatural amino acid (represented in red) is used in cells to incorporate non canonical amino acids into proteins. Adapted from (Wang et al., 2009b).

One of the first attempts to expand the genetic code *in vivo* was the incorporation of the synthetic amino acid O-methyl-l-tyrosine into proteins in response to an amber nonsense codon. Genes for a mutant $tRNA^{Tyr}$ and TyrRS from *Methanococcus jannaschii* were expressed in *E. coli*. Phylogenetic differences in tRNA identity elements prevented the recognition of this tRNA by *E. coli* aaRS (Wang et al., 2001). A similar strategy using orthogonal tRNA-aaRS pairs was then used to incorporate five tyrosine derivates into yeast proteins. In this case, an *E. coli* amber supressor $tRNA^{Tyr}$ and an TyrRS were used (Chin et al., 2003; Davis, 2004). More recently, pairs of $tRNA^{Tyr}$ and an TyrRS from *M. jannaschii* have been used to incorporate five unnatural amino acids in *M. smegmatis* and

M. tuberculosis, namely the photocrosslinkers p-azidophenylalanine and p-benzoylphenylalanine, the immunogenic amino acid p-nitrophenylalanine, the heavy atom containing amino acid p-iodophenylalanine, and the chemically reactive amino acid p-boronophenylalanine (Wang et al., 2010). The Schultz group has also managed to successfully incorporate unnatural amino acids into mammalian cells. For this, they manipulated the PylRS and its cognate $tRNA^{Pyl}$ from the archaeum *Methanosarcina maize* to incorporate o-nitrobenzyl-oxycarbonyl-Nε-L-lysine (ONBK) into HEK293 cells proteins in response to the amber nonsense codon (Chen et al., 2009).

Since the strategies mentioned above are limited to three codons, namely UGA, UAG and UAA, some authors attempted to expand the genetic code by using suppressor tRNAs with expanded anticodon loops (with five or four-base anticodons). Two tRNA/aaRS pair, derived from $tRNA^{Lys}$ and LysRS from *P. horikoshii*, and $tRNA^{Tyr}$-TyrRS pairs from *M. jannaschii*, were engineered to successfully incorporate L-homoglutamine and O-methyl-L-tyrosine in *E. coli*, in response to the quadruplet codon AGGA (Anderson et al., 2004; Magliery et al., 2001).

To date, more than 50 unnatural amino acids have been incorporated into *E. coli* and a dozen have been incorporated into yeast and mammalian cells. Although, this method cannot be used to incorporate unnatural amino acids that are unsuitable for the ribosome, such as D- and β-amino acids, or toxic to cells, namely amino acids analogues that can be recognized by cognate aaRSs. The benefits of incorporation of amino acid analogues that are fluorescent, photoresponsive, bio-orthogonally reactive or able to mimic various protein modifications are obvious. They are important for example, to understand cellular pathways, developmental programmes, protein signalling and moreover importantly for medical applications. Studies about genetic code alterations can provide additional insight about mRNA decoding fidelity, codon usage and reassignment in organisms, evolution of genomes and obviously to help understand the origin and evolution of the genetic code, and for these reasons genetic code engineering is attracting increasing interest from the scientific community (Wang et al., 2009b; Xie & Schultz, 2005).

Despite interest on the genetic code, the natural reassignment of codons is still poorly studied. Until now, despite the interest in understanding how and why genetic code alterations occurred, their evolutionary implications are far from being understood.

In our laboratory we are interested in understanding how and why the identity of the CUG codon was altered from Leu to Ser. This amino acid substitution is an unlikely event due to the distinct chemical properties of both amino acids, and therefore this is a highly unlikely genetic code alteration. Other studies from our laboratory have already demonstrated that misincorporation of Ser at Leu CUG codons reduces growth rate, but, under some stressful environmental conditions mistranslating cells can still have selective advantage (Santos et al., 1996; Santos et al., 1999). This suggests that genetic code alterations should be studied, and probably can only be understood in ecological and adaptative contexts.

In this chapter of this thesis we focus on engineering various genetic code reassignments in order to better understand the evolution of genetic code alterations. We were particularly motivated by the question of whether genetic code alterations could be engineered to reassigned codons involving similar amino acids, and also by the question of whether different amino acids reassignments could generate distinct selective advantages. For this, we have induced Ser misincorporation at various codons belonging to distinct amino acids families, using a tRNA engineering strategy based on creation of alternative anticodons in $tRNA_{UGA}^{Ser}$. We have created 8 mutant $tRNA^{Ser}$ that could misincorporate Ser at 8 distinct codons. The phenotypic consequences of these codon mistranslations were evaluated at the phenotypic and cellular levels using fitness and viability tests, organelle alterations, oxidative stress, protein aggregation, protein synthesis and also growth rate under various physiological conditions. Our data show that the cellular consequences of Ser misincorporation at different codons induce distinct phenotypic alterations that in some cases are beneficial and have adaptive potential.

3.2. Material and methods

3.2.1. Strains and growth conditions

E. coli, JM109 and DH5α, were grown at 37ºC in LB medium (formedium) supplemented with ampicilin (50 µg/ml). *S. cerevisiae* BY4743 strain (*MAT*a/α *his3Δ1/his3Δ1,leu2Δ0/leu2Δ0,LYS2/lys2Δ0,met15Δ0/MET15,ura3Δ0/ura3Δ0)* was grown at 30ºC in YPD (glucose: 2% (w/v), yeast extract: 0.5% (w/v) and peptone: 1%

(w/v)) (Formedium) or minimal medium (glucose: 2% (w/v), yeast nitrogen base without amino acids 0.67% (w/v), each required amino acids (100 µg/ml)) (Formedium).

3.2.2. Cloning of the *C. albicans* $tRNA_{UGA}^{Ser}$ in yeast pRS315 and pRS425 vectors

To select the *C. albicans* $tRNA^{Ser}$ for this study we have followed two criteria: the absence of an intron in the $tRNA^{Ser}$ gene and the existence of nucleotide mismatches between the *C. albicans* $tRNA^{Ser}$ and the homologous $tRNA^{Ser}$ from *S. cerevisiae*. This was important to allow us to monitor expression of the recombinant $tRNA^{Ser}$ by northern blot analysis. From the four $tRNA^{Ser}$ of *C. albicans* ($tRNA_{GCU}^{Ser}$, $tRNA_{CGA}^{Ser}$, $tRNA_{AGA}^{Ser}$ and $tRNA_{UGA}^{Ser}$) the $tRNA_{GCU}^{Ser}$ and the $tRNA_{CGA}^{Ser}$ were excluded because they contain an intron, the $tRNA_{AGA}^{Ser}$ was also excluded because its sequence differs in 2 mismatches from the homologous $tRNA_{AGA}^{Ser}$ from *S. cerevisiae*. Hence, the $tRNA_{UGA}^{Ser}$ was selected for this study because it does not contain an intron and when aligned to the homologous $tRNA_{UGA}^{Ser}$ from *S. cerevisiae* contains 14 nucleotide mismatches, which allow for its easy detection in *S. cerevisiae* by northern blot analysis. For heterologous expression of the *C. albicans* $tRNA_{UGA}^{Ser}$ gene in *S. cerevisiae* we have used the strategy that we use previously (chapter 2) to express the $tRNA_{CGA}^{Ser}$ (described in section 2.2.2.1). Briefly, a genomic DNA fragment of 285 bp containing the *C. albicans* $tRNA_{UGA}^{Ser}$ gene (annex I), was amplified by PCR using the oligonucleotides oUA2133 and oUA2134 (table 3.1) and was cloned into the yeast single copy pRS315 vector yielding the plasmid pUA261. The same tRNA gene was cloned into the yeast multicopy vector pRS425 yielding the plasmid pUA252 (table 3.2).

3.2.3. Construction of mutant $tRNA^{Ser}$ genes

tRNAs with degenerated anticodons were constructed by site directed mutagenesis (SDM) of the $tRNA_{UGA}^{Ser}$ gene cloned into plasmids pUA252 and pUA261, as described in section 2.2.2.1. The oligonucleotides used to introduce the anticodons CAG (Leu), GUA (Tyr), UUU (Lys), CGU (Thr), CAC (Val), UAU (Ile), UGC (Ala) and UCC (Gly) in Ser-$tRNA_{UGA}^{Ser}$ are mentioned in table 3.1, and the plasmids constructed are described in table 3.2.

Table 3.1: List of oligonucleotides used to construct mutant tRNA's

Name	Tm (ºC)	Sequence
$tRNA_{UGA}^{Ser}$ cloning into yeast pRS315 and pRS425		
oUA2133	60ºC	CGCGTCGACGTCCAGGACTGATTTATGTGCATC
oUA2134	60ºC	CGCGGATCCCAGTATGGATTGCTAGTCCTAGAG
tRNA isoacceptors produced by site directed mutagenesis of the $tRNA_{UGA}^{Ser}$ gene:		
$tRNA_{CAG(Leu)}^{Ser}$		
oUA2137	55ºC	GGTTAAGGAGAAAGACTCAGAATCTTTTGGGCTTTGC
oUA2138	55ºC	GCAAAGCCCAAAAGATTCTGAGTCTTTCTCCTTAACC
$tRNA_{GUA(Tyr)}^{Ser}$		
oUA2145	55ºC	GGTTAAGGAGAAAGACTGTAAATCTTTTGGGCTTTGC
oUA2146	55ºC	GCAAAGCCCAAAAGATTTACAGTCTTTCTCCTTAACC
$tRNA_{UUU(Lys)}^{Ser}$		
oUA2147	55ºC	GGTTAAGGAGAAAGACTTTTAATCTTTTGGGCTTTGC
oUA2148	55ºC	GCAAAGCCCAAAAGATTAAAAGTCTTTCTCCTTAACC
$tRNA_{CGU(Thr)}^{Ser}$		
oUA2153	55ºC	GGTTAAGGAGAAAGACTCGTAATCTTTTGGGCTTTGC
oUA2154	55ºC	GCAAAGCCCAAAAGATTACGAGTCTTTCTCCTTAACC
$tRNA_{CAC(Val)}^{Val}$		
oUA2155	55ºC	GTTAAGGAGAAAGACTCACAATCTTTTGGGCTTTG
oUA2156	55ºC	CAAAGCCCAAAAGATTGTGAGTCTTTCTCCTTAAC
$tRNA_{UAU(Ile)}^{Ser}$		
oUA2157	55ºC	GTTAAGGAGAAAGACTTATAATCTTTTGGGCTTTG
oUA2158	55ºC	CAAAGCCCAAAAGATTATAAGTCTTTCTCCTTAAC
$tRNA_{UGC(Ala)}^{Ser}$		
oUA2159	55ºc	GTTAAGGAGAAAGACTTGCAATCTTTTGGGCTTTG
oUA2160	55ºC	CAAAGCCCAAAAGATTGCAAGTCTTTCTCCTTAAC
$tRNA_{UCC(Gly)}^{Ser}$		
oUA2163	55ºC	GTTAAGGAGAAAGACTTCCAATCTTTTGGGCTTTG
oUA2164	55ºC	CAAAGCCCAAAAGATTGGAAGTCTTTCTCCTTAAC
Probe to detect wt and mutants versions of the $tRNA_{UGA}^{Ser}$ by northern blot analysis		
oUA2199	51.5ºC	TTAACCGCTCGGACAAGTT

Table 3.2: List of plasmids constructed in this work

Name	Description
pUA252	pRS425 plasmid containing one copy of *C. albicans* $tRNA_{UGA}^{Ser}$ gene cloned between BamHI and SalI restriction sites. For $tRNA_{UGA}^{Ser}$ expression in *S. cerevisiae*.
pUA253	Plasmid based on pUA252. Was constructed by SDM of the $tRNA_{UGA}^{Ser}$ gene and originated $tRNA_{CAG(Leu)}^{Ser}$. For multicopy expression of mutant mistranslating $tRNA^{Ser}$ (Leu) in *S. cerevisiae*.
pUA254	Plasmid based on pUA252. Was constructed by SDM of the $tRNA_{UGA}^{Ser}$ gene and originated $tRNA_{GUA(Tyr)}^{Ser}$. For multicopy expression of mutant mistranslating $tRNA^{Ser}$(Tyr) in *S. cerevisiae*.
pUA255	Plasmid based on pUA252. Was constructed by SDM of the $tRNA_{UGA}^{Ser}$ gene and originated $tRNA_{UUU(Lys)}^{Ser}$. For multicopy expression of mutant mistranslating $tRNA^{Ser}$(Lys) in *S. cerevisiae*.
pUA256	Plasmid based on pUA252. Was constructed by SDM of the $tRNA_{UGA}^{Ser}$ gene and originated $tRNA_{CGU(Thr)}^{Ser}$. For multicopy expression of mutant mistranslating $tRNA^{Ser}$(Thr) in *S. cerevisiae*.
pUA257	Plasmid based on pUA252. Was constructed by SDM of the $tRNA_{UGA}^{Ser}$ gene and originated $tRNA_{CAC(Val)}^{Ser}$. For multicopy expression of mutant mistranslating $tRNA^{Ser}$(Val) in *S. cerevisiae*.
pUA258	Plasmid based on pUA252. Was constructed by SDM of the $tRNA_{UGA}^{Ser}$ gene and originated $tRNA_{UAU(Ile)}^{Ser}$. For multicopy expression of mutant mistranslating $tRNA^{Ser}$(Ile) in *S. cerevisiae*.
pUA259	Plasmid based on pUA252. Was constructed by SDM of the $tRNA_{UGA}^{Ser}$ gene and originated $tRNA_{UGC(Ala)}^{Ser}$. For multicopy expression of mutant mistranslating $tRNA^{Ser}$(Ala) in *S. cerevisiae*.
pUA260	Plasmid based on pUA252. Was constructed by SDM of the $tRNA_{UGA}^{Ser}$ gene and originated $tRNA_{UCC(Gly)}^{Ser}$. For multicopy expression of mutant mistranslating $tRNA^{Ser}$(Gly) in *S. cerevisiae*.
pUA261	pRS315 plasmid containing one copy of *C. albicans* $tRNA_{UGA}^{Ser}$ gene cloned

	between BamHI and SalI restriction sites. For $tRNA_{UGA}^{Ser}$(Ser) expression in *S. cerevisiae*
pUA262	Plasmid based on pUA261. Was constructed by SDM of the $tRNA_{UGA}^{Ser}$ gene and originated $tRNA_{CAG(Leu)}^{Ser}$. For single-copy expression of mutant mistranslating $tRNA^{Ser}$(Leu) in *S. cerevisiae*.
pUA263	Plasmid based on pUA261. Was constructed by SDM of the $tRNA_{UGA}^{Ser}$ gene and originated $tRNA_{GUA(Tyr)}^{Ser}$. For single-copy expression of mutant mistranslating $tRNA^{Ser}$(Tyr) in *S. cerevisiae*.
pUA264	Plasmid based on pUA261. Was constructed by SDM of the $tRNA_{UGA}^{Ser}$ gene and originated $tRNA_{UUU(Lys)}^{Ser}$. For single-copy expression of mutant mistranslating $tRNA^{Ser}$(Lys) in *S. cerevisiae*.
pUA265	Plasmid based on pUA261. Was constructed by SDM of the $tRNA_{UGA}^{Ser}$ gene and originated $tRNA_{CGU(Thr)}^{Ser}$. For single-copy expression of mutant mistranslating $tRNA^{Ser}$(Thr) in *S. cerevisiae*.
pUA266	Plasmid based on pUA261. Was constructed by SDM of the $tRNA_{UGA}^{Ser}$ gene and originated $tRNA_{CAC(Val)}^{Ser}$. For single-copy expression of mutant mistranslating $tRNA^{Ser}$(Val) in *S. cerevisiae*.
pUA267	Plasmid based on pUA261. Was constructed by SDM of the $tRNA_{UGA}^{Ser}$ gene and originated $tRNA_{UAU(Ile)}^{Ser}$. For single-copy expression of mutant mistranslating $tRNA^{Ser}$(Ile) in *S. cerevisiae*.
pUA267	Plasmid based on pUA261. Was constructed by SDM of the $tRNA_{UGA}^{Ser}$ gene and originated $tRNA_{UGC(Ala)}^{Ser}$. For single-copy expression of mutant mistranslating $tRNA^{Ser}$(Ala) in *S. cerevisiae*.
pUA269	Plasmid based on pUA261. Was constructed by SDM of the $tRNA_{UGA}^{Ser}$ gene and originated $tRNA_{UCC(Gly)}^{Ser}$. For single-copy expression of mutant mistranslating $tRNA^{Ser}$(Gly) in *S. cerevisiae*.

3.2.4. Yeast fitness assays

Yeast growth curves were obtained from cell cultures grown in 100 ml Erlenmeyer flasks by inoculating cultures to an initial OD_{600}=0.02. At various time points aliquots of the cultures were taken and OD_{600} was measured. Growth rate corresponds to growth of yeast cells in exponential phase and was calculated for each mutant tRNA relative to control cells (transformed with empty plasmids pRS315 or pRS425).

Transformation efficiency of mutant tRNA genes expressed from single-copy plasmids was calculated as follows: number of transformants/1 µg plasmid/10^8 cells, normalized to the number of transformants obtained for the control plasmid (pRS315).

3.2.5. tRNA detection by northern blot analysis

250 ml of yeast cell cultures grown until middle exponential phase were harvested and frozen at -80ºC overnight. RNA was extracted as described in section 2.2.7.1.

In order to detect tRNAs expression by northern blot analysis we have followed the protocol (Español, unpublished) described in section 2.2.7.2. The probe used to detect mutant and Wt $tRNA_{UGA}^{Ser}$ was oUA2199 (table 3.1), while the positive control $tRNA_{CCC}^{Gly}$ was detected using the probe oUA2195 (table 2.8).

3.2.6. β-Galactosidase assays

Yeast cells transformed with the empty plasmid (pRS315) and the plasmids containing the wt $tRNA_{UGA}^{Ser}$ and the mutant tRNAs genes whose tRNAs misincorporated Ser at Leu, Tyr, Lys, Thr, Val, Ile, Ala and Gly codons were co-transformed with the pUKC815 plasmid, which contains the yeast phosphoglycerate kinase (PGK1) gene promoter plus the N-terminal 33 aminoacids of this gene fused in frame to the *E. coli* lacZ gene which encodes β-galactosidase (β-gal) (Stansfiled et al., 1995). Yeast cells expressing both vectors were selected in minimal medium -Leu-Ura.

β-gal thermoinactivation was monitored directly in *S. cerevisiae* cells as described previously (section 2.2.6), with few modifications. Middle exponentially growing *S. cerevisiae* double transformants (OD_{600}=0.5-0.7) were incubated at 47ºC for different periods of time, 0, 2, 4, 6, 8, 12 and 16 min and, relative β-Gal thermoinactivation for each strain was calculated as the percentage of variation of β-gal activity at each time point, relative to cells that were not incubated at 47ºC (Santos et al., 1996).

3.2.7. Cell death quantification

Cell death was determined using two distinct methods, namely the propidium iodide (PI) labeling and CFU tests. For PI method, cells ($1x10^6$) were collected, washed and ressuspended in 1X PBS. PI (0.5 mg/ml) was added to cells to a final concentration of 5 ng/µl. Cells were incubated in the dark, at 30ºC during 20 min and were washed twice with 1X PBS and analyzed by flow cytometry. Quantification of PI positive cells was carried out using FlowJo software.

In the CFUs test ~100 cells were plated in each agar plate and colonies were counted after 3 days of growth. Cell death was determined by the number of colonies relative to the plated cells.

3.2.8. Cell cycle analysis

The cell cycle was analysed by flow cytometry as described previously (Almeida et al., 2007b), with some modifications. For this, cells ($1x10^6$) were harvested, washed, fixed with ethanol 70% at 4ºC for 30 min, washed twice with sodium citrate 50 mM pH 7.5 and ressuspended in 800 µl of the same buffer. Cells were then treated at 50ºC for 1 hour with RNase A (2 mg/ml) to a final concentration of 0.25 mg/ml, followed by 1 mg/ml of Proteinase K, during 1 hour at 50ºC. The DNA (50 µl of previous sample) was stained with 1 µl of SYBR Green 10000x (diluted 10X in Tris-EDTA, pH 8.0) (Molecular Probes) at 4ºC, overnight, and cells were then sonicated (3 cycles 30W 2 seconds) after addition of 300 µl of Triton X-100 (0.25% v/v in 50 mM of sodium citrate buffer pH 7.5), and were analyzed

by flow cytometry. Determination of the cell cycle was carried out using the MODFIT LT software (Verity Software house).

3.2.9. Quantification of intracellular reactive oxygen species (ROS)

ROS were quantified with dihydrorhodamine 123 (DHR123) (Molecular Probes) and dihydroethidium (DHE) (Molecular Probes) as described previously (Almeida et al., 2007a). Briefly, for DHR123 labeling ~$1x10^6$ cells were collected, washed and ressuspended in 1X PBS. DHR123 (1 mg/ml in ethanol) was added to cells to a final concentration of 15 µg/ml. Cells were then incubated in the dark, at 30ºC during 90 min and were washed twice with 1X PBS and analyzed by flow cytometry. For quantification with DHE, cells ($1x10^6$) were collected, washed and ressuspended in 1X PBS. DHE (2.5 mg/ml in ethanol) was added to cells to a final concentration of 10 µg/ml. Cells were then incubated in the dark, at 30ºC during 10 min and after that washed twice with 1X PBS and analyzed by flow cytometry. Quantification of ROS level was carried out using FlowJo software.

3.2.10. Tunel assay for detection of yeast apoptosis

Evaluation of cell death was carried out using the Tunel method as described elsewere (Ludovico et al., 2001) with few modifications. DNA strand breaks were determined with *in situ* Cell Death Detection Kit (Roche). For this, $1x10^6$ yeast cells were collected, washed and fixed in 3.7% formaldehyde at room temperature for 45 min. After fixation, cells were washed three times and the cell wall was digested with 10 U/ml lyticase (Sigma), at 37ºC, during 15 min in phosphate-citrate buffer (0.2 M, 0.1 M pH 5.8). Cells were then washed and cytospins were prepared. Slides were rinsed with 1X PBS, incubated with permeabilization solution (0.1% (v/v) Triton-X 100 and 0.1% (p/v) sodium citrate) for 2 minutes on ice and rinsed twice with 1X PBS. 10 µl of the TUNEL mixture (terminal deoxynucleotidyl transferase and FITC-dUTP) was added and slides were incubated in a humidified chamber at 37ºC during 1 hour. Slides were then rinsed 3 times with 1X PBS and were incubated for 30 minutes at 37ºC in the dark with PI (50 µg/ml) and

RNase A (12.5 μg/ml). Slides were finally rinsed twice with 1X PBS and a drop of the anti-fading agent vectashield (Molecular Probes) was added before visualization in epifluorescente microscope (Olympus).

3.2.11. Mitochondria visualization

Mitochondrial morphology was assessed with MitoTracker Red CM-H2XRos as previously described (Ludovico et al., 2002) with few modifications. For this, $1x10^6$ yeast cells were collected, washed and ressuspended in 1X PBS. MitoTracker Red CM-H2XRos (Molecular Probes) was added to a final concentration of 0.5 μg/ml and cells were incubated for 30 min at 30ºC in the dark. Cells were then washed with 1X PBS and placed on a glass slide with a drop of the anti-fading agent vectashield (Molecular Probes) before visualization using confocal microscopy (Olympus Fluoview microscope) with a 60X oil objective. Images were analyzed with Olympus Fluoview advanced software.

3.2.12. Vacuole visualization

Vacuole morphology was visualized by taking $1x10^6$ yeast cells and resuspending them in 250 μl of YPD + 80 μM FM4-64 (Molecular Probes), prepared in dimethyl sulphoxide. Cells were then incubated for 30 min at 30ºC, washed once in YPD, incubated for 1h at 30ºC in YPD and were finally collected, placed on a glass slide with a drop of the anti-fading agent vectashield (Molecular Probes) and were visualized by confocal microscopy (Olympus Fluoview microscope) with a 60X oil objective (Belem Sampaio, unpublished). Images were analyzed with Olympus Fluoview advanced software.

3.2.13. DAPI staining

Nuclear morphological alterations were analyzed by microscopy after labeling with 4,6-diamino-2-phenyl-in-dole dihydrochloride (DAPI) staining, as described previously

(Almeida et al., 2007b). For this, cells ($1x10^6$) were collected, washed and ressuspended in 1X PBS. Next, DAPI (Molecular Probes) was added at a final concentration of 0.5 µg/ml and cells were further incubated in the dark for 10 min at room temperature, followed by washing with 1X PBS. Stained cells were visualized by confocal microscopy (Olympus Fluoview microscope) with a 60X oil objective and images were analyzed with Olympus Fluoview advanced software.

3.2.14. Insoluble protein quantification

The aggregation of soluble proteins was analyzed as described elsewere (Rand & Grant, 2006) with few modifications. Yeast cells ($3x10^8$) grown until middle exponential phase were collected, washed, resuspended in 300 µl of lysis buffer (50 mM potassium phosphate buffer pH 7, 1 mM EDTA, 5% (vol/vol) glycerol, 1 mM phenylmethylsulfonyl fluoride, and Complete Mini protease inhibitor cocktail (Roche)) plus 7.5 µl Lyticase (20 mg/ml) (Sigma) and incubated 30 min at 37ºC. About 2/3 of glass beads were added and cells were disrupted using the Precellys disrupter (5 cycles of 10 sec 5000 rpm + 2 min on ice). Disrupted cells were then centrifuged at 3000xg for 15 min to remove intact cells. Next, the membrane and aggregated proteins were isolated by high speed centrifugation at 15000xg for 20 min. The membrane proteins were then removed by washing with 320 µl of lyses buffer containing 80 µl of 10% Triton –X100 and centrifugation at 15000xg for 20 min. The final aggregated protein extract was ressuspended in lyses buffer and 6x sample buffer (30% glycerol, 10% SDS, 0.6 M DTT and 0.012% bromophenol blue in 0.5 M Tris-Cl/0.4% SDS, pH 6.8) and fractionated using 15% resolving acrylamide gels with 4% stacking gel. After electrophoresis, gels were stained with Coomassie Blue (0.25% Brilliant Blue R in 50% methanol and 10% acetic acid) and destained in a solution containing 25% methanol and 5% acetic acid. Gels were visualized using the Odyssey infra-red imaging system (*Li-Cor Biosciences*). Gel images obtained were analysed and the intensity of gel bands was determined with photoshop CS3 version (lasso tool and mean and pixel intensity quantification). The results are expressed as the relative percentage of insoluble protein for each sample relatively to that of the control cells (pRS315).

3.2.15. Determination of protein aggregation

Protein aggregates were analyzed as described previously (Erjavec et al., 2007). Briefly, an Hsp104-GFP fusion protein was expressed in the haploid yeast strain (MATa his3Δ1 leu2Δ0 met15Δ0 ura3Δ0) (Invitrogen) or in the diploid BY4743 strain (constructed during this thesis). In order to construct the Hsp104-GFP fusion protein the method described previously by Huh and colleagues (2003) was followed. For this, two oligonucleotides (oUA2403 and oUA2404, table 3.3) were designed to share complementary sequences to the GFP tag-marker cassette and to the C-terminal coding region of Hsp104 gene in order to construct a fusion cassette were the GFP tag was inframe fused to the C-terminal coding region of Hsp104 gene. The fusion cassette was generated by PCR using the plasmid pKT128 (pFA6a–GFP(S65T)–His3MX) as template. This plasmid contains the *S. pombe* his5 gene which is important for selection of transformants in histidine-free media, as template. The PCR products were purified using the QIAquick PCR purification kit (QIAGEN) and 1 µg of purified product was transformed into yeast BY4743 cells. Insertion of the fusion cassette by homologous recombination was confirmed by colony PCR using oUA2405 and oUA2406 primers (table 3.3). Positive clones were analyzed by fluorescence microscopy. The same strategy was used to construct the Hsp26-GFP fusion protein which was integrated into BY4743 cells. This fusion protein was constructed using the primers oUA2407 and oUA2408. Confirmation of the integration cassette was carried out using the PCR primers oUA2405 and oUA2409 (table 3.3).

Table 3.3: List of oligonucleotides used for GFP fusion proteins constriction

Name	Tm (ºC)	Sequence 5'-3'
Hsp104-GFP fusion construction		
oUA2403	57ºC	GACGATAATGAGGACAGTATGGAAATTGATGATGACCTA GATGGTGACGGTGCTGGTTTA
oUA2404	57ºC	GATTCTTGTTCGAAAGTTTTTAAAAATCACACTATATTAAA TCGATGAATTCGAGCTCG
Hsp104-GFP confirmation of fusion integration into the genome		
oUA2405	53ºC	CTTGAACATAACCTTCTGGC
oUA2406	53ºC	GACTTCTTGGCCAAATATGG

Hsp26-GFP fusion construction		
oUA2407	57ºC	GTCAAGAAGATTGAGGTTTCTTCTCAAGAATCGTGGGGT AACGGTGACGGTGCTGGTTTA
oUA2408	57ºC	GGTCCTCGCGAGAGGGACAACACTATAGAGCCAGGTCA CTTCGATGAATTCGAGCTCG
Hsp26-GFP confirmation of fusion integration into the genome		
oUA2409	53ºC	GTTTCTGGTGAAATTCCATC

Cells containing GFP fusion proteins were transformed with the mutant misreading tRNAs expressed from single-copy plasmids, and positive transformants were selected in minimal medium lacking Leu and His. Cells were grown up to middle exponential phase and were visualized using a fluorescence microscope (Zeiss) equipped with GFP and Brightfield filters and an oil-immersion objective, 100X (Zeiss). The presence of brilliant dots in cells was checked and their number was counted manually. At least 400 cells of each clone were analysed.

3.2.16. Proteasome activity quantification

Proteasome activity was quantified as described previously (Silva et al., 2007). For this, $3x10^8$ middle exponential phase cells were collected, washed and frozen at -30ºC. Cell pellets were ressuspended in 350 µl of lyses buffer (10 mM Hepes, 10 mM potassium chloride, 1.5 mM magnesium chloride), 2/3 volume of glass beads and were disrupted using a Precellys disrupter (3 cycles of 10 sec 5000 rpm + 2 min on ice between cycles). Pellets were centrifuged for 5 min at 3000xg followed by 10 min at 15000xg. Protein extracts were quantified using the BCA protein quantification kit (Pierce). 100 µg of protein extracts were ressuspended in assay buffer (10 mM Tris pH 8, 20 mM potassium chloride, 5 mM magnesium chloride) to a final volume of 2.5 ml and were incubated at 37ºC for 15 min. The proteasome substrate N-SLLVY-MCA (Sigma) was added to a final concentration of 50 µM, and cells were incubated at 37ºC during 60 min with agitation. Activity was measured using a Perkin Elmer Luminescence Spectrometer (LS 50B) at 365 nm (excitation) and 435 nm (emission). Relative proteasome activity was calculated by determining the increase of the amount of released MCA (difference between measured time 0 min and 60 min) relatively to control (pRS315) cells.

3.2.17. Protein synthesis quantification

The rate of protein synthesis was determined as described previously with minor alterations (Alamgir et al., 2008; Bernstein et al., 2007). Briefly, $2x10^8$ of middle exponential growing cells were collected, washed three times in pre-warmed minimal medium lacking Leu and Met and were ressuspended in 2 ml of the same medium. Cells were then starved for Met through incubation at 30ºC during 20 min with agitation. Then 2 µl of L- [^{35}S]-methionine (Perkin Elmer, 1175 Ci/mmol, 10.5 mCi/ml) were added and cultures were incubated for 8 min at 30ºC with agitation. Methionine incorporation was stopped by addition of 60 µl of cyclohexamide (20 mg/ml) and cells then were washed three times with cold water and frozen at -30ºC. Pellets were ressuspended in 200 µl of lysis buffer (50 mM potassium phosphate buffer pH 7, 1 mM EDTA, 5% (vol/vol) glycerol, 1 mM phenylmethylsulfonyl fluoride, and complete mini protease inhibitor cocktail (Roche) and 2/3 volume of glass beads. Cell lyses was performed using a Precellys disrupter (4 cycles of 10 sec 5000 rpm + 2 min on ice between each cycle) and extracts were centrifuged for 15 min at 3000xg and 20 min at 15000xg. 13 µl of protein extracts were applied onto GF/C filter paper disks (Whatman), dried at room temperature and the L-[^{35}S]-methionine incorporation into proteins was measured using a scintillation counter (Beckman). Protein extracts were quantified using the BCA protein quantification kit (Pierce). L- [^{35}S]-methionine incorporation was normalized to the total protein for each sample. Relative protein synthesis was calculated for each sample relatively to control (pRS315) cells.

3.2.18. Phenomics of mistranslating strains

The ability of mistranslating yeast cells to grow in different environmental conditions was determined as described by Kvitek and collaborators (2008) with few modifications. Yeast cells were grown until middle exponential phase and $1x10^8$ cells were collected and ressuspended in 1 ml of water. Six ten-fold serial dilutions were plated in minimal medium lacking Leu, supplemented with the stressors indicated in Table 3.4. Cells were plated using a liquid handling station (Caliper LifeSciences) and the diameter of the colonies was measured using Image J after 5 days of growth. The growth rate of each strain was calculated by dividing the diameter of each colony grown in the presence

of each stressor by the diameter of the control colonies grown in control medium lacking environmental stressors. These growth rate values were normalized to the corresponding growth rate of the control (pRS315 or pRS425) strain, producing the relative growth rate of each strain in each specific stress condition. A final percentual growth score was obtained by calculating the median growth rate of all dilutions for the same strain in each stress condition.

Table 3.4: List of environmental stressors and respective concentrations used.

Stress compound	Concentration
Caffeine	2 mM and 10 mM
Calcium chloride	0.5 M and 0.75 M
Cadmium chloride	50 µM and 100 µM
Copper sulfate	2.5 mM
Chromium trioxide	0.2 mM and 0.5 mM
Lithium chloride	150 mM and 300 mM
Sodium chloride	0.5 M and 1 M
Geneticin	75 mg/l and 200 mg/l
Paramomicine	0.5 mM and 1 mM
EDTA	0.5 mM
Sorbitol	1.5 M
Ethanol	2% and 5%
Medium without glucose	
Galactose	2%
Glycerol	2%
Menadione	90 µM and 150 µM
pH	6
Temperature	37ºC
SDS	0.01% and 0.015%

3.3. Results

3.3.1. Selection of mistranslating tRNAs

The misincorporation of Ser at Leu codons is an unlikely event, due to the distinct chemical properties of these two amino acids. In order to better understand why this unlikely substitution occurred at the CTG clade species we have decided to explore other types of mistranslation, involving different amino acids and compare the data to that of the Leu-for-Ser misincorporation.

In order to misincorporate Ser at different codon families we altered the anticodon of a $tRNA_{UGA}^{Ser}$ allowing it to recognize codons belonging to different amino acids. For this, we benefited from the observation that mutations introduced in $tRNA^{Ser}$ anticodon do not interfere with tRNA serylation, because SerRS do not recognize tRNA anticodon (Lenhard et al., 1999). Therefore, we have expressed in yeast cells variants of the *C. albicans* $tRNA_{UGA}^{Ser}$ containing anticodons that could recognize different codon families. The schematic diagram of the codon misreading strategy is outlined in figure 3.2 (i.e. Thr ACG codon).

In order to have a series of mistranslation toxicity and compare the results with the ones obtained for the Leu-for-Ser misincorporation, we decided to misincorporate Ser at codons of 8 different amino acids. Based on amino acids polarity and weight, we chose Ile and Val as the amino acids more similar to Leu, expected to induce more toxic alterations. Thr, Gly and Ala are the amino acids more similar in weight and polarity to Ser, and expected to induce the lowest toxicity. Lys was chosen from the polar basic amino acids group due to its smaller size, and Tyr was chosen from the aromatic amino acids group because it's polar like Ser (figure 3.3). The specific codon of each amino acid was chose relative to its usage in the genome of *S. cerevisiae* (codon usage similar to Leu-CUG codon), and abundance of tRNAs with homologous anticodons in yeast (competitors tRNAs). The characteristics of the codons mistranslated are represented in table 3.5.

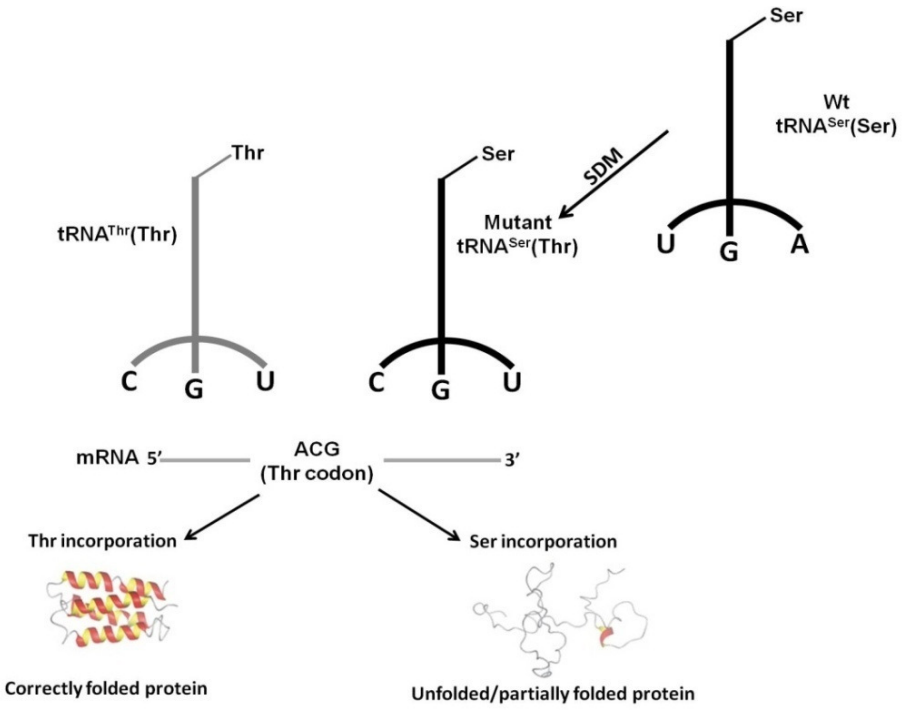

Figure 3.2: Mutant tRNAs as tools to misincorporate Ser at different codon families. A $tRNA_{UGA}^{Ser}$ was engineered by site directed mutagenesis (SDM) and its UGA-Ser anticodon was mutated to the CGU anticodon, which belongs to the Thr amino acid family. This mistranslating $tRNA^{Ser}$(Thr) maintained its serylation specificity and competed with the Wt $tRNA^{Thr}$(Thr) for the ACG codons during translation, leading to incorporation of Ser at Thr codons.

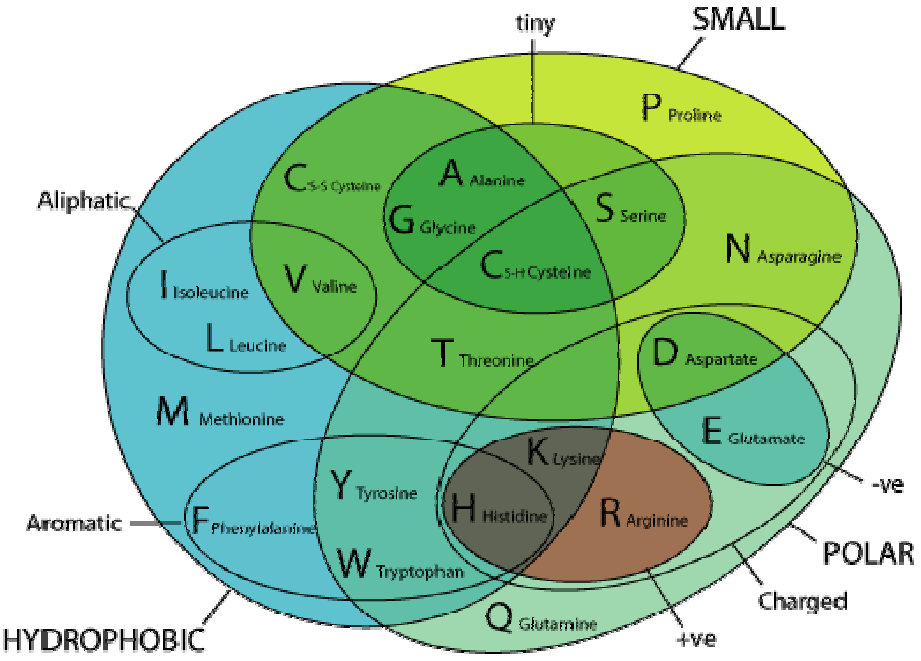

Figure 3.3: Amino acids chemical properties. Adapted from (Livingstone & Barton, 1993).

Table 3.5: Characteristics of the codons used for mistranslation of the genetic code

Amino acid	$tRNA^{Ser}$ engineered	Anticodon (5'→3')	Codon (5'→3')	Yeast tRNAs with same anticodon	aa MW	codon usage (per thousand)
Serine (Ser)	$tRNA^{Ser}$(Ser)	UGA	UCA [UCG, UCC, UCU]	3	105	UCA: 18.7
Glycine (Gly)	$tRNA^{Ser}$(Gly)	UCC	GGA [GGG, GGC, GGU]	3	75	GGA: 10.8
Threonine (Thr)	$tRNA^{Ser}$(Thr)	CGU	ACG	1	119	ACG: 8.0
Tyrosine (Tyr)	$tRNA^{Ser}$(Tyr)	GUA	UAC [UAU]	8	181	UAC: 14.8
Alanine (Ala)	$tRNA^{Ser}$(Ala)	UGC	GCA [GCG, GCU, GCC]	5	89	GCA: 16.2
Valine (Val)	$tRNA^{Ser}$(Val)	CAC	GUG	2	117	CAC: 10.6
Leucine (Leu)	$tRNA^{Ser}$(Leu)	CAG	CUG	0	131	CUG: 10.4
Isoleucine (Ile)	$tRNA^{Ser}$(Ile)	UAU	AUA [AUG, AUC, AUU]	2	131	AUA: 17.6
Lysine (Lys)	$tRNA^{Ser}$(Lys)	UUU	AAA [AAG]	7	146	AAA: 41.9

3.3.2. Expression of the mutant $tRNA^{Ser}$ in yeast

In order to evaluate the impact of Ser misincorporation at codons of chemically different amino acids in yeast, we have expressed the mutant mistranslating $tRNA^{Ser}$ from a multicopy plasmid (pRS425). Unexpectedly, the mistranslating $tRNA^{Ser}$(Leu), $tRNA^{Ser}$(Val) and $tRNA^{Ser}$(Ile), that misincorporated Ser at Leu, Val and Ile codons, respectively, did not reduced yeast growth rate. In opposition, the expression of the $tRNA^{Ser}$(Tyr), $tRNA^{Ser}$(Ala) and $tRNA^{Ser}$(Thr), which misincorporate Ser at Tyr, Ala and Thr codons, respectively, induced the highest reduction on growth rate (figure 3.4 A,B). These surprising results, contrary to the expected, prompted us to re-sequence the $tRNA^{Ser}$(Leu), $tRNA^{Ser}$(Val) and $tRNA^{Ser}$(Ile) genes extracted from those cells. Mutations were identified in all mistranslating $tRNA^{Ser}$ genes, suggesting that these $tRNA^{Ser}$ acquired mutations that inactivated them, explaining why they did not affect growth rate.

This result supported our previous studies (chapter 2) and indicated that above a certain level of toxicity the selective pressure is so high that the mistranslating tRNAs become lethal. It also showed that our experimental model was essentially correct since

different tRNAs produced different toxicities, as evaluated by the distinct alterations observed in the growth rate (figure 3.4).

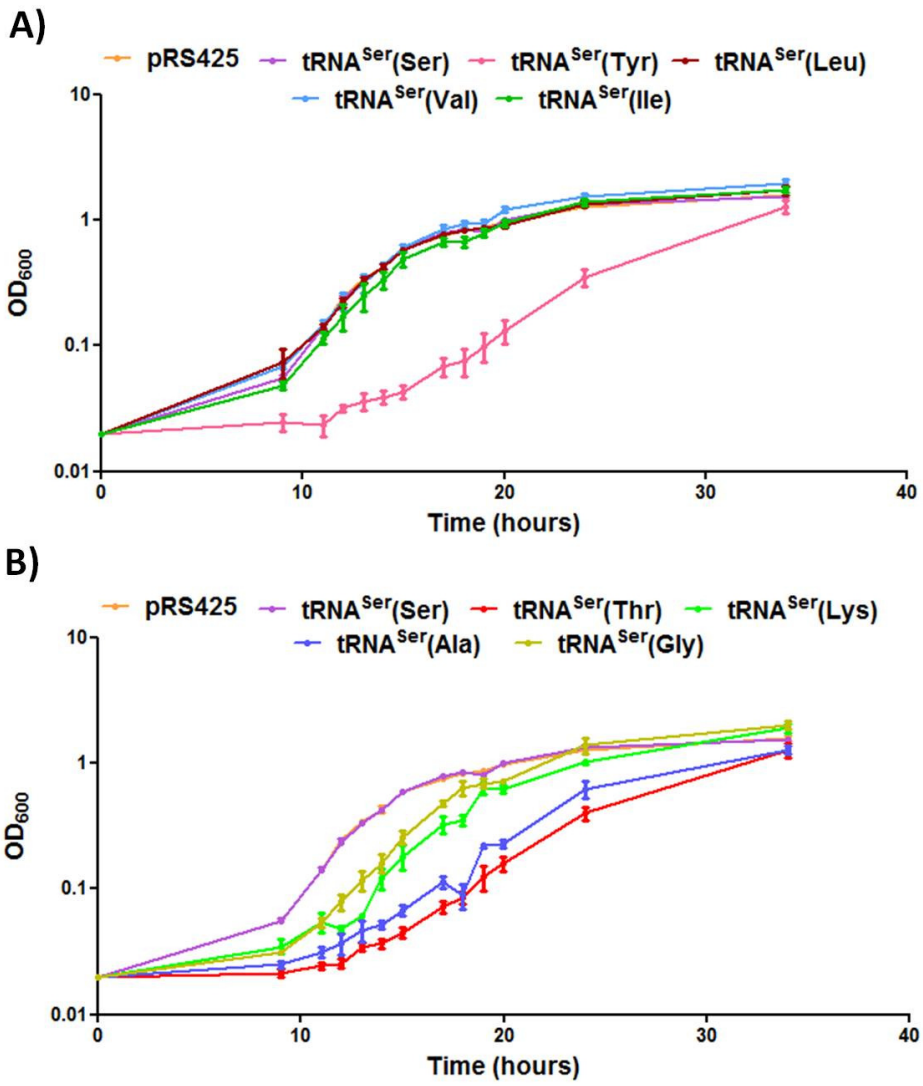

Figure 3.4: Growth curves of *S. cerevisiae* cells expressing mistranslating tRNAs from multicopy plasmids. Yeast cells transformed with pRS425, wt tRNA^{Ser}(Ser) and mistranslating tRNA^{Ser} expressed from multicopy plasmids, were grown at 30ºC in 100 ml culture flasks in selective medium until late stationary phase. Data represent the mean ± s.e.m. of duplicates of 3 independent clones.

The instability of some mistranslating tRNAs prompted us to express all tRNAs from the single-copy plasmid pRS315, in an attempt to decrease their toxicity. Growth curves, growth rate and transformation efficiencies were then determined for strains expressing the mistranslating tRNAs from single-copy plasmids (figure 3.5). Our data showed that all mistranslating tRNAs decreased cell growth and growth rate relative to the control cells containing the empty plasmid (pRS315) or the ones expressing the Wt $tRNA^{Ser}$ [$tRNA^{Ser}$(Ser)] (figure 3.5 A, B and C). Growth rate reduction was significant for all strains expressing the mistranslating tRNAs, except for the one expressing the $tRNA^{Ser}$(Lys), which misincorporates Ser at Lys codons, where the growth rate decrease was ~4% relative to the control strain (pRS315) (figure 3.5 C). The expression of $tRNA^{Ser}$(Ala), which misincorporates Ser at Ala codons, decreased yeast growth rate ~18%, while expression of $tRNA^{Ser}$(Thr), which misincorporates Ser at Thr codons, reduced growth rate ~23% relative to the control strain. The expression of $tRNA^{Ser}$(Gly), which misincorporate Ser at Gly codons, reduced yeast growth rate ~28%, while expression of $tRNA^{Ser}$(Val), $tRNA^{Ser}$(Tyr), $tRNA^{Ser}$(Leu) and $tRNA^{Ser}$(Ile), which misincorporated Ser at Val, Tyr, Leu and Ile codons, respectively, reduced more drastically yeast growth rate (above ~35%) (figure 3.5.C). These results were in agreement with those of the transformation efficiencies (figure 3.5 D). Indeed, the relative transformation efficiencies were higher for $tRNA^{Ser}$(Thr), $tRNA^{Ser}$(Lys) and $tRNA^{Ser}$(Ala), while $tRNA^{Ser}$(Gly) and $tRNA^{Ser}$(Tyr) reduced transformation efficiencies to ~40% relative to the control plasmid (pRS315). On the other hand, $tRNA^{Ser}$(Val) reduced the transformation efficiency to ~15% and, $tRNA^{Ser}$(Leu) and $tRNA^{Ser}$(Ile) yielded <1% of transformants, relative to control strain.

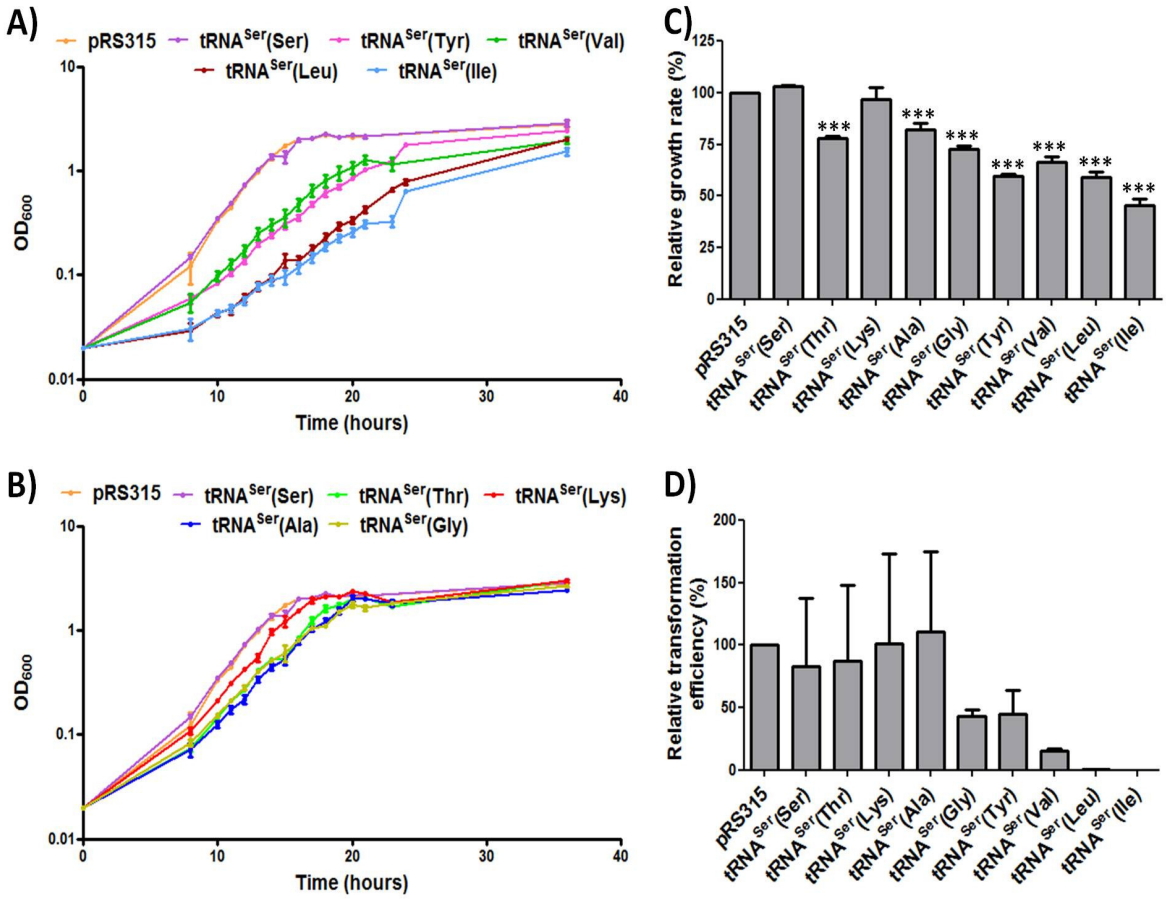

Figure 3.5: Effect of mistranslation on yeast growth rate and transformation efficiency. A, B) Growth curves of yeast cells transformed with the pRS315, tRNA^{Ser}(Ser), and mistranslating tRNA^{Ser} expressed from single-copy plasmids. Cultures were inoculated at an initial OD_{600} of 0.02 and were grown at 30ºC in selective medium until stationary phase. At various time points the OD_{600} was measured. Data represent the mean ± s.e.m. of duplicates of 3 independent clones. C) Relative growth rate of cells transformed with tRNA^{Ser}(Ser) and mistranslating tRNA^{Ser} expressed from single-copy plasmids was determined using exponential growth phase values, relative to control (pRS315) cells. Data represent the mean ± s.e.m. of duplicates of 3 independent clones (***p< 0.001 one-way Anova post Bonferroni's multiple comparison test with CI 95% relative to pRS315). D) Transformation efficiencies of yeast transformed with pRS315, tRNA^{Ser}(Ser) and mistranslating tRNA^{Ser} expressed from single-copy plasmids were determined relative to the control (pRS315) cells. Data represent the mean ± s.e.m. of three independent experiments.

The level of the mistranslating tRNA^{Ser} (expressed from single-copy plasmids) was monitored by northern blot analysis (see methods 3.2.5), and most interestingly, the

abundance of the mutant tRNAs varied significantly (figure 3.6 A,B). The mistranslating $tRNA^{Ser}$(Lys) and $tRNA^{Ser}$(Thr) were expressed at higher level, while $tRNA^{Ser}$(Leu), $tRNA^{Ser}$(Val) and $tRNA^{Ser}$(Ile) were expressed at lower level. The level of the control $tRNA_{CCC}^{Gly}$ remained constant in all strains.

There was, however, an interesting connection between expression level and toxicity as the most toxic tRNAs, namely $tRNA^{Ser}$(Leu), $tRNA^{Ser}$(Val) and $tRNA^{Ser}$(Ile) were expressed at lower level, and the less toxic tRNAs, namely $tRNA^{Ser}$(Thr), $tRNA^{Ser}$(Lys) and $tRNA^{Ser}$(Ala), were expressed at higher level. In order to ensure that the differential expression of the mistranslating tRNAs was not an artifact related to plasmid loss, we have amplified the tRNA gene by PCR in all mistranslating strains. For this, PCR reactions were setup using the same number of cells. Similar amplification intensity signals were obtained for all tRNA genes in all mistranslating strains, relative to the strain expressing the non-mistranslating tRNA [$tRNA^{Ser}$(Ser)] (figure 3.6 C). Therefore, the differential expression of the mistranslating tRNAs is likely related to the mechanism of tRNA downregulation uncovered in the previous chapter.

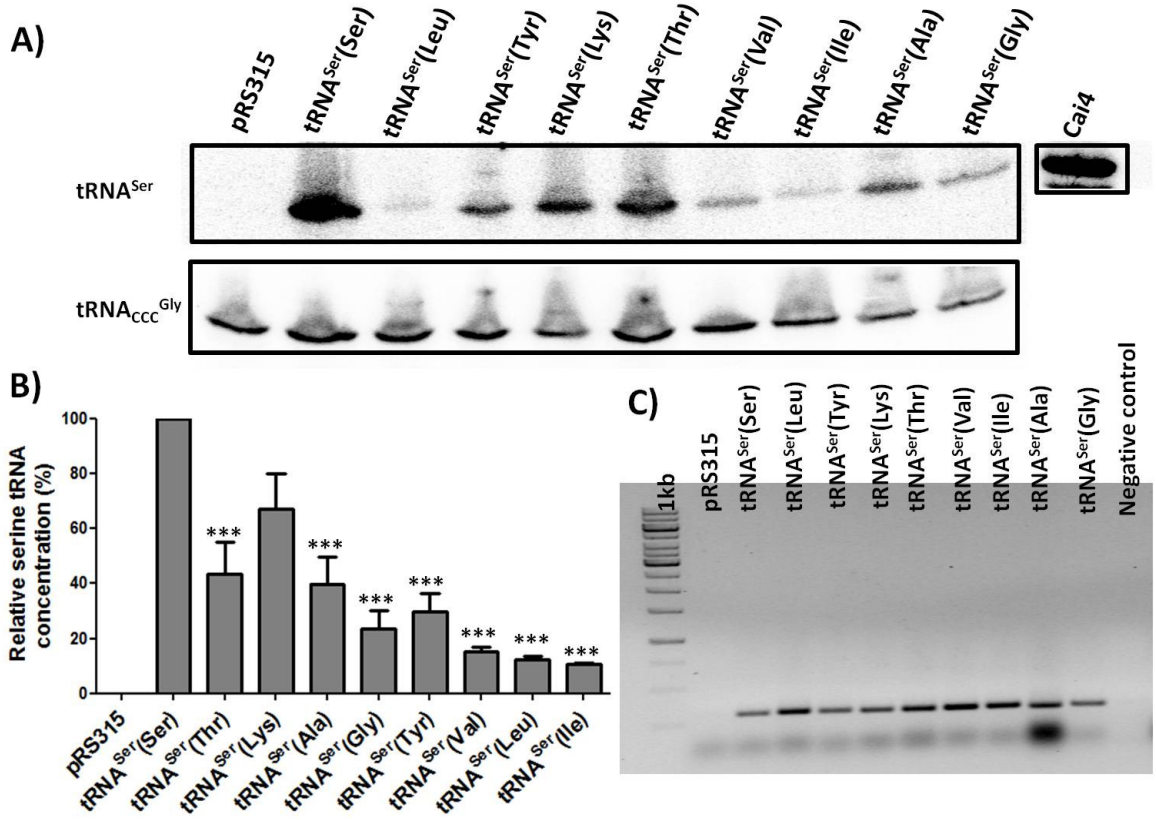

Figure 3.6: Mistranslation affects the expression of the mutant tRNA^{Ser} expressed from single-copy plasmids. A) Representative expression of mistranslating tRNAs detected by northern blot analysis. 50 µg of tRNAs extracted and purified under acidic conditions from yeast strains expressing tRNA^{Ser}(Ser) and mistranslating tRNA^{Ser} from single-copy plasmids, were fractionated on 12% polyacrylamide gels containing 8M urea at room temperature. Northern blot hybridizations were carried out using γ-^{32}P-ATP-tRNA$_{UGA}^{Ser}$ (oUA2199) and γ-^{32}P-ATP-tRNA$_{CCC}^{Gly}$ (oUA2195) probes (methods section 3.2.5). B) tRNAs were quantified relative to tRNA^{Ser}(Ser) after normalization to the control tRNA$_{CCC}^{Gly}$. Data represent the mean ± s.e.m. of 3 independent experiments. (***p< 0.001 one-way Anova post Bonferroni's multiple comparison test with CI 95% relative to the wt tRNA^{Ser}(Ser). C) Quantification of the mistranslating tRNA^{Ser} genes in yeast cells by colony PCR. tRNA genes were amplified by PCR using the same number of cells (5x10^6) for each strain, and the same volume of PCR product was loaded onto 1.2% agarose gels.

In order to confirm that the toxicity observed in yeast cells transformed with mistranslating tRNAs was due to mistranslation and was not related to secondary effects of heterologous tRNA expression, we have used the β-galactosidase (β-gal) reporter system to monitor Ser misincorporation (section 3.2.6). β-gal thermal stability decreased

in yeast expressing the mistranslating tRNAs relative to pRS315 and $tRNA^{Ser}$(Ser) strains (figure 3.7 A,B). However, the differences in β-gal stability correlated poorly with the growth rate data described above. One should note, however, that these β-gal assays are an indirect measure of mistranslation efficiency and do not permit comparative analysis of quantitative mistranslation, because the number of mistranslated codons, their location, and the impact of amino acid misincorporation are diverse.

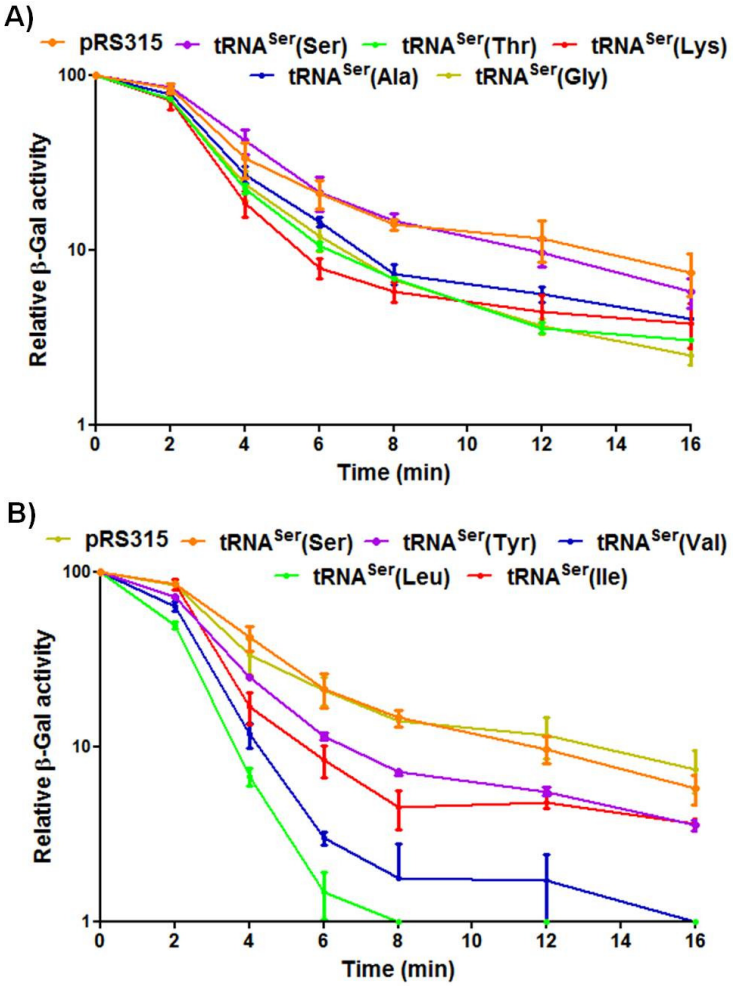

Figure 3.7: Mistranslation decreases protein stability. A, B) *E. coli* β-galactosidase (β-gal) was co-expressed in yeast cells with pRS315, $tRNA^{Ser}$(Ser) and mistranslating $tRNA^{Ser}$ expressed from single-copy plasmids. β-gal thermostability was determined for each time point relative to total activity measured in cells prior to denaturation (see methods 3.2.6). Data represent the mean ± s.e.m. of duplicates of 3 independent clones.

3.3.3. Mistranslation induces yeast cell death

In order to determine whether decreased growth rate of yeast cells was due to increased cell death we have evaluated this parameter by two methods, namely the propidium iodide (PI), a dye that stains cells with disrupted membranes and the colony forming units (CFU) method, which provides information about the percentage of viable cells that are able to form colonies. These assays were performed at various time points of the yeast growth curve to better understand the effect of mistranslation on growth. The time points chosen for this analysis were T10h, T15h, T20h, T25h and late stationary phase (times after culture inoculation).

Cell death determined by the PI method (figure 3.8) showed that at T10h of growth only $tRNA^{Ser}$(Ile) and $tRNA^{Ser}$(Leu) expression resulted in significant increase in death cells (PI positive), 45% and 55%, respectively, relative to the control cells (pRS315). This difference decreased at T15h to 25-15% and at T20h and T25h the percentage of PI positive cells was less than 10% for strains expressing the $tRNA^{Ser}$(Ile) and $tRNA^{Ser}$(Leu). In late exponential growth phase there was an increase of 30-40% in PI positive cells in the strains expressing the $tRNA^{Ser}$(Val), $tRNA^{Ser}$(Leu) and $tRNA^{Ser}$(Ile). These results suggested that cell death occurred mainly during the initial of stages of growth (T10h) and that cells recover viability over time. For the other strains there were no significant differences in PI positive cells relative to the control cells (pRS315).

The data obtained with the CFU test (figure 3.9) was in agreement with the PI test data because the highest percentage of cell death was also observed for strains expressing the $tRNA^{Ser}$(Val), $tRNA^{Ser}$(Leu) and $tRNA^{Ser}$(Ile). Although, while the CFU test showed continuous cell death along the growth curve, in particular for cells expressing $tRNA^{Ser}$(Leu) and $tRNA^{Ser}$(Ile), the PI method showed an unexpected maximal value of cell death at T10h, which then decreases over time. It is not clear why PI staining is maximal at T10h, but one possibility is that yeast cells may have some capacity to repair their membranes during late growth stages, thus preventing cell staining with PI, as observed previously (Davey & Haxley, 2010).

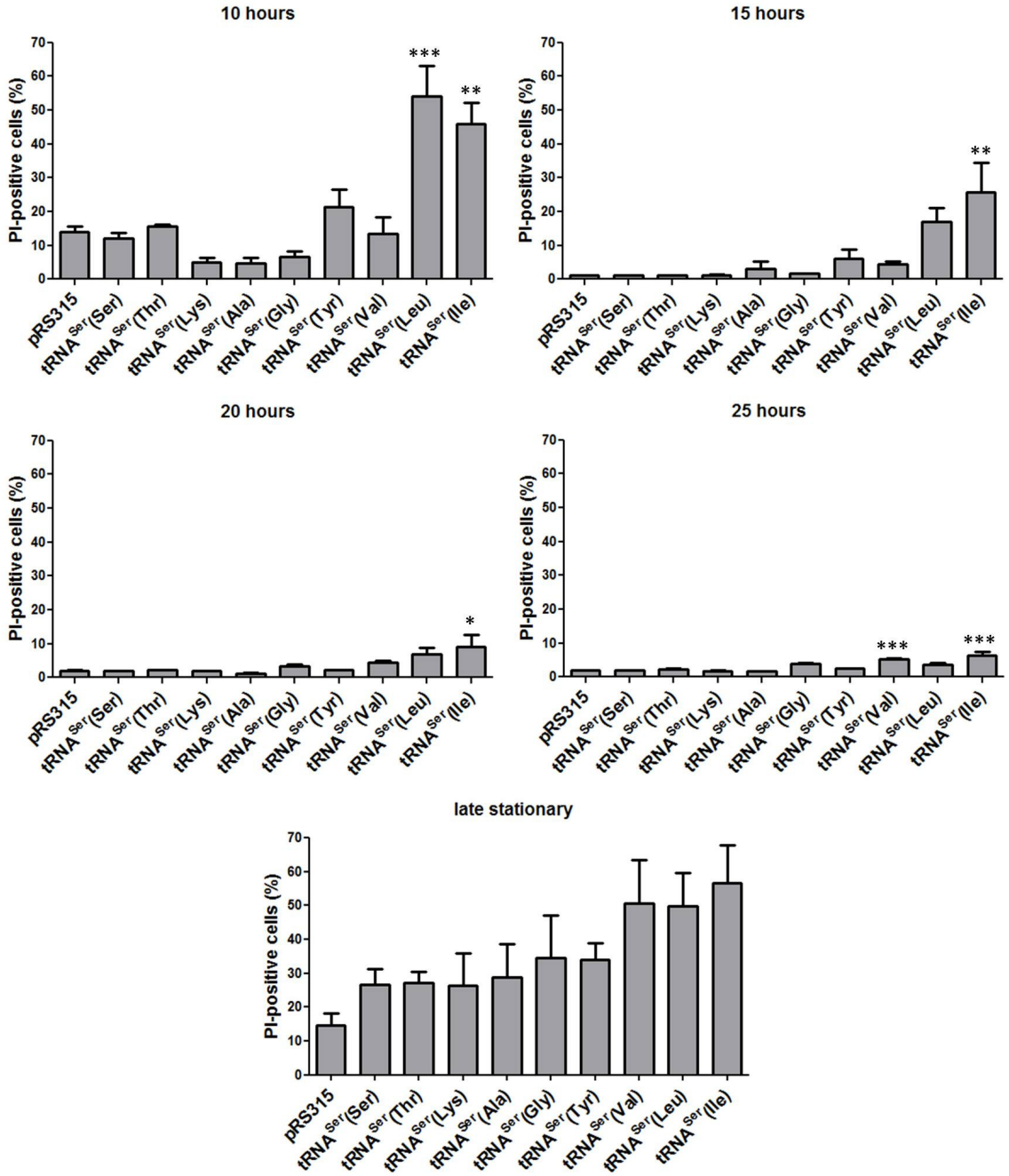

Figure 3.8: Mistranslation increases the percentage of PI-positive cells. Yeast cells transformed with pRS315, tRNA^{Ser}(Ser) and mistranslating tRNA^{Ser} expressed from single-copy plasmids, were grown in selective medium and were collected at T10h, T15h, T20h, T25h and in late stationary phase. Cells were labeled with PI (section 3.2.7) and were analyzed by flow cytometry. Data represent the mean ± s.e.m. of 3 independent clones. (***p< 0.001, **p< 0.01, *p< 0.05 one-way Anova post Bonferroni's multiple comparison test with CI 95% relative to pRS315).

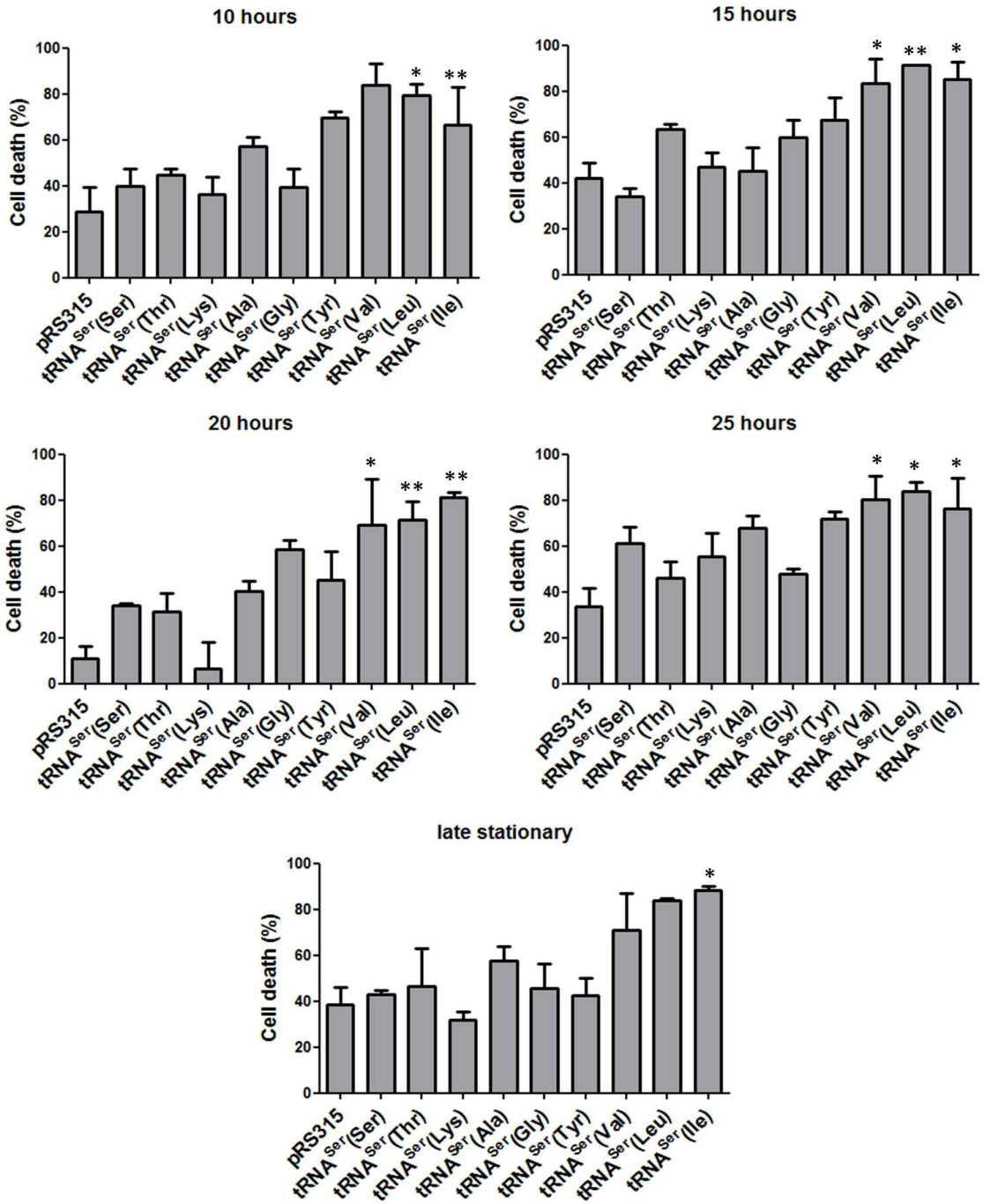

Figure 3.9: Mistranslation decreases yeast viability. Yeast cells transformed with pRS315, $tRNA^{Ser}$(Ser) and mistranslating $tRNA^{Ser}$ expressed from single-copy plasmids were grown in selective medium and were collected at T10h, T15h, T20h, T25h and in late stationary phase. ~100 cells were plated in each agar plate. After 3 days of growth colonies were counted (methods 3.2.7). Results are represented as cell death %. Data represent the mean ± s.e.m. of 3 independent clones. (**p< 0.01, *p< 0.05 one-way Anova post Bonferroni's multiple comparison test with CI 95% relative to pRS315).

Cell death and growth rate data were in good agreement as strains expressing the $tRNA^{Ser}$(Leu), $tRNA^{Ser}$(Ile), $tRNA^{Ser}$(Val) and $tRNA^{Ser}$(Tyr) were those that showed the highest decrease in growth rate and the highest percentage of cell death (~30-50%). While expression of the $tRNA^{Ser}$(Ala), $tRNA^{Ser}$(Thr), $tRNA^{Ser}$(Lys) and $tRNA^{Ser}$(Gly) had the lowest impact on growth rate and consequently on cell death. In other words, the decrease in growth rate induced by mistranslation seems to be directly correlated with an increase in cell death.

3.3.4. Mistranslation induces cell cycle alterations

Mistranslation induces cell cycle arrest and chromosome instability (Silva et al., 2007). In order to evaluate whether Ser misincorporation at codons belonging to different amino acid families had similar effects in the karyotype and in the cell cyle, we have analyzed the genome of the mistranslating cells. Briefly, the cell cycle of yeast cells can be divided into four phases, M (mitosis), G1 (Gap), S (Synthesis) and G2 (Gap). G1 corresponds to an increase in cell size and preparation for DNA replication which takes place in the S phase. Cells in G1 can stop dividing and enter a G0 phase instead of continuing to S phase. G2 corresponds to growth and preparation for mitosis, where nuclear division occurs (Singh et al., 2006).

Cell cycle analysis of yeast mistranslating cells showed significant differences relative to the control (pRS315) and to the cells expressing the non-mistranslating $tRNA^{Ser}$(Ser) (figure 3.10). These differences were more evident in cells expressing the $tRNA^{Ser}$(Val), $tRNA^{Ser}$(Leu) and $tRNA^{Ser}$(Ile), which resulted in production of aneuploid cells. In fact, in these three strains, aneuploid cells were more frequent (~70-80%) than diploid cells (~20-30%). Moreover, the analysis of the cell cycle showed differences in the percentage of mistranslating cells at each phase of the cell cycle relative to the controls pRS315 and $tRNA^{Ser}$(Ser). For example, expression of the $tRNA^{Ser}$(Val), $tRNA^{Ser}$(Leu) and $tRNA^{Ser}$(Ile) arrested cells in G2/M phase of the diploid population, more evident in late stationary phase, while the other mistranslating strains had no arrest. Furthermore, mistranslating $tRNA^{Ser}$(Tyr) delayed the cell cycle, because at T20h these cells were mainly in S and G2/M phases, while the control cells (pRS315) were in G1 phase, suggesting that these cells are still dividing at T20h, which is in agreement with the negative effect on growth rate (figure 3.5 A and B).

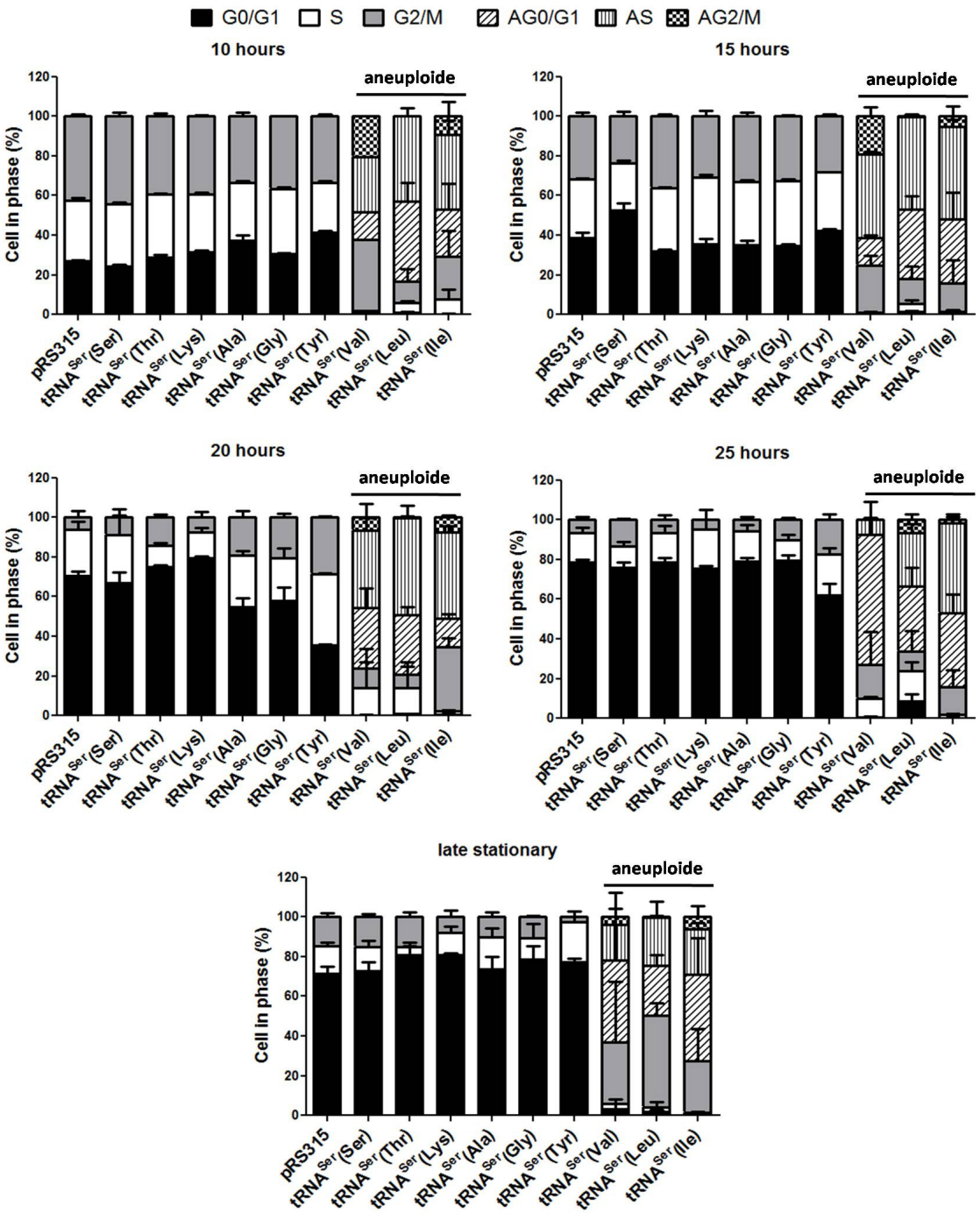

Figure 3.10: Mistranslation induces cell cycle alterations. Yeast cells transformed with pRS315, tRNA^{Ser}(Ser) and mistranslating tRNA^{Ser} expressed from single-copy plasmids, were grown in selective medium, collected at T10h, T15h, T20h, T25h and in late stationary phase and were labeled with SYBR green. Their cell cycle was evaluated using flow cytometry (methods 3.2.8). Bars without stripes correspond to G1, S and G2/M diploid phases, while bars with stripes correspond to aneuploid G1 (AG1), aneuploid S (AS), and aneuploid G2/M (AG2/M). Data represent the mean ± s.e.m. of 3 independent clones.

The progression or arrest of the cell cycle is governed by checkpoint controls, which ensure the accuracy of DNA replication and cell division. The DNA damage checkpoints can occur at G1, preventing entry into S phase or late in G2 and mitosis (DiPaola, 2002). The G2/M arrest of the cell cycle observed in our cells has been observed in other biological systems but the mechanism of inhibition is still unclear. One possibility is that it is linked to inhibition of regulatory proteins, namely cdks (Tyagi et al., 2002), or problems in the mitotic spindle structure that lead to impaired segregation of chromosomes (Holy, 2002). It was also observed in yeast cells defective in bud formation (Lew & Reed, 1995) and later related to cells with disruption of the actin cytoskeleton (McMillan et al., 1998). More recent studies showed that this checkpoint is triggered by failure to organize the septin scaffold at the mother-bud neck, a crucial event during bud formation, and that actin cytoskeleton perturbations have little effect on it (Longtine et al., 2000). Moreover, incomplete cytokinesis, a process that requires a functional actin cytoskeleton, may also inhibit cell cycle progression into mitosis (Liu & Balasubramanian, 2000).

To find out if the aneuploid population reached the tetraploid state, we determined the DNA index. This parameter is defined as the mean channel of G1 aneuploid cells relative to diploid G1 mean channel. In the case of a diploid population this index is 1 while in tetraploid cells is 2. Our results (table 3.6) show that cells expressing the $tRNA^{Ser}$(Val), $tRNA^{Ser}$(Leu) and $tRNA^{Ser}$(Ile) had a DNA index of ~1.7-2, which suggested that they are nearly tetraploid.

Table 3.6: DNA index calculation in cells expressing the tRNA^{Ser}(Val), tRNA^{Ser}(Leu) and tRNA^{Ser}(Ile). DNA index was determined after dividing the mean channel of G1 aneuploid cells by the mean channel of G1 diploid cells. Data represent the mean ± s.e.m. of 3 independent clones.

Hours	Strains	DNA index $\frac{\text{aneuploid G1 channel}}{\text{diploid G1 channel}}$
10	tRNA^{Ser}(Val)	1.867 ± 0.02186
	tRNA^{Ser}(Leu)	2.067 ± 0.03786
	tRNA^{Ser}(Ile)	1.897 ± 0.07572
15	tRNA^{Ser}(Val)	1.860 ± 0.01414
	tRNA^{Ser}(Leu)	2.033 ± 0.04726
	tRNA^{Ser}(Ile)	2.047 ± 0.1790
20	tRNA^{Ser}(Val)	1.80 ± 0.1980
	tRNA^{Ser}(Leu)	2.047 ± 0.1159
	tRNA^{Ser}(Ile)	1.847 ± 0.04163
25	tRNA^{Ser}(Val)	1.910 ± 0.2687
	tRNA^{Ser}(Leu)	1.963 ± 0.04619
	tRNA^{Ser}(Ile)	2.037 ± 0.1387
Late stationary	tRNA^{Ser}(Val)	1.797 ± 0.05033
	tRNA^{Ser}(Leu)	2.010 ± 0.2121
	tRNA^{Ser}(Ile)	1.883 ± 0.2421

In order to clarify the data shown in figure 3.10, in particular to determine whether the aneuploidies were correlated with amino acid toxicity and decreased growth rate, or whether they were specific for mistranslations of branched chain amino acids (Leu, Val and Ile), the cell cycle analysis was repeated using cells expressing mutant tRNA^{Ser} with anticodons for Thr, Lys, Ala, Gly and Tyr, from multicopy plasmids. These less toxic tRNAs expressed from single-copy plasmids were expected to be more toxic when expressed from multicopy plasmids. Our results (figure 3.11) did not show the presence of aneuploide cells in strains expressing the tRNA^{Ser}(Thr), tRNA^{Ser}(Lys), tRNA^{Ser}(Ala), tRNA^{Ser}(Gly) and tRNA^{Ser}(Tyr) from multicopy plasmids. In other words, our results demonstrated that aneuploidies are generated by mistranslating tRNA^{Ser} that misincorporate Ser at Leu, Ile and Val codons only.

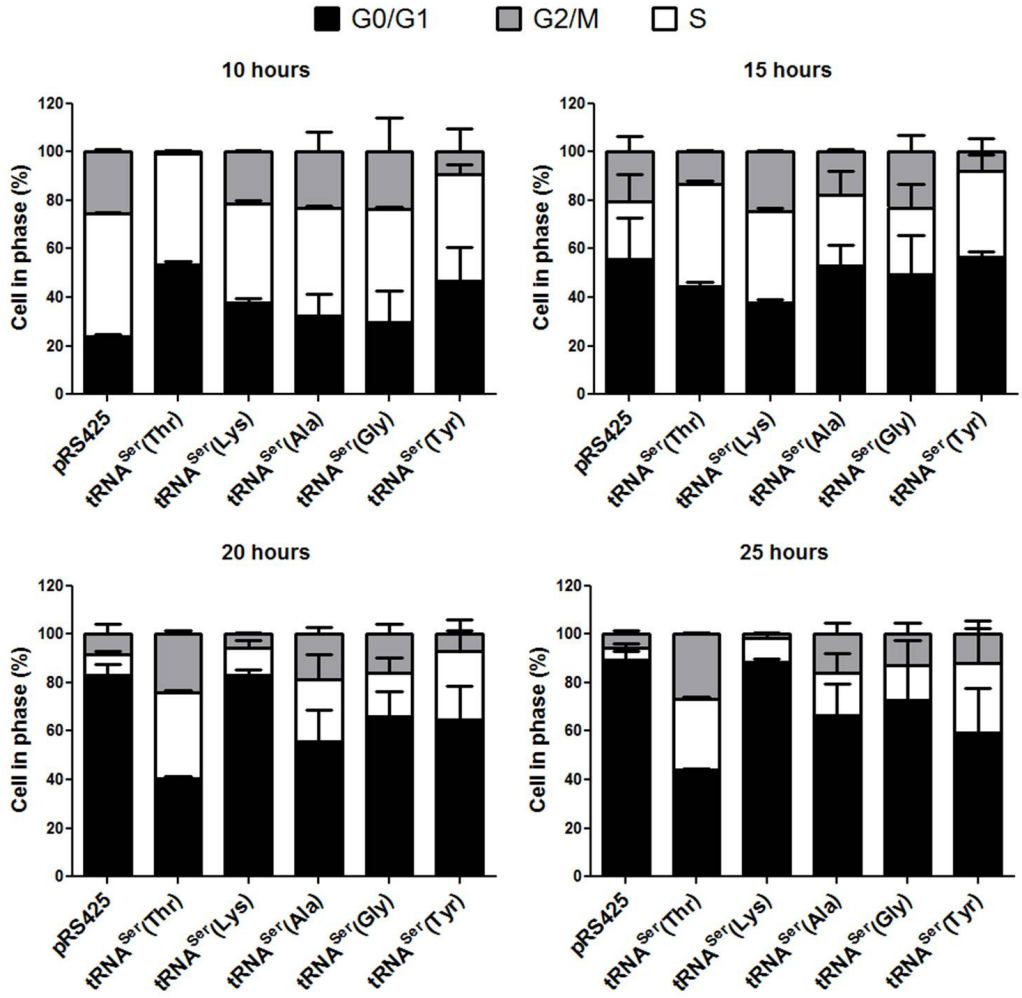

Figure 3.11: Cell cycle analysis of yeast cells expressing tRNA^{Ser} from multicopy plasmids. Yeast cells transformed with pRS425 and the mistranslating tRNA^{Ser} expressed from multicopy plasmids, were grown in selective medium and collected at T10h, T15h, T20h and T25h and then labeled with SYBR green (see methods 3.2.8). Cell cycle was evaluated using flow cytometry. Data represent the mean ± s.e.m. of 3 independent clones.

Interestingly, the cell cycle histograms showed an extra peak, before the G1 peak (figure 3.12), in some mistranslating strains, which is associated with cells in Sub G0/G1 phase. This cell population was significantly increased in the strains expressing the tRNA^{Ser}(Val), tRNA^{Ser}(Leu), tRNA^{Ser}(Ile) (figure 3.13). This Sub G0/G1 population is frequently associated with cells with lower DNA content related to UV exposure induced apoptosis (Del Carratore et al., 2002). This suggested that programmed cell death, namely apoptosis, may be occurring in these cells.

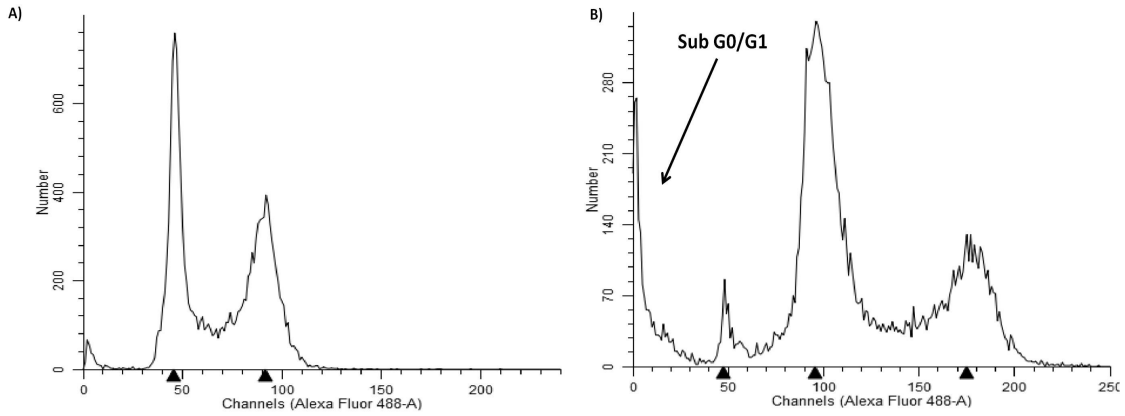

Figure 3.12: Representative histogram of the yeast cell cycle. The left histogram (A) corresponds to the control strain (pRS315), while the right corresponds to strain misincorporating Ser at Leu codons, both at T15h of growth. A sub G0/G1 population is observed in this case.

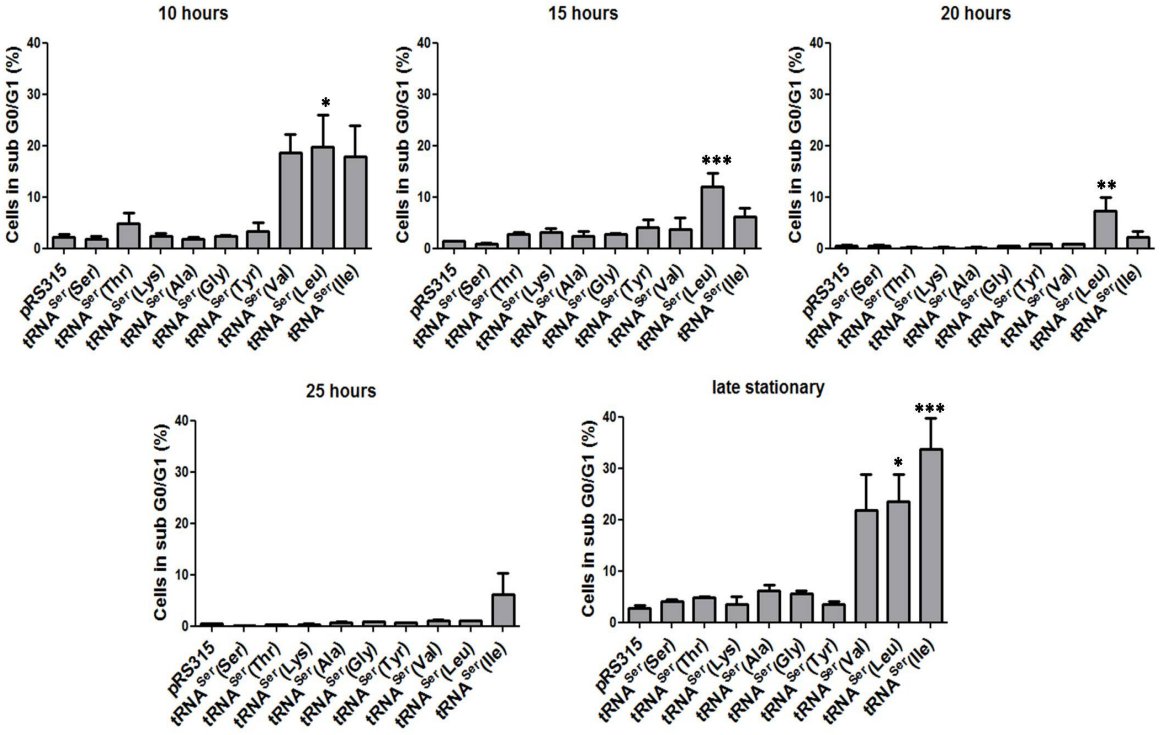

Figure 3.13: Quantification of cells in sub G0/G1 phase in mistranslating strains. Yeast cells transformed with pRS315, $tRNA^{Ser}$(Ser) and mistranslating $tRNA^{Ser}$ expressed from single-copy plasmids, grown in selective medium, were collected at T10h, T15h, T20h, T25h and in late stationary phase and were labeled with SYBR green (methods 3.2.8). The percentage of cells in sub G0/G1 was determined by flow cytometry. Data represent the mean ± s.e.m. of 3 independent clones. (***p< 0.001, **p< 0.01, *p< 0.05 one-way Anova post Bonferroni's multiple comparison test with CI 95% relative to pRS315).

3.3.5. Mistranslation increases reactive oxygen species (ROS) levels

Apoptosis is a programmed cell death mechanism which is extremely important for homeostasis (Menocal & D'Urso, 2004). The apoptotic cells, namely yeast, have markers, such as, externalization of phosphatidylserine to the outer leaflet of the plasma membrane, chromatin condensation, DNA fragmentation and cell breakage into membrane-enclosed vesicles (apoptotic bodies) (Madeo et al., 2002). Besides these characteristic phenotypes cells undergoing apoptosis have a high production of reactive-oxygen species, ROS, which are involved in initiation of apoptotic signaling (Fleury et al., 2002; Ling et al., 2003; Tan et al., 1998). In order to determine whether cell death in mistranslating strains was due to increased ROS production and consequently apoptosis, we decided to quantify ROS and DNA fragmentation in our mistranslating strains.

ROS accumulation in the mistranslating cells were evaluated by flow cytometry using two specific probes, DHR123 and DHE (see methods section 3.2.9). DHR123 data (figure 3.14) showed an increase number of cells with high intracellular ROS levels which was statistically significant in the case of the $tRNA^{Ser}$(Leu) and $tRNA^{Ser}$(Ile) at T20h. Unexpectedly, the number of cells with high level of ROS changed over time. For example, strains expressing the $tRNA^{Ser}$(Ile) showed decreased ROS levels from T10h to T15h and T20h and, then an increase at T25h and a decrease again in late stationary phase.

Determination of cells number with high level of intracellular ROS using the DHE probe (figure 3.15) gave more consistent results compared to the DHR123 probe. The increase in the number of cells with high ROS concentration was 7 times higher in the cases of the $tRNA^{Ser}$(Tyr) and $tRNA^{Ser}$(Val), 12 times for $tRNA^{Ser}$(Ile) and 18 times higher in the $tRNA^{Ser}$(Leu), relative to the control strain (pRS315) at T10h. At T15h the number of cells with high ROS levels decreased relative to the T10h. The values at T15h increased 11 and 14 fold in cells expressing the $tRNA^{Ser}$(Leu) and $tRNA^{Ser}$(Ile), but at T20h and T25h the ROS concentration in these strains was only 3-4 times higher than the control strain (pRS315). The decrease in the number of cells with high ROS concentration along the growth curve suggests that some defense mechanisms were activated in the strains expressing the $tRNA^{Ser}$(Tyr), $tRNA^{Ser}$(Val), $tRNA^{Ser}$(Leu) and $tRNA^{Ser}$(Ile).

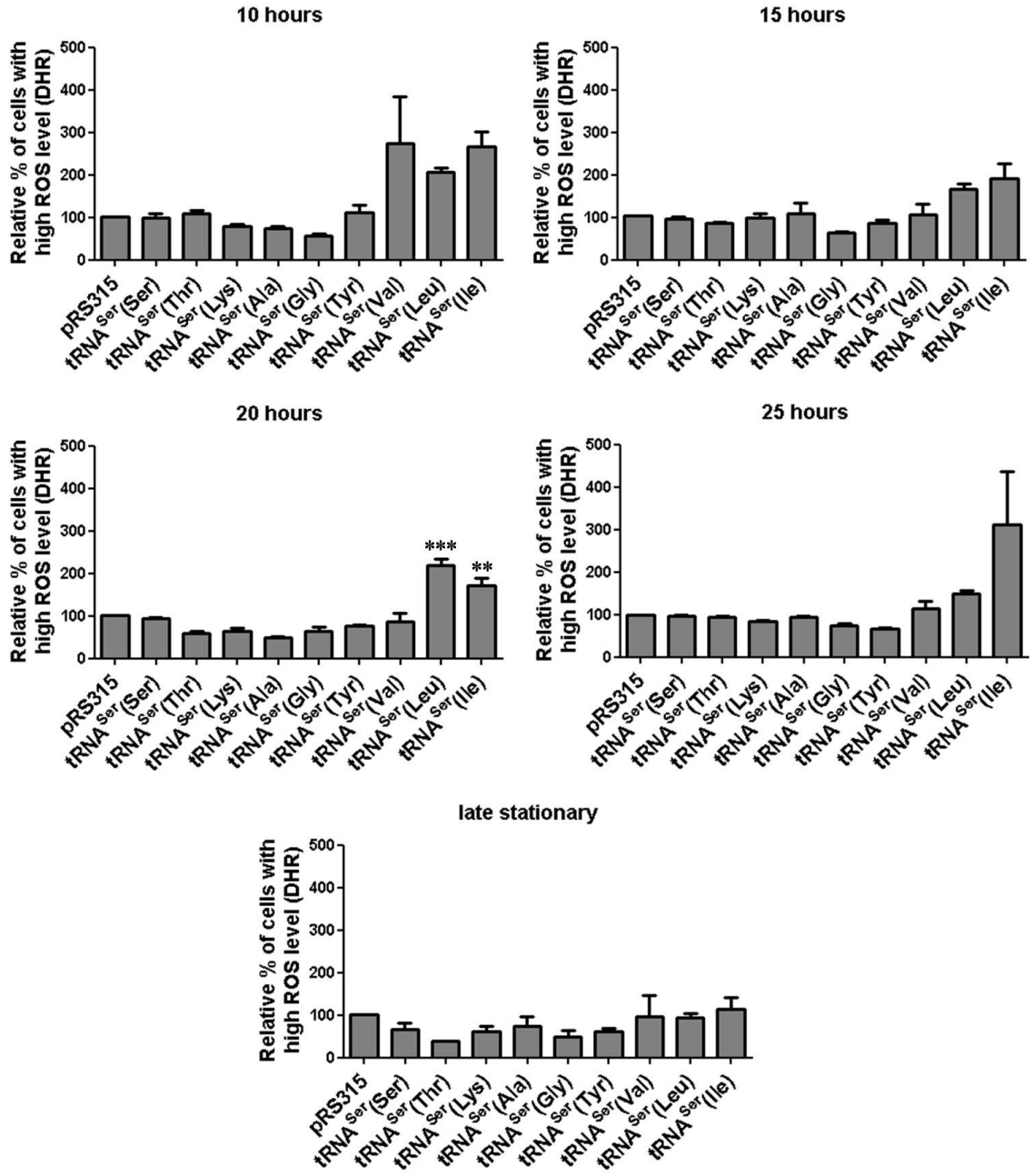

Figure 3.14: Mistranslation increases the level of ROS (DHR123 positive cells). Yeast cells transformed with pRS315, $tRNA^{Ser}$(Ser) and mistranslating $tRNA^{Ser}$ expressed from single-copy plasmids, were grown in selective medium and were collected at T10h, T15h, T20h, T25h and late in stationary phase, and were labeled with DHR123 (methods 3.2.9). Fluorescence was quantified by flow cytometry and is shown as the percentage of cells with increased ROS levels relative to that of the control strain (pRS315). Data represent the mean ± s.e.m. of 3 independent clones. (***p< 0.001, **p< 0.01 one-way Anova post Bonferroni's multiple comparison test with CI 95% relative to pRS315).

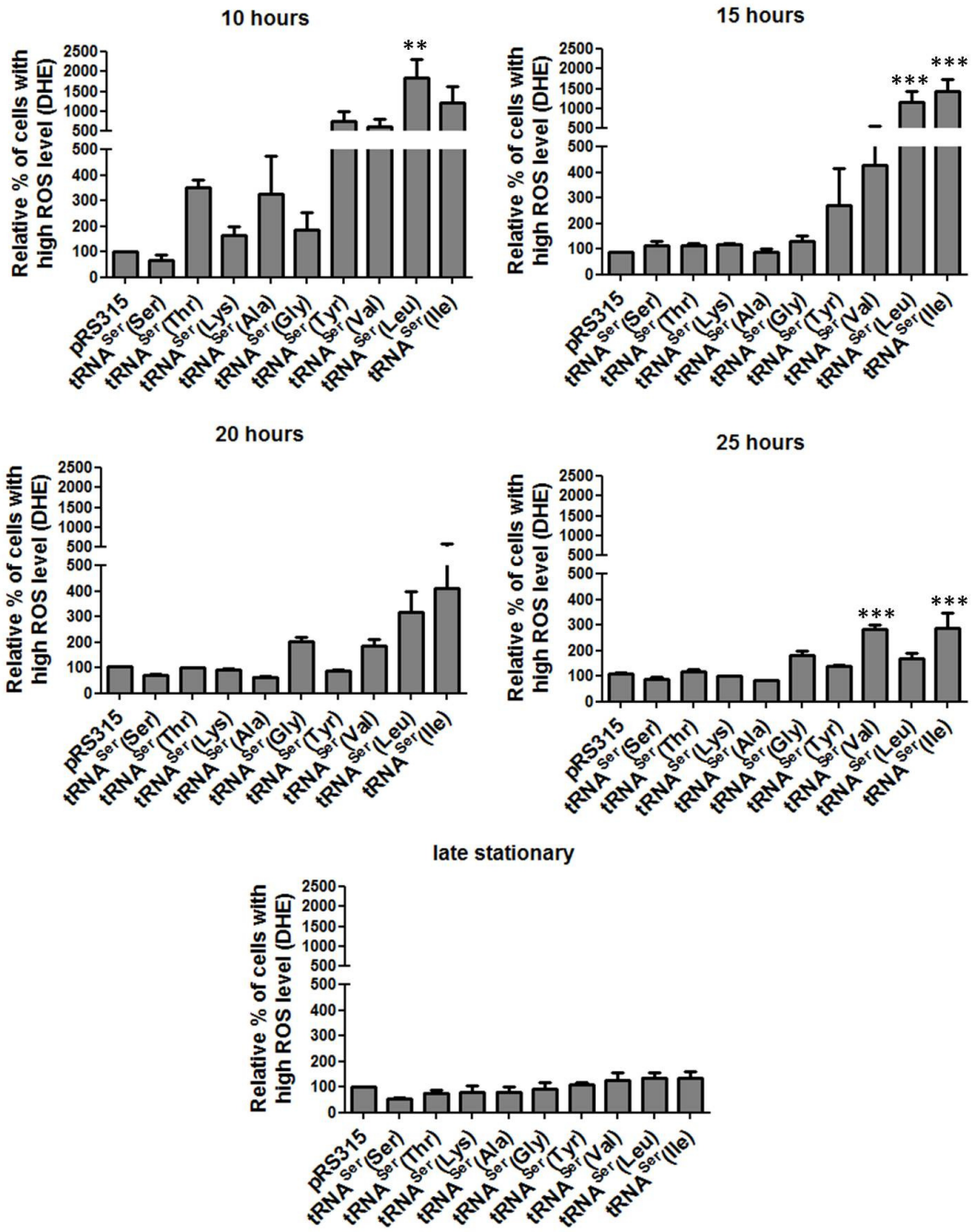

Figure 3.15: Mistranslation increases the level of ROS (DHE positive cells). Yeast cells transformed with pRS315, $tRNA^{Ser}$(Ser) and mistranslating $tRNA^{Ser}$ expressed from single-copy plasmids, were grown in selective medium and were collected at T10h, T15h, T20h, T25h and late in stationary phase, and were labeled with DHE (methods 3.2.9). Fluorescence was quantified by flow cytometry and is shown as the percentage of cells with increased ROS levels relative to that of the control strain (pRS315). Data represent the mean ± s.e.m. of 3 independent clones. (***p< 0.001, **p< 0.01 one-way Anova post Bonferroni's multiple comparison test with CI 95% relative to pRS315).

Yeast enzymatic antioxidant defenses include superoxide dismutase, catalases, glutathione peroxidases (Gpx), glutathione reductase (Glr), thiol peroxidases, thioredoxins, glutaredoxins, peroxiredoxins, sulfiredoxins, while the non-enzymatic, are ascorbic acid and its derivatives, glutathione, proline, trehalose, polyols, tocopherols, as well as pigments such as carotenoids and melanins (reviewed in Gessler et al., 2007).

The differences in ROS levels observed with the two probes used could be related to the specificity of each probe. Indeed, DHR123 is oxidized faster by hydrogen peroxide and peroxynitrite, while DHE is oxidized faster by superoxide (Janes et al., 2004). This could indicate that the superoxide anion is the most abundant ROS in our mistranslating strains. Moreover, detoxification of superoxide by SOD leads to formation of hydrogen peroxide (Gessler et al., 2007), which could be an explanation for the increased level of ROS detected with DHR123 probe at T20h.

ROS are normally produced at an early stage of the apoptotic suicide programme, preceding and contributing to the other events, such as, mitochondrial membrane depolarization, cytochrome c release, caspase activation and nuclear fragmentation (reviewed in Madeo et al., 2002; Menocal & D'Urso, 2004; Skulachev, 2002). In order to evaluate wheather ROS activated apoptosis in the mistranslating strains we have performed the Tunel assay, which is used to detect DNA fragmentation, a characteristic event in apoptosis. Our results showed a significant increase (25%) in tunel positive cells for the $tRNA^{Ser}$(Ile) only at T15h (figure 3.16). At T20h there was no detection of Tunel positive cells in mistranslating strains. These results were unexpected and we do not have a clear explanation for them.

Apoptosis was not the major cell death pathway in our mistranslating strains, but contributed in part to the increase in cell death observed when the $tRNA^{Ser}$(Ile) is expressed, suggesting that other types of cell death, namely necrosis, autophagy or mitotic catastrophe could also be involved. Autophagy refers to a cell death event that occurs without chromatin condensation and implies a massive autophagic vacuolization and excessive lysosomal activity inducing active destruction of the cytoplasm. Mitotic catastrophe is a cell death event that occurs during or shortly after deregulated or failed mitosis and can be accompanied by morphological alterations, such as formation of micronuclei and multinucleation. Necrosis is associated with disruption of the cell membrane and consequent release of cytoplasmatic content (reviewed in Kroemer et al., 2005; Ludovico et al., 2005). In other words, we need to clarify which of these processes are involved in cell death induced by mistranslation.

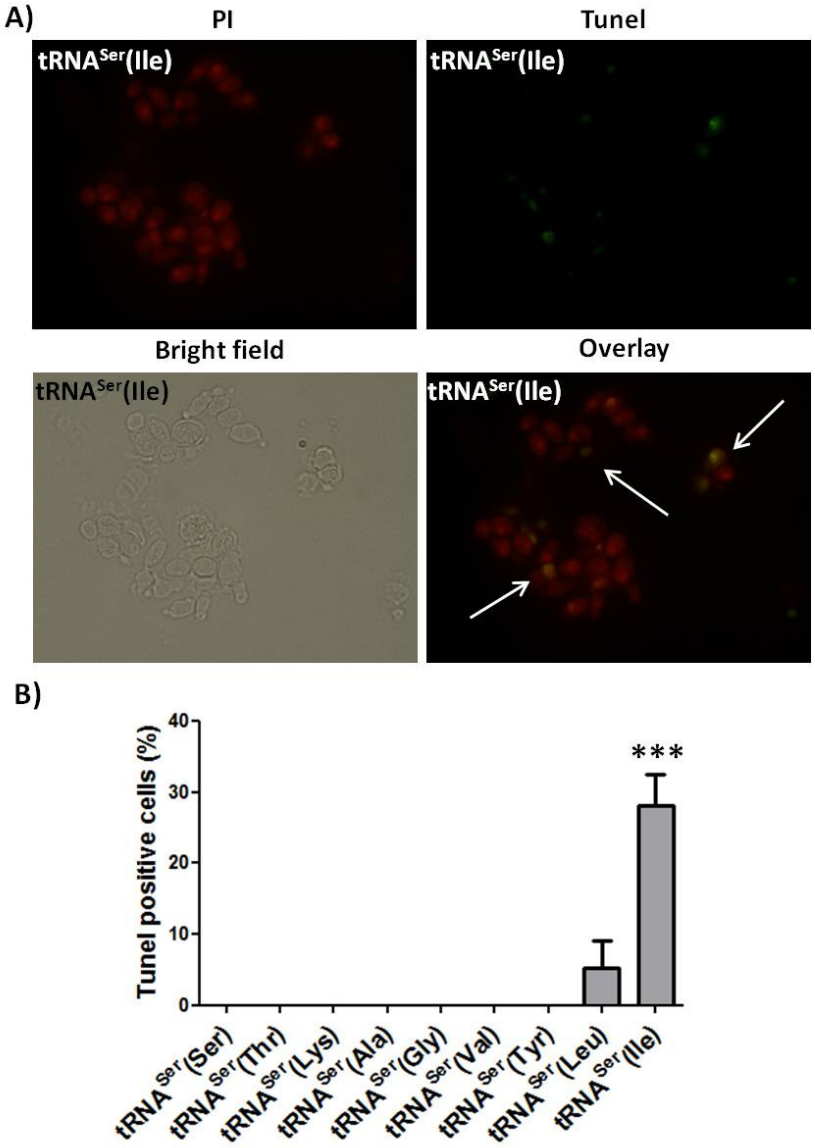

Figure 3.16: Certain types of mistranslation increase the frequency of Tunel positive cells. A) Yeast cells transformed with tRNA^{Ser}(Ser) and mistranslating tRNA^{Ser} expressed from single-copy plasmids, were grown in selective medium and were collected at T15h, labeled with the PI/Tunel kit (methods 3.2.10) and were then observed using an epifluorescence microscope (Olympus). tRNA^{Ser}(Ile) cells double positive for Tunel and PI are observed in the overlay image (arrows). B) Calculation of the percentage of Tunel positive cells showed that mistranslation of Ile codons as Ser was the most effective Tunel inducer followed by mistranslation of Leu codons. Data represent the mean ± s.e.m. of 3 independent clones. (***p< 0.001 one-way Anova post Bonferroni's multiple comparison test with CI 95% relative to tRNA^{Ser}(Ser).

3.3.6. Mistranslation induces nuclear and organelle alterations

ROS damages DNA, proteins, lipids, the cytoskeleton of yeast cells and also mitochondria. Some studies demonstrated that mitochondria are a source but also a target of ROS, because ROS can promote oxidation of mitochondrial pores, disrupte the mitochondrial membrane potential and finally contribute to cytochrome c release (Eisenberg et al., 2007; Simon et al., 2000). Due to the high level of intracellular ROS detected in cells expressing the $tRNA^{Ser}$(Val), $tRNA^{Ser}$(Leu) and $tRNA^{Ser}$(Ile) we have decided to evaluate the existence of morphological alterations in the mitochondria, vacuole and nuclear chromatin in these strains.

Mitochondrial morphology was assessed by confocal microscopy after labeling cells with the mitochondrial specific probe Mitotracker (methods 3.2.11). Our results showed significant differences in mitochondrial morphology of mistranslating strains relatively to the control pRS315 (figure 3.17). In the control strain a mitochondrial grid/network occupying the central parts of the cell was visible, while the expression of $tRNA^{Ser}$(Leu), $tRNA^{Ser}$(Val) and $tRNA^{Ser}$(Ile) seemed to inhibit the formation of a defined network structure but, independent peripheral spots were observed. These differences in mitochondrial morphology were more accentuated at T20h.

It is known that mitochondrial morphology varies according to environment and depends on the balance of fusion and fission activities. Indeed, mitochondrial fusion enables cells to build extended interconnected mitochondrial networks while fission produces small spherical organelles morphologically and functionally distinct (Hammermeister et al., 2010; Jensen et al., 2000; Palermo et al., 2007; Westermann, 2008). For instance, fusion is essential in embryonic development (Chen et al., 2003) and spermatogenesis (Hales & Fuller, 1997). On the other hand, fission is important for plasticity of spines and synapses (Li et al., 2004), and is linked to apoptosis because it normally occurs before cytochrome c release and caspase activation (Fannjiang et al., 2004; Youle & Karbowski, 2005). But, fission can also occur in the absence of apoptosis (Chen et al., 2003; Suen et al., 2008). Yeasts undergoing mitochondrial fission have mitochondrial DNA loss and are unable to grow on non-fermentable carbon sources, such as glycerol (reviewed in Mozdy & Shaw, 2003). The disruption of the mitochondrial network in cells expressing the $tRNA^{Ser}$(Leu), $tRNA^{Ser}$(Val) and $tRNA^{Ser}$(Ile) suggests a block in mitochondrial fusion or activation of fission.

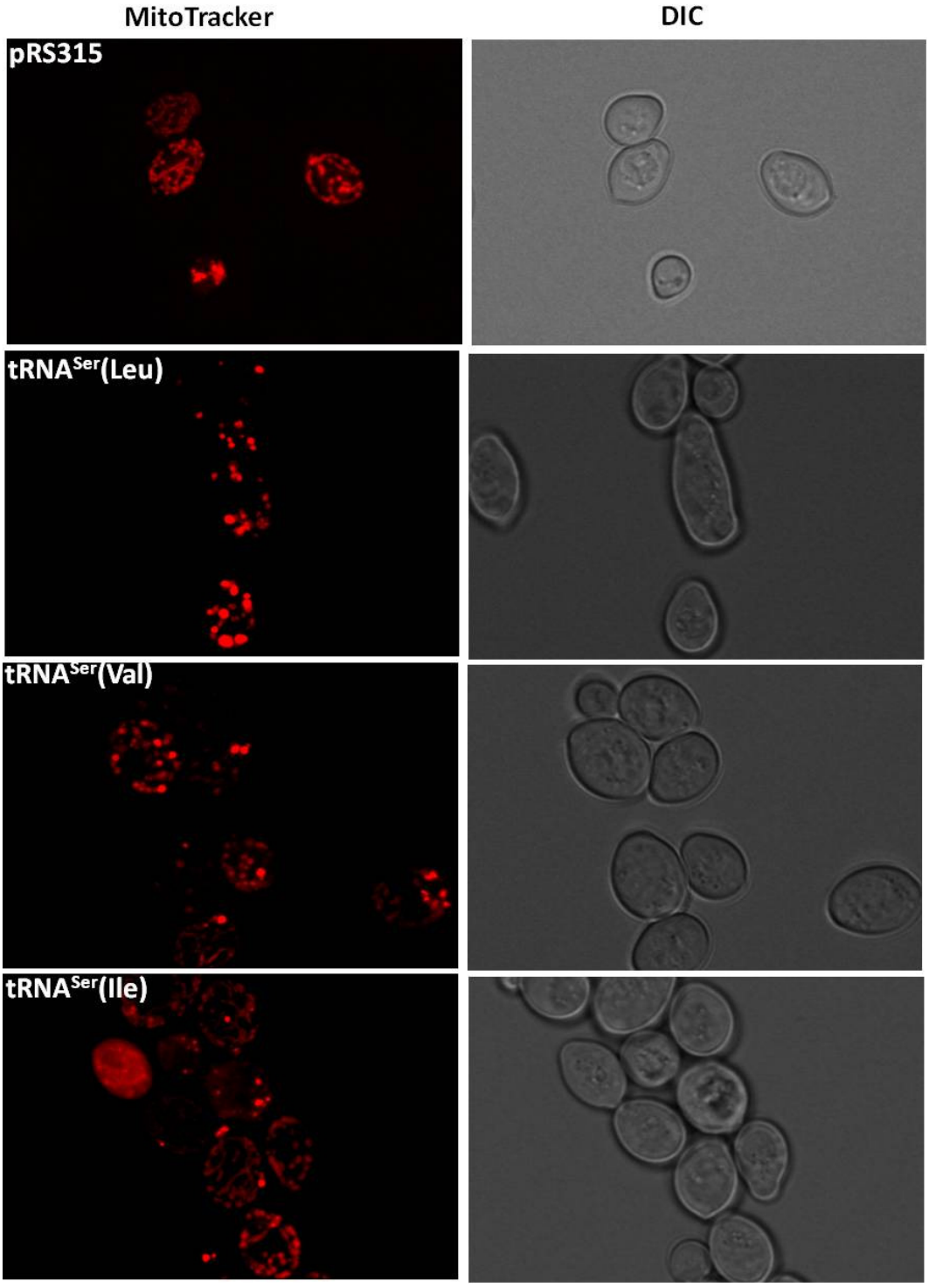

Figure 3.17: Mistranslation induces morphological alterations of yeast mitochondria. Yeast cells transformed with pRS315 and the mistranslating tRNA^{Ser} expressed from single-copy plasmids, were grown in selective medium and were collected at T20h for labeling with MitoTracker (methods 3.2.11). Cells were then visualized using a confocal microscope (Olympus) with an oil immersion objective of 60X.

The above mitochondrial alterations prompted us to evaluate the morphology of vacuoles of these mistranslating strains. For this, cells were labeled with the vital stain FM4-64 (see section 3.2.12), which is specific for vacuoles, and were observed using a confocal microscope. Our data showed significant differences in vacuolar morphology in these strains (figure 3.18). These differences were more evident in cells expressing the $tRNA^{Ser}$(Leu). While control strains had a typical single and large vacuole, expression of $tRNA^{Ser}$(Leu) induced the formation of multiple small vacuoles. This morphological alteration was similar to that described by others, either after yeast treatment with furfural biofuel (Allen et al., 2010) or in some yeast proteasome mutants (Hofmann et al., 2009; Kleijnen et al., 2007). The expression of $tRNA^{Ser}$(Val) and $tRNA^{Ser}$(Ile) did not produce the typical single large vacuole or the multiple small vacuoles, suggesting that these cells did not have distinct vacuolar structures, or that the vacuoles could be highly fragmented or disrupted.

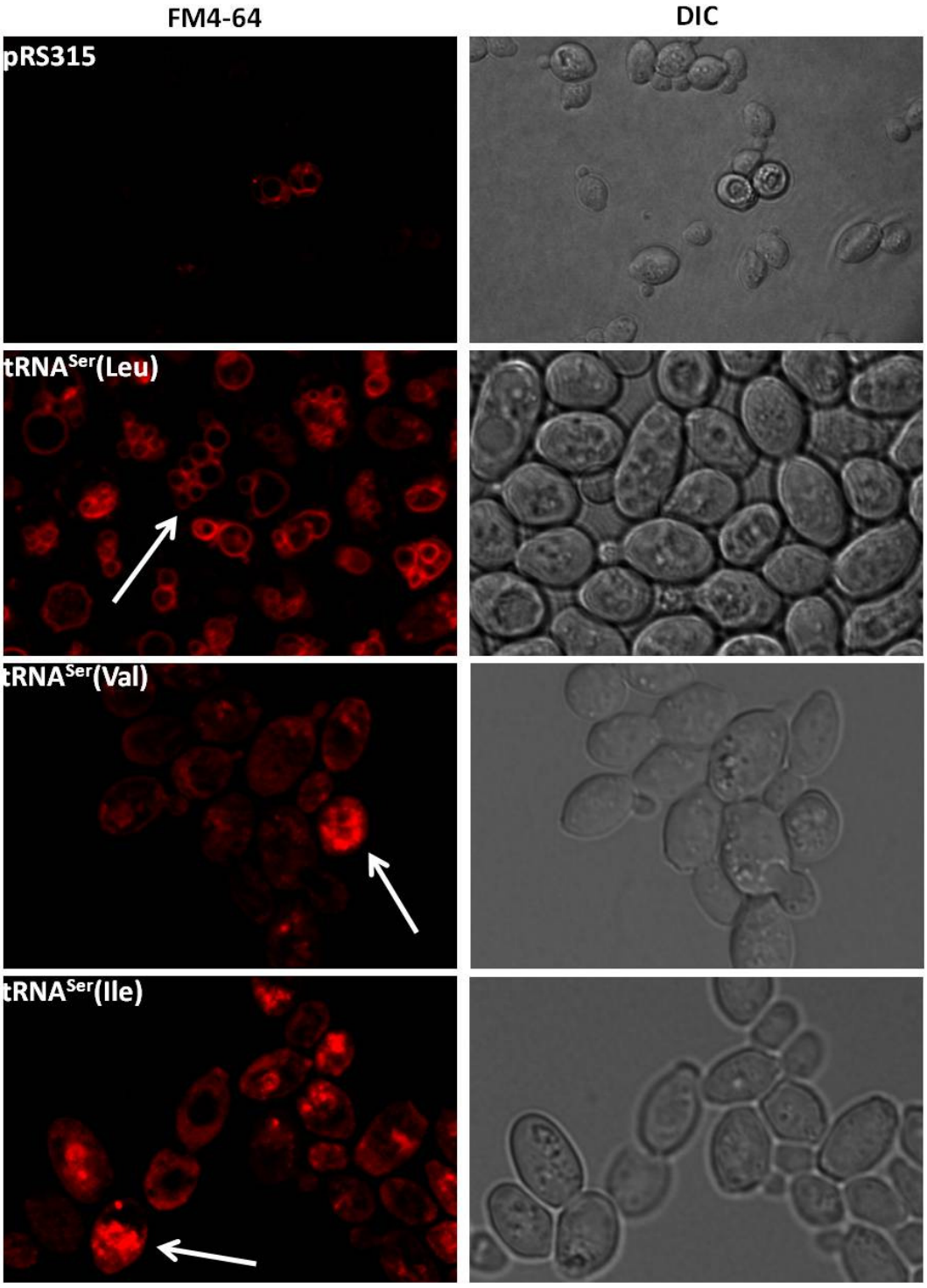

Figure 3.18: Mistranslation induces morphological alterations in the yeast vacuoles. Yeast cells transformed with pRS315 and the mistranslating tRNA^{Ser} expressed from single-copy plasmids, were grown in selective medium and were collected at T20h for labeling with FM4-64 (methods 3.2.12). Cells were then visualized using a confocal microscope (Olympus) with an oil immersion objective of 60X.

We then decided to test whether mistranslation also affect chromatin organization. For this, nuclear chromatin was labeled with 4',6-diamidino-2-phenylindole (DAPI) (see section 3.2.13) and cells were visualized using a confocal microscopy. We observed that cells expressing the $tRNA^{Ser}$(Val) had larger nuclei relative to the control cells (pRS315) (figure 3.19).

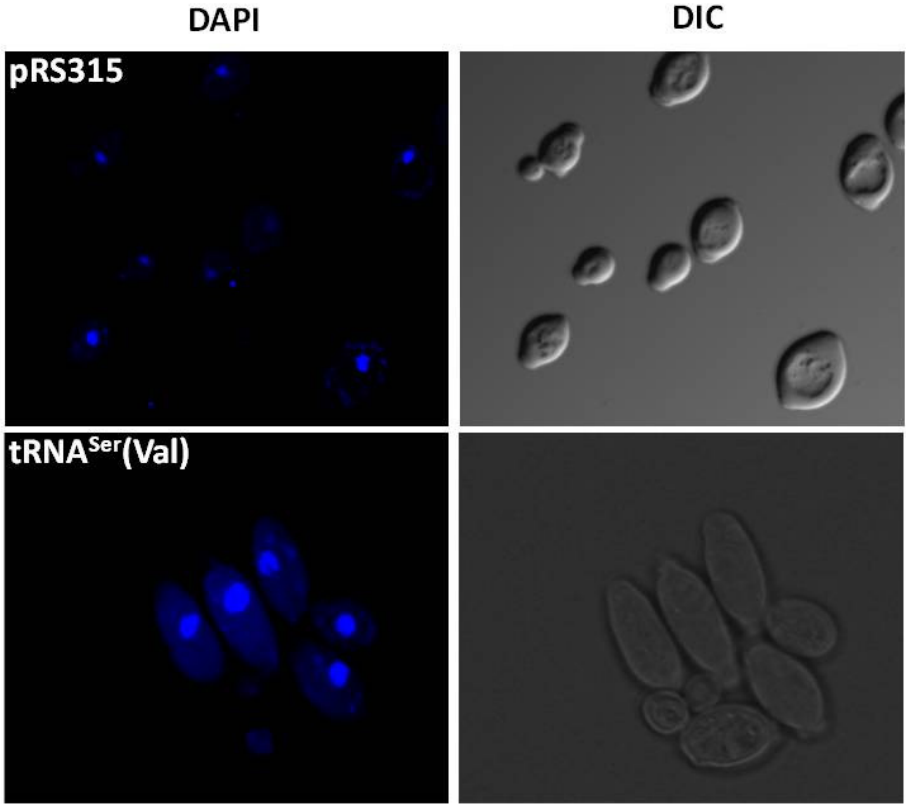

Figure 3.19: Morphology of chromatin in yeast control (pRS315) and cells expressing the $tRNA^{Ser}$(Val). Yeast cells were collected at T15h and were labeled with DAPI (methods 3.2.13). Cells were then visualized using confocal microscopy (Olympus) with an oil immersion objective of 60X.

Significant nuclear alterations were visible in cells expressing the $tRNA^{Ser}$(Leu). In this strain, cells with nuclear fragmentation (arrow 1), cells with two distinct nuclei (arrow 2), anucleated cells (arrow 3) and containing disorganized nuclear chromatin (arrow 4) were clearly visible (figure 3.20). In the case of the expression of the $tRNA^{Ser}$(Ile), cells with disorganized nuclear chromatin (arrow 1), cells with two nuclei (arrow 2) and without nucleus (arrow 3), were easily identified (figure 3.21).

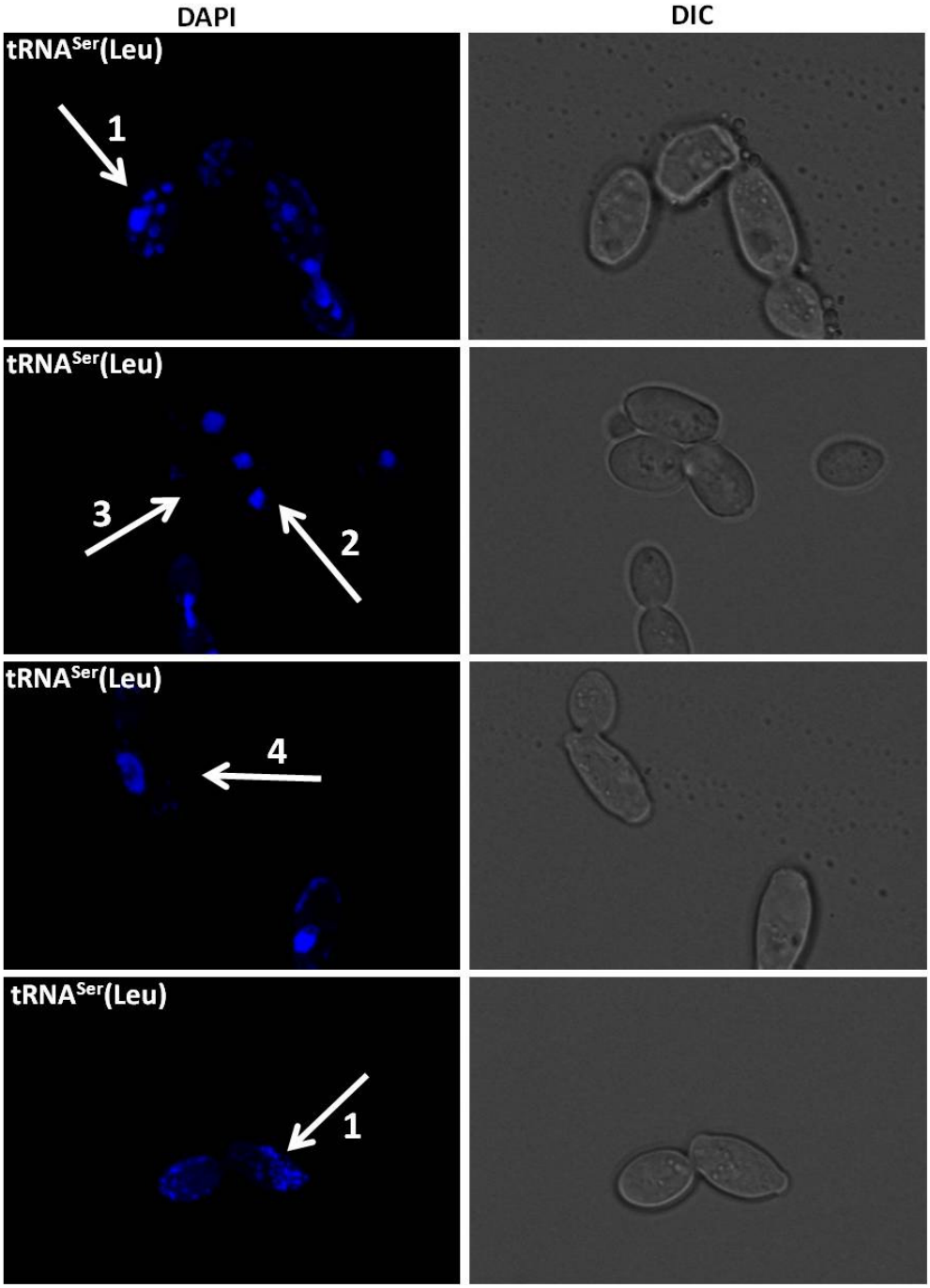

Figure 3.20: Morphological chromatin alterations in yeasts expressing the tRNA^{Ser}(Leu). Yeast cells were collected at T15h and were labeled with DAPI (methods 3.2.13). Cells were then visualized using confocal microscopy (Olympus) with an oil immersion objective of 60X. Alterations observed correspond to nuclear fragmentation (1), cells with two nuclei (2), anucleated cells (3) and with disorganized nuclear chromatin (4).

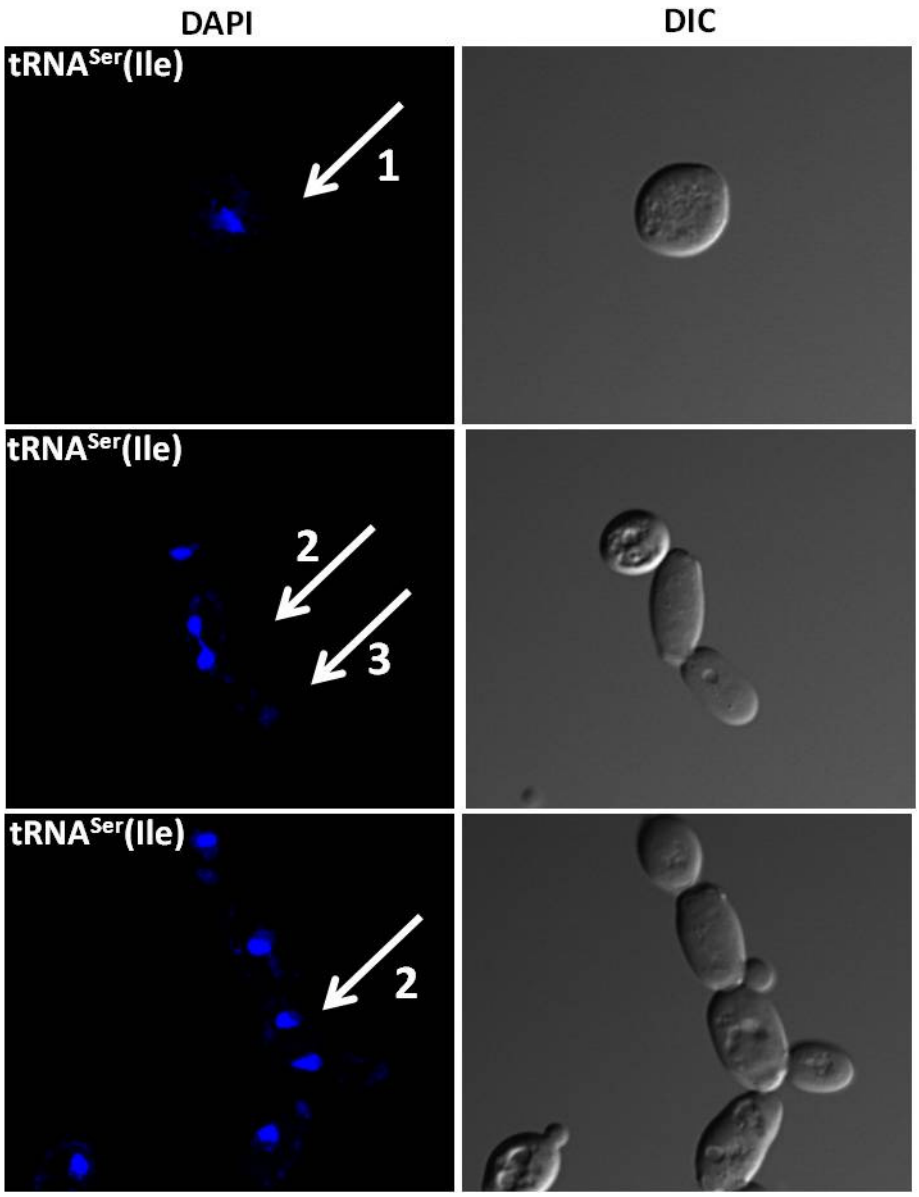

Figure 3.21: Morphological chromatin alteration induced by the expression of the tRNA^{Ser}(Ile). Yeast cells were collected at T15h and labeled with DAPI (methods 3.2.13). Cells were then visualized using confocal microscopy (Olympus) with an oil immersion objective of 60X. Alterations observed correspond to disorganized nuclear chromatin (1), cells with two nuclei (2) and anucleated cells (3).

The analysis of the number of cells with one, two or no nuclei (figure 3.22) showed that the percentage of cells with two nuclei were ~4% when tRNA^{Ser}(Val), tRNA^{Ser}(Leu) and tRNA^{Ser}(Ile) were expressed. In other words, most cells contained a typical single

nucleus. Although, cells without nuclei were also very frequent, being 45% and 37% of the cell population in the cases of the tRNA^{Ser}(Ile) and tRNA^{Ser}(Leu), respectively, and ~8% in the case of the tRNA^{Ser}(Val). This and the presence of cells with two nuclei suggest that mistranslation induces abnormal cell division, with high frequency of nuclei that do not migrate from mother to daughter cell.

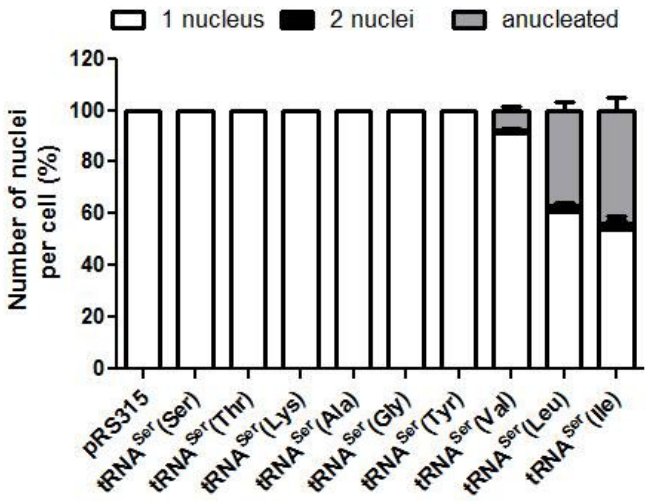

Figure 3.22: Mistranslation induces alterations in the number of nuclei in yeast strains. Yeast cells were observed using a fluorescence microscope (60-100x objectives) after DAPI staining. In order to quantify the number of cells with one, two or no nuclei around 100 cells were counted per clone. Data represent the mean ± s.e.m. of 3 independent clones.

While analyzing the morphology of organelles of the mistranslating strains we have noticed that some cells expressing the tRNA^{Ser}(Leu) and tRNA^{Ser}(Ile) had very different morphologies relative to the control cells (pRS315). Cells were bigger, more elongated and less spherical than control cells, and displayed atypical structures. These atypical filamentous elongated cells are usually identified as hyphae or pseudohyphae (figure 3.23, arrow 1). The appearance of these cellular structures can occur under nitrogen limitation (Dickinson, 1994), during growth in presence of low concentration of fusel alcohols (Dickinson, 1996), at reduced growth rate or under control of metabolic rate (reviewed in Dickinson, 2008). Besides hyphae or pseudohyphae it was also possible to observe other structures, namely the shmoos (figure 3.23, arrow 2), indicating that some cells were mating. Factors such as starvation, nitrogen, carbon, phosphate, sulfate,

guanine, methionine starvation can induce sporulation. After initiation of the sporulation program, spores originate through meiosis, and if mating is occurring shmoo structures are visible (reviewed in Mitchell, 1994).

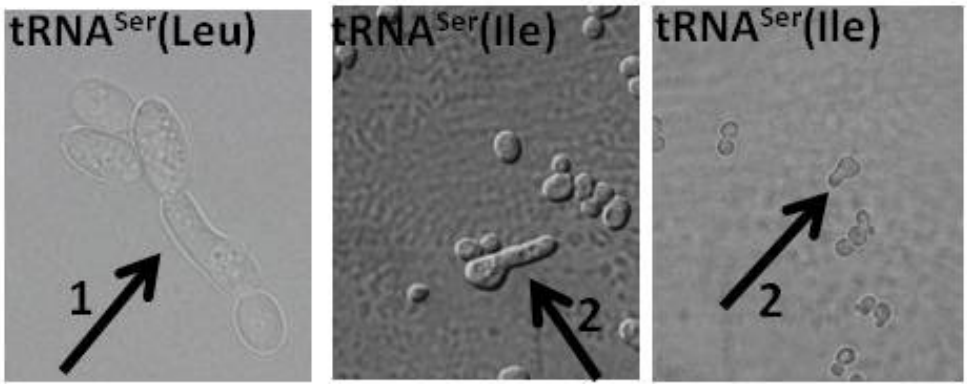

Figure 3.23: Morphological alterations of yeast mistranslating strains. Yeast cells were observed using a fluorescence microscope (60-100x objectives). Cells with atypical morphologies were visible in strains expressing tRNA^{Ser}(Leu) and tRNA^{Ser}(Ile). The atypical morphologies included pseudohyphae (1) and shmoos (2).

3.3.7. Mistranslation induces protein aggregation

Mistranslation is an important source of aberrant proteins that may misfold, aggregate or may be degraded. Erroneous proteins can be truncated translational polypeptides, misfolded intermediates and unassembled subunits of oligomeric protein complexes that expose their hydrophobic regions that are highly susceptible to aggregation. Moreover, mechanisms like protein oxidation, carbonylation, nitrosylation, unbalancing of protein synthesis, oxidative stress, heavy metals, and heat-shock may induce protein aggregation. These alterations occur frequently but at tolerable levels. In order to circumvent toxicity induced by protein aggregation cells activate mechanisms to remove aggregates. Usually, reparable aggregates are rescued by molecular chaperones, while irreparably aggregates are degraded. This degradation could be either via the ubiquitin–proteasome system or by autophagy in the case of aggregated proteins resistant to proteasomal degradation (reviewed in Dobson, 2003; Hampton, 2002). Failure of these quality control mechanisms are responsible for many human diseases, like diabetes and neurodegenerative disorders (reviewed in Vashist et al., 2010).

Our mistranslation system is expected to destabilize proteins, leading to protein misfolding and aggregation. In order to test this hypothesis, we have quantified the insoluble protein fraction in mistranslating strains and we then determined the presence of cytoplasmic aggregates using a Hsp104-GFP reporter system.

Quantification of protein aggregates by isolating the insoluble protein fraction and fractionating it on SDS-PAGE electrophoresis is commonly used (Galoubinoff et al., 1999; Halsbeck et al., 2005; Holland et al., 2007; Jang et al., 2004; Mogk et al., 1999; Rand & Grant, 2006). We have used this methodology (section 3.2.14) to isolate the insoluble protein fraction of our mistranslating strains. The mistranslating strains expressing the $tRNA^{Ser}$(Leu) and $tRNA^{Ser}$(Ile) showed increased levels of insoluble proteins (figure 3.24). For the other mistranslating strains no significant increase was detected.

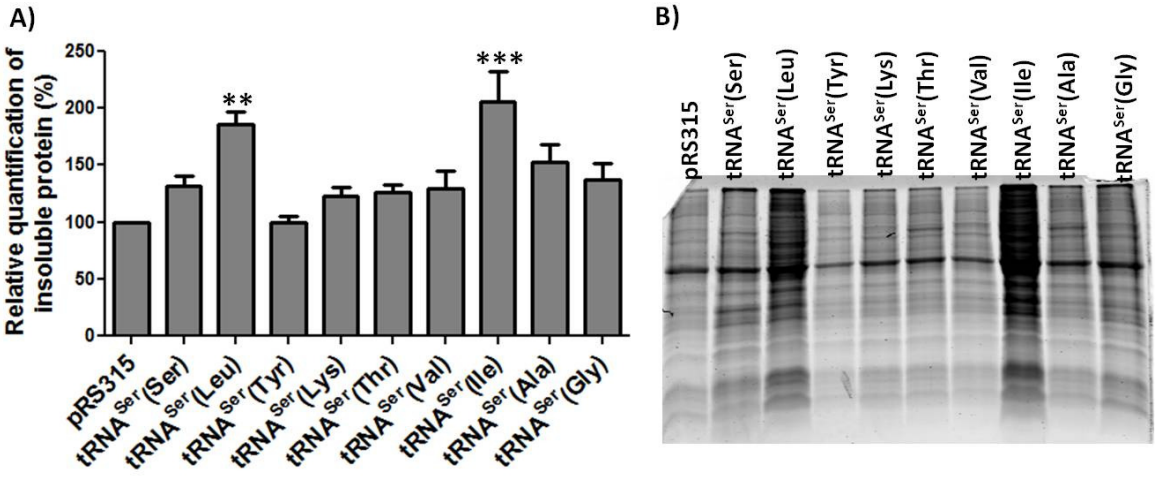

Figure 3.24: Mistranslation increases the level of insoluble proteins. A) The graph represents the relative quantification of insoluble proteins in mistranslating strains relative to the control strain (pRS315). Equal number of cells ($3x10^8$) expressing wt and mistranslating $tRNA^{Ser}$ from single-copy plasmids were collected and cytosolic extracts were prepared (methods 3.2.14). The insoluble protein fraction was fractionated by SDS-PAGE and gel lane intensities were then quantified. Results are represented as the percentage of insoluble protein of mistranslating strains relative to the control strain (pRS315). B) Representative gel showing the insoluble protein fraction of all mistranslating and control strains. Data represent the mean ± s.e.m. of duplicates of 3 independent clones. (***p< 0.001, **p< 0.01 one-way Anova post Bonferroni's multiple comparison test with CI 95% relative to pRS315 strain).

The data are in line with the higher toxicity of the $tRNA^{Ser}$(Leu) and $tRNA^{Ser}$(Ile) due to substitution of two hydrophobic amino acids by polar serine. Although, we were also

expecting to detect protein aggregation for the other mistranslating strains. In order to clarify whether the latter would also be able to produce aggregated proteins we have used an alternative method based on a Hsp104-GFP reporter protein. Hsp104p is a molecular chaperone involved in protein disaggregation which accumulates at the periphery of electron-dense aggregates under stress conditions that promote protein aggregation. In other words, in presence of protein aggregates, the Hsp104-GFP reporter forms distinct fluorescent foci and produces diffused fluorescence in absence of protein aggregates (Erjavec et al., 2007; Fujita et al., 1998; Lum et al., 2004). In order to monitor protein aggregates using the Hsp104-GFP reporter we have transformed a yeast strain containing this reporter integrated at the HSP104 locus, with single-copy plasmids carrying the mistranslating tRNAs. Since Ser misincorporation at Leu, Val and Ile codons is too toxic in haploid cells we have used diploid cells for these particular cases. In other words, the haploid strain harboring the Hsp104-GFP fusion was only transformed with pRS315, and with plasmids carrying less toxic $tRNA^{Ser}$ that misincorporate Ser at Ser, Tyr, Lys, Thr, Ala and Gly codons, while the diploid strain was transformed with plasmids carrying all mistranslating $tRNA^{Ser}$. Cells were grown up to middle exponential phase and were collected for observation by fluorescence microscopy (methods 3.2.15). Interestingly, only the expression of $tRNA^{Ser}$(Gly) produced discrete fluorescent foci, indicative of protein aggregation (figure 3.25). This was in sharp contrast with the SDS-PAGE results which showed poor protein aggregation in this strain.

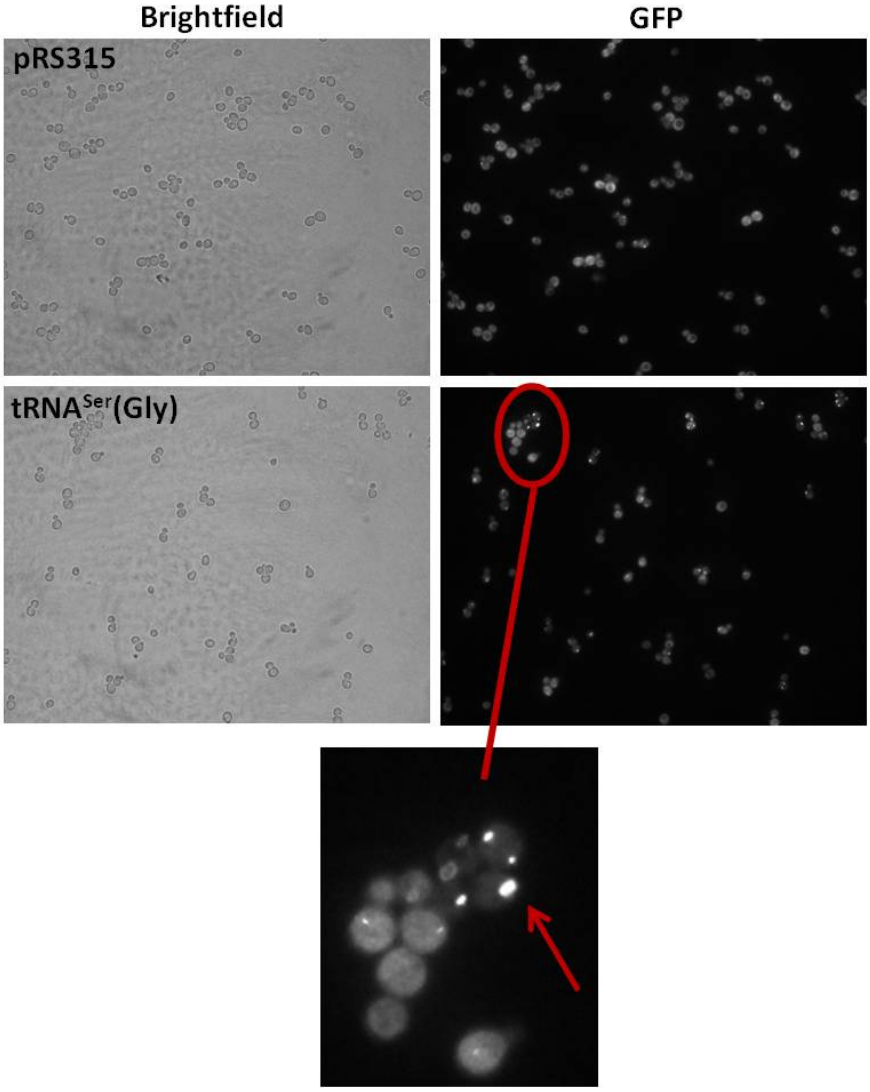

Figure 3.25: Mistranslation induces cytoplasmatic protein aggregates. Yeast cells expressing the Hsp104-GFP reporter protein were transformed with pRS315, tRNA^{Ser}(Ser) and mistranslating tRNA^{Ser} expressed from single-copy plasmids and were collected from middle exponential phase and observed by fluorescence microscopy (60x objective). Cells expressing the tRNA^{Ser}(Gly) showed localized Hsp104-GFP fluorescence, indicating the presence of protein aggregates.

The number of cells containing GFP fluorescent foci were quantified (figure 3.26A) and the data showed significant increase (37%) in localized Hsp104-GFP in cells expressing the tRNA^{Ser}(Gly). Mistranslation of Ala and Tyr codons to Ser also induced protein aggregation, but less extent. In the diploid strain, where mistranslation was less toxic, we were unable to identify protein aggregates (figure 3.26B), suggesting that such

aggregation is dependent on both the chemical nature of the amino acid and mistranslation efficiency.

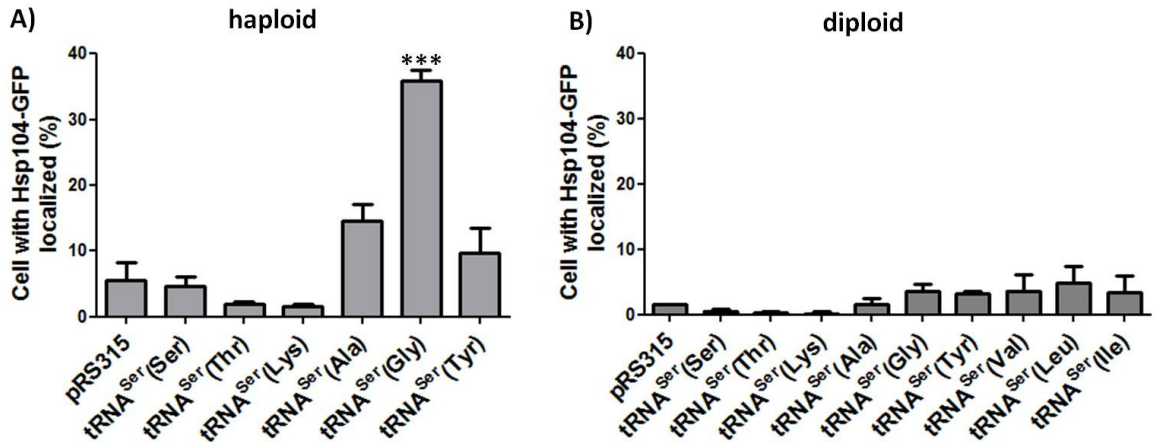

Figure 3.26: Quantification of localized Hsp104-GFP fluorescence in yeast haploid and diploid mistranslating strains. Yeast cells containing localized Hsp104-GFP fluorescent foci were counted. Results are expressed as the percentage of Hsp104-GFP foci positive cells present in a population of 400 cells. Data represent the mean ± s.e.m. of 3 independent clones. (***p< 0.001 one-way Anova post Bonferroni's multiple comparison test with CI 95% relative to pRS315).

These results prompted us to further confirm the formation of protein aggregates in the mistranslating cells. For this, we have constructed a new Hsp26-GFP reporter protein. Hsp26p helps Hsp104p during the initial stages of protein disaggregation and it also co-localizes with such aggregates. Therefore, we have constructed a yeast diploid strain harboring the Hsp26-GFP fusion protein (section 3.2.15), which was then transformed with single-copy plasmids expressing our mistranslating tRNAs. The data confirmed the Hsp104-GFP aggregation data. In other words, there was a significant increase in localized Hsp26-GFP fluorescence only in the cells expressing the $tRNA^{Ser}$(Gly) (figure 3.27).

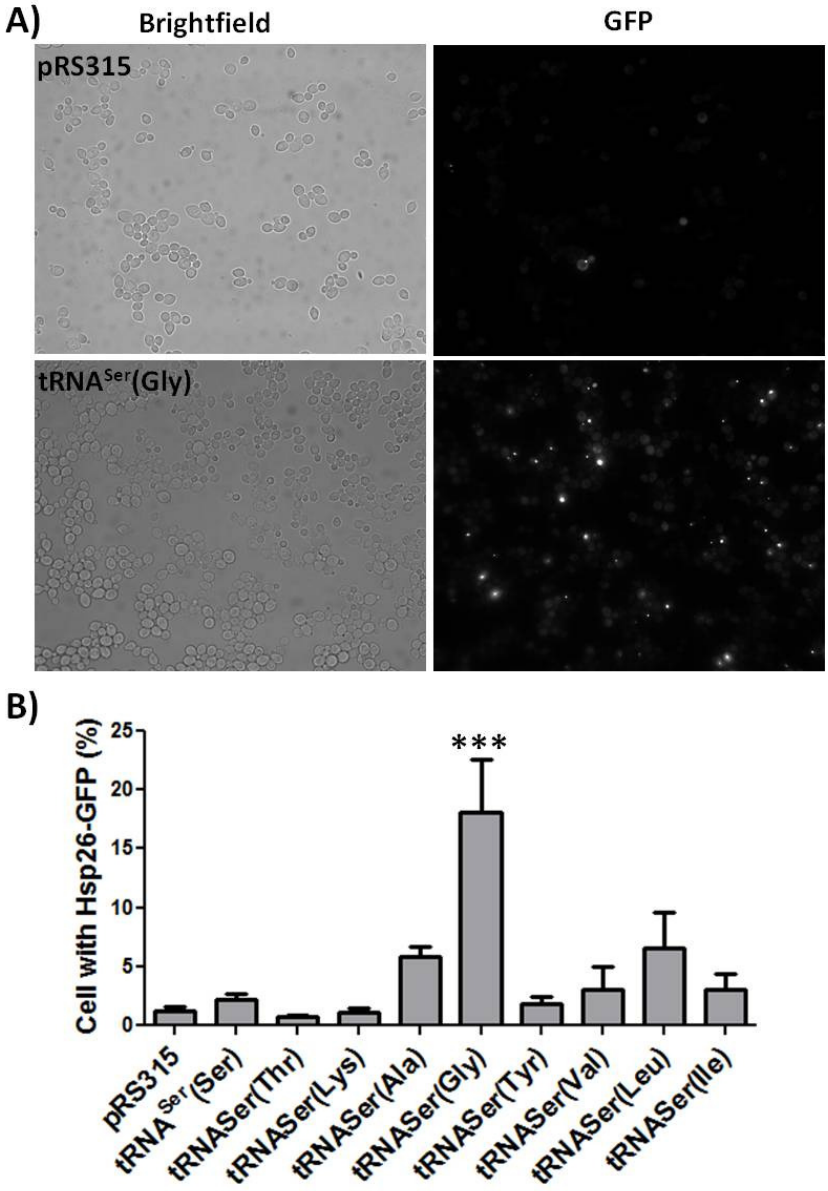

Figure 3.27: Monitoring protein aggregation using a Hsp26-GFP reporter protein. A) Cells expressing the Hsp26-GFP fusion protein were transformed with pRS315, $tRNA^{Ser}$(Ser) and mistranslating $tRNA^{Ser}$ expressed from single-copy plasmids and were allowed to grow to middle exponential phase. Cells were then collected and observed by fluorescence microscopy (60x objective). B) Quantification of cells with Hsp26-GFP localized fluorescence. The number of Hsp26-GFP foci was counted and the percentage of foci positive cells in a population of 400 cells was determined. Data represent the mean ± s.e.m. of 3 independent clones. (***p< 0.001 one-way Anova post Bonferroni's multiple comparison test with CI 95% relative to pRS315).

The cooperation between Hsp104p and Hsp26p in modulating protein disaggregation is well known. It seems that Hsp26p interacts first with misfolded proteins that have their hydrophobic residues exposed and binds to them, forming large protein aggregates which allow for their efficient recognition and disaggregation by Hsp104p (Cashikar et al., 2005). For this reason aggregates containing both misfolded proteins and small Hsps, like Hsp26p and Hsp42, acquired a structure which is more rapidly dissolved by Hsp104p. When the large protein aggregates are dissolved the small particles become accessible for refolding by the Hsp70/Hsp40 chaperone system, and Hsp26p or Hsp42p can be recycled to present new protein aggregates to Hsp104p (reviewed in Glover & Lindquist, 1998; Grimminger-Marquardt & Lashuel, 2009). Interestingly, Hsp26p is only activated by heat-shock and remains inactive under physiological conditions (Halsbeck et al., 1999), while Hsp42p is active under both physiological and stress conditions (Halsbeck et al., 2004).

Therefore, it is likely that mistranslation of Gly codons as Ser induces formation of protein aggregates that mobilized Hsp26p while the other types of aggregates originated by the other mutant mistranslating tRNAs may not trigger such modification of Hsp26p. If so, Hsp104p may not be mobilized. In other words, our data suggest that different types of mistranslation may induce formation of different types of aggregates.

As mentioned before, mistranslated proteins may misfold and aggregate or may be degraded through the ubiquitin-proteasome system (UPS) and/or autophagy (reviewed in Dobson, 2003). In order to better understand how mistranslated proteins are degraded we have quantified the activity of proteasome (methods 3.2.16) of our mistranslating strains. Interestingly, we did not detect a significant increase in its activity relative to the control cells (pRS315), with exception of cells expressing the $tRNA^{Ser}$(Leu) (30% increase) (figure 3.28). This result was unexpected because mistranslation of Ile codons as Ser was also very toxic, suggesting that this strain also contained high level of misfolded proteins (figure 3.24). Therefore, it is likely that mistranslated proteins are targeted to the autophagy pathway or somehow escape degradation.

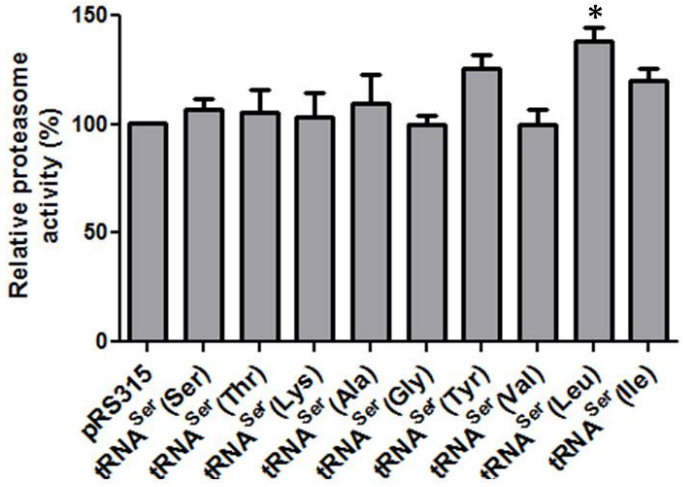

Figure 3.28: Mistranslation has a mild effect on proteasome activity. Yeast cells transformed with pRS315, tRNA^{Ser}(Ser) and mistranslating tRNA^{Ser} expressed from single-copy plasmids were grown and collected from middle exponential phase cultures and were incubated with the chymotrypsin-like substrate SucLLVY-AMC. Proteasome activity was quantified by measuring fluorescence emission at 435 nm (methods 3.2.16). Data represent the mean ± s.e.m. of triplicates of 3 independent clones. (*$p < 0.05$ one-way Anova post Bonferroni's multiple comparison test with CI 95% relative to pRS315).

3.3.8. Effect of mistranslation on protein synthesis rate

It is known that protein synthesis is reduced during stress, namely during oxidative, osmotic and heat stress. Some authors highlight that this reduction in protein synthesis may prevent gene expression during conditions that induce errors, allowing for efficient turnover of existing mRNAs and proteins, whilst gene expression is reprogrammed (Gasch, 2002; Geslain et al., 2009; Mager & Moradas Ferreira, 1993; Norbeck & Blomberg, 1998; Shenton et al., 2008). Since mistranslation induces proteotoxic stress we have evaluated its impact on global protein synthesis. For this, we have carried out pulse labeling experiments using [^{35}S]-methionine, as explained in section 3.2.17. Our results showed a significant decrease of protein synthesis rate in cells expressing the tRNA^{Ser}(Thr), tRNA^{Ser}(Val) and tRNA^{Ser}(Ile). No change was observed in cells expressing the tRNA^{Ser}(Lys) and tRNA^{Ser}(Leu) and a surprising increase was observed in the strains expressing the tRNA^{Ser}(Tyr), tRNA^{Ser}(Ala) and tRNA^{Ser}(Gly) (figure 3.29).

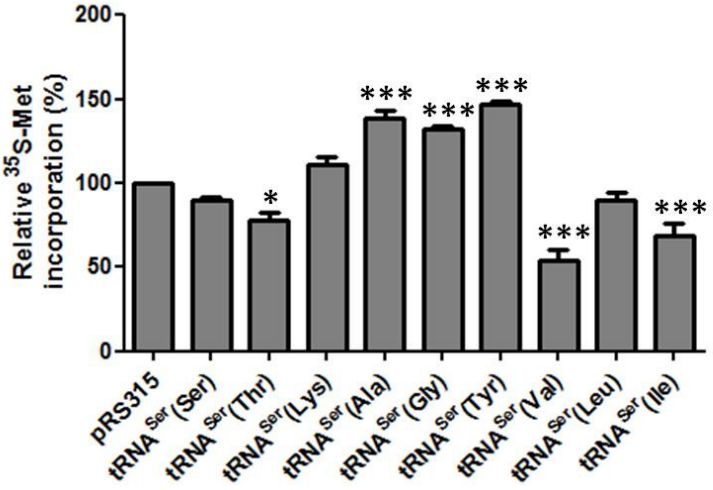

Figure 3.29: Effect of mistranslation on protein synthesis rate. Yeast cells transformed with pRS315, tRNA^{Ser}(Ser) and mistranslating tRNA^{Ser} expressed from single-copy plasmids were collected from exponentially growing cultures and were incubated for 20 min in media lacking methionine. Cells were labelled with [^{35}S]-Met for 8 min and protein synthesis was then stopped by addition of cyclohexamide. The efficiency of protein synthesis was calculated by determining the level of incorporation of [^{35}S]-Met into newly synthesized proteins. Results are expressed as percentage of [^{35}S]-Met incorporation in mistranslating strains relative to the control cells (pRS315). Data represent the mean ± s.e.m. of triplicates of 3 independent clones. (***p< 0.001, **p< 0.01, *p< 0.05 one-way Anova post Bonferroni's multiple comparison test with CI 95% relative to pRS315).

Since mistranslation affected growth rate in all strains, we were expecting a general decrease in protein synthesis in all cases, however only the strains expressing the tRNA^{Ser}(Thr), tRNA^{Ser}(Val) and tRNA^{Ser}(Ile) showed statistically significant reduction in protein synthesis. The tRNA^{Ser}(Lys) showed a clear correlation between growth rate and the rate of protein synthesis. The lack of a negative impact on protein synthesis in cells expressing the tRNA^{Ser}(Leu) was surprising because was one of the most toxic types of mistranslation that we have tested.

In order to clarify the above mentioned discrepancies we have investigated whether ribophagy was activated in our mistranslating cells. In this process, ribosomes are selectively translocated to vacuoles for degradation. Two major proteins are involved in this process, the Ubp3p and Bre5p, which are required for the degradation of 60S, but not 40S ribosomal subunits, during starvation (reviewed in Beau et al., 2008). Ribophagy

can be easily monitored in yeast using a RPL25-GFP reporter protein. The ribosomal RPL25-GFP reporter translocates to the vacuoles and provides an indirect indication of ribosome degradation (Dalley et al., 2008; Hurt et al., 1999). For this, mistranslating strains were transformed with a plasmid carrying the RPL25-GFP reporter gene. The level of RPL25-GFP fluorescence in all mistranslating strains was lower than that of control cells (figure 3.30), suggesting that mistranslation decreased the number of ribosomes per cell, which contradicts the protein synthesis rate data (figure 3.29).

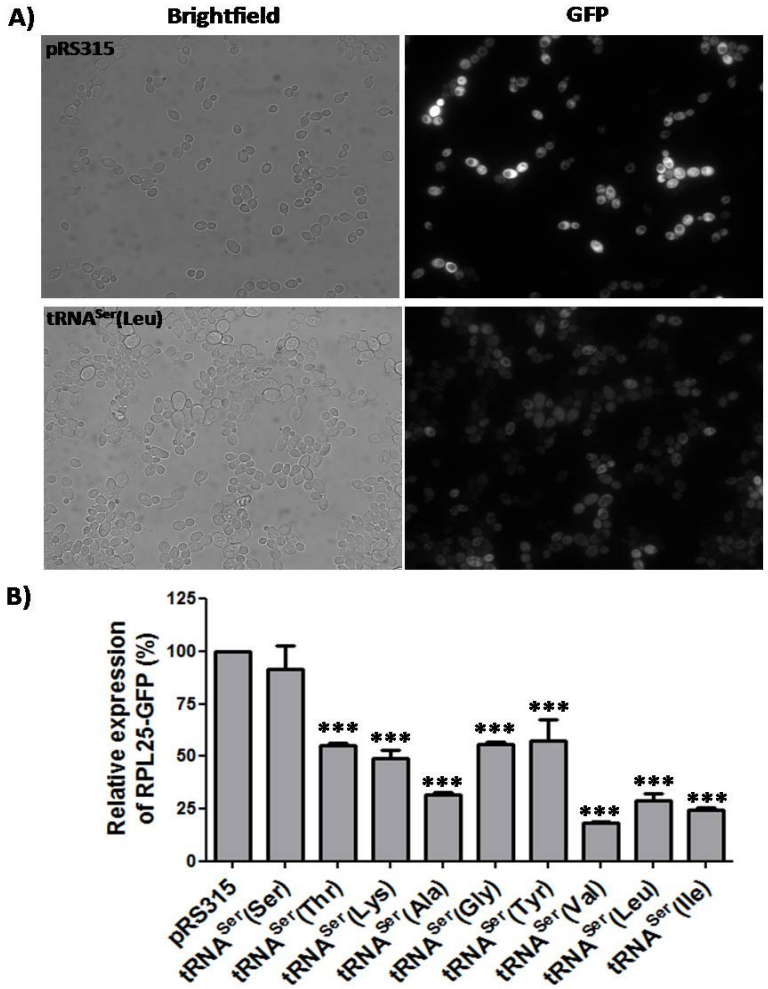

Figure 3.30: Quantification of the ribosomal protein RPL25 in mistranslating strains. A) Yeast cells transformed with pRS315, $tRNA^{Ser}$(Ser) and mistranslating $tRNA^{Ser}$ expressed from single-copy plasmids and the plasmid harboring the fusion protein RPL25-GFP were observed during exponential growing phase by fluorescence microscopy. B) Results are expressed as the percentage of GFP fluorescence, determined in mistranslating strains relative to the control strain (pRS315). Data represent the mean ± s.e.m. of triplicates of 3 independent clones. (***p< 0.001, **p< 0.01, *p< 0.05 one-way Anova post Bonferroni's multiple comparison test with CI 95% relative to pRS315 strain).

3.3.9. Phenomics of genome mistranslation

Our data, described above, showed that mistranslation is mainly degenerative, however a previous study showed that CUG decoding ambiguity in yeast creates a competitive advantage under specific stress conditions, mainly due to activation of the stress response and stress cross protection (Santos et al., 1999). We were interested in understanding whether our mistranslation induces selective advantages in an array of environmental conditions and also determine whether different types of mistranslation would produce phenotypic variation. We also wondered if mistranslating strains expressing the mutant $tRNA^{Ser}$(Lys), $tRNA^{Ser}$(Ala) and $tRNA^{Ser}$(Gly) from multicopy plasmids would have the same phenotypic variation as the strains expressing the same tRNAs from single copy plasmids.

In order to answer those questions we developed a phenotypic screening where the mistranslating strains expressing the mutant tRNAs $tRNA^{Ser}$(Ile), $tRNA^{Ser}$(Leu), $tRNA^{Ser}$(Val), $tRNA^{Ser}$(Tyr), $tRNA^{Ser}$(Gly), $tRNA^{Ser}$(Ala), $tRNA^{Ser}$(Lys), $tRNA^{Ser}$(Thr) and $tRNA^{Ser}$(Ser) from single-copy plasmids and the mutant tRNAs $tRNA^{Ser}$(Lys), $tRNA^{Ser}$(Ala) and $tRNA^{Ser}$(Gly) from multicopy plasmids, were grown in different stress conditions. These stressors varied from nutrient composition (without glucose, 2% galactose, 2% glycerol), temperature (37ºC), acidity (pH), presence of drugs (geneticin, paramomicine), toxics (caffeine, ethanol, sorbitol, SDS, EDTA), metals (cadmium, copper, chromium, lithium), oxidizing agent (menadione) and osmotic/ionic stress (calcium, sodium chloride). Cells were grown in solid medium supplemented with these stressors, as explained in section 3.2.18. Figure 3.31 shows the results of the phenotypic screening of yeast expressing the mutant tRNAs from single-copy plasmids and figure 3.32 shows the results of the phenotipyc screening of yeast expressing the mistranslating tRNAs from multicopy plasmids.

Our results show high phenotypic diversity among the mistranslating strains in presence of different environmental stressors. For example, the strain misincorporating Ser at Ile codons was sensitive to nearly all stressors tested, while Ser misincorporation at Lys codons increased tolerance to most conditions and generated significant selective advantages, relative to the control strain (pRS315) (figure 3.31). On the other hand, strains misincorporating Ser at Lys, Gly and Ala codons at high level (multicopy plasmids) had no advantage relative to the control strain (figure 3.32).

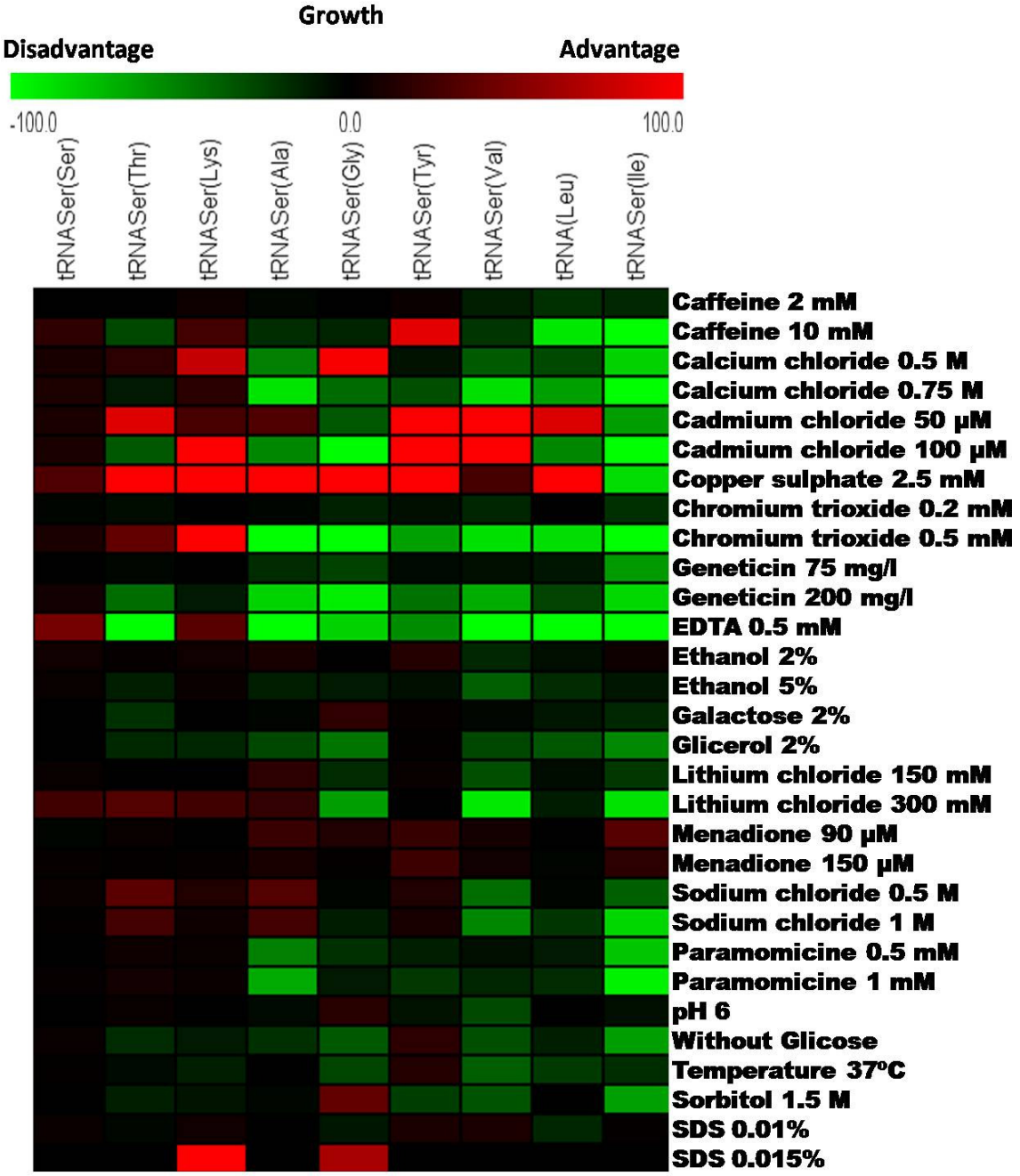

Figure 3.31: Phenomics of yeast strains misincorporating Ser at various non-cognate codons. The growth performance of yeast cells, transformed with $tRNA^{Ser}$(Ser) and mistranslating $tRNA^{Ser}$ expressed from single-copy plasmids, under 30 different environmental conditions was measured (section 3.2.18). Results are represented as growth advantage (red), or disadvantage (green), or identical growth (black), relative to the control strain (pRS315). The data represents the average of two independent growth cultures of three independent clones of each strain. For detailed data see annexes II.

Interestingly, the growth advantages observed in the presence of certain stressors for the strains that mistranslated at low level (single-copy plasmids) were not maintained at high mistranslation level (multicopy plasmids), showing that increased toxicity of mistranslation eliminates the advantages created by low level mistranslation.

The data also showed that mistranslation is not advantageous in media containing different nutrient composition, different pH or when strains were grown at a different temperature. Conversely, media containing copper sulphate and cadmium chloride produced the highest phenotypic variation and selective advantages. Ser misincorporation at Ile codons was not advantageous in the media tested, with the exception of menadione where was measured a growth advantage of 40% (90 µM menadione). In fact, Ser misincorporation at Ile codons produced the highest growth advantage in presence of menadione, which may be explained by the higher level of ROS in this strain that may induce antioxidant defenses and, therefore, stress cross protection.

Ser misincorporation at Leu codons produced selective advantages in presence of cadmium chloride and copper sulfate, with a relative growth advantage of 100% and 400%, respectively (annexes II). Cells misincorporating Ser at Ile and Leu codons had a significant disadvantage in presence of caffeine, EDTA and SDS, where no growth was observed. Ser misincorporation at Val codons showed relative advantages in presence of cadmium chloride and copper sulphate similar to cells with Ser misincorporation at Leu codons, and was disadvantageous in presence of SDS, EDTA and high concentration of calcium chloride and lithium chloride. Ser misincorporation at Tyr codons was advantageous in presence of copper sulphate and cadmium chloride, and was the only case where a growth advantage was scored in presence of caffeine. Ser misincorporation at Gly codons showed a relative growth advantage in media containing copper sulphate, calcium chloride, sorbitol and SDS, while Ser misincorporation at Ala codons did not induced any significant phenotypic variation, with exception of copper sulphate. Interestingly, Ser misincorporation at Lys codons was advantageous in almost all media, while Ser misincorporation at Thr codons did not induced significant phenotypes with exception of lack of growth in presence of EDTA and a high relative growth advantage in presence of copper sulphate and cadmium chloride.

The most important data of our phenotypic screening was the consistent resistance of mistranslating strains to cadmium chloride and copper sulphate. Indeed, the relative growth advantage in presence of cadmium chloride reached 500% (annexes II) for strains that misincorporated Ser at Tyr and Val codons, while the relative growth

advantage scored for copper sulphate was 1500% (annexes II) for the strain misincorporating Ser at Tyr codons.

The strains that mistranslated at high level (multicopy plasmids) did not show significant growth advantage in the media tested (figure 3.32), with the exception of Ser misincorporation at Lys codons in media containing menadione. Curiously, these strains did not show a relative growth advantage in presence of cadmium chloride and copper sulphate.

Our data demonstrates that different types of mistranslation produce different phenotypic outcomes. For instance, even strains with similar growth rate in standard minimal medium, namely those misincorporating Ser at Leu, Ile and Val codons, are phenotypically different. Interestingly, low level (single-copy tRNA expression) of Ser misincorporation at Lys, Ala and Gly codons was advantageous, i.e., in EDTA, SDS and copper sulphate media, but high mistranslation levels (tRNAs expressed from multicopy plasmids) were disadvantageous in the same media. This data suggest that there is a threshold of mistranslation where selective advantages can be observed and that beyond that line, toxicity likely becomes prohibitive and cell death is prominent.

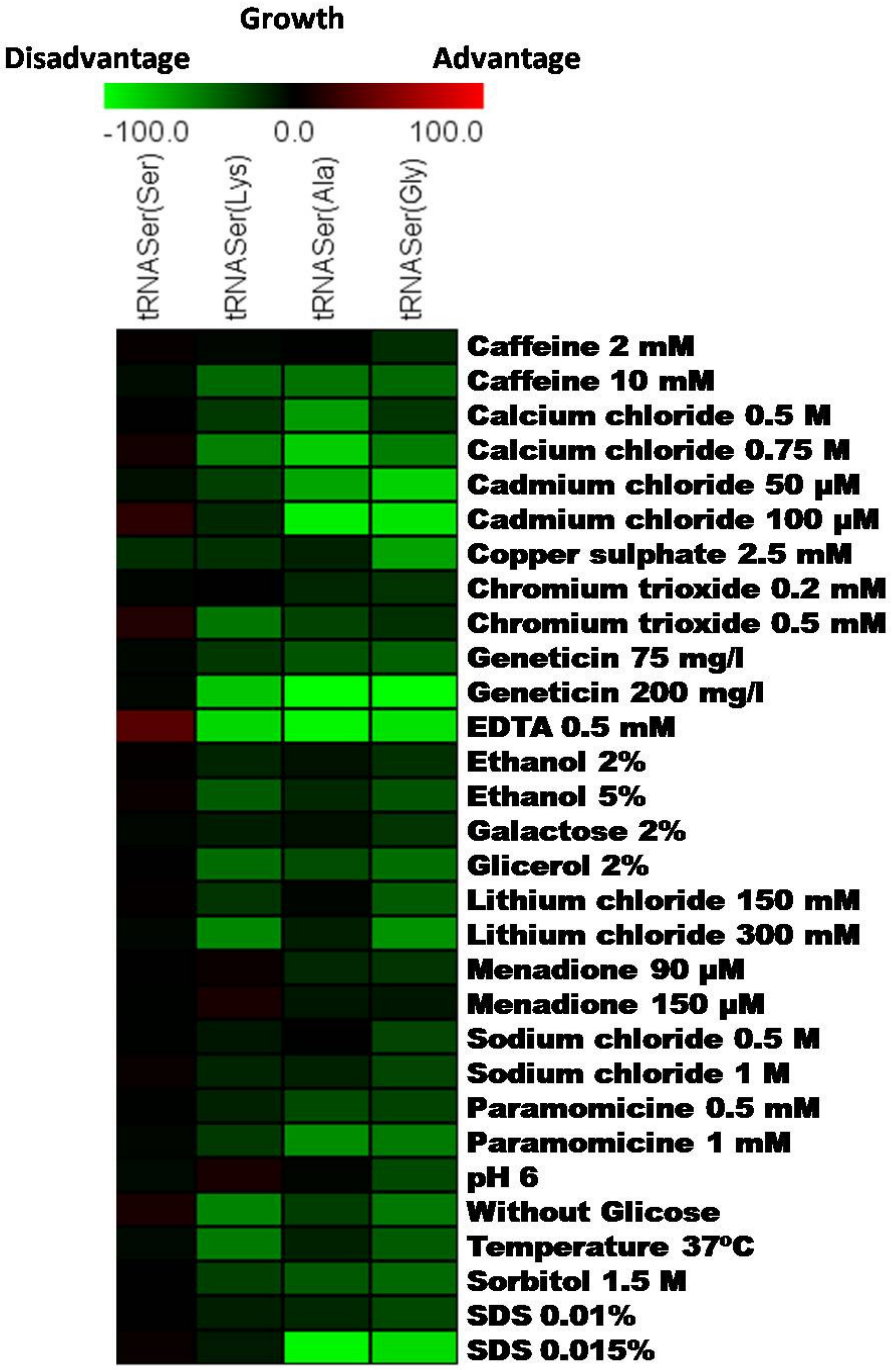

Figure 3.32: Phenomics of yeast strains mistranslating at high level. The growth performance of yeast cells, transformed with $tRNA^{Ser}$(Ser) and mistranslating $tRNA^{Ser}$ expressed from multicopy plasmids, in presence of 30 different environmental conditions was determined as described in methods (section 3.2.18). Results are represented as growth advantage (red), or disadvantage (green), or identical growth (black), relative to the control strain (pRS425). The data represents the average of two independent growth cultures of three independent clones of each strain. For detailed data see annexes II.

3.4. Discussion

In this chapter we have investigated the likelihood of altering the standard genetic code by misincorporating Ser at codons belonging to different amino acids. These alterations induced phenotypic advantages under specific conditions, despite the expected negative effect of amino acid substitutions on protein stability, structure and function. How mistranslation induces phenotypic advantages remains to be clarified, however a single amino acid substitution (Gln102-to-Arg) changes the specificity of *Bacillus stearothermophilus* lactate dehydrogenase from lactate to malate (Wilks et al., 1988), suggesting that some mistranslated proteins may acquire new functions. These dramatic effects of amino acid misincorporation are not surprising since amino acids have different physical, chemical and structural properties (table 3.7).

The position of the amino acids in the proteins is correlated with amino acid properties. Indeed, there is a negative correlation between amino acids accessibility and their polarity and conservation in proteins, in which the more conserved hydrophobic amino acids (Trp, Met, Phe, Ile, Leu, Val and Ala) are usually buried in the interior of the protein structure, while the less conserved hydrophilic amino acids (Thr, Ser, Asn, Gln, Arg, Asp, Glu, Lys) are more frequently exposed on the protein surface. Moreover, small proteins, with less than 100 amino acids, contain an increase in Cys, Arg and Lys, while Glu and Asp are less common (White, 1992). This tendency does not depend exclusively of the amino acid, but, also of the sequence context in which residues are located and on the restriction to rotate the proteins side chain (Padmanabhan et al., 1990). Gly is more frequent in protein U-turns (Wilmot & Thornton, 1988) and is equally exposed and buried in proteins, while Cys is the most conserved residue and the rarest at the surface (Fiser et al., 1996) due to its reactive side chain (Craighton, 1993). Interestingly, the distribution of the amino acids in the proteins sequences is most likely related to their tendency to stabilize or disrupt β-sheet or α-helical structures (Bahar et al., 1997). Amino acids with U at the second codon position, namely Leu, Val and Ile, are more prone to form β-sheet structures, while amino acids encoded by codons with A in the second position, namely Lys and Tyr, are more prone to form α-helical structures. Amino acids codify by codons with G in the second position do not exhibit any preference for specific protein structure, except Gly, which is more frequent in aperiodic structures, while amino acids codified by codons with C in the middle position do not have also any preference, except Ala, which is

more frequent in α-helix. Ser, whose codons may have G or C in the middle position does not have any preference for specific structure either (Chiusano et al., 2000).

Table 3.7: Amino acids classification. Amino acids are classified according to their polarity and charge.

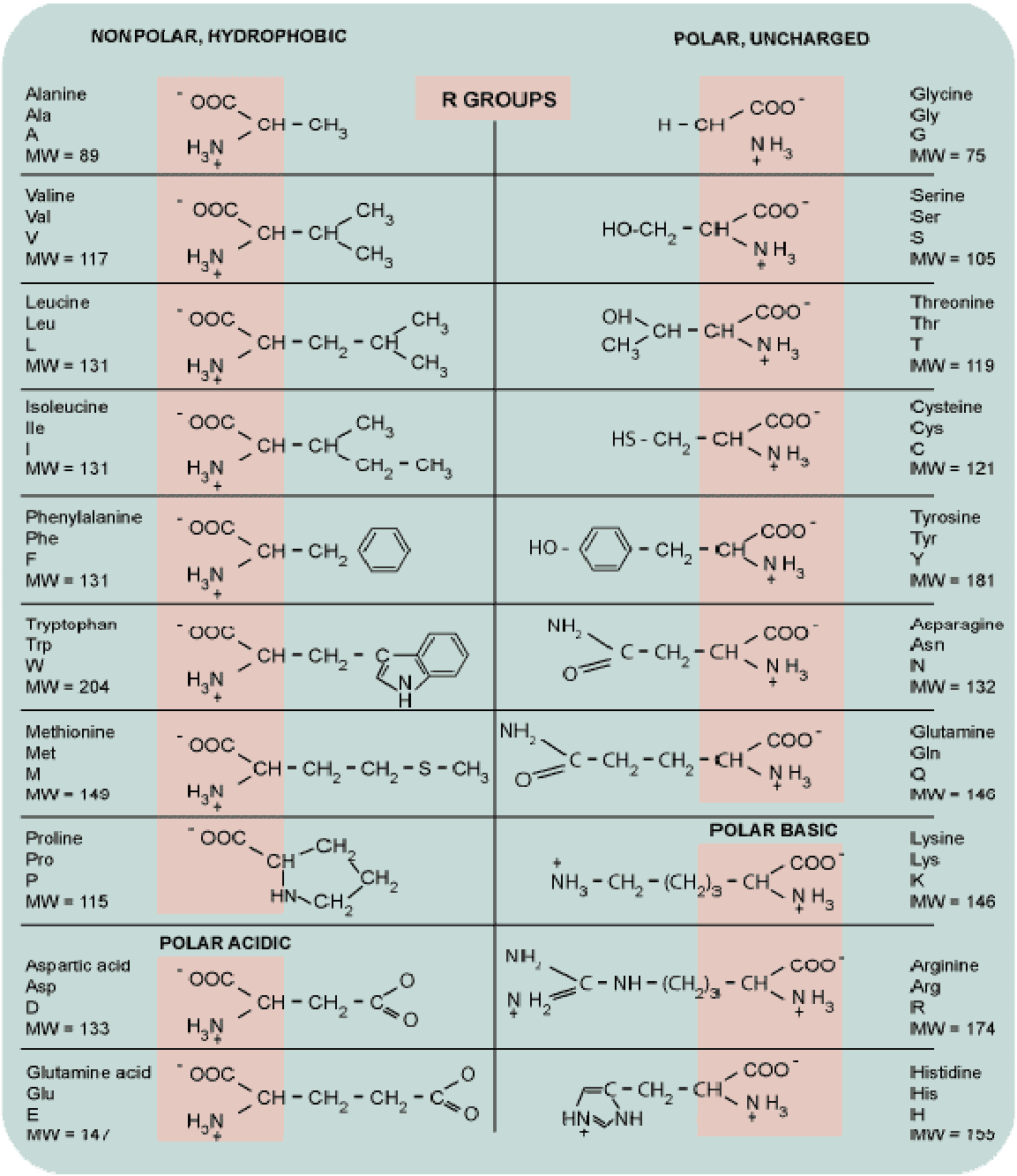

Previous studies have demonstrated that amino acids position regulates protein structure, but it is not the only determinant. For example, replacement of Ile by another hydrophobic residue, like Val, decrease protein stability because the removal of a CH2 group leaves an empty cavity in the protein core (Harpaz et al., 1994). In other words, correct protein folding requires contributions of hydrophobic effects and electrostatic and hydrogen bonding interactions between residues throughout the polypeptide chain (Pace et al., 1996). Furthermore, some studies classify the amino acids according to their order promoting state. Unstructured or incompletely structured proteins that retain a specific function, also known as IDPs (intrinsic disorders proteins) (reviewed in Radivojac et al., 2007), are depleted in order promoting amino acids (Ile, Leu, and Val, Trp, Tyr, Phe, Cys and Asn), are enriched in disorder promoting amino acids (Ala, Arg, Gly, Gln, Ser, Pro, Glu, and Lys), but are neither enriched or depleted in His, Met, Thr and Asp (Williams & Obradovic, 2001). This higher enrichment in disordering promoting amino acids in the IDPs is linked to their biological functions, such as signaling and control pathways (reviewed in Radivojac et al., 2007). Interestingly, proteins usually involved in the progression of some human diseases, such as cancer, cardiovascular disease, amyloidoses, diabetes, neurodegenerative diseases are enriched in IDPs (Uversky et al., 2009).

Other groups have previously induced amino acid misincorporation through engineered tRNAs containing anticodons that recognize codons belonging to different amino acids. The engineered $tRNA^{Phe}$ in *E. coli* (Kim et al., 2000) and the engineered $tRNA^{Ser}$ in mammalian cells (Geslain et al., 2009) induced different toxicities, where some amino acids substitutions are higly toxic and others do not have visible negative effects. In this context, we were expecting that Ser misincorporation at codons coding for different amino acids would produce variable toxicity, where misincorporation of Ser at Ile, Leu and Val codons was expected to be highly toxic, while misincorporation of Ser at Thr, Ala, Lys and Gly was expected to induce low toxicity, and toxicity of Ser misincorporation at Tyr codons was expected to be between these two extremes of toxicity.

Our data confirms our working hypothesis because we have observed that misincorporation of Ser at Ile, Leu and Val codons induced an accentuated growth rate decrease associated with high cell death, cell cycle alterations, aneuploidies and G2/M arrest. ROS, mitochondrial, vacuolar and nuclear alterations were also observed in these cells. Moreover, the expression of the mistranslating $tRNA^{Ser}$(Ile), $tRNA^{Ser}$(Leu) and $tRNA^{Ser}$(Val) from multicopy plasmids was lethal. Several studies have demonstrated that

ROS damages DNA, proteins and mitochondria and may culminate with cell death, mainly by apoptosis (Cheng et al., 2008; Herrera et al., 2001; Simon et al., 2000). Although, the mitochondrial, vacuolar and nuclear chromatin morphological alterations observed in our cells misincorporating Ser at Ile, Leu and Val did not induce significant increase in apoptosis. This is similar to the treatment of yeast cells with furfural, which also induces mitochondrial, vacuolar and nuclear chromatin morphological alterations through increased ROS, without apoptosis induction (Allen et al., 2010). It will be interesting to determine how Ser misincorporation at Ile, Leu and Val codons reduces growth rate and decreases cell viability, but in any case, the above cellular alterations strongly suggest that reassignments of Leu, Ile and Val codons to Ser is highly unlikely and difficult to be engineered in the laboratory.

According to the amino acids substitution matrix BLOSUM 62 (Henikoff & Henikoff, 1992), which compares the substitution rate of an amino acid by another (based in multiple alignments of proteins), substitution of Ile, Leu and Val for Ser has a value of -2, which indicates that is an extremely rare event (figure 3.33), likely due to the hydrophobic nature and location of these amino acids into the proteins core. These amino acids have non-reactive side chains and for this reason are rarely involved in catalysis, but can be involved in binding hydrophobic molecules such as lipids (Betts & Russell, 2003). For this reason, Ile substitution usually involves Leu and Val residues, as represented in BLOSUM 62 matrix (rate of 2 and 3, respectively). Conversely, Ser is a neutral polar amino acid containing a moderately reactive –OH group which is able to form hydrogen bounds with various polar molecules and, for this reason, it can remain at the surface of proteins or within the interior where it establishes hydrogen bounds with protein backbone residues (Betts & Russell, 2003).

Therefore, the misincorporation of Ser in positions normally occupied by Ile, Leu and Val likely disrupt protein structure because, as mentioned above, Leu, Ile and Val are order promoting residues, present mainly in β-sheet structures of protein hydrophobic cores, while Ser is a disording-promoter amino acid which is normally present at the protein surface (Bahar et al., 1997). Strong evidences for a disruptive rate of misincorporation of Ser at Ile and Leu codons was the high increase in the level of insoluble proteins detected in our recombinant yeast cells. It is unclear, however, why Ser misincorporation at Val codons does not induce protein aggregation. Substitution of amino acids placed in the hydrophobic core of proteins normally affects protein folding and solubility. For example, replacement of Leu and Ile by Ala residues at the hydrophobic

core of the small bacterial ribonuclease barnase reduces severely the free energy of folding and protein expression (Kellis et al., 1989). The substitutions Ile-to-Ala, Leu-to-Ala and Val-to-Ala in the hydrophobic core of the chymotrypsin inhibitor 2, reduces the free energy of folding by 3 fold above the reduction observed for the Ile-to-Val substitution, because loss of methyl groups (Jackson et al., 1993). The substitution Leu-to-Lys and Leu-to-Arg at the hydrophobic core of *E. coli* thioredoxin reduces protein stability, but do not affect catalysis (Ladbury et al., 1995). Interestingly, the substitution Phe-to-Tyr in *Rhodobacter sphaeroides* thioredoxin affect cell viability, but do not affect protein stability *in vitro* (Assemat et al., 1995).

	Ala	Arg	Asn	Asp	Cys	Gln	Glu	Gly	His	Ile	Leu	Lys	Met	Phe	Pro	Ser	Thr	Trp	Tyr	Val
Ala	4																			
Arg	-1	5																		
Asn	-2	0	6																	
Asp	-2	-2	1	6																
Cys	0	-3	-3	-3	9															
Gln	-1	1	0	0	-3	5														
Glu	-1	0	0	2	-4	2	5													
Gly	0	-2	0	-1	-3	-2	-2	6												
His	-2	0	1	-1	-3	0	0	-2	8											
Ile	-1	-3	-3	-3	-1	-3	-3	-4	-3	4										
Leu	-1	-2	-3	-4	-1	-2	-3	-4	-3	2	4									
Lys	-1	2	0	-1	-3	1	1	-2	-1	-3	-2	5								
Met	-1	-1	-2	-3	-1	0	-2	-3	-2	1	2	-1	5							
Phe	-2	-3	-3	-3	-2	-3	-3	-3	-1	0	0	-3	0	6						
Pro	-1	-2	-2	-1	-3	-1	-1	-2	-2	-3	-3	-1	-2	-4	7					
Ser	1	-1	1	0	-1	0	0	0	-1	-2	-2	0	-1	-2	-1	4				
Thr	0	-1	0	-1	-1	-1	-1	-2	-2	-1	-1	-1	-1	-2	-1	1	5			
Trp	-3	-3	-4	-4	-2	-2	-3	-2	-2	-3	-2	-3	-1	1	-4	-3	-2	11		
Tyr	-2	-2	-2	-3	-2	-1	-2	-3	2	-1	-1	-2	-1	3	-3	-2	-2	2	7	
Val	0	-3	-3	-3	-1	-2	-2	-3	-3	3	1	-2	1	-1	-2	-2	0	-3	-1	4

Figure 3.33: BLOSUM 62 matrix for amino acids positive and negative substitutions. Adapted and modified from (Henikoff & Henikoff, 1992).

The BLOSUM 62 matrix suggests that Ala-to-Ser, Asn-to-Ser and Thr-to-Ser substitutions are more likely because their BLOSUM values is +1. Our data is in line with the BLOSUM 62 theoretical prediction since Ser misincorporation at Thr and Ala codons were the less toxic of the amino acid substitutions studied. Thr is likely replaceable by Ser because the chemical differences between these amino acids reside in the presence of an

extra methyl group in Thr (table 3.7). Similarly, Ser misincorporation at Ala residues is a good candidate for codon reassignment because Ala is not a particularly hydrophobic residue and can be located either at the surface or can be buried in the proteins core (Betts & Russell, 2003). Our data also shows that misincorporation of Ser at Lys codons is possible and this is in agreement with the value (0) given by the BLOSUM 62 matrix.

The misincorporation of Ser at Gly codons according to BLOSUM 62 matrix (0) is not unlikely either, although our data shows that this replacement does induce some toxicity. This is likely related with the chemistry of this amino acid, which only contains a hydrogen in the side chain making it highly flexible and frequently located in specific positions of the proteins (U-turns) backbone, where others amino acids are forbidden. Indeed, a change of a conserved Gly for other amino acid could have a dramatic impact on protein structure (Betts & Russell, 2003) and may explain the protein aggregates that we have observed in the case of misincorporation of Ser at Gly codons. Clearly, these cytoplasmatic aggregates were recognized by Hsp104p and Hsp26p and were different from the other insoluble aggregates observed in cells misincorporating Ser at Ile and Leu codons. So, our results suggest that proteins containing Ser misincorporation at Gly codons are being targeted to assisted refolding by molecular chaperons, while proteins with Ser misincorporation at Ile and Leu codons are not targeted for refolding and accumulate in larger deposits (insoluble fraction), which may not be degraded by the ubiquitin-proteasome system. Indeed, the proteasome is not the major degradation pathway involved in aggregates removal because it can be inhibited by aggregates formation. In other words, protein aggregates are likely mainly degraded by autophagy (Bence et al., 2001).

The misincorporation of Ser at Tyr codons shows that Tyr codons are also unlikely candidates for Ser reassignment. Tyr is a large hydrophobic amino acid that contains an aromatic group and is usually located in the interior of protein molecules where its hydroxyl group is involved in hydrogen bonds. Indeed, Tyr-to-Ser substitution have a BLOSUM 62 value of -2 which despite the lower toxicity than Leu-to-Ser and Ile-to-Ser substitutions, measured by growth rate, cell death, ROS levels, disruption of mitochondria, vacuoles or chromatin, put them in the non-reassignable codons category.

According to the BLOSUM 62 matrix, the rarest substitution of Ser residues involves Trp (-3), which may only be replaced by other aromatic amino acids, namely Tyr and Phe, due to its unique size and chemical properties (Betts & Russell, 2003). It would be interesting to test the toxicity induced by this highly improbable substitution.

Our study shows that genetic code alterations are rare events because they are highly likely to induce dramatic cellular and phenotypic alterations, and even cell death. Despite this, misincorporation of Ser at different codons codifying distinct amino acids can be advantageous in certain environmental conditions. Clear advantages were observed in presence of copper sulphate and cadmium chloride. It is remarkable that the strains that displaced the highest selective advantages were those where Ser misincorporation was less disruptive, namely Lys-to-Ser substitution. It is also fascinating that different mistranslations produce distinct phenotypic outcomes. Although, these data strongly suggest that the evolution of the genetic code alterations can only be understood in an ecological context. In other words, the likelihood of reassigning codons depends on the toxicity of the initial misincorporation and on the selective advantages produced in the particular environments of the organism. This is in line with the incorporation of Pyl at UAG stop codons which is essential for *Methanosarcina acetivorans* to grow on monomethylamine as sole nitrogen source (Mahapatra et al., 2006), and also with the reassignment of Ile AUA codon to Met in the human and animal mitochondria, where increased Met content in proteins protects them from the oxidative environment of the inner mitochondrial membrane (Bender et al., 2008). In the same line of thought, misincorporation of Ser at Leu CUG codons confers a selective growth advantage to yeast growing in certain environmental conditions (Santos et al., 1999). In conclusion, the genetic code is flexible, but that flexibility is strictly linked to the ecology of each organism (Maeshiro & Kimura, 1998).

Chapter 4

Gene expression profiling of mistranslating yeast

4.1. Introduction

Since the discovery of the genetic code it became clear that it is not randomly organized, instead it is structured for maximal mRNA translation efficiency. Indeed, this level of organization was recognized from studies that demonstrated that closely related organisms had similar codon usage while distantly related organisms used codons in rather distinct ways (Grantham et al., 1980). Moreover, studies with yeast demonstrated gene specific codon usage biases (around 25) and that codon preference correlate with gene expression level. Indeed, preferred codons are more commonly used in the most expressed genes in yeast (Bennetzen & Hall, 1982) and in *E. coli* (Gouy & Gautier, 1982). This preference is correlated with the cellular abundance of tRNA isoacceptors suggesting that differences in synonymous codon usage between *E. coli* and yeast are at least, in part, explained by tRNA decoding efficiency (Ikemura, 1985). This is in line with the observation that expression of eukaryotic proteins containing high level of AGA codons (Arg) in *E. coli* lead to high level of amino acid misincorporation, because the AGA codon is rare in bacteria. This problem can, however, be overcome by increasing expression of the rare cognate $tRNA_{UCU}^{Arg}$ which decodes AGA codons in *E. coli* (Calderone et al., 1996). Moreover, the codon usage is also correlated with protein structure since α-helices tend to be coded by fast codons (highly used) while the β-strands and coil regions, whose folding requires more time, are usually codified by slow codons (used at low level) (Thanaraj & Argos, 1996).

Recent studies also demonstrated the existence of differences in synonymous codon usage between genes expressed in different human tissues (Plotkin et al., 2004), which are linked to differences in tRNA isoacceptor expression in these tissues. The brain seems to express the highest level of nuclear and mitochondrial encoded tRNAs (Dittmar et al., 2006). The same happens with yeast that transit from fermention to respiration, where a difference in the tRNA pool is observed (Tuller et al., 2010). Moreover, two distinct groups of genes with different codon preferences were identified in yeast and in the *Ashbya gossypii* multicellular mycelium, which were significantly enriched in cell cycle and metabolic functions, respectively (Jiang et al., 2008). Additionally, codon optimization was also observed for genes belonging to fermentative pathways in anaerobic species and for respiratory genes in aerobic species (Man & Pilpel, 2007).

In general, translation is a highly accurate biological process, however errors occur and previous studies have demonstrated that translational errors are in the order of 10^{-5} in

yeast (Stansfield et al., 1998). A recent study showed that translational errors can be as higher as 10^{-2} in *B. subtilis*, an organism that can decrease protein synthesis fidelity in adverse conditions, such as stationary phase, lower temperatures and starvation. These data suggest that errors in translation can contribute to organism robustness and confer a survival advantage in certain environments (Meyerovich et al., 2010). Indeed, misincorporation of Met residues at various codons in mammalian cells exposed to stress confers protein protection against the destructive action of ROS (Netzer et al., 2009). Interestingly, our previous results showed that mistranslation induces severe morphological alterations and growth disadvantages in yeast, but the latter can be overcome in stressful environments. Phenotypic diversity can also arise from noise in gene expression. For example, yeast strains isolated from different ecological niches display phenotypic variation in stress sensitivity associated to gene expression variability (Kvitek et al., 2008). Although, the gene expression variations are not always correlated with the phenotypes observed (Fay et al., 2004), it is interesting that both protein sequence variability and protein abundance variability can have positive selective outcomes and be adaptative.

In this context we were interested in determining the effects of the genetic code ambiguity generated through amino acid misincorporation in gene expression. Our hypothesis was that the proteotoxic stress induced by amino acid misincorporation could deregulate gene expression, activate the stress response and stress cross protection, which in turn could explain some of the phenotypes and selective advantages described in the previous chapter. For this, we have profiled our mistranslating yeast cells using DNA microarrays. Our results show large gene expression variation in the mistranslating strains that correlate, in part, with the phenotypic differences and stress sensitivity described in chapter 3.

4.2. Material and methods

4.2.1. RNA isolation

mRNA isolation was carried out as described elsewhere (van de Peppel et al., 2003). Briefly, 50 ml of exponentially growing yeast cells (OD_{600nm} = 0.5) were harvested

by centrifugation at 3200xg for 3 minutes at room temperature. Supernatants were quickly removed and tubes were immediately frozen by immersion on liquid nitrogen and were stored at -80ºC. Total RNA was isolated using the hot phenol method. Frozen cell pellets were ressuspended in 500 µl of acid phenol:chlorophorm (Sigma, 5:1, pH 4.7) and the same volume of TES-buffer (10 mM Tris pH 7.5, 10 mM EDTA, 0.5 % SDS) was vortexed for 20 seconds and incubated at 65ºC during 1 hour, with vortexing every 10 minutes. Samples were centrifuged for 20 min at 15000xg at 4ºC and the water-phase was transferred to new tubes containing 500 µl of acid phenol:chloroform. Tubes were vortexed and centrifuged for 15 minutes at 15000xg at 4ºC and the water-phase was transferred to new tubes containing 500 µl of chloroform:isoamyl-alcohol (Fluka, 25:1). Tubes were vortexed and centrifuged for 15 minutes at 15000xg at 4ºC. The water phases were transferred to new tubes containing 50 µl of sodium acetate (3 M, pH 5.2) and 800 µl of ice cold 100% ethanol. RNA was precipitated overnight at -30ºC. After precipitation, tubes were centrifuged for 10 minutes at 15000xg at 4ºC. The supernatant was removed and pellets were washed with 500 µl of 80% ice cold ethanol by centrifugation for 5 minutes at 15000xg. Dried RNA pellets were ressuspended in milliQ water and stored at -80ºC. mRNA enrichment was prepared using Oligotex dT beads according to the manufacturer instructions (Qiagen). Finally mRNA samples were ressuspended in mQ water to a final concentration of 1µg/µl.

4.2.2. Reverse transcription aminoallyl incorporation

cDNA synthesis was carried out using 3 µg of yeast mRNA, 1.5 µg of oligo dT_{12-18} primer and water to a final volume of 13 µl. Reactions were incubated at 70ºC for 10 min and immediately placed on ice. A mixture containing 3 µl of dGAC-mix (1 mM each), 0.9 µl dTTP (1 mM), 2.1 µl aa-dUTP (1 mM Sigma), 6 µl 5x first strand buffer (250 mM Tris-Cl pH 8.3, 375 mM KCl, 15 mM $MgCl_2$) and 3 µl DTT (0.1M) was added and samples were incubated at room temperature for 2 minutes. Then 2 µl of SuperScript™ II Reverse Transcriptase (200 U / µl, Gibco) was added and tubes were incubated at 42ºC for 60 minutes. Samples were incubated 2 min at 95ºC and were chilled on ice. 10 µl of NaOH (1M) and 10 µl of EDTA (0.5 M) were added to each cDNA reaction which were then incubated at 65ºC for 15 minutes. After a short spin, 25 µl of HEPES buffer (1M, pH 7.5)

were mixed with the samples, which were then cleaned using microcon-30 concentrator (Amicon microcon), according to the manufacturers instructions. To the eluate, 5 µl of Sodium-Bicarbonate buffer (0.5M, pH 9) were added and the sample was split in two identical aliquotes and stored at -20ºC for later use (van de Peppel et al., 2003).

4.2.3. Coupling of monofunctional NHS-ester Cy-dyes

cDNA samples purified as described above were mixed with 1.25 µl of Cy3 or Cy5 dyes and were ressuspended in DMSO and incubated for 1 hour in the dark at room temperature (van de Peppel et al., 2003). Reactions were then quenched to prevent cross coupling by adding 4.5 µl of 4 M hydroxylamine (SIGMA) and incubated in the dark at room temperature for 15 minutes. Free dyes were removed using chromaspin-30 columns (DEPC version, Clontech), according to the manufacturers instructions. Frequency of dye incorporation was calculated using the nano-drop spectrophotometer and samples were stored in a light hidden tube until hybridizations were carried out.

4.2.4. Hybridization protocol

Before hybridization, slides were prehybridized for 1 hour at 42ºC in 100 ml of prehybridization buffer, containing 5 x SSC (0.15 M NaCl and 0.015 M sodium citrate, pH 7.0), 25% formamide (Merck) 0.1% SDS and 1% of BSA filtered and pre-heated at 42ºC. Slides were washed by dipping 5 times in room temperature mQ water and room temperature isopropanol and air dried in a fume hood. Meanwhile, 250 µl of the 2x hybridization buffer (50% formamide, 10x SSC and 0.2% SDS) were mixed with 5 µl of Herring sperm DNA (stock 10 µg/µl), filtered and preheated to 42ºC. Samples were prepared by mixing 250 µl of target sample (300 ng of cDNA of mistranslating strain labelled with Cy3 or Cy5 plus 300 ng of control strain labelled respectively with Cy5 or Cy3) with 250 µl of 2x hybridization buffer, heated at 95ºC for 5 minutes and centrifuged at 13000xg for 4 minutes. Slides were prepared using Agilent gasket slides according to the manufacturer instructions. Hybridizations took place over 17 hours in a dark chamber (Agilent oven) at 42ºC at 12 rpm. Slides were then washed in three solutions during 5 min. Firstly, in 1x SSC/0.2 % SDS, then in 0.1x SSC/0.2 % SDS and finally in 0.1x SSC (van de Peppel et al., 2003). Slides were rapidly dried by centrifugation for 6 min at 130xg, room temperature, and scanned.

4.2.5. Data analysis

Images of the microarray hybridizations were acquired using the Agilent G2565AA microarray scanner (Agilent). Fluorescence intensities were quantified with QuantArray v3.0 software (PerkinElmer), bad spots were manually eliminated and the local background was subtracted. Using R2.2.1. limma software and BRB-ArrayTools v3.4.0, Log_2 intensity ratios (M values) were then median normalized, to correct for differences in genomic DNA labeling efficiency between samples. One class significance analysis of microarrays (SAM), with false discovery rate (FDR) of 0.001 was performed using MeV TM4.6.0 software. Individual hybridizations of two clones with two dye-swaps were used as the input data for each strain. In order to generate a list with significantly changed genes we selected all features that had -1> M >0.6. Functional classes and transcription factors enrichment analysis were performed using EXpression Analyzer and DisplayER (EXPANDER) 5 software, with the Tool for ANalysis of GO enrichments (TANGO), PRomoter Integration in Microarray Analysis (PRIMA) and the Kyoto Encyclopedia of Genes and Genomes (KEGG) pathway analysis, in all cases the p value cutoff was 0.05.

4.3. Results

4.3.1. Functional enrichment of up regulated genes

In order to compare the differences between all mistranslated strains we have selected all significant deregulated genes with values of M lower than -1 and higher than 0.6 and performed a functional enrichment analysis (Tango) using the Expander software package. Data obtained are expressed as -log(p values) for each gene class and are organized as a heat map with a color scale, where light colors (light red and green) correspond to higher deregulations.

The highest functional enrichment of genes was observed in the strain expressing the $tRNA^{Ser}$(Gly) from multicopy plasmid ($tRNA^{Ser}$(Gly)MC), were 22 classes of genes were up regulated, followed by the strains that misincorporated Ser at Tyr codon with 19, Ile codons with 18, Leu codon with 14, Val codons with 10, Gly codons with 9, Thr codons with 8, Ala codons with 5 and Lys codons with 2 (figure 4.1).

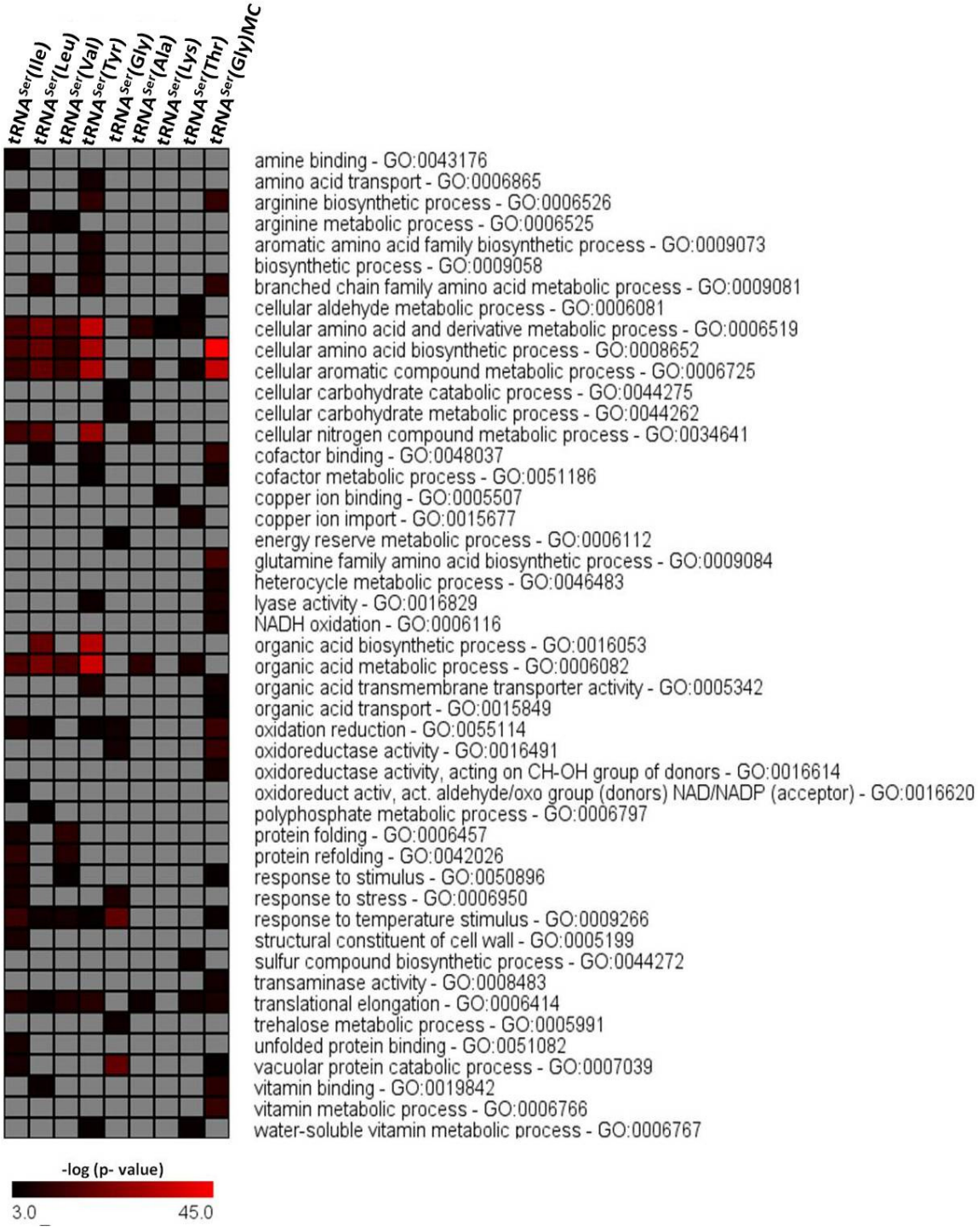

Figure 4.1: Functional class enrichment analysis of genes that are up regulated by mistranslation. Significantly up regulated genes identified using SAM analysis (FDR 0.001) and -1 > M >0.6 were functionally enriched using Tango analysis ($p< 0.05$). The significance of the enrichment is represented as a heat map where the color intensity corresponds to -log(p-values). GO identification numbers are identified for each category.

Misincorporation of Ser at Ile, Leu, Val and Tyr codons produced similar functional class enrichment, namely aromatic, organic acid and amino acid metabolic processes, response to temperature stimulus and translational elongation. Besides this, there were also specific differences between strains. For example, Ser misincorporation at Thr and Lys codons up regulated genes related to copper ion transport, while misincorporation of Ser at Gly codons up regulated genes involved in energy reserve, namely genes involved in trehalose and cellular carbohydrates metabolism. Ser misincorporation at Leu codons increased polyphosphate metabolism genes.

Functional enrichment analysis of metabolic pathways (KEGG) (figure 4.2), using the Expander software package with similar criteria to those used in the Tango analysis, as described above, showed variation in the up regulated pathways between strains, but also similarities, mostly for categories related to amino acids metabolism, which was in agreement with the Tango enrichment analysis. There was only one up regulated pathway that was common to all mistranslating strains, namely the pathway involved in vitamin B6 metabolism. Interestingly, vitamin B6 consists of six interconvertible compounds, namely pyridoxine, pyridoxal, pyridoxamine, pyridoxine 5'-phosphate, pyridoxal 5'-phosphate, and pyridoxamine 5'-phosphate (John, 1995), that allow *S. pombe* to grow in presence of the reactive oxygen generator menadione (Chumnantana et al., 2005). Therefore, this could be a defense against ROS generated by mistranslation.

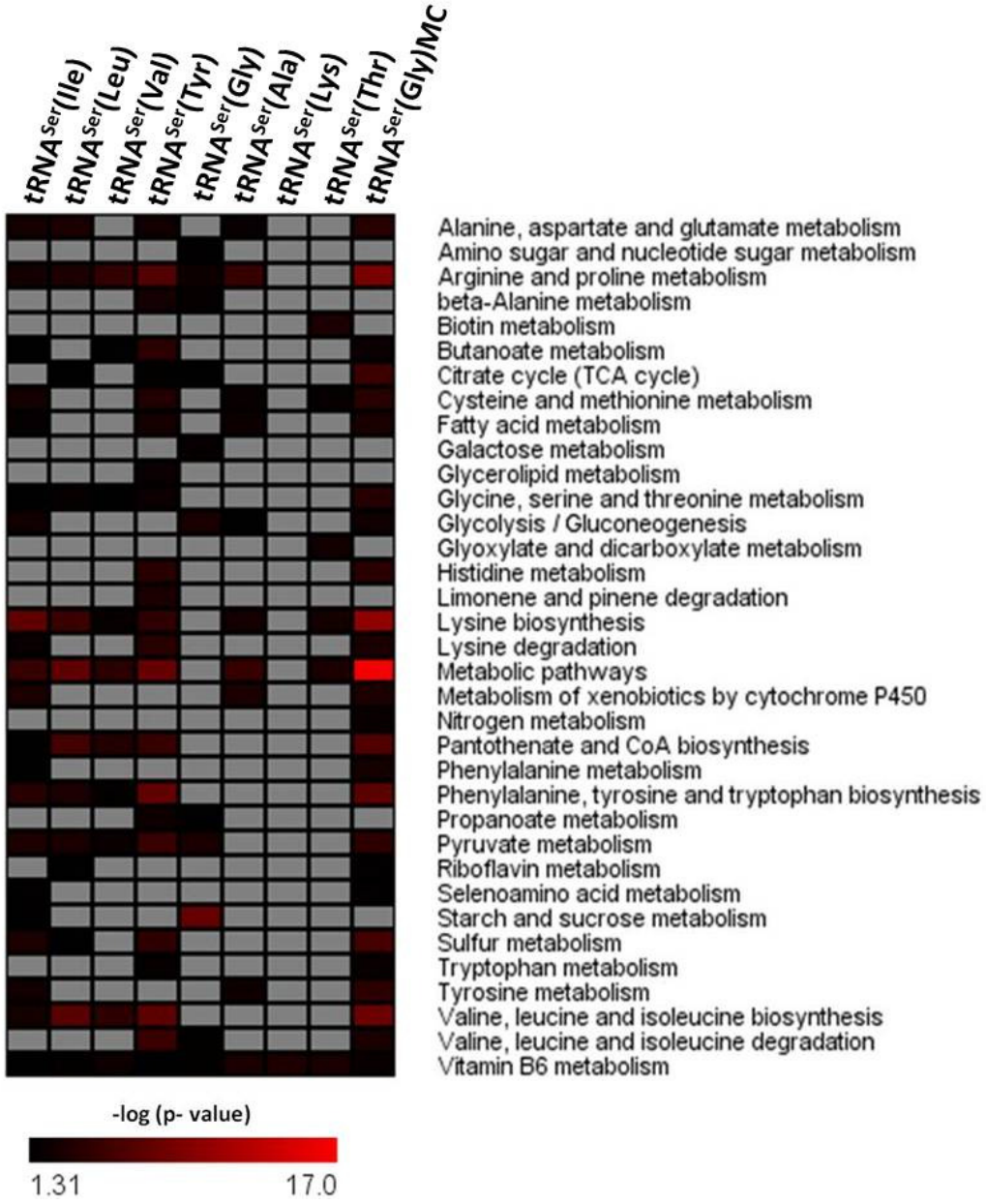

Figure 4.2: Functional pathways enrichment of genes that are up regulated by mistranslation. Significantly up regulated genes identified using the SAM analysis (FDR 0.001) and -1 > M >0.6 were functionally enriched using KEGG pathway analysis ($p < 0.05$). The significance of the enrichment is represented as a heat map where the color intensity corresponds to -log (p-values).

Several studies have already been performed to elucidate the transcriptional response of yeast exposed to diverse stimulus, namely amino acid starvation, nitrogen

deprivation, carbon source, osmotic stress, heat shock, reactive oxygen species generator, ethanol, acetic acid, drugs (Berry & Gasch, 2008; Gasch et al., 2000; Halbeisen & Gerber, 2009; Kuhn et al., 2001; Lee & Lee, 2008; Lewis et al., 2010; Melamed et al., 2008; Mira et al., 2010; Posas et al., 2000; Romero-Santacreu et al., 2009; Tucker & Fields, 2004). Large part of the deregulated genes (induced or repressed) during stress conditions are common and are generally designated as the environmental stress response (ESR). This response includes deregulation of 900 genes, of which 300 are up regulated and 600 are down regulated. The up regulated genes are mainly related to carbohydrate metabolism, metabolite transport, fatty acid metabolism, detoxification of reactive oxygen species, autophagy, protein folding and degradation, cell wall modification, DNA-damage repair, secretion, vacuolar and mitochondrial functions (Gasch, 2002). Our data, obtained using Tango and KEGG enrichment analysis of significantly up regulated genes, demonstrate that most of the categories deregulated by mistranslation belong to the ESR, although these categories are not regulated in the same way in all strains, indeed, some pathways are specific of particular types of missense translation.

Ser misincorporation at Ile codons induced the highest up regulation of genes belonging to the ESR, namely vacuolar protein catabolic processes, unfolded protein binding, protein folding and refolding, oxidation reduction, amino acid metabolism and transport, nitrogen metabolic process, structural constituents of the cell wall, response to stress and stimulus, fatty acid metabolism, butanoate metabolism, glycolysis and gluconeogenesis. This may be related to the high toxicity of that type of mistranslation since Ile and Ser are chemically distinct amino acids. One of the interesting genes whose expression was only up regulated by Ser misincorporation at Ile codons was the TIS11 gene. This gene was up regulated 3 fold in this strain and showed no significant variation in the other strains. TIS11 (also known as CTH2) is up regulated during iron starvation and is responsible for down regulation of steady-state levels of mRNAs coding for proteins involved in multiple Fe-dependent metabolic pathways, including the TCA cycle, respiration, lipid metabolism, heme biosynthesis and multiple Fe-S proteins, as well as many proteins of unknown function (Ihrig et al., 2010; Puig et al., 2005).

Misincorporation of Ser at Leu codons up regulated most of the genes that were also up regulated by Ser misincorporation at Ile codons, namely genes of amino acid transport and metabolic process, oxidation reduction, response to temperature, translation

elongation, but unexpectedly did not up regulated protein folding and refolding classes as in the case of Ser misincorporation at Ile and Val codons. Interestingly, Leu-to-Ser mistranslating strain was the only one that up regulated genes involved in polyphosphate metabolic processes. In *S. cerevisiae* phosphate transport is carried out by five phosphate transporters, namely Pho84p, Pho87p, Pho89p, Pho90p and Pho91p (reviewed in Lenburg & O'Shea, 1996). Under phosphate limitation, transcription of the high-affinity phosphate transporter genes, PHO84 and PHO89, is up regulated, while the low-affinity transporters, PHO87 and PHO90 are down regulated by physical interactions with SPL2. This induces positive feedback on the PHO pathway, increasing phosphate uptake and consequently down regulation of the PHO pathway (Wykoff et al., 2007; Wykoff & O'Shea, 2001). Ser misincorporation at Leu codons, conversely to the other cases, created an apparent phosphate limitation condition, since the gene that showed the highest up regulation was the high affinity phosphate transporter, PHO84 (102 fold), which was followed by increased expression of the low-affinity transporters repressor, SPL2 (35 fold). PHO89 expression increased 2.5 fold only, which was not surprising since activation of the Pho89p transporter takes place early during the growth phase, while Pho84p is maximally active during mid-log phase (Patisson-Granberg & Persson, 2000). PHO84 and SPL2 are regulated by the transcription factor PHO4. When the extracellular levels of Pi are low Pho81p is activated and represses the Pho80-Pho85 kinases, which in their active state repress Pho4p by phosphorylation. The hypophosphorylated Pho4p localizes mainly in the nucleus where it activates expression of PHO84. Besides these two genes activated by Pho4p, phosphate metabolism involves 21 genes (Ogawa et al., 2000). Ser misincorporation at Leu codons also up regulated VTC1 (7.8 fold), VTC3 (3.1 fold), VCT4 (2.7 fold), PHO8 (1.8 fold), PHM6 (4 fold), PHO11 (1.9 fold). Although, it is important to note that the VTC complex is also implicated in other cellular processes, namely in sorting of H^+-translocating ATPases, endocytosis, ER-Golgi trafficking, microautophagy and vacuole fusion besides, polyphosphate homeostasis (Cohen et al., 1999; Muller et al., 2002; Muller et al., 2003; Ogawa et al., 2000; Uttenweiler et al., 2007). Therefore, the lack of regulation of these genes in the other strains was surprising.

The transcriptome data of Ser misincorporation at Leu codons suggest that Spl2p represses the low affinity Pi transporters and up regulates Pho84p and Pho89p, increasing Pi transport from the extracellular medium, which will accumulate in vacuoles by the action of vacuolar transporter chaperon complex (vtc1, vtc2, vtc3, vtc4 proteins). The accumulated Pi will then be bound forming a polymer containing high energy bounds, namely the PolyP, by Phm1p, Phm2p, Phm3p and Phm4p. PolyP is cleaved by Phm5p

with release of Pi as an alternative energy source (ATP substitute) (Boyce et al., 2006; Ogawa et al., 2000).

But, why were phosphate metabolism genes deregulated only in the strain that misincorporated Ser at Leu codons? Could this be a way to repress the environmental stress response? Previous studies established a link between Pho84p and PKA signaling pathway (Giots et al., 2003). These authors showed that transport of inorganic phosphate, which increases phosphate levels in phosphate-starved cells, induces a rapid activation of protein kinase A (PKA) signaling. The PKA activation represses the ESR, suppresses Msn2 and Msn 4 transcription factors, leading to increased activation of ribosomal genes (Gasch et al., 2000). Moreover, PKA is a negative regulator of Pho84p, promoting its removal from the plasma membrane and consequent degradation in the vacuoles (Mouillon & Persson, 2005; Mouillon & Persson, 2006).

Misincorporation of Ser at Gly codons was also very interesting. Our Tango enrichment analysis showed that this type of missense translation up regulate genes related to energy reserve metabolic process (chemical reactions/pathways by which a cell derives energy from stored compounds such as fats or glycogen), carbohydrate catabolic and metabolic processes, and trehalose metabolic process (chemical reactions and pathways involving trehalose). Under stress situations yeast tends to induce a variety of genes that affect glucose metabolism as the latter is the main carbohydrate used by yeast. Glucose metabolism includes trehalose synthesis, glycogen storage, ATP synthesis through glycolysis, and NADPH regeneration by the pentose phosphate shuttle. Trehalose can be hydrolyzed to generate glucose, but can also be synthesized from glucose (reviewed in Bolat, 2008). Stress conditions like temperature (Virgilio et al., 1994), salinity (Posas et al., 2000; Romero-Santacreu et al., 2009) and oxidative stress (Pereira et al., 2001) increase trehalose accumulation in yeast. Trehalose is believed to stabilize and protect cellular membranes and is also a protein stabilizer that minimizes the aggregation of denatured proteins, by maintaining them in a partially-folded state that allows for their refolding by molecular chaperons (Singer & Lindquist, 1998). Although, if trehalose remains continuously bound to proteins after the chaperons attachment it will interfere and inhibit protein refolding, that is why trehalose needs to be hydrolyzed for the cell recover after heat-shock (Singer & Lindquist, 1998). Ser misincorporation at Gly codons increased expression of genes related to trehalose synthesis, namely TPS3 (1.75 fold), TSL1 (2.7 fold), PGM2 (3.1 fold), but this does not imply a direct increase in trehalose concentration,

because there was also a slight induction of trehalose degradation enzymes, namely NTH1 (1.54 fold) and ATH1 (2 fold), as previously observed by other authors (Parrou et al., 1997).

Another unique feature of Ser misincorporation occurred at Lys and Thr codons where the respective strains up regulated copper ion binding and copper import genes. Copper is an essential element that is incorporated as a catalytic or structural cofactor into a variety of proteins, for example cytochrome oxidase and Cu/Zn-superoxide dismutase (SOD1) (Linder & Hazegh-Azam, 1996). Yeast growing in low copper environments increase copper acquisition by activating the transcription factor MAC1 (Yamaguchi-Iway et al., 1997). Mac1 activation increases the transcription of 6 genes involved in copper uptake, namely genes encoding the high affinity plasma membrane copper ion permeases, CTR1 (Dancis et al., 1994) and CTR3 (Knight et al., 1996); genes encoding plasma membrane-associated Cu(II)-Fe(III) reductases, FRE1(Hassett & Kosman, 1995) and FRE7; and two uncharacterized ORF's, YFR055w/IRC7 and YJL217w/REE1 (Gross et al., 2000). Besides being regulated by Mac1, the FRE1 can also be regulated by Aft1 and Aft2, which are transcription factors activated during iron limitation conditions (Rutherford et al., 2003). Our results showed that mistranslation induces significant differences in copper related genes (table 4.1). FRE7 showed the highest up regulation in the strains that misincorporated Ser at Thr (24.5 fold), Lys (21.3 fold), Gly (16.5 fold) and Ile (7 fold) codons. REE1 was up regulated by Ser misincorporation at Thr (9.3 fold), Lys (7.7 fold), Ile (6.9 fold) and Gly (5.8 fold). CTR1 was up regulated between 2.6 fold to 2.8 fold by mistranslation of Ser at Thr, Lys and Gly codons. Finally, IRC7 was up regulated 2 fold by Ser misincorporation at Thr, Lys and Ala codons. Conversely, CTR1, FRE1 and FRE7 were down regulated in the strain that mistranslated Ser at Gly codons at high level ($tRNA^{Ser}$(Gly)MC). Interestingly, the ZPS1 and ADH4 genes, whose transcription is induced under low-zinc conditions by the Zap1 transcription factor (Lyons et al., 2000), were strongly down regulated by mistranslation (table 4.1). Indeed, ZPS1 was down regulated by Ser misincorporation at Ile (-32 fold), Leu (-6.9 fold), Tyr (-8.3 fold) and Ala (-4.5 fold) codons and at high level of mistranslation ($tRNA^{Ser}$(Gly)MC) (-2.5 fold), while ADH4 was down regulated by Ser misincorporation at Ile (-18.2 fold), Leu (-10.3 fold), Tyr (-14 fold) and Ala (-6.6 fold) codons and at high level of mistranslation (-4.7 fold). These results suggest that the level of zinc in these strains was elevated. However, it is not clear why different copper and iron metabolism genes were differentially regulated in the different mistranslating strains. These differences in ions concentration could be due to altered ion uptake in the different strains, or due to differential deregulation of ion sensors.

Interestingly, the deregulations of ion metabolism could affect other pathways and consequently be responsible, in part, for the phenotypic differences observed between strains.

Table 4.1: Expression of genes involved in copper and iron metabolism in the mistranslating strains. Values shown correspond to the fold variation. Positive values correspond to induced genes while negative values correspond to repressed genes.

Gene	$tRNA^{Ser}(Ile)$	$tRNA^{Ser}(Leu)$	$tRNA^{Ser}(Val)$	$tRNA^{Ser}(Tyr)$	$tRNA^{Ser}(Gly)$	$tRNA^{Ser}(Ala)$	$tRNA^{Ser}(Lys)$	$tRNA^{Ser}(Thr)$	$tRNA^{Ser}(Gly)MC$
FRE1	3.351168	1.304074	1.278269	-1.89675	2.376714	1.637538	3.003385	4.431902	-4.00096
FRE7	7.083527	3.33553	1.435419	-1.41258	16.51337	3.068215	21.35079	24.50939	-2.43894
CTR1	1.826943	1.127783	1.078464	-1.72862	2.59782	1.499654	2.797698	2.639334	-5.24748
IRC7	1.413357	1.273272	1.418597	1.282099	1.439484	2.329209	2.012346	2.159443	1.131287
REE1	6.907035	3.169347	2.665142	1.442123	5.815807	3.130023	7.739923	9.302885	1.693778
ZPS1	-32.4315	-6.89343	-1.90151	-8.31462	-1.40847	-4.5488	-1.87143	1.237248	-2.59081
ADH4	-18.186	-10.2952	-2.07646	-14.0806	-1.41593	-6.63281	-2.02272	-1.53881	-4.7849

Finally, Ser misincorporation at Thr codons up regulated significantly the biotin and the NAD(+) dependent formate dehydrogenase (FDH) genes, FDH1 and FDH2 (table 4.2). The FDH1 and FDH2 encode proteins responsible for protection of yeasts from formic acid toxicity by catalyzing its irreversible oxidation to CO_2 in presence of NAD^+ (Blanchard & Cleland, 1980; Schmidt et al., 2010). However, the level of formate in our strains is unknown and we are not able to fully understand the meaning of FDH1 and FDH2 deregulation. Moreover, Ser misincorporation at Thr codons up regulated BIO3, BIO4 and BIO5 genes, which are involved in biotin metabolism. Biotin is also known as vitamin H and is an essential nutrient usually used as a cofactor of many enzymes involved in gluconeogenesis, amino acid metabolism, fatty acid biosynthesis, and energy metabolism (Wu et al., 2005). *S. cerevisiae* is auxotrophic for biotin and requires it or intermediate metabolites of biotin synthesis, namely 7-keto-8-amino-pelargonic acid (KAPA) or 7,8-diamino-pelargonic acid (DAPA). For this reason, only the last three steps of the biotin

biosynthesis pathway, involving BIO3, BIO4, and BIO2 are activated in yeast. However, Ser misincorporation at Thr codons induced up regulation of BIO3, BIO4 and BIO5 while BIO2 did not change, suggesting that up regulation of some of the biotin genes is not related with increased biotin synthesis but, instead, could be related to the genomic localization of these genes. Indeed, our up regulated biotin genes are clustered in chromosome XIV and the gene encoding DAPA aminotransferase (BIO3) and dethiobiotin synthetase (BIO4) are linked to the gene that codes for the transport of KAPA (BIO5).

Table 4.2: Expression of FDH and biotin genes in the mistranslating strains. Values shown correspond to the fold variation. Positive values correspond to induced genes while negative values correspond to repressed genes.

Systematic name	Gene	$tRNA^{Ser}(Ile)$	$tRNA^{Ser}(Leu)$	$tRNA^{Ser}(Val)$	$tRNA^{Ser}(Tyr)$	$tRNA^{Ser}(Gly)$	$tRNA^{Ser}(Ala)$	$tRNA^{Ser}(Lys)$	$tRNA^{Ser}(Thr)$	$tRNA^{Ser}(Gly)MC$
YPL276W	FDH2	1.112985	1.06628	1.015392	-1.38221	-1.04321	-1.48942	1.081946	13.46537	-1.01745
YPL275W	FDH2	1.060146	1.443687	1.034109	-1.4095	1.18586	-1.50746	1.346166	29.29474	1.259918
YOR388C	FDH1	-1.01731	1.466887	1.086411	1.230097	1.286294	-1.24323	1.979347	38.79766	1.299364
YNR057C	BIO4	1.057266	-1.52121	-1.37027	-1.38222	-1.04988	-2.65397	1.678389	2.717522	-1.08937
YNR056C	BIO5	-1.4203	-2.55756	-1.80215	-1.85776	-1.07025	-4.39226	1.682644	2.726197	-1.79183
YNR058W	BIO3	-1.35609	-2.2982	-1.92321	-1.73365	-1.27094	-4.21245	1.282697	1.801327	-1.55583

4.3.2. Functional enrichment of down regulated genes

Functional enrichment analysis of down regulated genes using Tango and KEGG showed that Ser misincorporation at Lys, Thr and Gly codons failed to produce enriched functional classes lists, while Ser misincorporation at Ala codons produced the highest enrichment in functional pathways (figures 4.3 and 4.4).

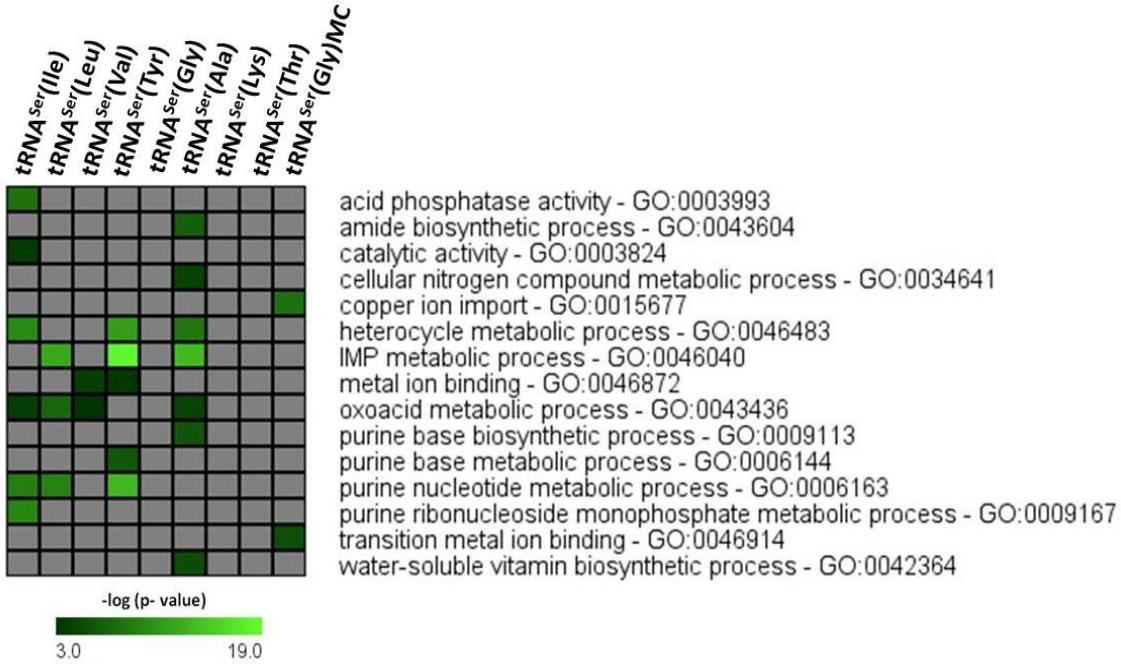

Figure 4.3: Functional class enrichment analysis of genes that are down regulated by mistranslation. Significantly down regulated genes identified using SAM analysis (FDR 0.001) and -1 > M >0.6 were functionally enriched using Tango analysis (p< 0.05). The significance of the enrichment is represented as a heat map where the color intensity corresponds to -log(p-values). GO identification numbers are indicated for each category.

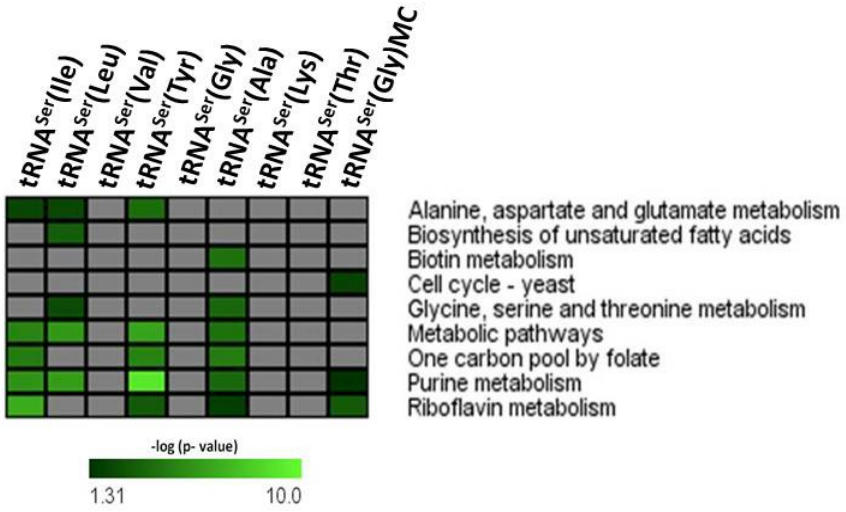

Figure 4.4: Functional pathways enrichment analysis of genes that are down regulated by mistranslation. Significantly down regulated genes identified using the SAM analysis (FDR 0.001) and -1 > M >0.6 were functionally enriched using KEGG pathway analysis (p< 0.05). The significance of the enrichment is represented as a heat map where the color intensity corresponds to -log (p-values).

Common classes of down regulated genes between strains were not identified, however some classes of down regulated genes are shared between the strains expressing the most toxic mistranslation, namely the Ser misincorporation at Ile, Leu and Val codons. Interestingly, misincorporation of Ser at Ala codons induced down regulation of biotin metabolism genes. Indeed, the expression of the BIO3, BIO4 and BIO5 genes was repressed (table 4.2). Also, copper ion import was down regulated in the strain that expressed the mutant tRNAs from multicopy plasmids ($tRNA^{Ser}$(Gly)MC), while in the others was not significantly affected. If we compare the level of FRE1, FRE7 and CTR1 it is possible to observe decreased expression in the MC strain and up regulation in other strains (table 4.1).

4.3.3. Enrichment of transcription factors

The deregulated genes described above were subjected to Prima transcription factor (TF) enrichment analysis (Expander software). All mistranslating strains showed enrichment of the CAD1 transcription factor (figure 4.5). CAD1 (Yap2) transcriptional activity is stimulated by aminotriazole and cadmium and confers resistance to various drugs and metals, such as cadmium and cyclohexamide (Fernandes et al., 1997; Rodrigues-Pousada et al., 2004). It also controls genes involved in stabilization and folding of proteins in oxidative environments (Cohen et al., 2002). Put3, a transcriptional activator of proline utilization genes, which is activated by phosphorylation in the absence of good nitrogen sources and in the presence of proline (Huang & Brandriss, 2000; Spitzner et al., 2008), was enriched in all strains except that misincorporating Ser at Thr codons (figure 4.5). The ADR1 gene, which encodes a transcription factor required to activate the expression of the glucose-repressible isoenzyme alcohol dehydrogenase II (ADH2) when glucose becomes depleted (Denis et al., 1981; Dombeck et al., 1993), was enriched in the up regulated genes in all strains except in the strain that misincorporated Ser at Ala codons.

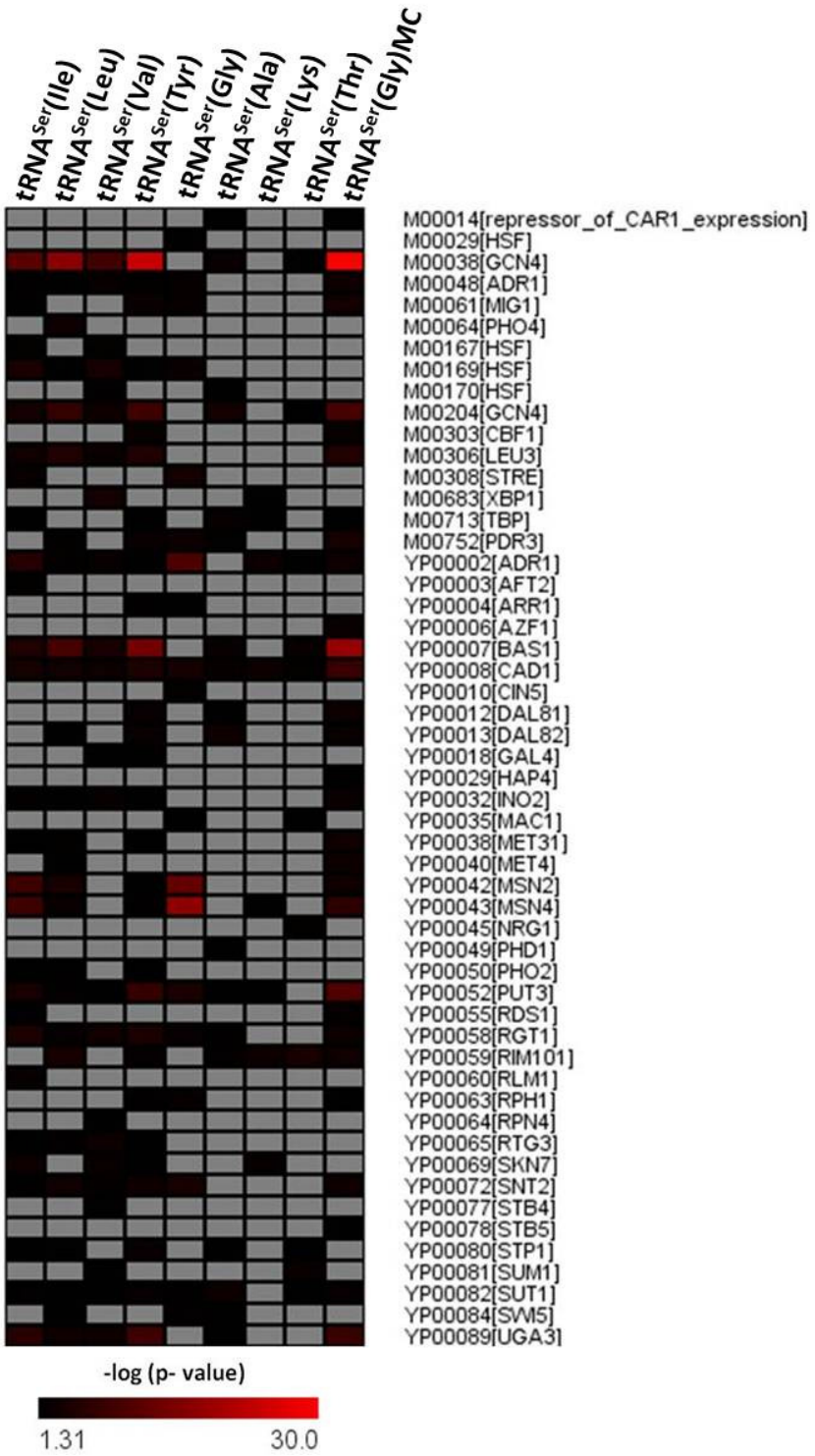

Figure 4.5: Transcription factors enrichment of the up regulated genes. The significantly up regulated genes identified using SAM analysis (FDR 0.001) and -1 > M >0.6 were functionally enriched using Prima transcription factor enrichment analysis ($p < 0.05$). The significance of enrichment is represented as a heat map in which the color intensity corresponds to –log (p-values).

The Leu3p, which interacts with the cis-acting element (UAS_{LEU}) located upstream of several unlinked genes and is involved in up regulation of branched-chain amino acid biosynthesis (LEU1, LEU2, LEU4, and ILV2) and nitrogen metabolism (GDH1) (Sze et al., 1993), was enriched in the up regulated genes list of strains that misincorporated Ser at Ile, Leu, Val and Tyr codons and in the strains that misincorporated Ser at Gly codons at high level (multicopy plasmid), and it was enriched in the down regulated genes list of the strains that misincorporated Ser at Ala, Gly and Ile codons (figure 4.6). Enrichment in GCN4 TF was observed in the list of up regulated genes for all strains except in those that misincorporated Ser at Gly and Lys codons (figure 4.5). GCN4 activates transcription of more than 30 amino acid biosynthesis genes representing 12 different pathways. Gcn4p synthesis is induced under various conditions, such as, amino acid and purine starvation, glucose limitation, growth in the nonfermentable carbon source ethanol, high hosmotic stress, treatment with methyl methanesulfonate and rapamycin. GCN4 is also regulated at the level of mRNA translation in amino acid starved cells (Filippi et al., 2007; Hinnebusch & Natarajan, 2002).

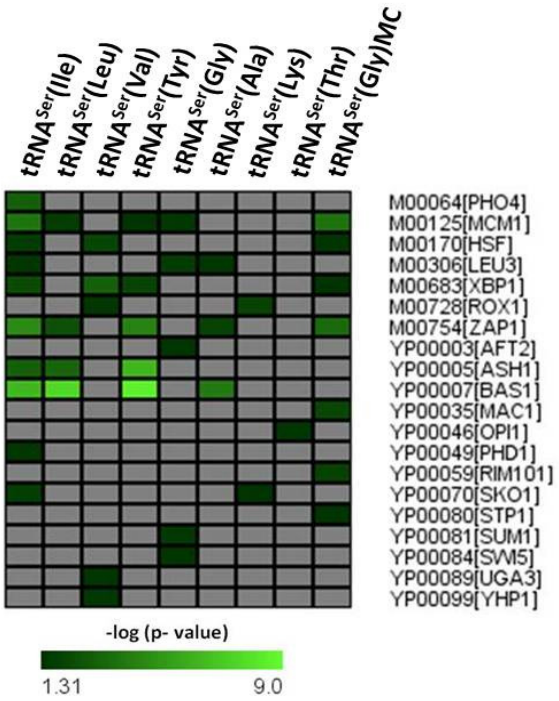

Figure 4.6: Transcription factors enrichment of the down regulated genes. The significantly down regulated genes identified using SAM analysis (FDR 0.001) and -1 > M >0.6 were functionally enriched using Prima transcription factor enrichment analysis ($p< 0.05$). The significance of enrichment is represented as a heat map in which the color intensity corresponds to –log (p-values).

The TF Bas1 was enriched in both up and down regulated gene lists (figure 4.5 and 4.6). This dual enrichment could be related to the control of genes encoding enzymes involved in histidine, arginine, pyrimidine and purine biosynthetic pathways. Genes down regulated by BAS1 (table 4.3) include ADE1, ADE2, ADE4, ADE5-7, ADE6, ADE8, which are required for IMP de novo biosynthesis. ADE 12 and ADE13 are involved in conversion of IMP into AMP, while all other ADE proteins are involved in synthesis of IMP from phosphorybosil pyrophosphate (Denis et al., 1998). The expression of these ADE genes was down regulated in the strains that misincorporated Ser at Ile, Leu, Tyr and Ala codons and in the strain that misincorporated Ser at Gly codons at high level (multicopy plasmid).

Table 4.3: Expression of ADE genes in the mistranslating strains. Values shown correspond to the fold variation. Positive values correspond to induced genes while negative values correspond to repressed genes.

Gene	$tRNA^{Ser}$(Ile)	$tRNA^{Ser}$(Leu)	$tRNA^{Ser}$(Val)	$tRNA^{Ser}$(Tyr)	$tRNA^{Ser}$(Gly)	$tRNA^{Ser}$(Ala)	$tRNA^{Ser}$(Lys)	$tRNA^{Ser}$(Thr)	$tRNA^{Ser}$(Gly)MC
ADE1	-1.90532	-2.95111	1.060482	-2.88135	1.46312	-4.14639	1.122642	1.029978	-1.84837
ADE2	-2.38154	-2.47949	1.113047	-2.72992	1.469147	-2.86361	1.439125	1.247176	-1.66117
ADE4	-1.90667	-1.998	1.064477	-2.08086	1.239318	-2.72147	1.051961	1.064117	-1.17002
ADE5,7	-3.66679	-3.06193	-1.41484	-3.17889	1.019253	-3.75793	-1.10334	-1.15045	-2.00096
ADE6	-1.84453	-2.0458	-1.49267	-2.06099	1.008631	-2.91638	-1.17586	-1.4051	-1.4914
ADE8	-1.77952	-1.38796	1.044374	-1.49618	-1.04001	-1.83773	1.06338	-1.01222	1.025719
ADE13	-5.54436	-5.07172	-1.58091	-5.79397	1.006695	-5.83528	-1.01811	-1.00403	-3.31653
ADE12	-2.48105	-2.22964	-1.13237	-2.10481	-1.27829	-1.97652	1.103403	1.132562	-1.41192
ADE16	-1.09918	1.017826	-1.03162	-1.22235	-1.01115	-1.47712	-1.02907	-1.35045	-1.19006
ADE17	-7.45872	-6.47711	-1.95484	-6.10826	1.404218	-7.66304	1.056739	-1.02184	-2.48516

The heat-shock TF (HSF) was up regulated in the strains that misincorporated Ser at Ile, Leu, Val, Tyr, Gly and Ala codons. It is unclear why HSF was not enriched in all strains and why its expression was even down regulated in the strains that misincorporated Ser at Ile and Val codons and in the strains that mistranslated at high

level (multicopy plasmid). HSF is activated in response to elevated temperatures, oxidants and heavy metals and binds the heat shock element (HSE) to activate transcription of the heat shock genes, resulting in accumulation of Hsps, which repair damaged proteins (Pirkkala et al., 2001). Besides HSF, MSN2 and MSN4 are also major regulators of the cytoplasmic heat shock response in yeasts, while in the endoplasmic reticulum (ER) the heat shock response is activated by the HAC1 transcription factor. Up regulated genes containing promoter elements recognized by Msn2 and Msn4 were enriched in the strains that misincorporated Ser at Ile, Leu, Tyr, Gly and Lys codons and in the strain that mistranslated at high level (multicopy plasmid). Msn2 and Msn4 accumulate in the nucleus in stressed cells where they bind the STRE element and activate transcription of stress genes. In the absence of stress conditions both factors localize in the cytosol. Although, HSF and MSN2/MSN4 play a role in heat stress they have different regulatory mechanisms. Hsf1 activates transcription of target genes after a severe heat shock and during the recovery period, while Msn2/4 are not involved in the recovery phase, suggesting that they play a role during the initial exposure to stress (Gasch, 2002; Yamamoto et al., 2008).

In addition to the TFs shared between mistranslating strains, other TFs were enriched in some strains only. For example, genes up regulated by Pho4 were identified only in the strain that misincorporated Ser at Leu codons. This was consistent with the deregulation of phosphate metabolism in the former strain, as mentioned before. Interestingly, these genes were down regulated in the strain that misincorporated Ser at Ile codons. The other case was the ZAP1 which binds to genes containing Zinc-Responsive Elements or "ZREs" in their promoters when zinc levels are low (Eide, 2009; Wu et al., 2008). This TF was down regulated in the strains that misincorporated Ser at Ile, Leu, Tyr and Ala codons and in the strain that mistranslated at high level. AFT2, a iron-regulated transcriptional activator involved in intracellular iron homeostasis (Blaiseau et al., 2001) was enriched in the list of up regulated genes in the strain that misincorporated Ser at Ile codons and, was also enriched in the Gly codon misreading strain in the down regulated genes list. The INO2 transcription factor, which is required for expression of phospholipid structural genes (Nikoloff & Henry, 1994), was enriched only in the strains where mistranslation was most toxic.

4.3.4. Gene expression deregulation is physically linked in the yeast genome

In order to explain the variability in gene deregulation patterns described above, we calculated the chromosomal median gene expression change in our strains (figure 4.7).

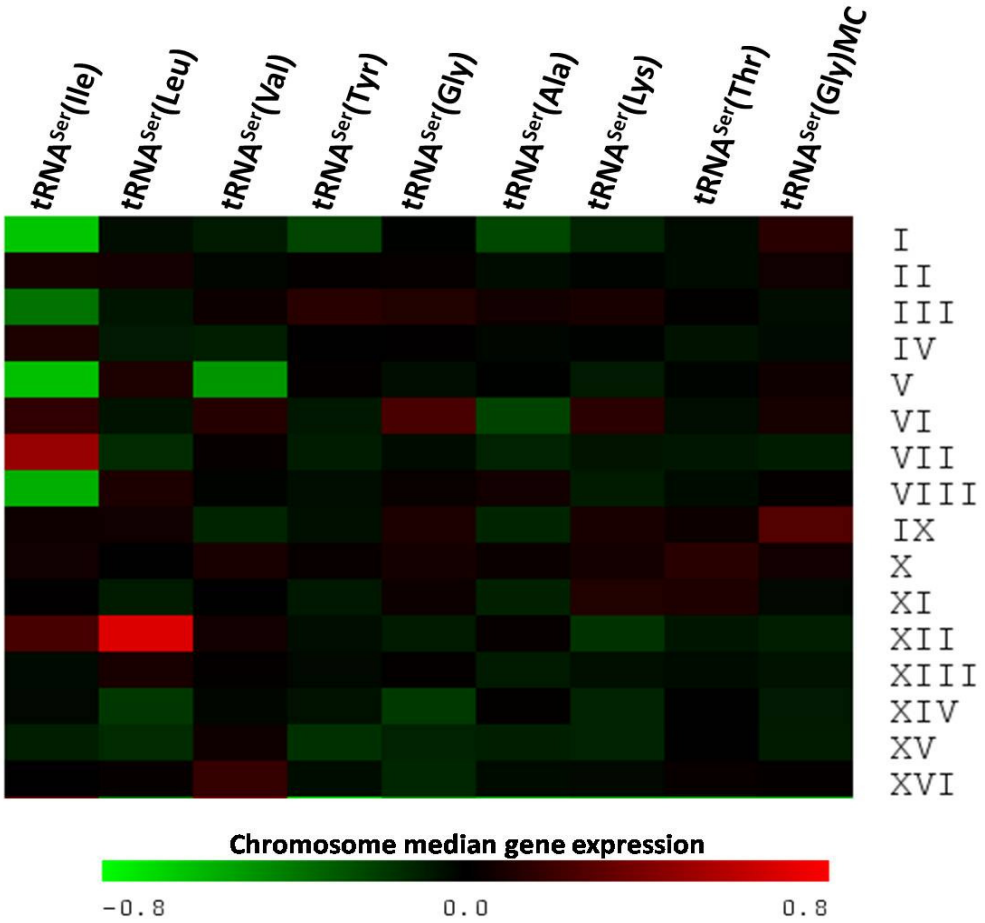

Figure 4.7: Chromosome median gene expression change in mistranslating strains. The median of gene expression change was calculated for each chromosome for mistranslating strain. The accumulation of up regulated genes (red) and down regulated genes (green) is represented as a heat map obtained using MEV software.

Surprisingly, in the strain that misincorporated Ser at Leu codons the chromosome XII showed an accumulation of up regulated genes, which was not observed in the other strains, while in the strain that misincorporated Ser at Ile codons there was an accumulation of up regulated genes located in chromosome VII and an accumulation of

down regulated genes located in chromosomes I, III, V and VIII. In the strain that misincorporated Ser at Val codons there was an accumulation of down regulated genes in chromosome V. The other mistranslating strains did not show physical association of the up or down regulated genes. This data suggested that some of the gene deregulation observed may result from chromosome rearrangements rather than other regulatory mechanisms, since there is a strong relationship between chromosomal median gene expression change and chromosome stoichiometry. Where, genes encoded on extranumerary chromosomes tend to be more highly expressed than genes on euploid chromosomes (Hughes et al., 2000; Rancati et al., 2008). Therefore, mistranslation generates chromosome instability which is variable between the strains analyzed. However, this data needs to be confirmed using karyotype analysis and comparative genomic hybridization analysis on array (aCGH).

4.4. Discussion

In order to understand the phenotypic variability observed in our mistranslating strains we have analysed the transcriptome of mistranslating cells using DNA microarray analysis. Usually, cellular responses to stress include gene expression reprogramming to adjust the proteome to the new physiological condition and, DNA microarrays are widely used to study transcriptional alterations of cells by comparing steady-state mRNA levels before and after the stress (Halbeisen et al., 2007; Halbeisen & Gerber, 2009; Romero-Santacreu et al., 2009). Previous studies demonstrated that yeast evolved mechanisms that allow it to adapt to various stressors. Yeast exposed to severe stress, namely to osmotic shock, acetic acid, carbon source variation, phosphate starvation, high or low doses of zinc, cadmium, iron, arsenic, heat shock, amino acid analogs (AZC), ethanol and calorie restriction deregulate the expression of ≈10-15% of its genes (Auesukaree et al., 2009; Berry & Gasch, 2008; Causton et al., 2001; Jin et al., 2008; Kuhn et al., 2001; Lee & Lee, 2008; Lu et al., 2009; Lyons et al., 2000; Ma & Liu, 2010; Melamed et al., 2008; Mira et al., 2010; Ogawa et al., 2000; Posas et al., 2000; Thorsen et al., 2010; Trotter et al., 2002; Wu et al., 2008), while in contrast, mild stress, namely low doses of Calcofluor-white or menadione, induced deregulation of ≈1% of the yeast genes (Halbeisen & Gerber, 2009). The response of yeast to severe stress is known as the environmental

stress response (ESR) (Gasch, 2002). This response induces deregulation of ≈900 genes from which ≈600 are down regulated and ≈300 are up regulated. The up regulated genes include gene ontology (GO) terms belonging to carbohydrate metabolism, detoxification of reactive oxygen species, cellular redox reactions, cell wall modification, protein folding and degradation, DNA damage repair, fatty acid metabolism, metabolite transport, vacuolar and mitochondrial functions and autophagy genes, while down regulated genes encode ribosomal proteins mainly (Gasch et al., 2000; Gasch, 2002). However, recent studies postulate that genes deregulated after the stress exposure (ESR genes) represent a growth rate response. Indeed, the correlation between ESR deregulated genes and growth rate suggest that yeast may not be responding directly to the stress but may instead respond to a reduction in growth rate caused by the stress (Brauer et al., 2008; Castrillo et al., 2007).

Mistranslation in yeast was previously related to the heat-shock response. Firstly, paramomicin, an aminoglycoside antibiotic that induces translation misreading, increases the level of aberrant proteins in yeast and triggeres the heat-shock response, as measured by induction of Hsp70 and thermotolerance acquisition (Grant et al., 1989). Secondly, the proline amino acid analog azetidine 2-carboxylic acid (AZC) causes protein instability and misfolding, induces cell cycle arrest, repression of expression of ribosomal proteins and expression of genes containing heat shock elements, namely heat shock proteins, through the activation of the heat shock factor (HSF) (Trotter et al., 2001; Trotter et al., 2002).

Our data showed similarities between the list of genes up regulated in our mistranslating strains and those of the ESR and AZC treatments, namely amino acid and carbohydrate metabolism, metabolite transport, protein folding and oxidative stress genes and also of genes regulated by the transcription factor (TF) HSF1. Conversely, the low functional class enrichment of down regulated genes in the mistranslating strains was very different from the ESR down regulated gene list, as the latter down regulates ≈600 genes. In our mistranslating strains the highest deregulation was observed in the case of expression of the $tRNA^{Ser}$(Gly) from the multicopy plasmid, where 6% of the genes (≈380 genes) were deregulated. Gene deregulation in the other strains was significantly lower than in $tRNA^{Ser}$(Gly) multicopy strain and in the ESR (10-15% of deregulated genes). This could be related to experimental design differences, since our yeast cells were mistranslating constitutively, while AZC and the other stressors were added to exponential growing cells for short period of time. In other words, ESR experiments used an inducible

experimental design while our experiments used a constitutive system. Our results showed also that the numbers of gene functional classes that are deregulated by mistranslation are dependent upon the level of mistranslation toxicity, as one would expect. In other words, mistranslation toxicity levels are directly correlated with gene expression deregulation. Interestingly, some studies suggest that toxicity is not always correlated with quantitative gene expression deregulation. For example, yeast exposed for 10 min to low doses of NaCl up regulate more genes than yeast exposed for 10 min to the double concentration of the same salt (Posas et al., 2000).

Besides the common response to mistranslation we observed peculiar differences in gene expression deregulation between our mistranslating strains. For example, the enrichment in up regulated polyphosphate genes was exclusive of the strain that misincorporated Ser at Leu codons. This strain increased expression of the high affinity phosphate transporter PHO84 gene (102 fold), suggesting that it accumulated Pi, which is usually bound forming a chain of Poly P. In certain cases, Poly P can reach up to 20% of cellular dry weight and most of it (99%) is stored in the vacuole (Brown & Kornberg, 2004; Kornberg et al., 1999). This suggests that the vacuolar alterations observed in this strain, namely the existence of multiples vacuoles per cell, could be related to an increase in Poly P. One of the functions of Poly P is to chelate a wide variety of metals, namely Zn2+, Fe3+, Cu2+ and Cd2+, which could explain the tolerance of this strain to copper sulphate and cadmium chloride (figure 3.31) (Brown & Kornberg, 2004; Kornberg et al., 1999). Indeed, intracellular polyphosphate protect bacterial and plant cells against toxicity induced by heavy metals, namely mercury and cadmium, through the sequestration of these ions (Keasling, 1997; Nagata et al., 2006; Pan-Hou et al., 2002). Conversely, increased phosphate uptake in yeast through deletion of Pho80 deregulates ion homeostasis and increases the uptake of iron, calcium and sodium cations that are toxic (Rosenfeld et al., 2010). Interestingly, the strains that grew better in the presence of cadmium chloride, namely those misincorporating Ser at Tyr and Val codons (figure 3.31), did not deregulate phosphate metabolism genes. Therefore, the role of phosphate metabolism in mistranslation remains to be elucidated in future studies. In order to clarify this issue one should quantify the level of phosphate in our mistranslating strains and correlate phosphate concentration with gene deregulation. Also, it will be important to quantify the level of the PHO84, at mRNA level using Real-Time PCR and at protein level using western blot analysis, because DNA microarrays are not quantitative and mRNA level does not always correlate with protein level. The difference between mRNA and protein levels are around 30% and under stress conditions these differences increase. For

example, in some situations mRNA levels may increase while protein levels remain constant, while in other cases mRNA levels remain constant and protein levels increase more than 30 fold. This incongruence between mRNA level and protein expression emphasize the importance of posttranscriptional regulatory mechanisms in cellular development (Castrillo et al., 2007; Griffin et al., 2002; Gygi et al., 1999). Interestingly, Cup1p mediates resistance to high concentrations of copper and cadmium (Winge et al., 1985), but we did not observe up regulation of CUP1 at mRNA level, suggesting that the tolerance of some mistranslating strains to grow in presence of cadmium chloride and copper sulphate is not directly related with the expression of CUP1. Our alternative explanation is that this tolerance results from an indirect effect of stress cross protection, which is activated by most environmental stressors (Lewis et al., 1995; Mahmud et al., 2010). For example, yeast exposure to cobalt activates cross protection against nickel, zinc and manganese (Çakar et al., 2009) and yeast growing in high osmotic medium become termotolerant (Trollmo et al., 1988).

Interestingly, Ser misincorporation at Gly codons up regulated genes involved in the galactose metabolism and result in a selective growth advantage of these cells in galactose containing media (figure 3.31). These cells and those that misincorporated Ser at Lys codons were also tolerant to SDS (figure 3.31). Although, our gene expression profiling data does not provide a clear explanation for the tolerance to SDS, suggesting that some of the phenotypes observed may arise from translational or post-translational control of gene expression.

Other interesting gene expression deregulations were observed in cells that misincorporated Ser at Thr codons. These cells showed a significant increase in the expression (>25 fold) of formate dehydrogenases (FDH1 and FDH2). The FDH enzymes catalyze the oxidation of formate (HCO_2^-) to CO_2 in the presence of $NAD(P)^+$ with the release of NAD(P)H (Blanchard & Cleland, 1980; Schmidt et al., 2010). Yeast can consume formate as an alternative energy source in aerobic glucose-limited conditions (Bruinenberg et al., 1985; Overkamp et al., 2002). For this reason, cells misincorporating Ser at Thr codons may have selective advantage relative to control and other mistranslating strains in presence of formate, which would be interesting to test in future studies.

The differences observed in gene expression in our mistranslating strains were partly expected and some were in agreement with the phenotypic variation observed. Our microarray analysis brought, therefore, insight on how genetic code ambiguity may create selective advantages, which are critical to understand the evolution of non-neutral genetic

code alterations. Our data also showed that mistranslation may induce chromosome alterations and that the latter may be responsible for part of the gene expression alterations observed. In other words, some of the gene deregulation may be a secondary effect of mistranslation. Nevertheless, this gene expression deregulation may also result in phenotypic alterations which could create selective advantages in specific ecological niches.

Chapter 5

General discussion

5.1. Evolution of CUG codon reassignment in the CTG clade

The genetic code table is not randomly organized, rather the distribution of codons seems to be optimized to avoid/reduce errors (Kurnaz et al., 2010; Woese, 1965; Woese et al., 1966). Indeed, mutations introduced in the third base of codons codify most of the time (69%) for synonymous codons that mediate the incorporation of the same or chemically similar amino acids (Davies et al., 1964; Freeland et al., 2002; Novozhilov et al., 2007). Moreover, codons containing uracil (the most hydrophilic nucleotide) in the midle position codify for hydrophobic amino acids, while codons containing an adenine (the most hydrophobic nucleotide) in the middle position codify hydrophilic amino acids (Haig & Hurst, 1991; Weber & Lacey, 1978). The tRNA-aaRS-codon system has also co-evolved as codons containing cytosine in the second nucleotide position codify for amino acids handled by class II aaRSs while those containing uracil at the second position codify for amino acids handled by class I aaRS (Wetzel, 1995). At the gene level, amino acids codified by codons with higher number of synonyms are incorporated more frequently into vertebrates proteins (King & Jukes, 1969), archaea, bacteria and eukaryotes proteins (Gilis et al., 2001). Moreover, amino acids with a smaller size (Hasegawa & Miyata, 1980) and with basic, polar and barophilic properties (Di Giulio, 2005a; Di Giulio, 2005b) are codified by a larger number of synonyms codons, demonstrating the existence of a correlation between the organization of the genetic code and the ecology of primordial organisms, suggesting that the genetic code structure took place under high hydrostatic pressure, in acidic pH conditions and at high temperature (Di Giulio, 2000; Di Giulio, 2005c).

The incorporation of selenocysteine (Sec) and pyrrolysine (Pyl) in the genetic code and the discovery of 23 alterations in the nuclear and mitochondrial genomes of various organisms show that the genetic code is flexible and is still evolving. One of these alterations occurs in the fungal CTG clade species (*C. albicans, C. dubliniensis, C. tropicalis, C. parapsilosis, C. lusitaniae, C. guilliermondii, L. elongisporus and D. hansenii*) (Butler & et al, 2009), where the Leu CUG codon is decoded as Ser. Molecular phylogeny studies showed that this decoding alteration of the CUG codon was initiated 272 ± 25 million years (MY) ago in an ancestor of fungi due to appearance of a mutant $tRNA_{CAG}^{Ser}$ that originated from a single mutation in the anticodon of the $tRNA_{CGA}^{Ser}$ gene (figure 5.1). This mutation involved the insertion of an Adenosine in the middle of the tRNA anticodon, which altered it from 5'-CGA-3' to 5'-CAG-3', permitting the recognition of Leu CUG

codons. In order to stabilize the mutant $tRNA_{CGA}^{Ser}$ two additional mutations were necessary, namely the $A_{37}\rightarrow G_{37}$ and $U_{33}\rightarrow G_{33}$ substitutions. In the yeast ancestor, the mutant $tRNA_{CAG}^{Ser}$ competed with the cognate $tRNA_{CAG}^{Leu}$ for CUG codons at the ribosome A-site, introducing genetic code ambiguity during translation of CUGs, which were translated as both Ser and Leu. For unknown reasons, the $tRNA_{CAG}^{Leu}$ gene disappeared from the genome and the $tRNA_{CAG}^{Ser}$ gene was selected, promoting the reassignment of the CUG codon from Leu to Ser (Massey et al., 2003; Santos et al., 2004).

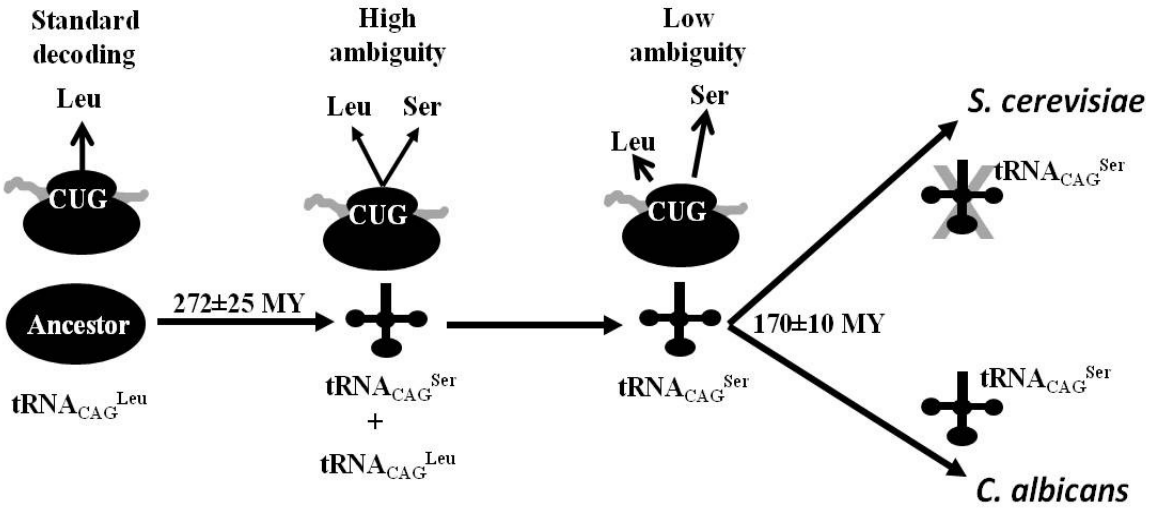

Figure 5.1: Evolutionary pathway of CUG reassignment in C. albicans. The mutant $tRNA_{CAG}^{Ser}$ appeared in a fungal ancestor 272±25 million years (MY) ago and competed with the cognate $tRNA_{CAG}^{Leu}$ for CUG decoding. The CUG codons were then translated as both Leu and Ser creating genetic code ambiguity. This ambiguity decreased over time due to loss of the $tRNA_{CAG}^{Leu}$ gene from genome of the ancestor. 170±10 MY ago the $tRNA_{CAG}^{Ser}$ was maintained in the lineage that originated *C. albicans* and was lost in the lineage that originated *S.cerevisiae*. Adapted and modified from (Miranda et al., 2007).

Interestingly, the $tRNA_{CAG}^{Ser}$ gene was lost in the lineage that originated the *S. cerevisiae* clade and was selected in the lineage that originated the CTG clade. In *C. albicans*, the reassignment did not proceed to completion as the CUG codon is still ambiguously decoded, 97% of the time Ser is incorporated and 3% of the time Leu is

incorporated. Such atypical ambiguity is due to dual recognition of the $tRNA_{CAG}^{Ser}$ by SerRS and LeuRS (Gomes et al., 2007). It is still unclear why such ambiguity was selected but our studies showed that codon ambiguity generates advantageous phenotypic variation (Miranda et al., 2007). Phylogenetic studies demonstrate that the CTG clade species reassigned 26000 to 30000 CUG codons present in ≈50% of its genes, which are occupied by Leu residues in *S. cerevisiae* genes, suggesting a highly dynamic evolution of CUG codons in fungi (Massey et al., 2003).

Our *in vivo* reconstruction studies of the $tRNA_{CAG}^{Ser}$ evolutionary pathway showed that mutations introduced in the anticodon of the $tRNA_{CGA}^{Ser}$ did not destabilize the tRNA, neither inhibited its expression, serylation or decoding. Our data are in agreement with a recent *in vitro* study which demonstrated that the reassignment of Leu CUN codon to Thr in yeast mitochondria was initiated by a mutation in a $tRNA_{GUG}^{His}$ gene that originated a mutant $tRNA_{UAG}^{Thr}$ that recognizes the 4 CUN Leu codons. This study also suggested that during reassignment of the CUN codons the cognate $tRNA_{UAG}^{Leu}$ was eliminated from the mitochondrial genome and that the original CUN codons were erased and then reappeared in positions occupied by other amino acids (Su et al., 2011).

Despite that genetic code flexibility, our data demonstrates unequivocally that reassignment of Leu CUG codons to Ser was a highly unlikely evolutionary event due to its high toxicity and the negative fitness impact of Ser misincorporation at CUG codons. Our data shows that the toxicity of Ser misincorporation at CUG codons was minimized by low expression of the mutant $tRNA_{CAG}^{Ser}$, but, nevertheless the negative effects of low level of Ser misincorporation at CUGs were clear. This low abundance of the mutant mistranslating tRNAs and the apparent positive correlation between mistranslation toxicity and tRNA abundance suggest the existence of a novel mechanism that regulates the expression of mistranslating tRNAs. In other words, cells may have a specific defense mechanism that either repress transcription or target mistranslating tRNAs to degradation.

Small RNA sequencing using deep sequencing technologies have identified tRNA fragments in human cells depending on the tissue type and cell line (Kawaji *et al.*, 2008), and in the urine and sera of cancer patients, with levels correlated with tumor burden (Thompson, 2009b). The metabolism of tRNAs is controlled by specific RNA degradation pathways and can be induced by several factors, namely nucleotide base pair disruptions (Li *et al.*, 2002), nucleotide substitutions in the variable arm (Lee & Mcclain, 2004),

absence of base modifications (Alexandrov et al., 2006; Chernyakov et al., 2008; Kadaba et al., 2004; Kadaba et al., 2006; Ozanick et al., 2008; Wang et al., 2008), chemical RNA methylation (Ougland R. *et al.*, 2004), amino acid starvation (Lee, 2005), and treatment with colicin D (Shigematsu *et al.*, 2009). Oxidative stress also induces tRNA degradation in yeast (Thompson, 2009b) and mammalian cells (Fu *et al.*, 2009) through endonucleolytic cleavage in the anticodon loop, originating tRNA halves with ≈35 nucleotides, or in other loops originating other types of tRNA fragments (Kawaji *et al.*, 2008). The nucleases responsible for the oxidative stress-induced tRNA cleavage are Rny1p in yeast (Thompson, 2009b) and angiogenin in mammalian cells (Fu *et al.*, 2009). These nucleases are secreted or released from the vacuole into the cytosol and gain access to tRNAs during stress. Usually full-length tRNA levels do not decline significantly and tRNA fragments levels are lower than those of full-length tRNAs (Fu *et al.*, 2009;Thompson, 2009a;Thompson, 2009b).

The degradation of hypomodified and misprocessed tRNAs leads to undetectable tRNA halves and to accentuated decrease of the misprocessed or hypomodified tRNA. Two different regulatory pathways are involved in degradation of hypomodified and misprocessed tRNAs, namely the cytoplasmic and the nuclear pathways (figure 5.2) (Doma & Parker, 2007). Indeed, tRNAs can be degraded from the 5' to the 3' in the cytosol (Alexandrov *et al.*, 2006;Chernyakov *et al.*, 2008) or adenylated and degraded from the 3' to the 5' in the nucleus (Kadaba *et al.*, 2004;Kadaba *et al.*, 2006;Li *et al.*, 2002;Ozanick *et al.*, 2008;Wang *et al.*, 2008). The nuclear pathway acts through the action of the TRAMP complex and the nuclear exosome (Kadaba *et al.*, 2004;Kadaba *et al.*, 2006;Vanacova *et al.*, 2005). The TRAMP complex is a polyadenylation complex that contains a non-canonical poly(A) polymerase (Trf4p or Trf5p in yeast), an RNA-binding protein (Air1p or Air2p) and an RNA helicase (Mtr4p) (Doma & Parker, 2007). This tRNA degradation pathway always involves polyadenylation of tRNAs by the TRAMP complex and downstream 3′ to 5′ degradation by Rrp6p and/or the nuclear exosome (Kadaba *et al.*, 2006). The cytoplasmic tRNA degradation pathway, also known as the rapid tRNA decay (RTD) pathway is responsible for degradation of mature hypomodified tRNAs, such as the yeast $tRNA_{ACC}^{Val}$ and include the 5' to 3' exonucleases Rat1p, Xrn1p and also Met22p, which likely acts indirectly trough Rat1p and Xrn1p (Chernyakov *et al.*, 2008).

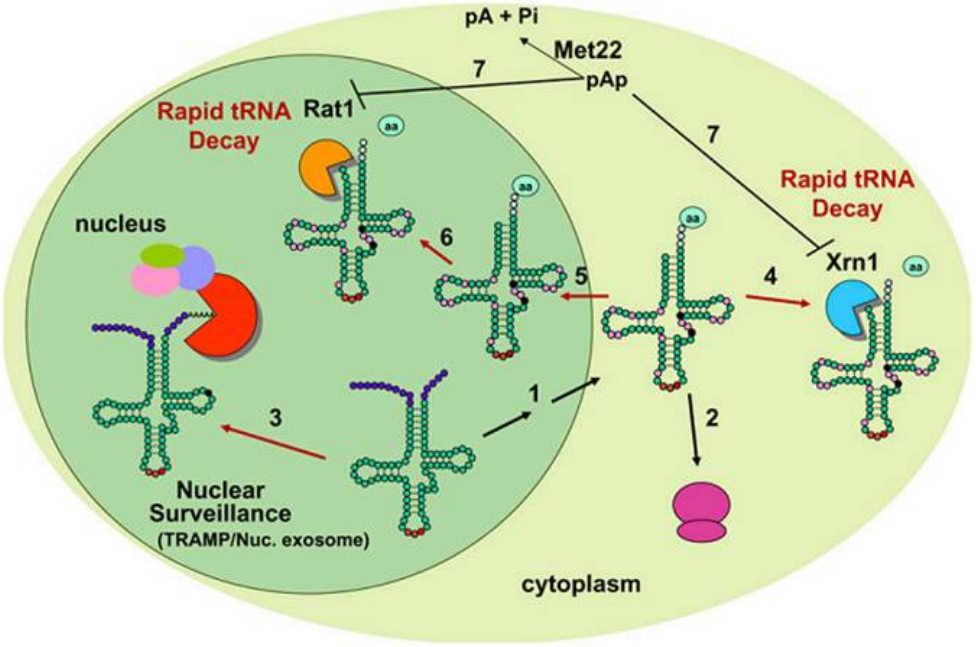

Figure 5.2: Two different tRNA degradation pathways in yeast. After transcription by RNA polymerase II pre-tRNAs are processed in the nucleus and in the cytoplasm (step 1) in order to remove the 5' leader and 3' trailer. This precedes the addition of the CCA to the 3' end and the modification of the canonical bases. Fully processed tRNA can then be used in translation by the ribosome (step 2). But, if the tRNA is not processed, it is degraded by the nuclear surveillance pathway (step 3) in which the pre-tRNA is first polyadenylated by the TRAMP complex and then degraded from the 3' end by the nuclear exosome. Lack of nucleotide modifications in tRNA, targets it for degradation by the Xrn1 rybonuclease in the cytoplasm (step 4) (RTD pathway), or by Rat1 in the nucleus (step 6) after nuclear import (step 5). The elevated presence of pAp in MET22 mutants inhibits the RTD pathway by inhibiting both Xrn1 and Rat1 (step 7). Adapted from (Phizicky & Hopper, 2010).

Our northern blot results of the mistranslating $tRNA_{CGA}^{Ser}$, $tRNA_{CAG}^{Ser}$ and $tRNA_{UGA}^{Ser}$ did not show the presence of tRNA halves, suggesting that the decrease in the abundance of the mistranslating tRNAs is not regulated by the oxidative-stress induced tRNA cleavage pathway. Moreover, the expression of our mutant $tRNA_{CGA}^{Ser}$ was not restored in the yeast ΔRNY1 knockout strain confirming that in our cells tRNA degradation is independent of Rny1p. Indeed, the observation that the level of our mutant $tRNA_{CGA}^{Ser}$ was not restored in any of the knock-out strains tested suggests that other protein(s)

(pathways) may be involved in the specific degradation of mistranslating tRNAs. This pathway should be investigated in future studies.

5.2. Effects of genetic code ambiguity

Genetic code engineering has attracted significant interest over the last few years. Indeed, recent attempts to engineer the genetic code have succeeded in incorporating 70 unnatural amino acids (UAAs) into *E. coli*, yeast and mammalian proteins. The UAAs incorporated include photocrosslinked, glycosylated, chemically reactive (containing keto, alkene, or alkyne groups) and fluorescent chemistries (reviewed in Liu & Schultz, 2010). The incorporation of UAAs, namely those with heavy atoms and isosteric analogues are a powerful tool for X-ray crystallography and protein folding, stability and activity studies. These UAAs also allow for engineering proteins with novel properties, namely proteins with improved pharmacological properties, with fluorescence and with *in vivo* photoregulated activity. Furthermore, the incorporation of UAAs can provide information about the evolution of the genetic code and about the possibility of creating organisms with new genetic codes (Wang & Schultz, 2005).

Most of the UAA experiments were carried out in *E. coli* using nonsense codons and mutant aaRS. For example, mutant TyrRS, LeuRS and PheRS have been selected to misincorporate 3H-azatyrosine (Hamano-Takaku F, 2000), norvaline and norleucine (Tang & Tirrell, 2002) and p-CI-phenylalanine (Ibba & Hannecke, 1995), respectively, in response to the UAG nonsense codon. The strategy to incorporate UAAs was then improved with the engineering of heterologous aaRS:tRNA pairs, named orthogonal pairs. For example, the yeast mutant PheRS:$tRNA^{Phe}$ orthogonal pair that permitted the incorporation of L-3-2-naphthyl-alanine (Nal) at Phe codons (Kwon et al., 2003) and the incorporation of p-fluoro-phenylalanine (p-F-Phe) at UAG codons (Further, 1998), while the mutant *Methanococcus jannaschii* TyrRS:$tRNA^{Tyr}_{CUA}$ orthogonal pair was engineered to incorporate the photocrosslinking amino acid p-benzoyl-l-phenylalanine (Chin et al., 2002) at UAG codons. The misincorporation of canonical amino acids in response to stop codons was also tested using the *Halobacterium sp*. LeuRS:$tRNA^{Leu}$ orthogonal pair which misincorporated Leu (Anderson & Shcultz, 2003) and the *S. cerevisiae* TrpRS:$tRNA^{Trp}_{CUA}$ orthogonal pair which misincorporated Trp (Hughes & Ellington, 2010) in response to UAG codons in *E. coli*. Mutant aaRS that recognized

cognate tRNAs containing an atypical 8bp anticodon, namely the *Pyrococcus horikoshii* $tRNA^{Lys}$ and the *Methanococcus jannaschii* $tRNA^{Tyr}$, were also used to misincorporate L-homoglutamine (hGln) and O-methyl-L-tyrosine in *E. coli*, respectively, in response to the quadruplet codons (AGGA) (Anderson et al., 2004). Recently, the incorporation of UAAs was improved by expressing in *E. coli* synthetically designed mRNA, ribosomes (ribo-Q1) and *Methanosarcina barkeri* and *Methanococcus jannaschii* mutant PylRS:$tRNA^{Pyl}$ orthogonal pairs to misincorporate several UAAs in response to UAG codons and to quadruplet AGGA codons (Neumann et al., 2010).

Various UAAs have also been incorporated in yeast and in mammalian cells. For example, mutant *E. coli* TyrRS:$tRNA_{CUA}^{Tyr}$ orthogonal pair has been used to misincorporate p-acetyl-L-phenylalanine, p-benzoyl-L-phenylalanine, p-azido-L-phenylalanine, O-methyl-L-tyrosine and p-iodo-L-phenylalanine in yeast (Chin et al., 2003) and 3-iodo-L-tyrosine and 4-azido-L-phenylalanine in *D. melanogaster* S2 cells (Mukai et al., 2009) in response to UAG codons. While mutant TyrRS:$tRNA_{CUA}^{Tyr}$ and PylRS:$tRNA^{Pyl}$ orthogonal pairs have been used to incorporate 3-iodo-L-tyrosine (Sakamoto et al., 2002) and N(epsilon)-tert-butyloxycarbonyl-l-lysine (Boc-lysine) (Mukai et al., 2008), respectively, in Chinese hamster ovary cells.

The above data show unequivocally, within certain limits, that genetic code ambiguity is not lethal and that is possible to incorporate new amino acids into the code. Indeed, the full reassignment of the nonsense UAG codons was recently achieved in *E. coli*. Although, genetic modifications were needed to circumvent the lethal effect of this reassignment (Mukai et al., 2010), the engineered strain adapted to the new genetic code and remained viable. In this thesis, we have explored the possibilities of engineering Ser misincorporation at codons coding for amino acids with distinct chemical properties. Our data show that genetic code ambiguity is mainly disadvantageous, but it also generates morphological alterations and gene expression variation, in particular when Ser was misincorporated at codons coding for amino acids with distinct chemical properties. These data are in agreement with previous studies showing growth rate disadvantages in the phage Qβ (Bacher et al., 2003) and in *E. coli* (Bacher & Ellington, 2001) misincorporating the Trp analogues 6-fW and 4-fW, respectively, and also in *E. coli* expressing an editing defective IleRS that misincorporated norvaline at Ile codons (Bacher et al., 2005).

The toxicity observed in our mistranslating strains is related to the synthesis of mutant proteins whose structure and function may be disrupted, which may lead to their degradation or aggregation and accumulation in the cell. Indeed, mistranslation induced by an editing defective AlaRS leads to accumulation of misfolded proteins in mouse neurons and to cerebellar Purkinje cell loss and ataxia (Lee et al., 2006). Our data show that mistranslation generates aggregates that are recognized by Hsp26 and Hsp104 (Ser misincorporation at Gly codons) and other types of insoluble proteins which also trigger overexpression of the Hsps but do not form Hsp104-GFP or Hsp26-GFP foci (Ser misincorporation at Leu and Ile codons). In some cases, mistranslation did not lead to formation of aggregates that could be detected by the methods used here. These data suggest that different types of mistranslation can have distinct proteomic outcomes, which in turn may lead to phenotypic differences. These data are also in line with studies carried out by others which show that there are at least three different types of cytoplasmatic protein aggregates, namely aggregates that form juxtanuclear inclusions (JUNQs), insoluble protein deposits (IPODs) and “aggresomes”. The JUNQs appear after severe stress conditions and contain misfolded ubiquitylated proteins that cannot be refolded or degraded by the ubiquitin–proteasome system. These structures usually co-localize with proteasomes and with Hsp104 (Kaganovich et al., 2008). The IPODs are large perivacuolar inclusions located at the cell periphery and are formed by non-ubiquitylated proteins. These structures can be formed either in stress and non-stressed cells and usually co-localize with the autophagosome marker ATG8 and with Hsp104 (Kaganovich et al., 2008). The protein aggregates formed by Ser misincorporation at Gly codons may correspond to the the juxtanuclear inclusions (JUNQs) or to the insoluble protein deposits (IPODs) as both types of protein aggregates are recognized by Hsp104. The third type of protein aggregates correspond to the aggresomes, usually observed in mammalian cells in which the ubiquitin proteasome system is overloaded (Johnston et al., 1998). These structures have also been observed in yeast (Wang et al., 2009c) and correspond to insoluble perinuclear inclusions usually targeted for degradation via autophagy (Pankiv et al., 2007) that co-localize with the microtubule organizing centre, but not with Hsp104 (reviewed in Kopito, 2000). Yeast cells misincorporating Ser at Ile and Leu codons may produce insoluble protein aggregates that correspond to yeast aggresomes because the insoluble protein did not co-localize with Hsp104. It will be interesting to study the structure of these different types of protein aggregates generated in our mistranslating strains.

Interestingly, our results also show that Ser misincorporation at Ile and Leu codons increase ROS production. Previous studies demonstrated that high levels of Cu^{2+} and Fe^{3+}, in the brain of patients with Alzheimer's disease (Butterfield et al., 2001), can interact with Aβ (β-amyloid) aggregates and may induce the formation of hydrogen peroxide (H_2O_2) and hydroxyl radical (OH•) through electron transfer interactions in the presence of oxygen (reviewed in Valko et al., 2005). Both ROS are responsible for the early oxidative damage detected in this disease (Huang et al., 2004; Huang et al., 1999b; Huang et al., 1999a). Therefore, it would be interesting to determine the concentration of Cu^{2+} and Fe^{3+} in our mistranslating strains as our gene expression data shows deregulation of genes involved in ion homeostasis.

Misincorporation of Ser at Ile, Leu and Val codons generates aneuploidies. Interestingly, polyploidy increases plant diversification (Vamosi & Dickinson, 2006) and the ability of insects (Lokki & Saura, 1979) and plants (reviewed in Otto & Whitton, 2000) to occupy new ecological niches. However, yeast genome instability and consequent protein imbalance induced by aneuploidy cause cell cycle progression deffects, proliferative disadvantages and higher sensitivity to protein synthesis inhibitors (Torres et al., 2007). Aneuploidy also reduces proliferation and decreases cellular fitness in mouse (Williamns et al., 2008), *S. pombe* (Niwa et al., 2006) and human cells (Segal & McCoy, 1974). In other words, the genomic instability observed in cells that misincorporate Ser at Ile, Leu and Val codons may contribute to the observed gene expression variation, reduction of cell proliferation, viability and protein synthesis, cell cycle arrest, but, it may also generate advantageous phenotypes. Our data are in line with previous studies suggesting that in yeast (Pavelka et al., 2010; Rancati et al., 2008) and *Candida sp.* (Selmecki et al., 2008) the genomic instability induced by aneuploidy increases gene expression variation and proteome diversification, which despite its negative effect may confer growth advantages under adverse conditions. Moreover, a selective growth advantage is observed under Ile limiting conditions in *E. coli* (Pezo et al., 2004) and Acinetobacter baylyi (Bacher et al., 2007) expressing an editing defective IleRS that misincorporated Ile analogues, and bacterial resistance to a new generation of antibiotics (cephalosporin) is conferred by amino acid substitutions in the TEM1-β-lactamase enzyme (Wang et al., 2002). Furthermore, mistranslation induced by streptomycin causes genetic instability and promote the appearance of new phenotypes in *E. coli* (Nagel & Chan, 2006), while *S. cerevisiae* grown under stress conditions display significant increase in [PSI+] prion formation, which induces readthrough of stop codons (Tyedmers et al., 2008), promotting genetic variation and consequent phenotypic diversity (True et al., 2004; True

& Lindquist, 2000). Unfortunately, our gene expression data does not explain the selective advantages of mistranslating cells in presence of cadmium and copper. In yeast the CUP1 gene mediates cadmium and copper resistance (Jeyaprakash et al., 1991), but its expression was not altered in our mistranslating strains. These results are not unexpected because gene expression variation does not always correlate with a specific phenotype (Fay et al., 2004; Hillenmeyer et al., 2008).

5.3. The evolution of genetic code alterations

Two theories have been proposed to explain the evolution of the genetic code alterations that have been discovered during the last 30 years, namely the “codon capture” and the “ambiguous intermediate” theories. The “codon capture” also known as the codon disappearance theory postulates that G+C genome biases force certain codons to disappear from the genome. In other words, the translational machinery loses capacity to use the entire set of codons. Following codon loss the respective cognate tRNAs become functionless and their genes are also erased from the genome. At a later stage, changes in G+C biases and mutational drift may re-introduce the erased codons which can be decoded by mutant tRNAs or wild-type tRNAs belonging to non-cognate amino acid families. Codon misreading by new-cognate tRNAs assume here a critical role since they are needed to decode the re-introduced codons (Osawa et al., 1992). This theory is supported by the effect of G+C pressure on codon usage and by genetic code degeneracy which permits replacement of one codon by a synonymous one without disruption of protein structure (Osawa & Jukes, 1995; Seaborg, 2010). This theory is however unable to explain most of the sense codon reassignments (Swire et al., 2005). Conversely, the “ambiguous intermediate” theory postulates that a mutant tRNA can decode at least two codons, a cognate and a non-cognate codon, permitting amino acid misincorporation and synthesis of ambiguous proteins (Schultz & Yarus, 1994; Schultz & Yarus, 1996). This theory does not explain how such deleterious reassignments are driven (Moura et al., 2010), but is supported by the reassignment of the Leu CUG codon to Ser in the fungal CTG clade (Massey et al., 2003).

Our results demonstrate that codon ambiguity introduced by Ser misincorporation at various codons in yeast is not lethal supporting the “ambiguous intermediate” theory. Indeed, our data show that ambiguity induced by Ser misincorporation at codons codying

for chemically similar amino acids (Thr, Lys, Ala) reduce slightly growth rate and cause minor gene expression variations, while Ser misincorporation at codons codying for chemically different amino acids (Ile, Leu and Val) has strong negative effects on growth rate, induce major phenotypic variations and high gene expression alterations. Interestingly, our data demonstrates that despite its deleterious effects, mistranslation may confer growth advantages under specific stressful environments. In other words, the toxic effects of mistranslation can be overcome (at least in part) in ecological niches where mistranslation is advantageous, permitting the gradual evolution of codon reassignments (figure 5.3). These data are in line with recent studies which suggest that reassignment of the Ile AUA codon to Met, in the mitochondrial genome of various organisms, has been driven by the positive cytoprotective effect of Met under highly oxidative environments (oxidative inner mitochondrial membrane) as Met has antioxidant properties (Bender et al., 2008). Moreover, the ambiguous decoding of the Leu CUG codon as Ser increases tolerance to various environmental stressors, namely arsenite, cadmium and cyclohexamide, in yeast (Santos et al., 1999), while in *C. albicans* it is an important generator of phenotypic diversity (Miranda et al., 2007).

Our studies support the “ambiguous intermediate” theory and confirm previous theories suggesting that maintenance of ambiguous proteomes occur if amino acid misincorporation is neutral (similar amino acids) or if it provides a selective advantage that can overcome the instability associated to ambiguous proteomes (Bacher et al., 2004; Moura et al., 2009).

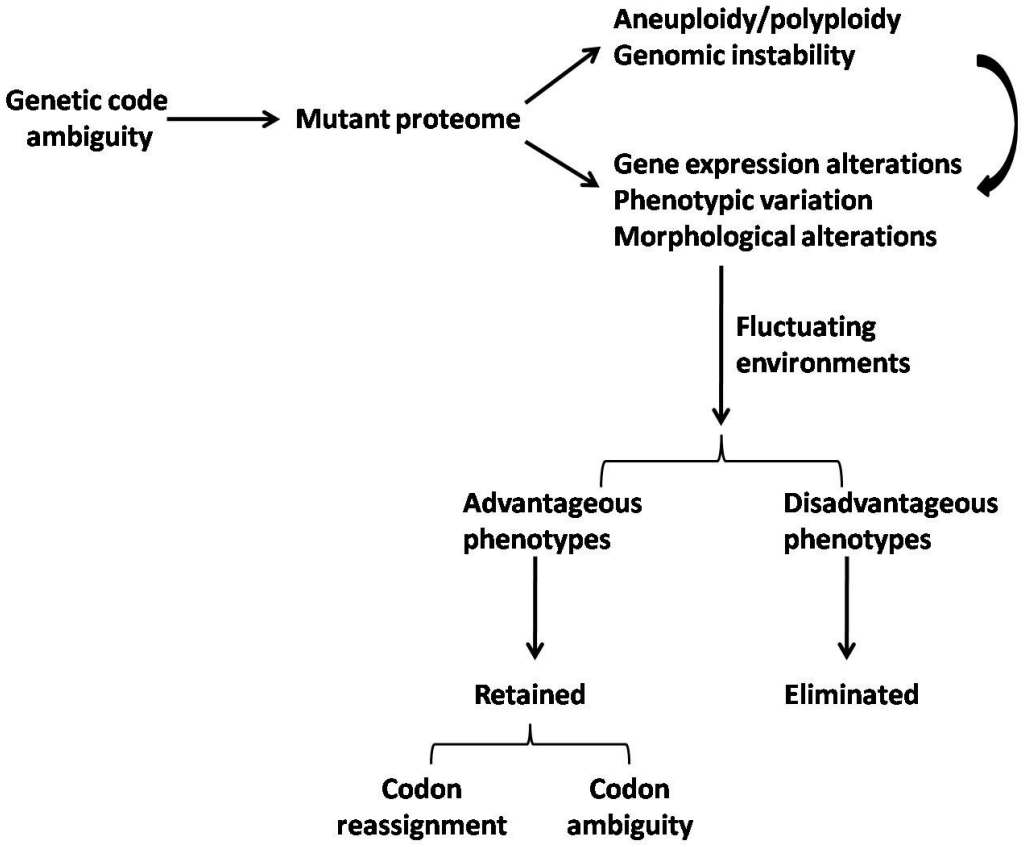

Figure 5.3: Evolutionary model of genetic code alterations. Genetic code ambiguity induces the synthesis of mistranslated proteins and generates a mutant proteome. This mutant proteome could induce genomic instability, polyploidy and aneuploidy which together with protein misfolding and aggregation (proteotoxic stress) induce gene expression alterations, phenotypic variation and morphological alterations. Under fluctuating environments organisms or cells with ambiguous genetic codes may be eliminated if fitness is negatively affected. Alternatively, they may be selected if the genomic and proteomic alterations produce advantageous phenotypes that allow for adaptation to new ecological conditions.

5.4. General conclusions and future studies

Previous molecular evolution studies suggested that the reassignment of the *C. albicans* Leu CUG codon to Ser was mediated by an ambiguous $tRNA_{CAG}^{Ser}$ derived from an ancestral $tRNA_{CGA}^{Ser}$ gene (Massey et al., 2003). In order to validate this hypothesis we have reconstructed *in vivo* the putative evolutionary pathway of the $tRNA_{CGA}^{Ser}$. Our data demonstrates that the various mutant $tRNA_{CAG}^{Ser}$ that represent the critical evolutionary steps of CUG reassignment are expressed, aminoacylated and misread the yeast CUG codon, indicating that a single mutation was sufficient to allow the ancestral $tRNA_{CAG}^{Ser}$ to decode Leu CUG codons. However, these mutant mistranslating $tRNA^{Ser}$ could only be expressed at low level, suggesting that tRNA down regulation, induced by an unknown pathway, played a critical role in the evolution of CUG reassignment, likely by minimizing the toxic effects of CUG misreading. Our data also suggest that the replacement of the conserved U_{33} in $tRNA_{CAG}^{Ser}$ by an atypical G_{33} stabilized and increased the cellular abundance of the $tRNA_{CAG}^{Ser}$, probably because the $tRNA_{CAG}^{Ser}$ G_{33} was less toxic than the $tRNA_{CGA}^{Ser}$ U_{33} and, for that reason, better tolerated. Our data also shows that the acceptor stem and extra-arm contain nucleotides that are important for $tRNA_{CAG}^{Ser}$ stability and/or function.

We have also demonstrated that the likelyhood of Ser beeing misincorporated and selected at Leu CUG codons was very low due to its high negative impact on fitness. Other types of mistranslation involving chemically similar amino acids were less toxic and could have been selected. However, mistranslation events involving chemically distinct amino acids produce the highest level of genomic instability, gene expression variation, morphological alterations and phenotypic diversity, which bring genomic and phenotypic plasticity to adaption under dynamic environments. In other words, the evolution of genetic code alterations can only be understood in ecologically favorable contexts.

The overall data clarifies the “ambiguous intermediate” theory by demonstrating that ambiguous codon can be selected due to its capacity to generate phenotypic variation of high adaptation potential. In other words, our data allows for reformulation of the “ambiguous intermediate” theory as follows: *genetic code alterations evolve through codon ambiguity in ecological contexts where phenotypic advantages, arising from statistical proteomes, are sufficiently robust to overcome the negative impact of genetic code ambiguity on fitness.*

Our data also raises new questions which need to be clarified in future studies, namely:

1. Which tRNA degradation pathway is activated by misreading tRNAs? This could be assessed by monitoring the expression of mistranslating tRNAs using the yeast gene knock-out strain collection.

2. Why do different types of missense translation generate different types of protein aggregates, namely aggregates that are recognized by Hsp104 and aggregates that are not recognized by this molecular chaperone. And, how are the protein aggregates that are not recognized by Hsp104, recovered or eliminated? Could autophagy play a role in the elimination of these aggregates, or do they accumulate and ultimately kill the cell? This could be studied by investigating the activation of autophagy and formation of amorphous protein aggregates by transmission electron microscopy.

3. Why does mistranslation generate aneuploidies and polyploidies? Are chromosome rearrangements common and similar in strains with different types of missense translation? This question could be addressed using comparative genomic hybridization on array (aCGH) and karyotype analysis.

4. Why is the PHO84 gene so sensitive to mistranslation, in particular to misincorporation of Ser at Leu CUG codons? Does up-regulation of PHO84 increase phosphate uptake and is it advantageous? Answering this question may provide new clues to understand the ecological context of the CUG reassignment in the fungal CTG clade.

References

Abelson, J., Trotta, C., & Li, H. (1998). tRNA splicing. The Journal of Biological Chemistry 273[21], 12685-12688.

Achsel, T. & Gross, H. J. (1993). Identity determinats of human $tRNA^{Ser}$: sequence elements necessary for serylation and maturation of a tRNA with a long extra arm. The EMBO Journal 12[8], 3333-3338.

Agris, P. F., Vendeix, F. A. P., & Graham, W. D. (2007). tRNA's Wobble Decoding of the Genome: 40 Years of Modification. *J.Cell Biol., 366,* 1-13.

Ahel, I., Korencic, D., Ibba, M., & Soll, D. (2003). Trans-editing of mischarged tRNAs. *Proc.Natl.Acad.Sci.USA, 100,* 15422-15427.

Ahsen, U. V., Green, R., Schroeder, R., & Noller, H. F. (1997). Identification of 2-hydroxyl groups required for interaction of a tRNA anticodon stem-loop region with the ribosome. *RNA, 3,* 49-56.

Alamgir, MD., Eroukova, V., Jessulat, M., Xu, J., & Golshani, A. (2008). Chemical-genetic profile analysis in yeast suggests that a previously uncharacterized open reading frame, YBR261C, affects protein synthesis. BMC Genomics 9:583.

Alexandrov, A., Chernyakov, I., Gu, W., Hiley, S. L., Hughes, T. R., Grayhack, E. J. et al. (2006). Rapid tRNA decay can esult from lack of nonessential modifications. *Molecular Cell, 21,* 87-96.

Allen, E. H., Glassman, E., Cordes, E., & Schweet, R. S. (1959). Incorporation of amino acids into ribonucleic acid. II. Amino acid transfer ribonucleic acid. *J.Biol.Chem., 235,* 1074.

Allen, S., Clark, W., McCaffery, J., Cai, Z., Lanctot, A., Slininger, P. et al. (2010). Furfural induces reactive oxygen species accumulation and cellular damage in S. cerevisiae. Biotechnology for Biofuels 3[2].

Almeida, B., Buttner, S., Ohlmeier, S., Silva, A., Mesquita, A., Sampaio-Marques, B. et al. (2007a). NO-mediated apoptosis in yeast. *Journal of Cell Science, 120,* 3279-3288.

Almeida, B., Sampaio-Marques, B., Carvalho, J., Silva, M. T., Leão, C., Rodrigues, F. et al. (2007b). Anatypical active cell death process underlies the fungicidal activity of ciclopiroxolamine against the yeast Saccharomyces cerevisiae. *FEMS Yeast Research, 7,* 404-412.

Anderson, J., Wu, N., Santoro, S., Lakshman, V., Kind, D., & Schultz, P. G. (2004). An expanded genetic code with a functional quadruplet codon. *Proc.Natl.Acad.Sci.USA, 101,* 7566-7571.

Anderson, J. C. & Shcultz, P. G. (2003). Adaptation of an orthogonal archaeal leucyl-tRNA and synthetase pair for four-base, amber, and opal suppression. *Biochemistry, 42,* 9598-9608.

Araiso, Y., Palioura, S., Ishitani, R., Sherrer, R. L., O'Donoghue, P., Yuan, J. et al. (2008). Structural insights into RNA-dependent eukaryal and archaeal selenocysteine formation. *Nucleic Acids Research, 36,* 1187-1199.

Ardell, D. H. (2010). Computational analysis of tRNA identity. *FEBS Letters, 584,* 325-333.

Asahara, H., Himeno, H., Tamura, K., Nameki, N., Hasegawa, T., & Shimizu, M. (1994). Escherichia coli seryl-tRNA synthetase recognizes $tRNA^{Ser}$ by its characteristics tertiary structure. Journal of Molecular Biology 236[3], 738-748.

Aschel, T. & Gross, H. J. (1993). Identity determinates of human tRNASer: sequence elements necessary for serylation and maturation of a tRNA with a long extra-arm. *The EMBO Journal, 12,* 3333-3338.

Ashraf, S. S., Ansari, G., Guenther, R., Sochacka, E., Malkiewicz, A., & Agris, P. F. (1999). The uridine in "U-turn": Contributions to tRNA ribosomal binding. RNA 5, 503-511.

Assemat, K., Alzari, P. M., & Clement-Metral, J. (1995). Conservative substitutions in the hydrophobic core of Rhodobacter sphaeroides thioredoxin produce distinct functional effects. *Protein Science, 4,* 2510-2516.

Auesukaree, C., Damnernsawad, A., Kruatrachue, M., Pokethitiyook, P., Boonchird, C., Kaneko, Y. et al. (2009). Genome-wide identification of genes involved in tolerance to various environmental stresses in Saccharomyces cerevisiae. J Appl Genet 50[3], 301-310.

Bacher, J., Bull, J., & Ellington, A. D. (2003). Evolution of phage with chemically ambiguous proteomes. *BMC Evolutionary Biology, 3:24*.

Bacher, J., Crecy-Lagard, V., & Schimmel, P. (2005). Inhibited cell growth and protein functional changes from an editing-defective tRNA synthetase. Proc.Natl.Acad.Sci.USA 102[5], 1697-1701.

Bacher, J. & Ellington, A. D. (2001). Selection and Characterization of Escherichia coli Variants Capable of Growth on an Otherwise Toxic Tryptophan Analogue. *Journal of Bacteriology, 183,* 5414-5425.

Bacher, J., Hughes, R. A., Wong, J., & Ellington, A. D. (2004). Evolving new genetic codes. *TRENDS in Ecology and Evolution, 19,* 69-75.

Bacher, J., Waas, W. F., Metzgar, D., Crecy-Lagard, V., & Schimmel, P. (2007). Genetic Code Ambiguity Confers a Selective Advantage on Acinetobacter baylyi. *Journal of Bacteriology, 189,* 6494-6496.

Bahar, I., Kaplan, M., & Jernigan, R. L. (1997). Short-range conformational energies, secondary structure propensities, and recognition of correct sequence-structure matches. Proteins 29, 292-308.

Barrell, B. G., Bankier, A. T., & Drouin, J. (1979). A different genetic code in human mitochondria. *Nature, 282,* 189-194.

Beau, I., Esclatine, A., & Codogno, P. (2008). Lost to translation: when autophagy targets mature ribosomes. Trends in Cell Biology 18[7], 311-314.

Beebe, K., Ribas de Pouplana, L., & Schimmel, P. (2003). Elucidation of tRNA-dependent editing by a class II tRNA synthetase and significance for cell viability. *EMBO Journal, 22,* 668-675.

Bellinger, F. P., Raman, A. V., Reeves, M. A., & Berry, M. J. (2009). Regulation and function of selenoproteins in human disease. *Biochem.J., 422,* 11-22.

Bence, N., Sampat, R., & Kopito, R. (2001). Impairment of the ubiquitin-proteasome system by protein aggregation. Science 292, 1552-1555.

Bender, A., Hajieva, P., & Moosmann, B. (2008). Adaptive antioxidant methionine accumulation in respiratory chain complexes explains the use of a deviant genetic code in mitochondria. *Proc.Natl.Acad.Sci.USA, 105,* 16496-16501.

Bennetzen, J. L. & Hall, B. D. (1982). Codon selection in yeast. *J.Biol.Chem., 257,* 3026-3031.

Bernstein, K., Bleichert, F., Bean, J., Cross, F., & Baserga, S. (2007). Ribosome biogenesis is sensed at the start cell cycle checkpoint. Molecular Biology of the Cell 18, 953-964.

Berry, D. & Gasch, A. P. (2008). Stress-activated Genomic Expression Changes Serve a Preparative Role for Impending Stress in Yeast. Mol Cell Biol 19, 4580-4587.

Betts, M. J. & Russell, R. B. (2003). Amino Acid Properties and Consequences of Substitutions. In Michael R.Barnes and Ian C.Gray (Ed.), *Bioinformatics for Geneticists.* (pp. 289-316). John Wiley & Sons, Ltd.

Bjork, G. (1995). Byosinthesis and function of modified nucleosides. In D.Soll & U. RajBhandary (Eds.), *tRNA: structure, biosynthesis and function* (pp. 165-205). Washington D.C.: American Society for Microbiology.

Blaiseau, P., Lesuisse, E., & Camadro, J. (2001). Aft2p, a Novel Iron-regulated Transcription Activator That Modulates, with Aft1p, Intracellular Iron Use and Resistance to Oxidative Stress in Yeast. The Journal of Biological Chemistry 276[36], 34221-34226.

Blanchard, J. S. & Cleland, W. W. (1980). Kinetic and Chemical Mechanisms of Yeast Formate Dehydrogenase. *Biochemistry, 19,* 3543-3550.

Blank, A., Gallant, J. A., Burgess, R. R., & Loeb, L. A. (1986). An RNA polymerase mutant with reduced accuracy of chain elongation. *Biochemistry, 25,* 5920-5928.

Blight, S. K., Larue, R. C., Mahapatra, A., Longstaff, D. G., Chang, E., Zhao, G. et al. (2004). Direct charging of tRNA(CUA) with pyrrolysine in vitro and in vivo. *Nature, 431,* 333-335.

Bock, A., Forchhammer, K., Heider, J., Leinfelder, W., Sawers, G., Veprek, B. et al. (1991). Selenocysteine: the 21st amino acid. *Molecular Microbiology, 5,* 515-520.

Bolat, I. (2008). THE IMPORTANCE OF TREHALOSE IN BREWING YEAST SURVIVAL. Innovative Romanian Food Biotechnology 2.

Boyce, K., Kretshcmer, M., & Kronstad, W. (2006). The vtc4 Gene Infuences Polyphosphate Storage, Morphogenesis,and Virulence in the Maize Pathogen Ustilago maydis. Eukaryotic Cell 5[8], 1399-1409.

Brauer, M., Huttenhower, C., Airoldi, E., Rosenstein, R., Matese, J., Gresham, D. et al. (2008). Coordination of Growth Rate, Cell Cycle, Stress Response, and Metabolic Activity in Yeast. *Molecular Biology of the Cell, 19,* 352-367.

Breitchopf, K., Achsel, T., Busch, K., & Gross, H. J. (1995). Identity elements of human $tRNA^{Leu}$: structural requirements for converting human $tRNA^{Ser}$ into a leucine acceptor in vitro. *Nucleic Acids Research, 23,* 3633-3637.

Breitchopf, K. & Gross, H. J. (1994). The exchange of the discriminator base A73 for G is alone sufficient to convert human $tRNA^{Leu}$ into a serine-acceptor in vitro. *The EMBO Journal, 13,* 3166-3169.

Breitchopf, K. & Gross, H. J. (1996). The discriminator bases G73 in human $tRNA^{Ser}$ and A73 in $tRNA^{Leu}$ have significantly different roles in the recognition of aminoacyl-tRNA synthetases. *Nucleic Acids Research, 24,* 405-410.

Brown, M. R. W. & Kornberg, A. (2004). Inorganic polyphosphate in the origin and survival of species. *Proc.Natl.Acad.Sci.USA, 101,* 16085-16087.

Bruinenberg, P. J. R., van Dijken, P., & Sheffers, W. A. (1985). Utilization of formate as an additional energy source by glucose limited chemostat cultures of Candida utilis CBS621and Saccharomyces cerevisiae CBS8066. *Arch Microbiol, 142,* 302-306.

Budisa, N. (2006). *Engineering the genetic code : Expanding the amino acid reportoire for the desigh of novel proteins*. Wiley, VCH, Verlag GmbH & Co.

Burke, D., Dawson, D., & Stearns, T. (2000). *Methods in yeast genetics, a cold spring harbor laboratory course manual*.

Butler, G. & et al (2009). Evolution of pathogenicity and sexual reproduction in eight Candida genomes. *Nature, 459,* 657-662.

Butterfield, D., Drake, J., Pocernich, C., & Castegna, A. (2001). Evidence of oxidative damage in Alzheimer's disease brain: central role for amyloid beta-peptide. Trends Mol.Med. 7[12], 548-554.

Çakar, Z. P., Alkim, C., Turanli, B., Tokman, N., Akman, S., Sarikaya, M. et al. (2009). Isolation of cobalt hyper-resistant mutants of Saccharomyces cerevisiae by in vivo evolutionary engineering approach. *Journal of Biotechnology, 143,* 130-138.

Calderone, T. L., Stevens, R. D., & Oas, T. G. (1996). High-level Misincorporation of Lysine for Arginine at AGA Codons in a Fusion Protein Expressed in Escherichia coli. *J.Mol.Biol., 262,* 407-412.

Cashikar, A., Duennwald, M., & Lindquist, S. (2005). A Chaperone Pathway in Protein Disaggregation: HSP26 ALTERS THE NATURE OF PROTEIN AGGREGATES TO FACILITATE REACTIVATION BY HSP104S. J.Biol.Chem. 280[25], 23869-23875

Castresana, J., Fuchs, G., & Paabo, S. (1998). Codon reassignment and amino acid composition in hemichordate mitochondria. *Proc.Natl.Acad.Sci.USA, 95,* 3703-3707.

Castrillo, J., Zeef, L., Hoyle, D., Zhang, N., Hayes, A., Gradner, D. et al. (2007). Growth control of the eukaryote cell: a systems biology study in yeast. *J.Biol., 6:4*.

Causton, H., Ren, B., Koh, S., Harbison, C., Kanin, E., Jennings, E. et al. (2001). Remodeling of Yeast Genome Expression in Response to Environmental Changes. Molecular Biology of the Cell 12, 323-337.

Cerini, C., Kerjan, P., Astier, M., Gratecos, D., Mirande, M., & Semeriva, M. (1991). A component of the multisynthetase complex is a multifunctional aminoacyl-tRNA synthetase. *EMBO Journal, 10,* 4267-4277.

Chan, C., Dyavaiah, M., DeMott, M., Taghizadeh, K., Dedon, P., & Begley, T. (2010). A Quantitative Systems Approach Reveals Dynamic Control of tRNA Modifications during Cellular Stress. *PLoS Genetics, 6,* e1001247.

Chen, H., Detmer, S., Ewald, A., Griffin, E., Fraser, S., & Chan, D. (2003). Mitofusins Mfn1 and Mfn2 coordinately regulate mitochondrial fusion and are essential for embryonic development. J.Cell Biol. 160[2], 189-200.

Chen, P., Groff, D., Guo, J., Ou, W., Cellitti, S., Geierstanger, B. et al. (2009). A Facile System for Encoding Unnatural Amino Acids in Mammalian Cells. *Angew.Chem., 48,* 4052-4055.

Cheng, W., Leach, K., & Hardwick, J. (2008). Mitochondrial death pathways in yeast and mammalian cells. Biochim Biophys Acta 1783[3], 1272-1279.

Chernyakov, I., Whipple, J. M., Kotelawala, L., Grayhack, E. J., & Phizicky, E. M. (2008). Degradation of several hipomodified mature tRNA species in Saccharomyces cerevisiae is mediated by Met22 abd the 5' 3' exonuleases Rat1 and Xrn1. *Genes & Development, 22,* 1369-1380.

Chimnaronk, S., Jappesen, M. G., Suzuki, T., Nyborg, J., & Watanabe, K. (2005). Dual-mode recognition of noncanonical tRNAs^{Ser} by seryl-tRNA synthetase in mammalian mitochondria. The EMBO Journal 24[19], 3369-3379.

Chin, J., Cropp, T. A., Anderson, J. C., Mukherji, M., Zhang, Z., & Schultz, P. G. (2003). An expanded eukaryotic genetic code. *Science, 301,* 964-967.

Chin, J. W., Martin, A. B., King, D. S., Wang, L., & Schultz, P. G. (2002). Addition of a photocrosslinking amino acid to the genetic code of Escherichia coli. *Proc.Natl.Acad.Sci.USA, 99,* 11020-11024.

Chiusano, M., Alvarez-Valin, F., Giulio, M., D'Onofrio, G., Ammirato, G., Colonna, G. et al. (2000). Second codon positions of genes and the secondary structures of proteins.Relationships and implications for the origin of the genetic code. Gene 261, 63-69.

Chumnantana, R., Yokochi, N., & Yagi, T. (2005). Vitamin B6 compounds prevent the death of yeast cells due to menadione, a reactive oxygen generator. Biochimica et Biophysica Acta (BBA) 1722[1], 84-91.

Cohen, A., Perzov, N., Nelson, H., & Nelson, N. (1999). A novel family of yeast chaperons involved in the distribution of V-ATPase and other membrane proteins. J.Biol.Chem. 274[38], 26885-26893.

Cohen, B., Pilpel, Y., Mitra, R., & Church, G. (2002). Discrimination between Paralogs using Microarray Analysis: Application to the Yap1p and Yap2p Transcriptional Networks. Molecular Biology of the Cell 13, 1608-1614.

Craighton, T. E. (1993). *Proteins: Structures and Molecular Properties*. (2nd ed.).

Crick, F. H. (1966a). Codon-anticodon pairing: The wobble hypothesis. *J.Cell Biol., 19,* 548-555.

Crick, F. H. (1966b). The genetic code--yesterday, today, and tomorrow. *Cold Spring Harb Symp Quant Biol., 31,* 1-9.

Czerwoniec, A., Dunin-Horkawicz, S., Purta, E., Kaminska, K., Kasprzak, J., Bujnicki, J. et al. (2009). MODOMICS: a database of RNA modification pathways. *Nucleic Acids Research, 37,* D118-D121.

Dalley, J., Selkirk, A., & Pool, M. (2008). Access to Ribosomal Protein Rpl25p by the Signa Recognition Particle Is Required for Efficient Cotranslational Translocation. Molecular Biology of the Cell 19, 2876-2884.

Dancis, A., Haile, D., Yuan, D., & Klausner, R. (1994). The Saccharomyces cereuisiae Copper Transport Protein (Ctrlp). The Journal of Biological Chemistry 269[41], 25660-25667.

Davey, H. & Haxley, P. (2010). Red but not dead? Membranes of stressed Saccharomyces cerevisiae are permeable to propidium iodide. Environmental Microbiology .

Davies, J., Gilbert, W., & Gorini, L. (1964). Streptomycin, supression and the code. *Biochemistry, 51,* 883-890.

Davis, B. (2004). Expansion of the genetic code in yeast: making life more complex. *Bioessays, 26,* 111-115.

Daviter, T., Gromadski, K., & Rodnina, M. (2006). The ribosome's response to codon–anticodon mismatches. Biochimie 88, 1001-1011.

Del Carratore, R., Della Croce, C., Simili, M., Taccini, E., Scavuzzo, M., & Sbrana, S. (2002). Cell cycle and morphological alterations as indicative of apoptosis promoted by UV irradiation in S. cerevisiae. Mutat.Res. 15[513], 183-191.

Denis, C. L., Ciriacy, M., & Young, E. T. (1981). A positive regulatory gene is required for accumulation of the functional messenger RNA for the glucose-repressible alcohol dehydrogenase from Saccharomyces cerevisiae. *Journal of Molecular Biology, 148,* 355-368.

Denis, V., Boucherie, H., Monribot, C., & Fornier, B. (1998). Role of the Myb-like protein Bas1p in Saccharomyces cerevisiae: a proteome analysis. Molecular Microbiology 30[3], 557-566.

Deutscher, P. (1995). tRNA processing nucleases. In D.Soll & U. RajBhandary (Eds.), *tRNA: structure, biosynthesis and function* (pp. 51-65). Washington D.C.: American Society for microbiology.

Di Giulio, M. (2000). The late stage of genetic code structuring took place at a high temperature. *Gene, 261,* 189-195.

Di Giulio, M. (2005a). A comparison of proteins from Pyrococcus furiosus and Pyrococcus abyssi: barophily in the physicochemical properties of amino acids and in the genetic code. *Gene, 346,* 1-6.

Di Giulio, M. (2005b). Structuring of the genetic code took place at acidic pH. *Journal of Theoretical Biology, 237,* 219-226.

Di Giulio, M. (2005c). The origin of the genetic code: theories and their relationships, a review. *Biosystems, 80,* 175-184.

Dickinson, J. (1994). Irreversibel formation of pseudohyphae by haploid S. cerevisiae. FEMS Microbiol Letters 119, 99-104.

Dickinson, J. (1996). Fusel alcohols induce hyphael-like extensions and pseudohyphael formation in yeasts. Microbiology 142, 1391-1397.

Dickinson, J. (2008). Filament formation in S. cerevisiae - a review. Folia Microbiol. 53[1], 3-14.

DiPaola, R. (2002). To Arrest or Not To G2-M Cell-Cycle Arrest. Clinical Cancer Research 8, 3311-3314.

Dirheimer, G., Keith, G., Dumas, P., & Westhof, E. (1995). Primary, secondary and tertiary structures of tRNA's. In D.Soll & U. RajBhandary (Eds.), *tRNA structure, biosynthesis and function* (pp. 93-126). Washington D.C.: American Society for Microbiology.

Dittmar, K., Goodenbour, J. M., & Pan, T. (2006). Tissue-Specific Differences in Human Transfer RNA Expression. *PLoS Genetics, 2,* e221.

Dobson, C. (2003). Protein folding and misfolding. Nature 426, 884-890.

Doma, M. K. & Parker, R. (2007). RNA Quality Control in Eukaryotes. *Cell, 131,* 660-668.

Dombeck, K., Camier, S., & Young, E. (1993). ADH2 Expression Is Repressed by REG1 Independently of Mutations That Alter the Phosphorylation of the Yeast Transcription Factor ADR1. Molecular and Cellular Biology 13[7], 4391-4399.

Ehrenreich, A., Forchhammer, K., Tormay, P., Veprek, B., & Bock, A. (1992). Selenoprotein synthesis in E. coli. Purification and characterisation of the enzyme catalysing selenium activation. ***Eur.J.Biochemistry, 206,*** **767-773.**

Eide, D. (2009). Homeostatic and Adaptive Responses to Zinc Deficiency in Saccharomyces cerevisiae. The Journal of Biological Chemistry 284[28], 18565-18569.

Eisenberg, T., Buttner, S., Kroemer, G., & Madeo, F. (2007). The mitochondrial pathway in yeast apoptosis. Apoptosis 12, 1011-1023.

Ellman, J., Mendel, D., Anthony-Cahill, S. J., Noren, C. J., & Schultz, P. G. (1991). Biosynthetic method for introducing unnatural amino acids site-specifically into proteins. ***Methods in Enzymology, 202,*** **301-336.**

Engelke, D. R. & Hopper, A. K. (2006). Modift view of tRNA: stability amid sequence diversity. Molecular Cell 21, 144-145.

Erjavec, N., Larsson, L., Grantham, J., & Nystrom, T. (2007). Accelerated aging and failure to segregate damaged proteins in Sir2 mutants can be suppressed by overproducing the protein aggregation-remodeling factor Hsp104p. Genes and Development 21, 2410-2421.

Fannjiang, Y., Cheng, W., Lee, S., Qi, B., Pevsner, J., McCaffery, J. et al. (2004). Mitochondrial fission proteins regulate programmed cell death in yeast. Genes and Development 18, 2785-2797

Fay, J. C., McCullough, H. L., Sniegowski, P. D., & Eisen, M. B. (2004). Population genetic variation in gene expression is associated with phenotypic variation in Saccharomyces cerevisiae. ***Genome Biology, 5:R26*****.**

Fernandes, L., Rodrigues-Pousada, C., & Struhl, K. (1997). Yap, a Novel Family of Eight bZIP Proteins in Saccharomyces cerevisiae with Distinct Biological Functions. Mol Cell Biol 17[12], 6982-6993.

Filippi, L., Founier, M., Cameroni, E., Linder, P., De Virgilio, C., Foti, M. et al. (2007). Membrane stress is coupled to a rapid translational control of gene expression in chlorpromazine-treated cells. Curr.Genet. 52, 171-185.

Fiser, A., Simon, I., & Barton, G. (1996). Conservation of amino acids in multiple alignments: aspartic acid as unexpected conservation. FEBS Letters 397, 225-229.

Fleury, C., Mignotte, B., & Vayssiere, J. L. (2002). Mitochondrial reactive oxygen species in cell death signaling. Biochimie 84[2], 131-141.

Francklyn, C. (2008). DNA Polymerases and Aminoacyl-tRNA Synthetases: Shared Mechanisms for Ensuring the Fidelity of Gene Expression. Biochemistry 47[45], 11695-11703.

Frechin, M., Senger, B., Brayé, M., Kern, D., Martin, R. P., & Becker, H. D. (2009). Yeast mitochondrial Gln-tRNAGln is generated by a GatFAB-mediated transamidation pathway involving Arc1p-controlled subcellular sorting of cytosolic GluRS. ***Genes and Development, 23,*** **1119-1130.**

Fredriksson, A., Ballesteros, M., Peterson, C., Persson, O., Silhavi, T., & Nystrom, T. (2007). Decline in ribosomal fidelity contributes to the accumulation and stabilization of the master stress response regulator σ upon carbon starvation. Genes and Development 21, 862-874.

Freeland, S., Wu, T., & Keulmann, N. (2002). THE CASE FOR AN ERROR MINIMIZING STANDARD GENETIC CODE. ***Origins of Life and Evolution of the Biosphere, 33,*** **457-477.**

Fu, H., Feng, J., Liu, K., Sun, F., Tie, Y., Zhu, J. et al. (2009). Stress induces tRNA cleavage by angiogenin in mammalian cells. *FEBS Letters, 583,* 437-442.

Fujita, K., Kawai, R., Iwahashi, H., & Komatsu, Y. (1998). Hsp104 Responds to Heat and Oxidative Stress with Different Intracellular Localization in Saccharomyces cerevisiae. Biochemical and Biophysical Research Communications 248, 542-547.

Further, R. (1998). Expansion of the genetic code: Site-directed p-fluoro-phenylalanine incorporation in Escherichia coli. *Protein Science, 7,* 419-426.

Galoubinoff, P., Mogk, A., Zvi, A., Tomoyasu, T., & Bukau, B. (1999). Sequential mechanism of solubilization and refolding of stable protein aggregates by a bichaperone network. Proc.Natl.Acad.Sci.USA 96[24], 13732-13737.

Gasch, A. P. (2002). The environmental stress response: a common yeast response to diverse environmental stresses. In S.Hohmann and P.Mager (ed) (Ed.), *Yeast Stress Responses.* (pp. 11-70). Springer-Verlag Heidelberg.

Gasch, A. P., Spellman, P., Kao, C., Carmel-Harel, O., Eisen, M., Storz, G. et al. (2000). Genomic Expression Programs in the Response of Yeast Cells to Environmental Changes. Molecular Biology of the Cell 11, 4241-4257.

Geslain, R., Cubells, L., Bori-Sanz, T., Alvarez-Medina, R., Rosell, D., Marti, E. et al. (2009). Chimeric tRNAs as tools to induce proteome demage and identify components of stress response. Nucleic Acids Research , 1-11.

Gessler, N., Aver'Yanov, A., & Belozerskaya, T. (2007). Reactive Oxygen Species in Regulation of Fungal Development. Biochemistry (Moscow) 72[10], 1091-1109.

Giannouli, S., Kyritsis, A., Malissovas, N., Becker, H. D., & Stathopoulos, C. (2009). On the role of an unusual tRNAGly isoacceptor in Staphylococcus aureus. *Biochemie, 91,* 344-351.

Giege, R. & Eriani, G. (2002). Transfer RNA recognition by synthetases. In *Encyclopedia of Life Sciences* (Nature Publishing Group.

Giege, R., Sissler, M., & Florentz, C. (1998). Universal rules and idiosyncratic features in tRNA identity. *Nucleic Acids Research, 26,* 5017-5035.

Gietz, R. D. & Woods, R. A. (1994). High efficiency transformation with lithium acetate. In *Molecular genetics of yeast: a pratical approach* (Johnston JR (ed) ed., pp. 121-134).

Gilis, D., Massar, S., Cerf, N., & Rooman, M. (2001). Optimality of the genetic code with respect to protein stability and amino-acid frequencies. *Genome Biology, 2*.

Giots, F., Donaton, M., & Thevelein, J. (2003). Inorganic phosphate is sensed by specific phosphate carriers and acts in concert with glucose as a nutrient signal for activation of the protein kinase A pathway in the yeast Saccharomyces cerevisiae. Molecular Microbiology 47[4], 1163-1181.

Glover, J. & Lindquist, S. (1998). Hsp104, Hsp70, and Hsp40: A Novel Chaperone System that Rescues Previously Aggregated Proteins. Cell 94, 73-82.

Goldman, E. (2002). Transfer RNA. In *Encyclopedia of Life Science* (Macmillan Publishers Ltd, Nature Publishing Group.

Gomes, A. C., Miranda, I., Silva, R. M., Moura, G., Thomas, B., Akoulitchev, A. et al. (2007). A genetic code alteration generates a proteome of high diversity in the human pathogen *Candida albicans*. *Genome Biology, 8,* R206.

Gouy, M. & Gautier, c. (1982). Codon usage in bacteria: correlation with gene expressivity. *Nucleic Acids Research, 10,* 7055-7074.

Grant, C. M., Firoozan, M., & Tuite, M. F. (1989). Mistranslation induces the heat-shock response in the yeast Saccharomyces cerevisiae. *Molecular Microbiology, 3,* 215-220.

Grantham, R., Gautier, c., Gouy, M., Mercier, R., & Pavé, A. (1980). Codon catalog usage and the genome hypothesis. *Nucleic Acids Research, 8,* 49-62.

Griffin, T. J., Gygi, S., Ideker, T., Rist, B., Eng, J., Hood, L. et al. (2002). Complementary Profiling of Gene Expression at the Transcriptome and Proteome Levels in Saccharomyces cerevisiae. *Molecular and Cellular Proteomics, 1.4,* 323-333.

Grimminger-Marquardt, V. & Lashuel, H. (2009). Structure and function of the molecular chaperon Hsp104 from Yeast. Biopolymers 93[3], 252-276.

Grosjean, H., Droogmans, L., Roovers, M., & Keith, G. (2007). Detection of Enzymatic Activity of Transfer RNA Modification Enzymes Using Radiolabeled tRNA Substrates. In *Methods in Enzymology* (425 ed., pp. 57-101).

Gross, C., Kelleher, M., Iyer, V., O.Brown, P., & Winge, D. (2000). Identification of the Copper Regulon in Saccharomyces cerevisiae by DNA Microarrays. The Journal of Biological Chemistry 275[41], 32310-32316

Gruic-sovulj, I., Landeka, I., Soll, D., & Weygand-Durasevic, I. (2002). tRNA dependet amino acid discrimination by yeast seryl-tRNA synthetase. Eur.J.Biochemistry 269, 5271-5279.

Gustilo, E. M., Vendeix, F., & Agris, P. F. (2008). tRNAs modification bring order to gene expression. Current opinion in Microbiology 11, 134-140.

Gygi, S., Rochon, Y., Franza, B., & Aebersold, R. (1999). Correlation between Protein and mRNA Abundance in Yeast. Mol Cell Biol 19[3], 1720-1730.

Haig, D. & Hurst, L. D. (1991). A quantitative measure of error minimization in the genetic code. *J.Mol.Evol., 33,* 412-417.

Halbeisen, R., Galgano, A., Scherrer, T., & Gerber, A. P. (2007). Post-transcriptional gene regulation: From genome-wide studies to principles. Cell.Mol.Life Sci.

Halbeisen, R. & Gerber, A. P. (2009). Stress-Dependent Coordination of Transcriptome and Translatome in Yeast. PLoS Biol 7[5], e1000105.

Hales, K. & Fuller, M. (1997). Developmentally regulated mitochondrial fusion mediated by a conserved, novel, predicted GTPase. Cell 90[1], 121-129.

Halsbeck, M., Braun, N., Stromer, T., Richter, B., Model, N., Weinkauf, S. et al. (2004). Hsp42 is the general small heat shock protein in the cytosol of Saccharomyces cerevisiae. The EMBO Journal 23, 638-649.

Halsbeck, M., Miess, A., Stromer, T., Walter, S., & Buchner, J. (2005). Disassembling Protein Aggregates in the Yeast Cytosol. The Journal of Biological Chemistry 280[25], 23861-23868.

Halsbeck, M., Wlake, S., Stromer, T., Ehrnsperger, M., White, H., Chen, S. et al. (1999). Hsp26: a temperature-regulated chaperone. The EMBO Journal 18[23], 6744-6751.

Hamano-Takaku F, I. T. S.-Y. S. T. K. M. Y. K. M. S. D. N. S. (2000). A mutant Escherichia coli tyrosyl-tRNA synthetase utilizes the unnatural amino acid azatyrosine more efficiently than tyrosine. *J.Biol.Chem., 275,* 40324-40328.

Hammermeister, M., Schodel, K., & Westermann, B. (2010). Mdm36 Is a Mitochondrial Fission-promoting Protein in Saccharomyces cerevisiae. Molecular Biology of the Cell 21, 2443-2452.

Hampton, R. (2002). ER-associated degradation in protein quality control and cellular regulation. Current Opinion in Cell Biology 14, 476-482.

Hao, B., Gong, W., Fergunson, T. K., James, C. M., Krzycki, J. A., & Chan, M. K. (2002). A new UAG-encoded residue in the structure of a methanogen methyltransferase. *Science, 296,* 1462-1466.

Hao, R., Yao, Y. N., Zheng, Y. G., Xu, M. G., & Wand, E. D. (2004). Reduction of $tRNA^{Leu}$ (UUR) aminoacylation by some MELAS-associated mutations. FEBS Letters 578, 135-139. Ref Type: Journal (Full)

Harpaz, Y., Gerstein, M., & Chothia, C. (1994). Volume changes on protein folding. *Structure, 2,* 641-649.

Hasegawa, M. & Miyata, T. (1980). On the antisymmetry of the amino acid code table. *Orig.Life, 10,* 265-270.

Hassett, R. & Kosman, D. J. (1995). Evidence for Cu(II) reduction as a component of copper uptake by Saccharomyces cerevisiae. *J.Biol.Chem., 270,* 128-134.

Helm, M. (2006). Post-transcriptional nulceotide and modification and alternative folding of RNA. Nucleic Acids Research 34[2], 721-733.

Henikoff, S. & Henikoff, J. G. (1992). Amino acid substitution matrices from protein blocks. *Proc.Natl.Acad.Sci.USA, 89,* 10915-10919.

Herrera, B., Alvarez, A., Sanchez, A., Fernandez, M., Roncero, C., Benito, M. et al. (2001). Reactive oxygen species (ROS) mediates the mitochondrial-dependent apoptosis induced by transforming growth factor b in fetal hepatocytes. The FASEB Journal 15, 741-751.

Hillenmeyer, M. E., Fung, E., Wildenhain, J., Pierce, S. E., Hoon, S., Lee, W. et al. (2008). The Chemical Genomic Portrait of Yeast: Uncovering a Phenotype for All Genes. *Science, 320,* 362-365.

Himeno, H., Hasegawa, T., Ueda, T., Watanabe, K., Miura, K., & Shimizu, M. (1989). Role of the extra G-C pair at the end of the acceptor stem of tRNA(His) in aminoacylation. *Nucleic Acids Research, 17,* 7855-7863.

Himeno, H., Hasegawa, T., Ueda, T., Watanabe, K., & Shimizu, M. (1990). Conversion of aminoacylation specificity from tRNA(Tyr) to tRNA(Ser) in vitro. Nucleic Acids Research 18[23], 6815-6819.

Himeno, H., Yoshida, S., Soma, A., & Nishikawa, K. (1997). Only one nucleotide insertion to the long variable arm confers and efficiente serine acceptor activity upon *S. cerevisiae* tRNALeu *in vitro*. *J.Mol.Biol., 268,* 704-711.

Hinnebusch, A. & Natarajan, K. (2002). Gcn4p, a Master Regulator of Gene Expression, Is Controlled at Multiple Levels by Diverse Signals of Starvation and Stress. Eukaryotic Cell 1[1], 22-32.

Hofmann, L., Saunier, R., Cossard, R., Esposiito, M., Rinaldi, T., & Delahodde, A. (2009). A nonproteolytic proteasome activity controls organelle fission in yeast. J Cell Sci 122, 3673-3683.

Holland, S., Lodwing, E., Sideri, T., Reader, T., Clarke, I., Gkargkas, K. et al. (2007). Application of the comprehensive set of heterozygous yeast deletion mutants to elucidate the molecular basis of cellular chromium toxicity. Genome Biology 8[12], R268.

Holy, J. M. (2002). Curcumin disrupts mitotic spindle structure and induces micronucleation. Mutat.Res. 518[1], 71-84.

Hou, Y. & Schimmel, P. (1988). A simple structural feature is a major determinant of the identity of a transfer RNA. *Nature, 333,* 140-145.

Huang, H. & Brandriss, M. (2000). The Regulator of the Yeast Proline Utilization Pathway Is Differentially Phosphorylated in Response to the Quality of the Nitrogen Source. Mol Cell Biol 20[3], 892-899

Huang, H., Moir, R., Tanzi, R., Bush, A., & Rogers, J. (2004). Redox-Active Metals, Oxidative Stress, and Alzheimer's Disease Pathology. Annals of the New York Academy of Sciences 1012, 153-163.

Huang, X., Atwood, C., Hartshorn, M., Multhaup, G., Goldstein, L., Scarpa, R. et al. (1999a). The Aß Peptide of Alzheimer's Disease Directly Produces Hydrogen Peroxide through Metal Ion Reduction. Biochemistry 38[24], 7609-7616.

Huang, X., Cuajungco, M., Atwood, C., Hartshorn, M., Tyndall, J., Hanson, G. et al. (1999b). Cu(II) Potentiation of Alzheimer Ab Neurotoxicity. The Journal of Biological Chemistry 274[52], 37111-37116.

Hughes, R. A. & Ellington, A. D. (2010). Rational design of an orthogonal tryptophanyl nonsense suppressor tRNA. *Nucleic Acids Research, 38,* 6813-6830.

Hughes, T. R., Roberts, C. J., Dai, H., Jones, A. R., Meyer, M. R., Salde, D. et al. (2000). Widespread aneuploidy revealed by DNA microarray expression profiling. *Nature Genetics, 25,* 333-337.

Hurt, E., Hannus, S., Schmelzl, B., Lau, D., Tollervey, D., & Simos, G. (1999). A Novel In Vivo Assay Reveals Inhibition of Ribosomal Nuclear Export in Ran-Cycle and Nucleoporin Mutants. The Journal of Cell Biology 144, 389-401.

Ibba, M. & Hannecke, H. (1995). Relaxing the substrate specificity of an aminoacyl-tRNA synthetase allows in vitro and in vivo synthesis of proteins containing unnatural amino acids. *FEBS Letters, 364,* 272-275.

Ihrig, J., Hausmman, A., Hain, A., Richter, N., Hamza, I., Lill, R. et al. (2010). Iron Regulation through the Back Door: Iron-Dependent Metabolite Levels Contribute to Transcriptional Adaptation to Iron Deprivation in Saccharomyces cerevisiae. Eukaryotic Cell 9[3], 460-471.

Ikemura, T. (1985). Codon usage and tRNA content in unicellular and multicellular organisms. *Mol.Biol.Evol., 2,* 13-34.

Ishimaru, Y., Ohama, T., Kawatsu, Y., Nakamura, K., & Osawa, S. (1996). UAG is a sense codon in several chlorophycean mitochondria. *Curr.Genet., 30,* 29-33.

Jackson, S. E., Moracci, M., elMasry, n., Johnson, c. M., & Fersht, A. R. (1993). Effect of cavity-creating mutations in the hydrophobic core of chymotrypsin inhibitor 2. *Biochemistry, 32,* 11259-11269.

Jakubowski, H. & Goldman, E. (1992). Editing of errors in selection of amino acids for protein synthesis. *Microbiological Reviews, 56,* 412-429.

Janes, M., Hill, D., Cardon, C., Robison, C., Walls, J., Leung, W. et al. (2004). Fluorogenic Detection of Mitochondrial Superoxide in Live Cells. American Society for Cell Biology 44th Annual Meeting .

Jang, H., Lee, K., Chi, Y., Jung, B., Park, S., Park, J. et al. (2004). Two Enzymes in One: Two Yeast Peroxiredoxins Display Oxidative Stress-Dependent Switching from a Peroxidase to a Molecular Chaperone Function. Cell 117, 625-635.

Jensen, R., Hobbes, A., Hobbes, A., Cerveny, K., & Sesaki, H. (2000). Yeast Mitochondrial Dynamics: Fusion, Division, Segregation, and Shape. MICROSCOPY RESEARCH AND TECHNIQUE 51, 573-583.

Jeyaprakash, A., welch, J. W., & Fogel, S. (1991). Multicopy CUP1 plasmids enhance cadmium and copper resistance levels in yeast. *Mol.Gen.Genetics, 225,* 363-368.

Jiang, H., Zhang, Y., Sun, J., Wang, W., & Gu, Z. (2008). Differential selection on gene translation efficiency between the filamentous fungus Ashbya gossypii and yeasts. *BMC Evolutionary Biology, 8:343*.

Jin, Y., Dunlap, P., McBride, S., Al-Refai, H., Bushel, P., & Freedman, J. (2008). Global Transcriptome and Deletome Profiles of Yeast Exposed to Transition Metals. PLoS Genetics 4[4], e1000053.

John, R. A. (1995). Pyridoxal phosphate-dependent enzymes. *Biochem Biophys Acta, 1248,* 81-96.

Johnston, J. A., Ward, C. L., & Kopito, R. R. (1998). Aggresomes: a cellular response to misfolded proteins. *J.Cell Biol., 143,* 1898.

Jones, C. N., Jones, C. I., Graham, W. D., Agris, P. F., & Spremulli, L. L. (2008). A disease causing point mutation in Human mitochondrial $tRNA^{Met}$ results in tRNA misfolding leading to defects in translational initiation and elongation. The Journal of Biological Chemistry 283[49], 34445-34456.

Jones, O. W. & Nirenberg, M. W. (1966). Degeneracy in the amino acid code. *Biochim Biophys Acta, 119,* 400-406.

Kadaba, S., Krueger, A., Trice, T., Krecic, A. M., Hinnebusch, A. G., & Anderson, J. T. (2004). Nuclear surveillance and degradation of hypomodified initiator $tRNA^{Met}$ in *S. cerevisiae*. *Genes & Development, 18,* 1227-1240.

Kadaba, S., Wang, X., & Anderson, J. T. (2006). Nuclear RNA Surveillance in *Saccharomyces cerevisiae*: Trf4p-dependent polyadenylation of nascent hypomethylated tRNA and an aberrant form of 5S rRNA. *RNA, 12,* 508-521.

Kaganovich, D., Kopito, R., & Frydman, J. (2008). Misfolded proteins partition between two distinct quality control compartments. Nature 454, 1088-1095.

Kano, A., Andachi, Y., Ohama, T., & Osawa, S. (1991). Novel anticodon composition of transfer RNAs in Micrococcus luteus, a bacterium with a high genomic G + C content. Correlation with codon usage. *Journal of Molecular Biology, 221,* 387-401.

Kavran, J. M., Gundllapalli, S., O'Donoghue, P., Englert, M., Soll, D., & Steitz, T. (2007). Structure of pyrrolysyl-tRNA synthetase, an archaeal enzyme for genetic code innovation. *Proc.Natl.Acad.Sci.USA, 104,* 11268-11273.

Kawaji, H., Nakamura, M., Takahashi, Y., Sandelin, A., Katayama, S., kuda, S. et al. (2008). Hidden layers of human small RNAs. *BMC Genomics, 9*.

Keasling, J. D. (1997). Regulation of intracellular toxic metals and other cations by hydrolysis of polyphosphate. *Ann N Y Acad Sci., 829,* 242-249.

Kellis, J. T., Nyberg, K., & Fersht, A. R. (1989). Energetics of complementary side-chain packing in a protein hydrophobic core. *Biochemistry, 28,* 4914-4922.

Kim, H. S., Kim, I. Y., Soll, D., & Lee, S. Y. (2000). Transfer RNA Identity Change in Anticodon Variants of E. coli tRNAPhe in vivo. *Molecules and Cells, 10,* 76-82.

Kim, S. H., Suddath, F. L., Quigley, G. J., McPherson, A., Sussman, J. L., Wang, A. H. et al. (1974). Three-dimensional tertiary structure of yeast phenylalanine transfer RNA. *Science, 185,* 435-440.

King, J. L. & Jukes, T. (1969). Non darwinian evolution. *Science, 164,* 788-798.

Kleijnen, M., Kirkpatrick, D., & Gygi, S. (2007). The ubiquitin–proteasome system regulates membrane fusion of yeast vacuoles. The EMBO Journal 26, 275-287.

Knight, R., Freeland, S., & Landweber, L. (2001). REWIRING THE KEYBOARD: EVOLVABILITY OF THE GENETIC CODE. *Nat.Rev.Genet., 2,* 49-58.

Knight, S. A., Labbe, S., Kwon, L. F., Kosman, D., & Thiele, D. (1996). A widespread transposable element masks expression of a yeast copper transport gene. *Genes and Development, 10,* 1917-1929.

Kopito, R. (2000). Aggresomes, inclusion bodies and protein aggregation. *Trends in Cell Biology, 10,* 524-530.

Korencic, D., Polycarpo, C., Weygand-Durasevic, I., & Soll, D. (2004). Differential modes of transfer RNA^{Ser} recognition in *Methanosarcina barkeri*. The Journal of Biological Chemistry 279[47], 48780-48786.

Kornberg, A., Rao, N. N., & Ault-Riche, D. (1999). INORGANIC POLYPHOSPHATE:A MOLECULE OF MANY FUNCTIONS. *Annu.Rev.Biochem, 68,* 89-125.

Kroemer, G., El-Deiry, W., Golstein, P., Peter, M., Vaux, D., Vandenabeele, P. et al. (2005). Classification of cell death: recommendations of the Nomenclature Committee on Cell Death. Cell Death and Differentiation 12, 1463-1467.

Kryukov, G. V., Castellano, S., Novoselov, S. V., Lobanov, A. V., Zehtab, O., Guigo, R. et al. (2003). Characterization of mammalian selenoproteomes. *Science, 300,* 1439-1443.

Kuhn, K., DeRisi, J., Brown, P., & Sarnow, P. (2001). Global and Speci?c Translational Regulation in the Genomic Response of Saccharomyces cerevisiae to a Rapid Transfer from a Fermentable to a Nonfermentable Carbon Source. Mol Cell Biol 21[3], 916-927

Kunkel, T. A. & Bebenek, K. (2000). DNA replication fidelity. Annu.Rev.Biochem. 69, 497-529.

Kurnaz, M. L., Bilgin, T., & Kurnaz, A. (2010). Certain Non-Standard Coding Tables Appear to be More Robust to Error Than the Standard Genetic Code. *J.Mol.Evol., 70,* 13-28.

Kvitek, D., Will, J., & Gasch, A. P. (2008). Variation in stress sensitivity and genomic expression in deiverse S. cerevisiae isolates. PLoS Genetics 4[10: e1000223].

Kwon, I., Kirshembaum, K., & Tirrell, D. A. (2003). Breaking the degeneracy of the genetic code. *J Am Chem Soc, 125,* 7512-7513.

Lackner, D. H. & Bahler, J. (2008). Translational control of gene expression: from transcripts to transcriptomes. *International Review of Cell and Molecular Biology, 271,* 199-251.

Ladbury, J. E., Wynn, R., Thomson, J. A., & Sturtevant, J. M. (1995). Substitution of charged residues into the hydrophobic core of Escherichia coli thioredoxin results in a change in heat capacity of the native protein. *Biochemistry, 34,* 2148-2152.

Lee, D. & Mcclain, W. H. (2004). Aptamer redesigned tRNA is nonfunctional and degraded in cells. *RNA, 10,* 7-11.

Lee, J. W., Beebe, K., Nangle, L., Jang, J., Longo-Guess, C., Cook, S. et al. (2006). Editing-defective tRNA synthetase causes protein misfolding and neurodegeneration. *Nature, 443,* 50-55.

Lee, S. a. C. K. (2005). Starvation-induced Cleavage of the tRNA Anticodon Loop in *Tetrahymena thermophila*. *Journal of Biological Chemistry, 280,* 42744-42749.

Lee, Y. & Lee, C. (2008). Transcriptional Response According to Strength of Calorie Restriction in Saccharomyces cerevisiae. Molecules and Cells 26, 299-307.

Lenburg, M. E. & O'Shea, E. K. (1996). Signaling phosphate starvation. *TRENDS in Biochemical Sciences, 21,* 383-387.

Lenhard, B., Orellana, O., Ibba, M., & Weygand-Durasevic, I. (1999). tRNA recognition and evolution of determinants in seryl-tRNA synthesis. Nucleic Acids Research 27[3], 721-729.

Levine, M. & Tarver, H. (1951). Studies on ethionine: incorporation of ethionine into rat protein. *J.Biol.Chem., 192,* 835-850.

Lew, D. J. & Reed, S. I. (1995). A cell cycle checkpoint monitors cell morphogenesis in budding yeast. J.Cell Biol. 129, 739-749.

Lewis, J., Elkon, I., McGee, M., Higbee, A., & Gasch, A. P. (2010). Exploiting natural variation in Saccharomyces cerevisiae to identify genes for increased ethanol resistance. Genetics Epub ahead of print[10.1534/genetics.110.121871].

Lewis, J. G., Learmonth, R. P., & Watson, K. (1995). Induction of heat, freezing and salt tolerance by heat and salt shock in Saccharomyces cerevisiae. *Microbiology, 141,* 687-694.

Li, Z., Okamoto, K., Hayashi, Y., & Sheng, M. (2004). The importance of dendritic mitochondria in the morphogenesis and plasticity of spines and synapses. Cell 119[6], 873-887.

Li, Z., Reimers, S., Pandite, S., & Deutscher, M. P. (2002). RNA quality control: degradation of defective transfer RNA. *The EMBO Journal, 21,* 1132-1138.

Lincecum, T. L. & Martinis, S. (2005). Leucyl-tRNA synthetases. In M.Ibba, C. Francklyn, & S. Cusack (Eds.), *The aminoacyl-tRNA synthetases* (pp. 36-46). Landes Biosciences.

Linder, M. C. & Hazegh-Azam, M. (1996). Copper biochemistry and molecular biology. *Am.J.Clin.Nutr, 63,* 797-811.

Ling, J., So, R. B., Yadavalli, S. S., Roy, H., Shoji, S., Fredrick, K. et al. (2009). Resampling and Editing of Mischarged tRNA Prior to Translation Elongation. *Molecular Cell, 33,* 654-660.

Ling, J. & Soll, D. (2010). Severe oxidative stress induces protein mistranslation through impairment of an aminoacyl-tRNA synthetase editing site. Proc.Natl.Acad.Sci.USA 107[9], 4028-4033.

Ling, Y., Liebes, L., Zou, Y., & Perez-Soler, R. (2003). Reactive Oxygen Species Generation and Mitochondrial Dysfunction in the Apoptotic Response to Bortezomib, a Novel Proteasome Inhibitor, in Human H460 Non-small Cell Lung Cancer Cells. J.Biol.Chem. 278[36], 33714-33723.

Liu, C. C. & Schultz, P. G. (2010). Adding New Chemistries to the Genetic Code. *Annu.Rev.Biochem, 79,* 413-444.

Liu, J. & Balasubramanian, M. K. (2000). A checkpoint that monitors cytokinesis in Schizosaccharomyces pombe. J Cell Sci 113[7], 1223-1230.

Livingstone, C. D. & Barton, G. (1993). Protein Sequence Alignments: A Strategy for the Hierarchical Analysis of Residue Conservation. *Comput.Appl.Biosci, 9,* 745-756.

Lobanov, A. V., Kryukov, G. V., Hatfield, D. L., & Gladyshev, V. N. (2006). Is there a twenty third amino acid in the genetic code. *TRENDS in Genetics, 22,* 357-360.

Lokki, J. & Saura, A. (1979). Polyploidy in insect evolution. *Basic Life Sci, 13,* 277-312.

Longtine, M., Theesfeld, C., McMillan, J. N., Weaver, E., Pringle, J., & Lew, D. J. (2000). Septin-dependent assembly of a cell cycle-regulatory module in Saccharomyces cerevisiae. Mol Cell Biol 20[11], 4049-4061.

Lu, C., Brauer, M., & Botstein, D. (2009). Slow Growth Induces Heat-Shock Resistance in Normal and Respiratory-deficient Yeast. Molecular Biology of the Cell 20, 891-903.

Ludovico, P., Madeo, F., & Silva, M. (2005). Yeast Programmed Cell Death: An Intricate Puzzle. IUBMB Life 57, 129-135.

Ludovico, P., Rodrigues, F., Almeida, A., Silva, M. T., Barrientos, A., & Corte-Real, M. (2002). Cytochrome c Release and Mitochondria Involvement in Programmed Cell Death Induced by Acetic Acid in Saccharomyces cerevisiae. *Molecular Biology of the Cell, 13,* 2598-2606.

Ludovico, P., Sousa, M. J., Silva, M. T., Leao, C., & Corte-Real, M. (2001). Saccharomyces cerevisiae commits to a programmed cell death process in response to acetic acid. *Microbiology, 147,* 2409-2415.

Lum, R., Tkach, J., Vierling, E., & Glover, J. (2004). Evidence for an Unfolding/Threading Mechanism for Protein Disaggregation by Saccharomyces cerevisiae Hsp104. The Journal of Biological Chemistry 279[28], 29139-29146.

Lyons, T., Gasch, A. P., Gaither, A., Botstein, D., O.Brown, P., & Eide, D. (2000). Genome-wide characterization of the Zap1p zinc-responsive regulon in yeast. Proc.Natl.Acad.Sci.USA 97[14], 7957-7962.

Ma, M. & Liu, L. (2010). Quantitative transcription dynamic analysis reveals candidate genes and key regulators for ethanol tolerance in S. cerevisiae. BMC Microbiology 10[169].

Madeo, F., Engelhardt, S., Herker, E., Lehmann, N., Maldener, C., Proksch, A. et al. (2002). Apoptosis in yeast: a new model system with applications in cell biology and medicine. Curr.Genet. 41, 208-216.

Maeshiro, T. & Kimura, M. (1998). The role of robustness and changeability on the origin and evolution of genetic codes. *Proc.Natl.Acad.Sci.USA, 95,* 5093.

Mager, W. & Moradas Ferreira, P. (1993). Stress response of yeast. Biochem.J. 290, 1-13.

Magliery, T., Anderson, J. C., & Schultz, P. G. (2001). Expanding the Genetic Code: Selection of Efficient Suppressors of Four-base Codons and Identification of "Shifty" Four-base Codons with a Library Approach in Escherichia coli. *Journal of Molecular Biology, 307,* 755-769.

Mahapatra, A., Patel, A., Soares, J. A., Larue, R. C., Zhang, J. K., Metcalf, W. W. et al. (2006). Characterization of a Methanosarcina acetivorans mutant unable to translate UAG as pyrrolysine. *Molecular Microbiology, 59,* 56-66.

Mahmud, S. A., Hirasawa, T., & Shimizu, H. (2010). Differential importance of trehalose accumulation in Saccharomyces cerevisiae in response to various environmental stresses. *Journal of Bioscience and Bioengineering, 109,* 262-266.

Man, O. & Pilpel, Y. (2007). Differential translation efficiency of orthologous genes is involved in phenotypic divergence of yeast species. *Nature Genetics, 39,* 415-421.

Martinis, S. & Boniecki, M. (2010). The balance between pre- and post-transfer editing in tRNA synthetases. *FEBS Letters, 584,* 455-459.

Massey, S. E., Moura, G., Beltrão, P., Almeida, R., Garey, J. R., Tuite, M. F. et al. (2003). Comparative evolutionary genomics unveils the molecular mechanism of reassignment of the CTG codon in *Candida spp*. *Genom Research, 13,* 544-557.

Mata, J., Marguerat, S., & Bahler, J. (2005). Post-transcriptional control of gene expression: a genome-wide perspective. *TRENDS in Biochemical Sciences, 30,* 506-514.

McClain, W. (1993). Rules that govern tRNA identity in protein synthesis. *Journal of Molecular Biology, 234,* 257-280.

McKee, A. E. & Silver, P. A. (2007). Systems perspectives on mRNA processing. *Cell Research, 17,* 590.

McMillan, J. N., Sia, R. A., & Lew, D. J. (1998). A morphogenesis checkpoint monitors the actin cytoskeleton in yeast. J.Cell Biol. 142[6], 1487-1499.

Meinnel, T., Mechulam, Y., & Blanquet, S. (1995). Aminoacyl-tRNA synthetases: Occurrence, structure and function. In D.Soll & U. RajBhandary (Eds.), *tRNA: structure, biosinthesis and function* (pp. 251-292). Washington,D.C.: ASMPress.

Melamed, D., Pnueli, L., & Arava, Y. (2008). Yeast translational response to high salinity: Global analysis reveals regulation at multiple levels. RNA 14, 1337-1351.

Menocal, L. & D'Urso, G. (2004). Programmed cell death in fission yeast. FEMS Yeast Research 5, 111-117.

Metzger, A. U., Heckl, M., Willbold, D., Breitchopf, K., RajBhandary, U. L., Rosch, P. et al. (1997). Structural studies on tRNA acceptor stem microhelices: exchange of the discriminator base A73 for G in human $tRNA^{Leu}$ switches the acceptor specificity from leucine to serine possibly by decreasing the stability of the terminal G1-C72 base pair. *Nucleic Acids Research, 25,* 4551-4556.

Meyerovich, M., Mamou, G., & Ben-Yehuda, S. (2010). Visualizing high error levels during gene expression in living bacterial cells. *Proc.Natl.Acad.Sci.USA, 107,* 11543-11548.

Mira, N., Palma, M., Guerreiro, J., & Sá-Correia, I. (2010). Genome-wide identification of Saccharomyces cerevisiae genes required for tolerance to acetic acid. Microbial Cell Factories 9[79].

Miranda, I., Rocha, R., Santos M.C., Mateus D.D., Moura, G., Carreto L. et al. (2007). A Genetic Code Alteration Is a Phenotype Diversity Generator in the Human Pathogen *Candida albicans*. *PLoS ONE, 2,* e996.

Miranda, I., Silva, R. M., & Santos, M. A. S. (2006). Evolution of the genetic code in yeasts. *Yeast, 23,* 203-213.

Mitchell, A. (1994). Control of Meiotic Gene Expression in Saccharomyces cerevisiae. Microbiological Reviews 58[1], 56-70.

Mogk, A., Tomoyasu, T., Galoubinoff, P., Rudiger, S., Roder, D., Langen, H. et al. (1999). Identi?cation of thermolabile Escherichia coli proteins: prevention and reversion of aggregation by DnaK and ClpB. The EMBO Journal 18[24], 6934-6949.

Morl, M. & Marchfelder, A. (2001). The final cut. *EMBO reports, 21,* 17-20.

Mouillon, J. M. & Persson, B. L. (2005). Inhibition of the protein kinase A alters the degradation of the high-affinity phosphate transporter Pho84 in Saccharomyces cerevisiae. Curr.Genet. 48[4], 226-234.

Mouillon, J. M. & Persson, B. L. (2006). Newaspectson phosphate sensingandsignalling inSaccharomyces cerevisiae. FEMS Yeast Research 6, 171-176.

Moura, G., Carreto L., & Santos, M. A. S. (2009). Genetic code ambiguity: an unexpected source of proteome innovation and phenotypic diversity. *Current Opinion in Microbiology, 12,* 1-7.

Moura, G. R., Paredes, J. A., & Santos, M. A. (2010). Development of the genetic code: Insights from a fungal codon reassignment. *FEBS Letters, 584,* 334-341.

Mozdy, A. & Shaw, J. (2003). A fuzzy mitochondrial fusion aparatus comes into focus. Nat.Rev.Mol Cell Biol. 4[6], 468-478.

Mukai, T., Hayashi, a., Iraha, F., Sato, A., Ohtake, K., Yokoyama, S. et al. (2010). Codon reassignment in the Escherichia coli genetic code. *Nucleic Acids Research, 38,* 8188-8195.

Mukai, T., Kobayashi, T., Hino, N., Yanagisawa, T., Sakamoto, K., & Yokoyama, S. (2008). Adding l-lysine derivatives to the genetic code of mammalian cells with engineered pyrrolysyl-tRNA synthetases. *Biochemical and Biophysical Research Communications, 371,* 818-822.

Mukai, T., Wakiyama, M., Sakamoto, K., & Yokoyama, S. (2009). Genetic encoding of non-natural amino acids in Drosophila melanogaster Schneider 2 cells. *Protein Science, 19,* 440-448.

Muller, O., Bayer, M. J., Peters, C., Anderson, J. S., Mann, M., & Mayer, A. (2002). The Vtc proteins in vacuole fusion: coupling NSF activity to V(0) trans-complex formation. EMBO Journal 21[3], 259-269.

Muller, O., Neumann, H., Bayer, M. J., & Mayer, A. (2003). Role of the Vtc proteins in V-ATPase stability and membrane trafficking. J Cell Sci 116[6], 1107-1115.

Murphy, M. H. & Baralle, F. E. (1983). Directed semisynthetic point mutational analysis of an RNA polymerase III promoter. *Nucleic Acids Research, 11,* 7695-7700.

Nagao, A., Suzuki, T., Katoh, T., Sakagushi, Y., & Suzuki, T. (2009). Biogenesis of glutaminyl-mt tRNAGln in human mitochondria. *Proc.Natl.Acad.Sci.USA, 106,* 16209-16214.

Nagata, T., Kiyono, M., & Pan-Hou, H. (2006). Engineering expression of bacterial polyphosphate kinase in tobacco for mercury remediation. *Appl Microbiol Biotechnol, 72,* 777-782.

Nagel, R. & Chan, A. (2006). Mistranslation and genetic variability: The effect of streptomycin. *Mutation Research, 601,* 162-170.

Nakanishi, K. & Nureki, O. (2005). Recent progress of structural biology of tRNA processing and modification. *Molecules and Cells, 19,* 157-166.

Nangle, L., Motta, C., & Schimmel, P. (2006). Global Effects of Mistranslation from an Editing Defect in Mammalian Cells. Chemistry and Biology 13, 1091-1100.

Negri, D. N., Fabbri, S., Bufardeci, E., Baldi, M. I., Attardi, D. G., Mattoccia, E. et al. (1997). The Eucaryal tRNA Splicing Endonuclease Recognizes a Tripartite Set of RNA Elements. *Cell, 89,* 859-866.

Netzer, N., Goodenbour, J. M., David, A., Dittmar, K., Jones, R., Schneider, J. et al. (2009). Innate Immune and Chemically Triggered Oxidative Stress Modifies Translational Fidelity. *Nature, 462,* 522-526.

Neumann, H., Wang, K., Davis, L., Garcia-Alai, M., & Chin, J. W. (2010). Encoding multiple unnatural amino acids via evolution of a quadruplet-decoding ribosome. *Nature, 464,* 441-444.

Nierhaus, K. (2001). Gene expression: decoding and accuracy. In *Encyclopedia of Life Sciences* (Nature Publishing Group.

Nikoloff, D. & Henry, S. (1994). Functional Characterization of the IN02 Gene of Saccharomyces cerevisiae. The Journal of Biological Chemistry 269[10], 7402-7411.

Nirenberg, M. W., Leder, P., Bernfield, M., Brimacombe, R., Trupin, J., Rottman, F. et al. (1965). RNA Codewords and protein synthesis, VII. On the general nature of the RNA code. *Biochemistry, 53,* 1161-1168.

Niwa, O., Tange, Y., & Kurabayashi, A. (2006). Growth arrest and chromosome instability in aneuploid yeast. *Yeast, 23,* 937-950.

Nobles, K. N., Yarian, C. S., Liu, G., Guenther, R., & Agris, P. F. (2002). Highly conserved modified nulceosides influence Mg2+ dependent tRNA folding. Nucleic Acids Research 30[21], 4751-4760.

Norbeck, J. & Blomberg, A. (1998). Amino acid uptake is strongly a¡ected during exponential growth of Saccharomyces cerevisiae in 0.7 M NaCl medium. FEMS Microbiol Letters 158, 121-126.

Noren, C. J., Anthony-Cahill, S. J., Griffith, M. C., & Schultz, P. G. (1989). A general method for site-specific incorporation of unnatural amino acids into proteins. *Science, 244,* 182-188.

Normanly, J., Ogden, R., Horvath, S., & Abelson, J. (1986). Changing the identity of a transfer RNA. *Nature, 321,* 213-219.

Normanly, J., Ollick, T., & Abelson, J. (1992). Eight base changes are sufficient to convert a leucine-inserting tRNA into a serine-inserting tRNA. Proc.Natl.Acad.Sci.USA 89, 5680-5684.

Novozhilov, A., Wolf, Y., & Koonin, E. (2007). Evolution of the genetic code: partial optimization of a random code for robustness to translation error in a rugged fitness landscape. *Biology Direct, 2:24*.

Nowak, M. W., Kearney, P. C., Sampson, J. R., Saks, M. E., Labarca, C. G., et al et al. (1995). Nicotinic receptor binding site probed with unnatural amino acid incorporation in intact cells. ***Science, 268,*** **439-442.**

Oba, T., Andachi, Y., Muto, A., & Osawa, S. (1991). CGG: an unassigned or nonsense codon in Mycoplasma capricolum. ***Proc.Natl.Acad.Sci.USA, 88,*** **921-925.**

Ogawa, N., DeRisi, J., & O.Brown, P. (2000). New Components of a System for Phosphate Accumulation and Polyphosphate Metabolism in Saccharomyces cerevisiae Revealed by Genomic Expression Analysis. Molecular Biology of the Cell 11, 4309-4321.

Ogle, J. M. & Ramakrishnan, V. (2005). STRUCTURAL INSIGHTS INTO TRANSLATIONAL FIDELITY. Annu.Rev.Biochem. 74, 129-177.

Ohama, T., Muto, A., & Osawa, S. (1990). Role of GC-biased mutation pressure on synonymous codon choice in Micrococcus luteus, a bacterium with a high genomic GC-content. ***Nucleic Acids Research, 18,*** **1565-1569.**

Ohama, T., Suzuki, T., Mori, M., Osawa, S., Ueda, T., Watanabe, K. et al. (1993). Non-universal decoding of the leucine codon CUG in several ***Candida*** **species.** ***Nucleic Acids Research, 21,*** **4039-4045.**

Osawa, S. & Jukes, T. (1989). Codon reassignment (codon capture) in evolution. ***J.Mol.Evol., 28,*** **271-278.**

Osawa, S. & Jukes, T. (1995). On codon reassignment. ***J.Mol.Evol., 41,*** **247-249.**

Osawa, S., Jukes, T., Watanabe, K., & Muto, A. (1992). Recent evidence for the evolution of the gentic code. ***Microbiological Reviews, 56,*** **229-264.**

Otto, S. P. & Whitton, J. (2000). POLYPLOID INCIDENCE AND EVOLUTION. ***Annu.Rev.Genet., 34,*** **401-437.**

Ougland R., Zhang C., Liiv A., Johansen R.F., Seeberg E., Hou W. et al. (2004). AlkB Restores the Biological Function of mRNA and tRNA Inactivated by Chemical Methylation. ***Molecular Cell, 16,*** **107-116.**

Overkamp, K., Kotter, P., Van der Hoek, R., Schoondermark-Stolk, S., Luttik, M., van Dijken, P. et al. (2002). Functional analysis of structural genes for NAD+ dependent formate dehydrogenase in Saccharomyces cerevisiae. ***Yeast, 19,*** **509-520.**

Ozanick, S., Wang, X., Costanzo, M., Brost, R., oone, C., & Anderson, J. T. (2008). Rex1p deficiency leads to accumulation of precursor initiator tRNAMet and polyadenylation of substrate RNAs in ***Saccharomyces cerevisiae*****.** ***Nucleic Acids Research, 37,*** **298-308.**

Pace, C., Shirley, B., Mcnutt, M., & Kajiwala, K. (1996). Forces contributing to the conformational stability of proteins. FASEB J. 10, 75-83.

Padmanabhan, S., Marqusse, s., Ridgeway, T., Alue, T. M., & Baldwin, R. L. (1990). Relative helix-forming tendencies of nonpolar amino acids. ***Nature, 344,*** **268-270.**

Palermo, V., Falcone, C., & Mazzoni, C. (2007). Apoptosis and Aging in Mitochondrial Morphology Mutants of S. cerevisiae. Folia Microbiol. 5, 479-483.

Pallanck, L., Pak, M., & Schulman, L. (1995). tRNA discrimination in aminoacylation. In D.Soll & U. RajBhandary (Eds.), ***tRNA: structure, biosynthesis and function*** **(pp. 371-394). Washington D.C.: American Society for Microbiology.**

Pan-Hou, H., Kiyono, M., Omura, H., Omura, T., & Endo, G. (2002). Polyphosphate produced in recombinant Escherichia coli confers mercury resistance. *FEMS Microbiol Letters, 207,* 159-164.

Pankiv, S., Clausen, T. H., Lamark, T., Brech, A., Bruun, J. A., Outzan, H. et al. (2007). p62/SQSTM1 binds directly to Atg8/LC3 to facilitate degradation of ubiquitinated protein aggregates by autophagy. *J.Biol.Chem., 282,* 24131-24145.

Paolella, G., Lucero, M. A., Murphy, M. H., & Baralle, F. E. (1983). The Alu family repeat promoter has a tRNA-like bipartite structure. *EMBO Journal, 2,* 691-696.

Parrou, J., Teste, M., & Francois, J. (1997). Effects of various types of stress on the metabolism of reserve carbohydrates in Saccharomyces cerevisiae: genetic evidence for a stress-induced recycling of glycogen and trehalose. Microbiology 143, 1891-1900.

Patisson-Granberg, J. & Persson, B. (2000). Regulation of Cation-Coupled High-Affinity Phosphate Uptake in the Yeast Saccharomyces cerevisiae. Journal of Bacteriology 182[17], 5017-5019.

Pavelka, N., Rancati, G., Zhu, J., Bradford, W. D., Saraf, A., Florens, L. et al. (2010). Aneuploidy confers quantitative proteome changes and phenotypic variation in budding yeast. *Nature, 468,* 321-325.

Pereira, M., Eleutherio, E., & Panek, A. (2001). Acquisition of tolerance against oxidative damage in Saccharomyces cerevisiae. BMC Microbiology 1[11].

Perreau, V. M., Keith, G., Holmes, W. M., Przykorska, A., Santos, M. A., & Tuite, M. F. (1999). The Candida albicans CUG-decoding ser-tRNAa has an atypical anticodon stem-loop structure. Journal of Molecular Biology 293[1039], 1053.

Pezo, V., Metzgar, D., Hendrickson, T. L., Wass, w. F., Hazebrouck, S., Doring, V. et al. (2004). Artificially ambiguous genetic code confers growth yield advantage. *Proc.Natl.Acad.Sci.USA, 101,* 8593-8597.

Phizicky, E. M. & Hopper, A. K. (2010). tRNA biology charges to the front. Genes and Development 24, 1832-1860.

Pirkkala, L., Nykanan, P., & Sistonen, L. (2001). Roles of the heat shock transcription factors in regulation of the heat shock response and beyond. FASEB J. 15, 1118-1131.

Plotkin, J. B., Robins, H., & Levine, A. J. (2004). Tissue-specific codon usage and the expression of human genes. *Proc.Natl.Acad.Sci.USA, 101,* 12588-12591.

Polycarpo, C., Ambrogelly, A., Berube, A., Winbush, S. M., McCloskey, J. A., Crain, P. F. et al. (2004). An aminoacyl-tRNA synthetase that specifically activates pyrrolysine. *Proc.Natl.Acad.Sci.USA, 101,* 12450-12454.

Posas, F., Chambers, J., Heyman, J., Hoeffler, J., Nadal, E., & Ariño, J. (2000). The Transcriptional Response of Yeast to Saline Stress. The Journal of Biological Chemistry 275[23], 17249-17255.

Preiss, T. & Hentze, M. W. (2003). Starting the protein synthesis machine: eukaryotic translation initiation. *Bioessays, 25,* 1201-1211.

Puig, S., Askeland, E., & Thiele, D. (2005). Coordinated Remodeling of Cellular Metabolism during Iron Deficiency through Targeted mRNA Degradation. Cell 120, 99-110.

Quesne, J., Spriggs, K., Bushell, M., & Willis, A. (2010). Dysregulation of protein synthesis and disease. Journal of Pathology 220, 140-151.

Radivojac, P., Iakoucheva, L., Oldfield, C., Obradovic, Z., Uversky, V., & Keith Dunker, A. (2007). Intrinsic Disorder and Functional Proteomics. Biophysical Journal 92, 1439-1456.

RajBhandary, U. (1997). Once there were twenty. *Proc.Natl.Acad.Sci.USA, 94,* 11761-11763.

RajBhandary, U. & Soll, D. (1995). Transfer RNA in its fourth decade. In D.Soll & U. RajBhandary (Eds.), *tRNA: structure, biosynthesis and function* (pp. 1-4). Washington D.C.: ASM Press.

Rancati, G., Pavelka, N., Fleharty, B., Noll, A., Allen, R., Walton, K. et al. (2008). Aneuploidy and polyploidy underlie adaptive evolution of yeast cells deprived of a conserved cytokinesis motor. *Cell, 135,* 879-893.

Rand, J. D. & Grant, C. M. (2006). The thioredoxin system protects ribosomes against stress-induced aggregation. Molecular Biology of the Cell 17, 387-401.

Rennell, D., Bouvier, S. E., Hardy, L. W., & Poteete, A. R. (1991). Systematic mutation of bacteriophage T4 lysozyme. *Journal of Molecular Biology, 222,* 67-88.

Reynolds, N., Lazazzera, B., & Ibba, M. (2010). Cellular mechanisms that control mistranslation. Nature Reviews - Microbiology 8, 849-856.

Ribas de Pouplana, L. & Schimmel, P. (2001). Aminoacyl-tRNA synthetases: potential markers of genetic code development. *TRENDS in Biochemical Sciences, 26,* 591-596.

Rich, A. & Kim, S. H. (1978). The three-dimensional structure of transfer RNA. *Scientific American, 38,* 52-62.

Rocha, R., Barbosa Pereira, P. J., Santos, M. A., & Macedo-Ribeiro, S. (2011). Purification, crystallization and preliminary X-ray diffraction analysis of the seryl-tRNA synthetase from Candida albicans. *Acta Crystallogr Sect F Struct Biol Cryst Commun, 67,* 153-156.

Rodrigues-Pousada, C., Nevitt, T., Menezes, R., Azevedo, D., Pereira, J., & Amaral, C. (2004). Yeast activator proteins and stress response: an overview. FEBS Letters 567, 80-85.

Romero-Santacreu, L., Moreno, J., Perez-Ortin, J., & Alepuz, P. (2009). Specific and global regulation of mRNA stability during osmotic stress in Saccharomyces cerevisiae. RNA 15, 1110-1120.

Rosenberger, R. F. & Hilton, J. (1983). The frequency of transcriptional and translational errors at nonsense codons in the lacZ gene of Escherichia coli. Mol.Gen.Genetics 191[2], 207-212.

Rosenfeld, R., Reddi, A. R., Leung, E., Aranda, K., Ensen, L. T., & Cullota, V. C. (2010). The effect of phosphate accumulation on metal ion homeostasis in Saccharomyces cerevisiae. *J.Biol.Inog.Chem., 15,* 1051-1062.

Ruan, B., Palioura, S., Sabina, J., Marvin-Guy, L., Kochhar, S., LaRossa, R. A. et al. (2008). Quality control despite mistranslation caused by an ambiguous genetic code. *Proc.Natl.Acad.Sci.USA, 105,* 16502-16507.

Rutherford, J. C., Jaron, S., & Winge, D. R. (2003). Aft1p and Aft2p mediate iron-responsive gene expression in yeast through related promoter elements. *J.Biol.Chem., 278,* 27636-27643.

Sakamoto, K., Hayashi, a., Sakamoto, A., Kiga, D., Nakayama, H., Soma, A. et al. (2002). Site-speci®c incorporation of an unnatural amino acid into proteins in mammalian cells. *Nucleic Acids Research, 30,* 4692-4699.

Sambrook, J., Fritsch, E. F., & Maniatis, T. (2008). *Molecular cloning: a laboratory manual*. (2nd ed.) Cold Spring Harbor Laboratory Press.

Sampson, J. R. & Uhlenbeck, O. C. (1988). Biochemical and physical characterization of an unmodified yeast phenylalanine transfer RNA transcribed in vitro. *Proc.Natl.Acad.Sci.USA, 85,* 1033-1037.

Sankaranarayanan, R. & Moras, D. (2001). The fidelity of the translation of the genetic code. Acta Biochimica Polonica 48[2], 323-335.

Santos, M. A., Keith, G., & Tuite, M. F. (1993). Non-standard translational events in Candida albicans mediated by an unusual seryl-tRNA with a 5'-CAG-3' (leucine) anticodon. *The EMBO Journal, 12,* 607-616.

Santos, M. A., Moura, G., Massey, S., & Tuite, M. F. (2004). Driving change: the evolution of alternative genetic codes. *TRENDS in Genetics, 20,* 95-102.

Santos, M. A. & Tuite, M. F. (2004). Extant variations in the genetic code. In Lluis Ribas de Pouplana (Ed.), *The genetic code and the origin of life* (pp. 184-200). Eureka/Kluwer Academic/Plenum Publishers.

Santos, M. A. S., Cheesman, C., Costa, V., Moradas-Ferreira, P., & Tuite, M. F. (1999). Selective advantages created by codon ambiguity allowed for the evolution of an alternative genetic code in *Candida spp. Molecular Microbiology, 31,* 937-947.

Santos, M. A. S., Perreau, V. M., & Tuite, M. F. (1996). Tranfer RNA structural change is a key element in the reassignment of the CUG codon in *Candida albicans*. *The EMBO Journal, 15,* 5060-5068.

Santos, M. A. S. & Tuite, M. F. (1995). The CUG codon is decoded in vivo as serine and not leucine in *Candida albicans*. *Nucleic Acids Research, 23,* 1481-1486.

Schimmel, P., Giege, R., Moras, D., & Yokoyama, S. (1993). An operational RNA code for amino acids and possible relationship to genetic code. *Proc.Natl.Acad.Sci.USA, 90,* 8763-8768.

Schmidt, T., Michalik, C., Zavrel, M., Spiess, A., Marquardt, W., & Ansorge-Schumacher, M. B. (2010). Mechanistic Model for Prediction of Formate Dehydrogenase Kinetics Under Industrially Relevant Conditions. *Biotechnol.Prog, 26,* 73-78.

Schulman, L. & Pelka, H. (1988). Anticodon switching changes the identity of methionine and valine transfer RNAs. *Science, 242,* 765-768.

Schultz, D. W. & Yarus, M. (1994). Transfer RNA mutation and the malleability of the genetic code. *Journal of Molecular Biology, 235,* 1377-1380.

Schultz, D. W. & Yarus, M. (1996). On Malleability in the Genetic Code. *J.Mol.Evol., 42,* 597-601.

Seaborg, D. M. (2010). Was Wright Right? The Canonical Genetic Code is an Empirical Example of an Adaptive Peak in Nature; Deviant Genetic Codes Evolved Using Adaptive Bridges. *J.Mol.Evol., 71,* 87-99.

Segal, D. J. & McCoy, E. E. (1974). Studies on Down's syndrome in tissue culture. I. Growth rates and protein contents of fibroblast cultures. *J.Cell Physiol, 83,* 85-90.

Selmecki, A., Gerami-Nejad, N., Paulson, C., Forche, A., & Berman, J. (2008). An isochromosome confers drug resistance in vivo by amplification of two genes, ERG11 and TAC1. *Molecular Microbiology, 68,* 624-641.

Shawk, K., Westaway, & Abelson, J. (1995). Splicing of tRNA precursors. In D.Soll & U. RajBhandary (Eds.), *tRNA: structure, biosynthesis and function* (pp. 79-92). Washington D.C.: American Society for Microbiology.

Shenton, D., Mascaranhas, C., & Grant, C. M. (2008). Regulation of protein synthesis in yeast by oxidative stress. In *Stress in Yeast and Filamentous Fungi* (British Mycological Society Symposia Series ed., pp. 221-233).

Sheppard, K., Yuan, J., Hohn, M., Jester, B., Devine, K., & Soll, D. (2008). From one amino acid to another: tRNA-dependent amino acid biosynthesis. Nucleic Acids Research 36[6], 1813-1825.

Shigematsu, M., Tetsuhiro Ogawa, T., Atsuhiro Kido, A., Kitamoto, H. K., Hidaka, M., & Masaki, H. (2009). Cellular and transcriptional responses of yeast to the cleavage of cytosolic tRNAs induced by colicin D. *Yeast*.

Silva, R. M., Paredes, J. A., Moura, G., Manadas, B., Lima Costa, T., Rocha, R. et al. (2007). Critical roles for a genetic code alteration in the evolution of the genus Candida. *The EMBO Journal,* 1-11.

Simon, H., Haj-Yehia, A., & Levi-Schaffer, F. (2000). Role of reactive oxygen species (ROS) in apoptosis induction. Apoptosis 5, 415-418.

Singer, M. & Lindquist, S. (1998). Multiple Effects of Trehalose on Protein Folding In Vitro and In

Singh, G., Volpe, G., Creely, C., Grotsch, H., Geli, I., & Petrov, M. (2006). The lag phase and G1 phase of a single yeast cell monitored by Raman microspectroscopy. JOURNAL OF RAMAN SPECTROSCOPY 37, 858-864.

Skulachev, V. (2002). Programmed death in yeast as adaptation? FEBS Letters 528, 23-26.

Sohmen, D., Harms, J., Schlunzen, F., & Wilson, D. (2009). SnapShot: Antibiotic Inhibition of Protein Synthesis II. Cell 139.

Soma, A., Kumagai, R., Nishikawa, K., & Himeno, H. (1996). The anticodon loop is a major identity determinant of *Saccharomyces cerevisiae* $tRNA^{Leu}$. *J.Mol.Biol., 263,* 707-714.

Spitzner, A., Perzlmaier, A., Geillinger, K., Reihl, P., & Stolz, J. (2008). The Proline-Dependent Transcription Factor Put3 Regulates the Expression of the Ribo?avin Transporter MCH5 in Saccharomyces cerevisiae. Genetics 180, 2007-2017.

Sprinzl, M., Brown, M., Ioudovitch, A., & Steinberg, S. (1998). Compilation of tRNA sequences and sequences of tRNA genes. *Nucleic Acids Research, 26,* 148-153.

Srinivasan, G., James, C., & Krzycki, J. A. (2002). Pyrrolysine encoded by UAG in Archaea: charging of a UAG-decoding specialized tRNA. *Science, 296,* 1459-1462.

Stansfield, I., Jones, K. M., Herbert, P., Lewendon, A., Shaw, W. V., & Tuite, M. F. (1998). Missense translation errors in Saccharomyces cerevisiae. *J.Mol.Biol., 282,* 13-24.

Stansfiled, I., Akhmaloka, & Tuite, M. F. (1995). A mutant alele of the SUP45 (SAL 4) gene of S. cerevisiae shown temperature-dependent allosupressor and omnipotent supressor phenotypes. Curr.Genet. 27, 417-426.

Steitz, T. (2008). A structural understanding of the dynamic ribosome machine. Nat.Rev.Mol Cell Biol. 9, 242-253.

Su, D., Lieberman, A., Lang, F. B., Simonovic, M., Soll, D., & Ling, J. (2011). An unusual tRNAThr derived from tRNAHis reassigns in yeast mitochondria the CUN codons to threonine. *Nucleic Acids Research, Epub ahead of print*.

Suen, D., Norris, K., & Youle, R. (2008). Mitochondrial dynamics and apoptosis. Genes and Development 22, 1577-1590.

Sugita, T. & Nakase, T. (1999). Non-universal usage of the leucine CUG codon and the molecular phylogeny of the genus Candida. *Syst.Appl.Microbio., 22,* 79-86.

Suzuki, T., Ueda, T., & Watanabe, K. (1997). The "polysemous" codon - a codon with multiple amino acid assignment caused by dual specificity of tRNA identity. *The EMBO Journal, 16,* 1122-1134.

Suzuki, T., Ueda, T., Yokogawa, T., Nishikawa, K., & Watanabe, K. (1994). Characterization of serine and leucine tRNAs in an asporogenic yeast *Candida cylindracea* and evolutionary implications of genes for $tRNA^{Ser}CAG$ responsible for translation of a non-universal genetic code. *Nucleic Acids Research, 22,* 115-123.

Swire, J., Judson, O. P., & Burt, A. (2005). Mitochondrial Genetic Codes Evolve to Match Amino Acid Requirements of Proteins. *J.Mol.Evol., 60,* 128-139.

Sze, J., Remboutsika, E., & Kohlhaw, G. (1993). Transcriptional Regulator Leu3 of Saccharomyces cerevisiae: Separation of Activator and Repressor Functions. Molecular and Cellular Biology 13[9], 5702-5709.

Szymanski, M. & Barciszewski, J. (2007). The genetic code — 40 years on. *Acta Biochimica Polonica, 54,* 51-54.

Tan, S., Sagara, Y., Liu, Y., Maher, P., & Schubert, D. (1998). The regulation of reactive oxygen species production during programmed cell death. J.Cell Biol. 141[6], 1423-1432.

Tang, Y. & Tirrell, D. A. (2002). Attenuation of the editing activity of the Escherichia coli leucyl-tRNA synthetase allows incorporation of novel amino acids into proteins in vivo. *Biochemistry, 41,* 10635-10645.

Taylor, F. & Coates, D. (1989). The code within the codons. *Biosystems, 22*.

Thanaraj, T. A. & Argos, P. (1996). Protein secondary structural types are differentially coded on messenger RN. *Protein Science, 5,* 1973-1983.

Thompson, D. M. a. P. R. (2009a). Stressing out over tRNA cleavage. *Cell, 138,* 215-219.

Thompson, D. M. a. P. R. (2009b). The RNase Rny1p cleaves tRNAs and promotes cell death during oxidative stress in *Saccharomyces cerevisiae*. *Journal of Cell Biology, 185,* 43-50.

Thompson, R. C. & Karim, A. M. (1982). The accuracy of protein biosynthesis is limited by its speed: high fidelity selection by ribosomes of aminoacyl-tRNA ternary complexes containing GTP[gamma S]. *Proc.Natl.Acad.Sci.USA, 79,* 4922-4926.

Thorsen, M., Perrone, G., Kristiansson, E., Traini, M., Ye, T., Dawes, Y. et al. (2010). Genetic basis of arsenite and cadmium tolerance in Saccharomyces cerevisiae. BMC Genomics 10[105].

Torres, E. M., sokolsky, T., Tucker, C. M., Chan, L. Y., Boselli, M., Dunham, M. J. et al. (2007). Effects of Aneuploidy on Cellular Physiology and Cell Division in Haploid Yeast. *Science, 317,* 916-924.

Trollmo, C., André, L., Blomberg, A., & Adler, A. (1988). Physiological overlap between osmotolerance and thermotolerance in Saccharomyces cerevisiae. *FEMS Microbiol Letters, 56,* 321-325.

Trotter, E. W., Berenfeld, L., Krause, S. A., Petsko, G. A., & Gray, J. (2001). Protein misfolding and temperature up-shift cause G1 arrest via a common mechanism dependent on heat shock factor in Saccharomyces cerevisiae. *Proc.Natl.Acad.Sci.USA, 98,* 7313-7318.

Trotter, E. W., Kao, C., Berenfeld, L., Botstein, D., Petsko, G., & Gray, J. (2002). Misfolded Proteins Are Competent to Mediate a Subset of the Responses to Heat Shock in Saccharomyces cerevisiae. J.Biol.Chem. 277[47], 44817-44825.

True, H., Berlin, I., & Lindquist, S. (2004). Epigenetic regulation of translation reveals hidden genetic variation to produce complex traits. Nature 431, 184-187.

True, H. & Lindquist, S. (2000). A yeast prion provides a mechanism for genetic variation and phenotypic diversity. Nature 407, 477-483.

Tucker, C. & Fields, S. (2004). Quantitative genome-wide analysis of yeast deletion strain sensitivities to oxidative and chemical stress. Comparative and Functional Genomics 5, 216-224.

Tuite, M. F. & Santos, M. A. (1996). Codon reassignment in Candida species: An evolutionary conundrum. *Biochimie, 78,* 993-999.

Tuller, T., Carmi, A., Vestsingian, K., Navon, S., Drofan, Y., Zaborske, J. et al. (2010). An Evolutionarily Conserved Mechanism for Controlling the Efficiency of Protein Translation. *Cell, 141,* 344-354.

Tumbula, D. L., Becker, H. D., Chang, W. Z., & Soll, D. (2000). Domain-specific recruitment of amide amino acids for protein synthesis. *Nature, 407,* 106-110.

Tyagi, A., Singh, R., & Agarwal, C. (2002). Silibinin strongly synergizes human prostate cancer DU145 cells to doxorubicin-induced growth inhibition, G2-M arrest, and apoptosis. Clinical Cancer Research 8[11], 3512-3519.

Tyedmers, J., Madariaga, M. L., & Lindquist, S. (2008). Prion Switching in Response to Environmental Stress. *PLoS Biol, 6,* e294.

Ueda, T. & Watanabe, K. (2001). tRNA synthesis and regulation. In *Encyclopedia of Life Sciences* (Nature Publishing Group.

Uttenweiler, A., Schwarz, H., Neumann, H., & Mayer, A. (2007). The Vacuolar Transporter Chaperone (VTC) Complex Is Required for Microautophagy. Molecular Biology of the Cell 18, 166-175.

Uversky, V., Oldfield, C., Midic, O., Xie, H., Xue, B., Vucetic, S. et al. (2009). Unfoldomics of human diseases: linking protein intrinsic disorder with diseases. BMC Genomics 10[Suppl1].

Uy, R. & Wold, F. (1977). Posttranslational covalent modification of proteins. *Science, 198,* 890-896.

Valko, M., Morris, H., & Cronin, M. (2005). Metals, Toxicity and Oxidative Stress. Current Medicinal Chemistry 12, 1161-1208.

Vamosi, J. C. & Dickinson, T. A. (2006). POLYPLOIDY AND DIVERSIFICATION: A PHYLOGENETIC INVESTIGATION IN ROSACEAE. *Int.J.Plant Sci., 167,* 349-358.

van de Peppel, J., Kemmeren, P., van Bakel, H., Radonjic, M., van Leenan, D., & Holstege, F. C. (2003). Monitoring global messenger RNA changes in externally controlled microarray experiments. *EMBO reports, 4,* 387-393.

Vanacova, S., Wolf, J., Martin, G., Blank, D., Dettwiler, S., Friedlain, E. et al. (2005). A new yeast poly(A) polymerase complex involved in RNA quality control. *PLoS Biology, 3,* e189.

Vashist, S., Cushman, M., & Shorter, J. (2010). Applying Hsp104 to protein-misfolding disorders. Biochem.Cell.Biol. 88, 1-13.

Virgilio, C., Hottiger, T., Dominguez, J., Boller, T., & Wiemken, A. (1994). The role of trehalose synthesis for the acquisition of thermotolerance in yeast. I. Genetic evidence that trehalose is a thermoprotectant. Eur.J.Biochemistry 219, 179-186.

Walker, G. & Weller, G. (1994). he structure of the small mitochondrial DNA of Kluyveromyces thermotolerans is likely to reflect the ancestral gene order in fungi. *J.Mol.Evol., 38,* 593-601.

Wang, F., Robbins, S., Guo, J., Shen, W., & Schultz, P. G. (2010). Genetic Incorporation of Unnatural Amino Acids into Proteins in Mycobacterium tuberculosis. *PLOs ONE, 5,* e9354.

Wang, H., Xu, Z., Gao, L., & Hao, B. (2009a). A fungal phylogeny based on 82 complete genomes using the composition vector method. *BMC Evolutionary Biology, 9*.

Wang, L., Brock, A., Herberich, B., & Schultz, P. G. (2001). Expanding the genetic code of Escherichia coli. *Science, 292,* 498-500.

Wang, L. & Schultz, P. G. (2005). Expanding the Genetic Code. *Angew.Chem., 44,* 34-66.

Wang, Q., Parrish, A., & Wang, L. (2009b). Expanding the Genetic Code for Biological Studies. *Chem.Biol., 16,* 323-336.

Wang, X., Jia, H., Jankowsky, E., & Anderson, J. T. (2008). Degradation of hypomodified $tRNA_i^{Met}$ in vivo involves RNA-dependent ATPase activity of the DExH helicase Mtr4p. *RNA, 14,* 107-116.

Wang, X., Minasov, G., & Shoichet, B. K. (2002). Evolution of an Antibiotic Resistance Enzyme Constrained by Stability and Activity Trade-offs. *J.Mol.Biol., 320,* 85-95.

Wang, Y., Merrin, A., Zaarur, N., Romanova, N., Chernoff, Y., Costello, C. et al. (2009c). Abnormal proteins can form aggresome in yeast: aggresome-targeting signals and components of the machinery. FASEB J. 23, 451-463.

Watanabe, K. & Ueda, T. (2001). Evolution of the genetic code. In *Encyclopedia of Life Sciences* (Nature Publishing Group.

Weber, A. L. & Lacey, J. C. (1978). Genetic code correlations: amino acids and their anticodon nucleotides. *J.Mol.Evol., 11,* 199-210.

Westermann, B. (2008). Molecular Machinery of Mitochondrial Fusion and Fission. J.Biol.Chem. 283[20], 13501-13505.

Wetzel, R. (1995). Evolution of the aminoacyl-tRNA synthetases and the origin of the genetic code. *J.Mol.Evol., 40,* 545-550.

Weygand-Durasevic, I. & Cusack, S. (2005). Seryl-tRNA synthetases. In M.Ibba, C. Francklyn, & S. Cusack (Eds.), *The aminoacyl-tRNA synthetases* (pp. 177-192). Lands Bioscience.

White, S. (1992). Amino acids prferences of small proteins: Implication for protein stability and evolution. Journal of Molecular Biology 227, 991-995.

Wilks, H. M., Hart, K. M., Feeney, R., Dunn, C. R., Muirhead, H., Chia, W. N. et al. (1988). A specific, highly active malate dehydrogenase by redesign of a lactate dehydrogenase framework. *Science, 242,* 1541-1544.

Williamns, B. R., Prabhu, V. R., Hunter, K. E., Glazier, C. M., Whittaker, C. A., Housman, D. E. et al. (2008). Aneuploidy affects proliferation and spontaneous immortalization in mammalian cells. *Science, 322,* 703-709.

Williams, R. & Obradovic, Z. (2001). THE PROTEIN NON-FOLDING PROBLEM: AMINO ACID DETERMINANTS OF INTRINSIC ORDER AND DISORDER. Pacific Symposium on Biocomputing 6, 89-100.

Wilmot, C. M. & Thornton, J. M. (1988). Analysis and prediction of the different types of beta-turn in proteins. *Journal of Molecular Biology, 203,* 221-232.

Winge, D., Nielson, K. B., Gray, W. R., & Hamer, D. H. (1985). yeast metallothionein. Sequence and metal-binding properties. *J.Biol.Chem., 260,* 14464-14470.

Woese, C. R. (1965). Order in the genetic code. *Proc.Natl.Acad.Sci.USA, 54,* 71-75.

Woese, C. R., Dugre, D. H., Saxinger, W. C., & Dugre, S. A. (1966). The molecular basis for the genetic code. *Proc.Natl.Acad.Sci.USA, 55,* 974.

Wu, C., Bird, A., Chung, L., Newton, M., Winge, D., & Eide, D. (2008). Differential control of Zap1-regulated genes in response to zinc deficiency in Saccharomyces cerevisiae. BMC Genomics 9[370].

Wu, H., Ito, K., & Shimoi, H. (2005). Identification and Characterization of a Novel Biotin Biosynthesis Gene in Saccharomyces cerevisiae. Applied and Environmental Microbiology 71[11], 6845-6855.

Wu, X. Q. & Gross, H. J. (1993). The long extra arms of human $tRNA^{(Ser)Sec}$ and $tRNA^{Ser}$ function as major identity elements for serylation in an orientation-dependent, but not sequence-specific manner. Nucleic Acids Research 21[24], 5589-5594.

Wykoff, D. & O'Shea, E. (2001). Phosphate Transport and Sensing in Saccharomyces cerevisiae. Genetics 149[1491], 1499.

Wykoff, D., Rizvi, A., Raser, J., Margolin, B., & O'Shea, E. (2007). Positive Feedback Regulates Switching of Phosphate Transporters in S. cerevisiae. Molecular Cell 27, 1005-1013.

Xie, J. & Schultz, P. G. (2005). Adding amino acids to the genetic repertoire. *Current Opinion in Chemical Biology, 9,* 554.

Yamaguchi-Iway, Y., Serpe, M., Haile, D., Yang, W., Kosman, D., Klausner, R. et al. (1997). Homeostatic Regulation of Copper Uptake in Yeast via Direct Binding of MAC1 Protein to Upstream Regulatory Sequences of FRE1 and CTR1. The Journal of Biological Chemistry 272[28], 11711-11718.

Yamamoto, N., Maeda, Y., Ikeda, A., & Sakurai, H. (2008). Regulation of Thermotolerance by Stress-Induced Transcription Factors in Saccharomyces cerevisiae. Eukaryotic Cell 7[5], 783-790.

Yarian, C. S., Basti, M. M., Cain, R. J., Ansari, G., Guenther, R. H., Sochacka, E. et al. (1999). Structural and functional roles of the N1- and N3-protons of ψ at tRNA's position 39. Nucleic Acids Research 27[17], 3543-3549.

Yoshihisa, T., Ohshima, C., Yunoki-Esaki, K., & Endo, T. (2007). Cytoplasmic splicing of tRNA in Saccharomyces cerevisiae. *Genes Cells, 12,* 285-297.

Yoshihisa, T., Yunoki-Esaki, K., Ohshima, C., Tanaka, N., & Endo, T. (2003). Possibility of cytoplasmic pre-tRNA splicing: the yeast tRNA splicing endonuclease mainly localizes on the mitochondria. *Molecular Biology of the Cell, 14,* 3266-3279.

Yoshizawa, S. & Bock, A. (2009). The many levels of control on bacterial selenoprotein synthesis. *Biochimica et Biophysica Acta (BBA), 1790,* 1404-1414.

Youle, R. & Karbowski, M. (2005). Mitochondrial fission in apoptosis. Nat.Rev.Mol Cell Biol. 6[8], 657-663.

Yuan, J., O'Donoghue, P., Ambrogelly, A., Gundllapalli, S., Sherrer, R. L., Palioura, S. et al. (2010). Distinct genetic code expansion strategies for selenocysteine and pyrrolysine are reflected in different aminoacyl-tRNA formation systems. *FEBS Letters, 584,* 342-349.

Zaher, H. S. & Green, R. (2009). Fidelity at the Molecular Level: Lessons from Protein Synthesis. Cell 136, 746-762.

Zhang, Y., Baranov, P. V., Atkins, J. F., & Gladyshev, V. N. (2005). Pyrrolysine and Selenocysteine Use Dissimilar Decoding Strategies. *The Journal of Biological Chemistry, 280,* 27740-27751.

Annexes

Annexe I: Map of the plasmids constructed and sequences

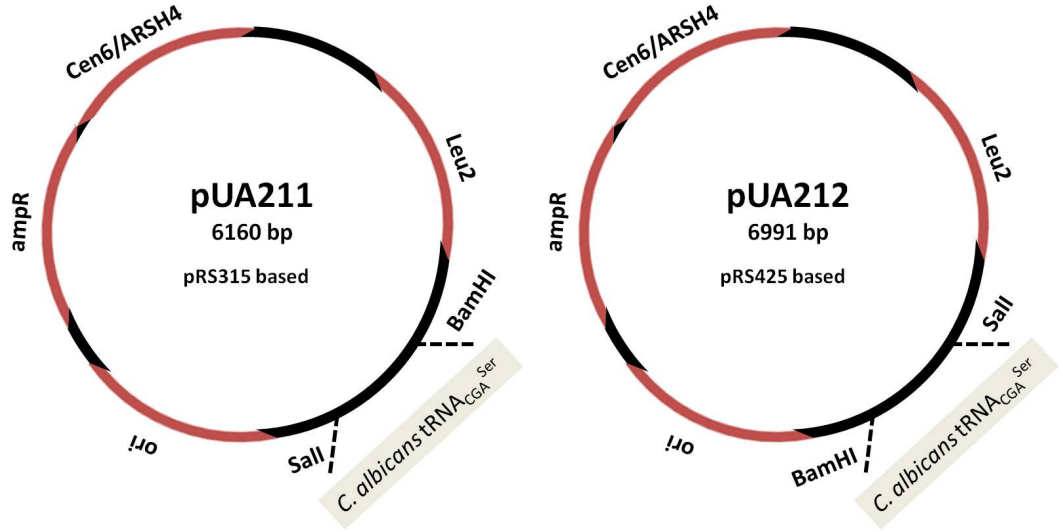

Figure A1: Plasmids pUA211 and pUA212 constructed for this work. Single copy and multicopy plasmids, based respectively in pRS315 and pRS425, for the expression of *C. albicans* $tRNA_{CGA}^{Ser}$ in *S.cerevisiae* cells.

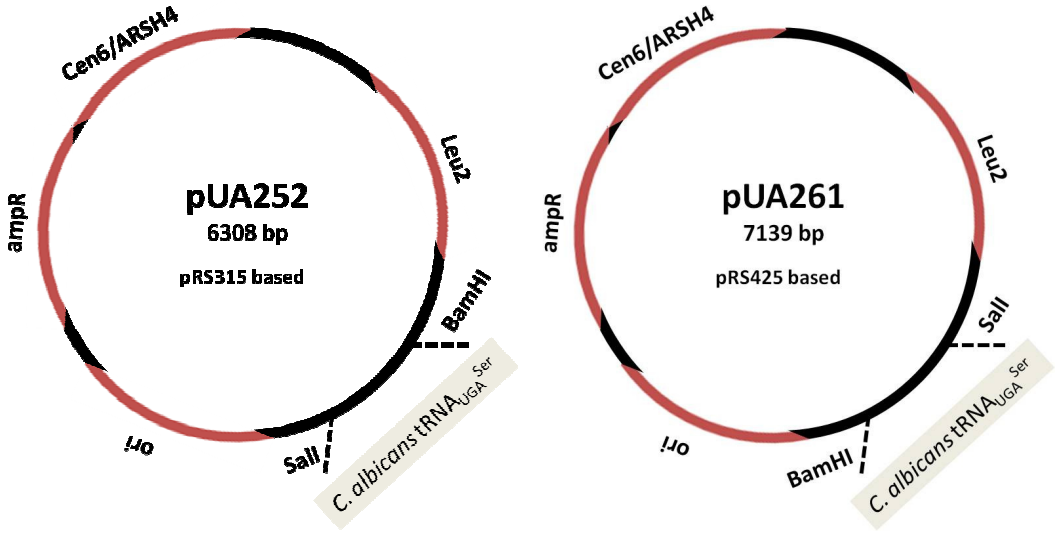

Figure A2: Plasmids pUA261 and pUA252 constructed for this work. Single copy and multicopy plasmids, based respectively in pRS315 and pRS425, for the expression of *C. albicans* $tRNA_{UGA}^{Ser}$ in *S.cerevisiae* cells.

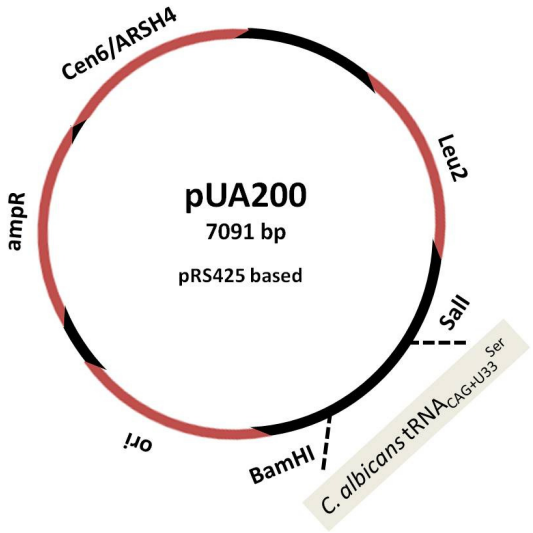

Figure A3: Plasmid pUA200 constructed for this work. Multicopy plasmid based in pRS425, for the expression of *C. albicans* $tRNA_{CAG}^{Ser}$ in *S.cerevisiae* cells.

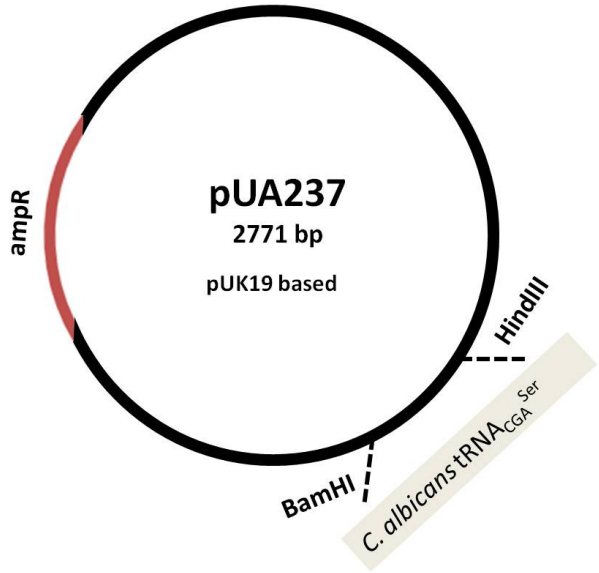

Figure A4: Plasmid pUA237 constructed for this work. Plasmid based in pUK19 containing the sequence of *C. albicans* $tRNA_{CGA}^{Ser}$ for tRNA *"in vitro"* transcription.

Sequence of *C. albicans* $tRNA_{CGA}^{Ser}$ cloned in plasmids pUA211 and pUA212

The tRNA sequence with 1000 bp upstream and downstream.

At grey is the region cloned.

Assembly 21, Chr1 (2164418, 2164324)

ATAAAGAGAATATACAAACAACTACTACTAAGGGTTCTACACCGGATATAAAAGAGTACC
TTCTACAATTGTGAAATAATCAGACCACAGCACCCTCAGTTACGAGAAACATATTAGTAT
ATTGTTTTCTTTTTTGCATATATTTGGACAATACATGCTTTTTTTGACCATGTTATAAGC
ATACTTATTTCAAACATATATAGCAATTGCAATTCAGTTTACATATGATTCTTTTATAGT
AGTTCGCATTCATGTTCCATTATTCTTATATCTCTTAGCAACTTTTTTTGCATTAGTTAT
CTTTTATGTTTACCCCAAGTTGCTTTACAAGCTTTTTATTAATACCATAGAGTGAAGGAA
TTATTTATTGTAAGAGACTCTTTTGTACAGAAAAATTAAGGGGTTGAATAAATTCGCTGT
ACCAACAGAGAACATTATTTTGCATTGCAGGACTGTAATACATTTATTGTTAATGAAACC
GACAAATCAAACCCCGATTAAGTCTTTTCAGAATTTATATAGTATTTGATATCTCCGAGT
AATGTAAAAGCTGGTGATAAATATGGGCCCATGAACTACTGAGCAAATTAGCTGCAACAA
TATGTACTTGATAAGCAAGAAAAGGGTGATTGATACAACCTGTTTGTTTATGCATCAATT
TTCCTAATCTAGGTCTTAAAACAGTTCTAGAATTATTGTAGACCTAGCTCAGATATTGTA
AATCAAGTGATGATGCTCGATGAAATAGTTAAAATCATTCAATGCTGGTGTGGTTTTTTG
TAATAATTTTTGCACCAAATTTTATCTAAACTTATAACGGAAAAAGGAAAAGCATTCAAG
ACAATCCACTTTAACCACTTAAGAACCTTTTGCCAATATCATACTAAATTACTTTAAAAA
AGCGGTATTTATATATTAGATTACTGCCATTCATCTATCTAAAAGCTATAGAAAGAATTT
CCCGATATAATATTCTGGGAGCCTAAAATTCAAAAAATTTGACAGTGTGGCCGAGCGGTT
AAGGCGTCTGACTCGAATCTTATTCGCGTTATCAGTTGGGCTTTGCCCGCGCAGGTTCGA
ATCCTGCTGCTGTCGTCATAAGTTATTTTTTTGTTTCTTGAATATTTTTTTCCCACTTAA
ATCAATCACAGTTGTCCACTGTAATGTGCTTTATAAAAGCATGTAAAGTATCTGGTTAGA
TATCAAAGTATTCTCTTATTTTCAAGAGTCTTTTTTAAAACATGTTGAATAAAGAACTCA
CTATCTAACAAAAGTGGTTGACAAAAAGTAATGAGGATGCGCAAAAAAAAAATGTCAAAA
AAAGTATTTTGCTGCTTCACTTACAAACAACTCCTTTAACACTCTTACATTCAATGCCAA
AGATAAAAAAACCGAAAAAGAATGGTCCACCGCCTGAAGGGTACTCTAAAATAGAACCTA
CATTGACAAAGTATCGTAACAAATTGAAATCAGCCCAAGCTAATCCTGACCCAACCAAAT
CCAAACAATCATCATTATGGATAATATATCAATTAAATTACAAAATCACTCGATATGTTT
ATGATACATATGTGGCGAAACGAATATCTAAAGAATTATACGACTGGCTATTACTTCAAA
ATGATATAAATAAGGACCTTATTGCTAAATGGAAAAAACCTGGTTATGAAAAGTTATGTT
GTATTAATTGTATATCTACCAATACCAATGGTGGTGGAACTTGTGTTTGTAGAGTTCCTA
AAGCCAAATTATTAGAAAAAGATCCCGAAAAAGTGAATATTGAATGTATCACTTGTGGTT
GCCGAGGCTGTGCTTCTAGTGATTAATCTTGTAAATATATATATGTATATATGTATATTG
GTTATTAAAGAAGAAAATTATATAAAAAAAAAAACAAATGATAATAATACAAAACTAATCT
ACTCATCAAACAAATAAAAAAAAATAACCAACCTTAAAAACTCCCTATAAGTAGATTATA
AAAAAGTAATAATAATAATGACCATTAAATATCTTAATCCAAGAAATGAAACAAAAATAG
AATAAAAATATGGAAAAAGTAAGAGAACACTAATTAAAAGTGATTTGCCCATTCC

Sequence of *C. albicans* $tRNA_{UGA}^{Ser}$ cloned in plasmids pUA252 and pUA261

The tRNA sequence with 1000 bp upstream and downstream.

At grey is the region cloned.

Assembly 21, chr1 (335138-337219)

GAACATGAAGATTATCAAGATTCAATATTATGTGAAATCTTGAAAAGTCATTTATTTGTT
TATATTGGTCATGGTGGTTGTGATCAATATATTAAAGTATCAAAATTATTTAAAAAATGT
GGCAATAATCAAGATTTACTGAATAAATTACCTCCTAGTTTATTGTTAGGTTGTTCATCA
GTTAAATTAGATAATTGTAATTATAACTATAATTCCAGTATGTTACAACCACTGGGTAAT
ATTTATAATTGGTTGAACTGTAAATCGTCAATGATACTCGGGAATCTATGGGATGTTACT
GATAAAGACATTGATATTTTTACACTTTCATTACTACAAAAATGGGGGTTAATAGATGAT
TATAATGGCAGTGGCCATGATTATGGTATGAAGAAATTGGATTTGACTAATTGTGTTGTT
CAAAGTCGAAGTAAATGTACTTTGAAATACTTGAATGGATCAGCACCTGTGGTTTATGGT
CTACCAATGTATTTAAAATAGACATTCTGTTTGCATATAAGTTTATATATTTTAATAATA
AGAAAAAGAGCATAATTTGGATCTTGATTTTGTATTGTTTGGTTTGTTATGAACAAATTT
TGCACCCAATCACTATCGAACTTTCTTTTTTAAACAGAGAACATTTAATCAACATTTATG
TTACATTTAAGCGTTTAAATACATATTTGTGTTAGATAGTTATATAATGTTGGCATTTTC
TGATGGAATTGTTGATATTCATTTTTTTTAGCATTTTTTTCGCCAAAATTCATAATCAAA
AATTGATTTGATTGCGAATGTAATGATGAGTTCAGAAATGAATAATCTCAACAACTTAAC
CAGTATTAATTAAAAATAAAGTACGGACTGAATGATCTACAGCCATATTTGAGTCTTGAA
TTACCCTTATTACGTCTGAAGATAAAAATTATTGTTGTGGAAAAGCAAAACAATTTGTCC
AGGACTGATTTATGTGCATCCCTAATTTCAGCGAGATTTAGGCAACTTGTCCGAGCGGTT
AAGGAGAAAGACTTGAAATCTTTTGGGCTTTGCCCGCGCAGGTTCGAGTCCTGCAGTTGT
CGTTATTTTTTTTGCTCCGCCAAACGCCCTCTTTTTTTTTACATCAATTTTGGAGCTGAT
TCACAAAGCTCATGCAAATATATATATATTGTTATCTAACCTTCTATGAAATCAATTAAA
TCGTCTAAAATGGCCACGGTTTCTCTAGGACTAGCAATCCATACTGTGCAAGCACTTAAT
CTGGCTTTAAAATCATTAGCACCCAAACTAGCAAATTGATCACCAATATGTAAACTTTCC
GATTTACCAATAGGACAAACATGATCAACTGTTTCGTCATGACAAATGTATTTTTGAAGT
GATTCTACCCCTAAGGCTTTATCACCAATATCTACCCAAACATCGCTACCACCATTAAAG
GCACAAACTTTAATATCATCAACACAAAGAGCTTCAGTGGAATCGGCAAAATTTGACGAT
GACGTTAGAATAGTATTTAATTTTCTTGAACAAGATAATACCATTTCTTCCAATTGTTCA
CGTAAGATGCGACATCCTGAATTAGGTATAATCCCAACAGATCTTTCCTTTTTAATGATG
GTAGTTGAATCTTCTAAATTGAAATTATTTCTTAAATAAATCAAATGTTTATAAAGAGTA
TCCATAATATAATTGATTTTACCAATATTCCAATTTTTCACTTGTGGTAAAAACCATTCT
TCATCATCAATGAATTTTAAACCTTTCATTTCATTATTATATCGGAATAAATAATTCGAT
TCAGCTCCCATGACTAATAAATTCTCTTTTTGATATGTTTTCAAAGTACAGTGATTGCTA
TTTAAATGATCAATTAATCCCTTCAATCGTTCATAATATTTTTCAGCTCCAGATTGACGA
GGGTACCCTGCAGCAGTAACAACACCAACATATAATCCTAATGATAATAATTTAACTAGT
CTTTGAACAACTTCACTATTTTCATCTAATGATTTCCCATCTTCATATAATGTCACATCA
CCATCAAATGTAATCAACTTCAACTTTTGTTGTTGCTGTTGT

Sequence of *C. albicans* $tRNA_{CGA}^{Ser}$ cloned in plasmids pUA200

The tRNA sequence with 1000 bp upstream and downstream.

At grey is the region cloned.

Contig19-10080 (91580, 91661)

ATAGAATTGAGCCGTTTCACACGACGTGGCAATAATAATCAACTGATATGACGTTTTATC
AGAGATTGTCGAGTTTTGTGTTACTATTTTGAAAGGAAGAACTAACGAAATAAGGCACAG
GTTTCCTACTACATTTTTCTAACTCTTGATAAGTTTTGAAAAAACGTATGTTGTATGTTA
GAGAGTATTTAGTCAAAAAAAGAAGGGAAATTATTACATCCATTTCGAACCAGTGGCTGT
TTGTTTCCAGTTGCAACAAATTTGTCACGTGACCCGTGTTTAGAACTTGGCAAATTATAT
CAGATTAATAAGTTTTCACATCCTTTTTTACTTGTCTGTTGTAGAGTCTGGTTGCTTAGC
TGGATCTCTGCTTATTAATTTAGAAAATAAACTATCGGTCATCAAGTTTGGTCACTTTAA
CAATGATCGAATGCCACTACAATAAGTTGACTACATAGGTTTGATGTTAGAAGATGCTCG
TATTTGACAGCTGAATAGTATTGCTATAAATACGTTATTTGCTAGATTATTCTCTAATTA
TATTTACTTTAAGTCTGAAGTAGTAAAGCTGTTATGTCTCAATGTGGAGTTGAATTCACT
AGGAAACTTTTTTGGTTGCAAATGTAATCCAAATTTTAACTAAAAAGAAAATTTTGCTAA
ATGATCCCCAAAAGCAATAACAACTAAGCACAGATGTATTTGATATTAGAAACTCTACAT
TTAAGCTTATAACTGGAAGAAATATGTATGCAATCGTTGTCTGTAATGTAGTCCACAAAA
AACGTCACGTGATACGCTATAAATGATATCACATCGAATGAGCACCTTTGCACACCAAAT
TCATATCCTTCCATTATAGTTTAGCTAGAAAACAATATTAAAATGCTTTCCTAATTGATT
AAACTCAAATTTACTAGTTGAAACACCAAACAAAAGATGCTAATCGTCAGCATACATCAA
TTGTCATAATCATTCGTGCTTGCCTCCGGGTAGTTGCAACGATACGATGGCCGAGTGGTT
AAGGCGAAGGATGCAGGTTCCTTTGGGCATTGCCCGCGCAGGTTCGAACCCTGCTCGTGT
CGTCATTTTTTTTCAACAAATTTTGTTTTTCCCAATTTGTTAATAAGTATGCATGTAATA
AAGTCAATCATCTGTACATCGTAATTAATGTGACGTTGTGCCAATTATTTTTTTTAAATA
TTATTTATCATGTATATGAAATGATGAAACAGTTAACGAGATTGATAGTGTGACTTTGCC
AAAGACATTAAAAAATATAAAACTAAACAAAACAAAGGAAAGAGACAAACTAAACCACAT
AATGAAAAAAAAAAAAGAAAACAAAAAAAATAATATAAAGAACAGAGGACAGACTATTCA
AGACAGCACACTACCGCCCTATTCCATTCGATATGCTAGAAACAGATCTATACGATGTTC
TTGAAATAGATAGATCAGCCACTAATGCGGAGATTAAGAAAGCATACAGAAAACTAGCTT
TAAAATATCATCCCGATAAAGTGGCGGAAGAAGAACGAGAATACTCTGAAACAAAATTCA
AAGAGATATCATTTGCATACGAAATATTGATTGATGACGTAAAGAGAGATGAGTATGATA
GATATGGTACTACCGATGGATTAAATGGAATGCCCGATTTTGAATTCGCAGGAAATCCTT
TTGATCAATTTTACGGTGCAGGTGCAGGTGCCCAGTTTAACGAATATGGTGGTGATGACT
TTTATAATTTCTTCAATAACATGAATGGTGGTGGAGGTGCCCGTCACCAGACAAAAACAA
ACAGAACCGAGGATGCACATATAGAGGTTGACTTGACTTTAGAAGATCTATACAAAGGTA
AAGTTATCAAAACCACATCAACCAGGAATATTATTTGCACTCAGTGTAAAGGATCAGGCG
TTAAATCGTCATCAGTGGTCTCAAAACAATGCTCTACTTGTAAGGGAGAAGGACAAGTTA
GAAAAATAAAGCGTGTTGGGCCTGGCATGGTTGCACAGACATATGTTGATTGTTCTACAT
GTCAAGGAATTGGGAAGATATATCGAACCAAAGATAAATGTA

Annexe II: Phenotypic screening data

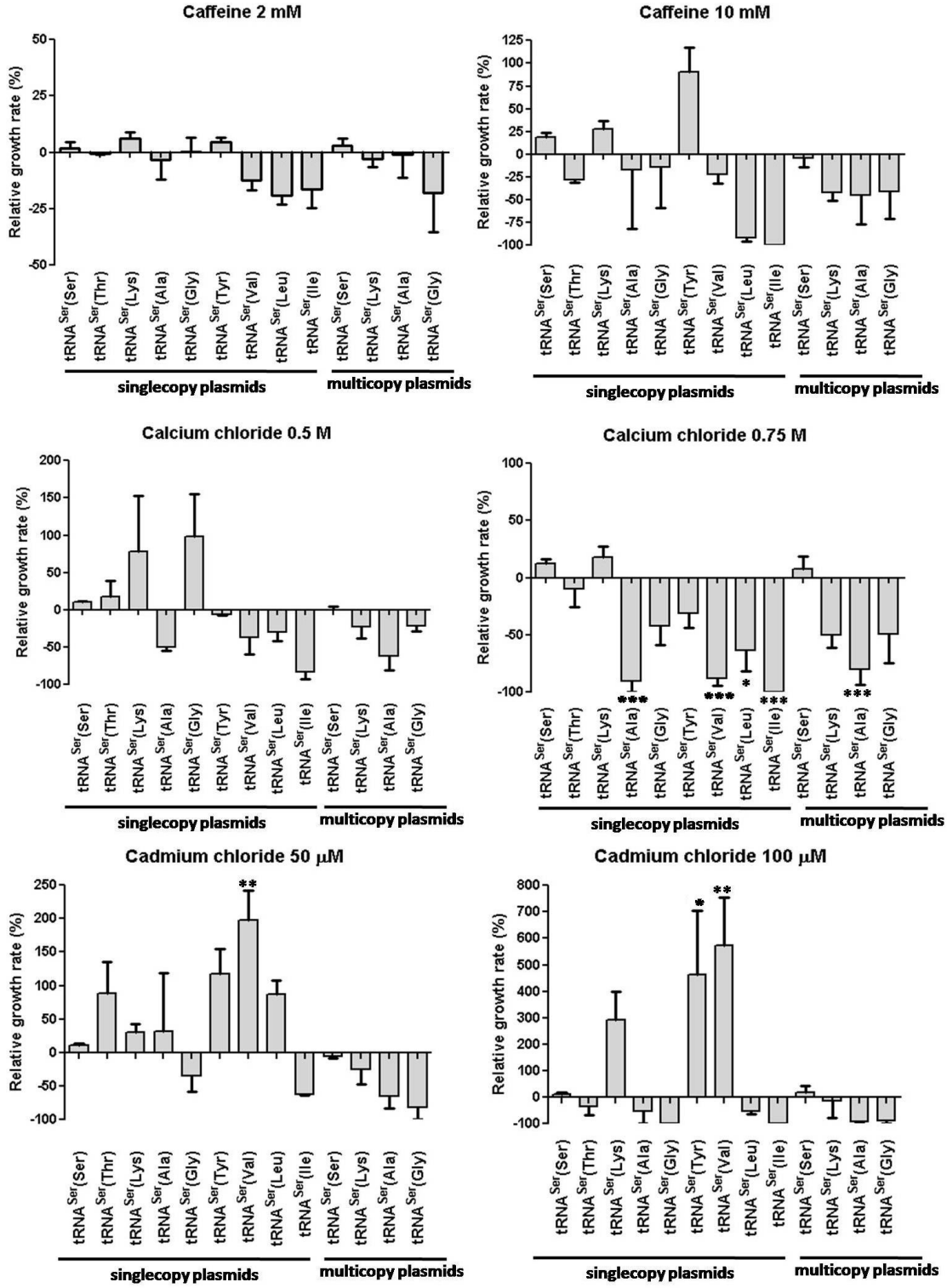

Figure 5A: Phenomics of yeast mistranslating strains. The growth performance of yeast cells, transformed with $tRNA^{Ser}$(Ser) and mistranslating $tRNA^{Ser}$ expressed from single-copy and multicopy plasmids, in the conditions indicated was determined as described in methods (section 3.2.18). Data represent the mean ± s.e.m. of duplicates of 3 independent clones (***p< 0.001, **p< 0.01, *p< 0.05 one-way Anova post Dunnett's multiple comparison test with CI 95% relative to pRS315 or pRS425 strain).

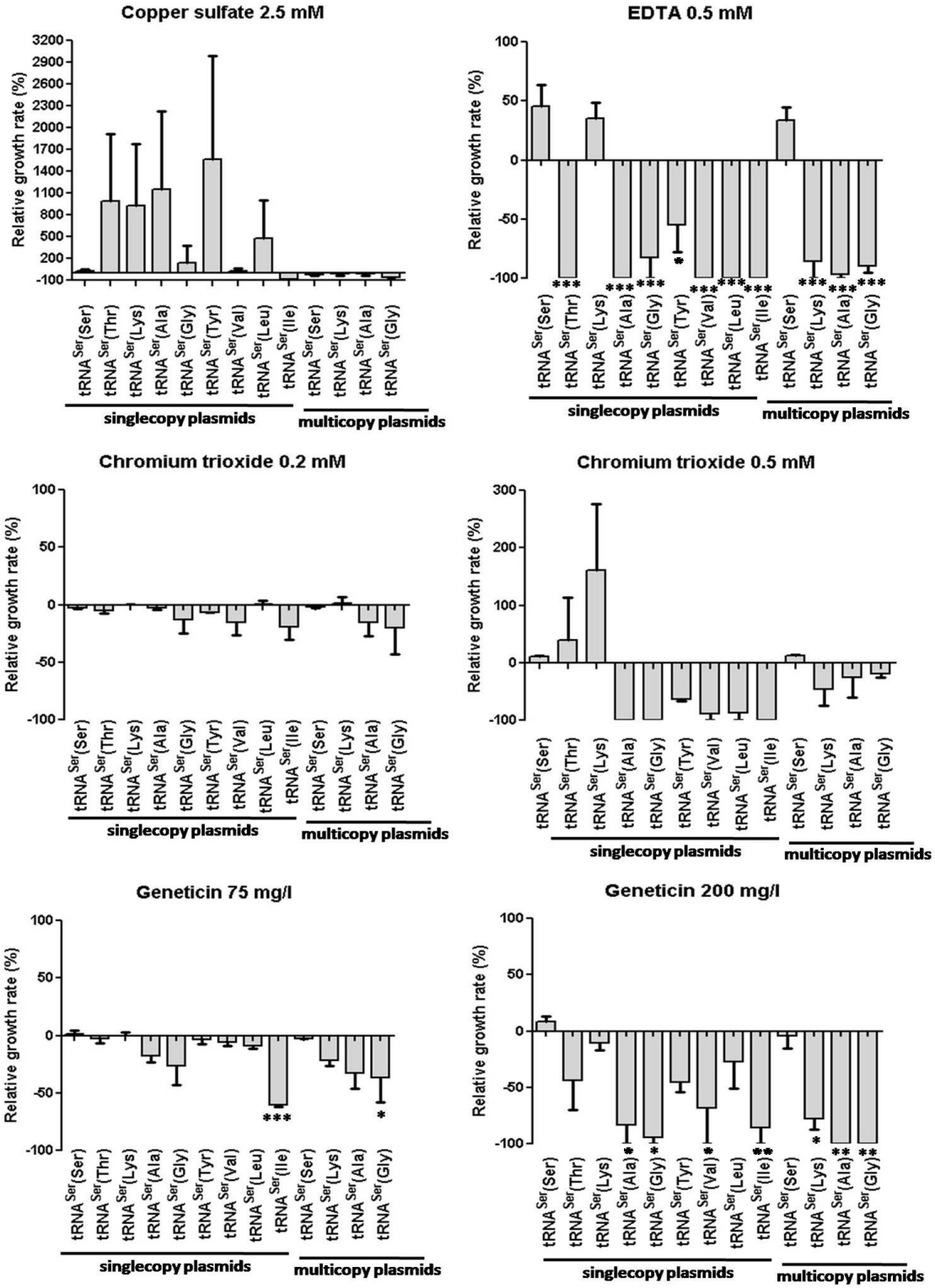

Figure 6A: Phenomics of yeast mistranslating strains. The growth performance of yeast cells, transformed with $tRNA^{Ser}$(Ser) and mistranslating $tRNA^{Ser}$ expressed from single-copy and multicopy plasmids, in the conditions indicated was determined as described in methods (section 3.2.18). Data represent the mean ± s.e.m. of duplicates of 3 independent clones (***p< 0.001, **p< 0.01, *p< 0.05 one-way Anova post Dunnett's multiple comparison test with CI 95% relative to pRS315 or pRS425 strain).

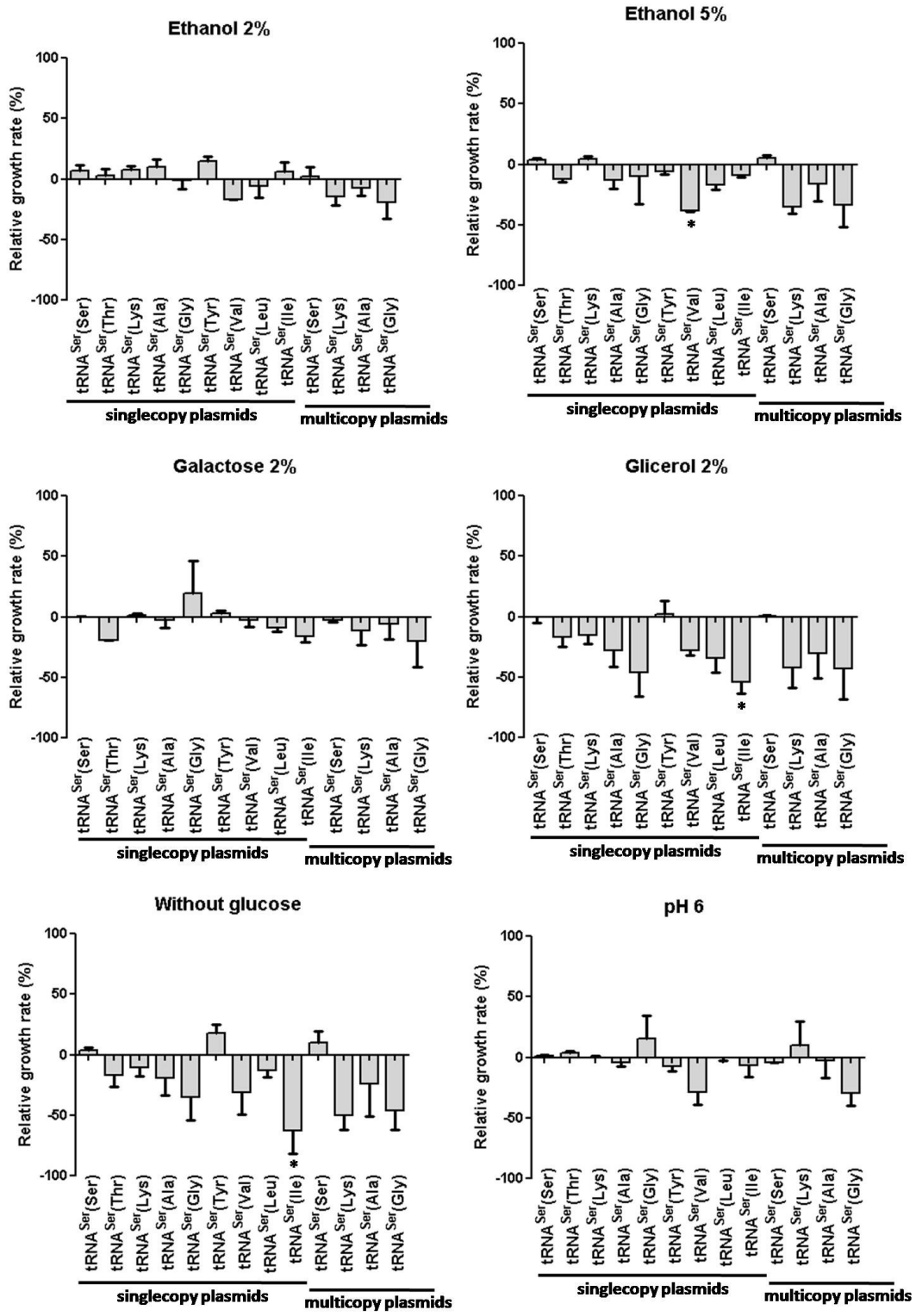

Figure 7A: Phenomics of yeast mistranslating strains. The growth performance of yeast cells, transformed with $tRNA^{Ser}$(Ser) and mistranslating $tRNA^{Ser}$ expressed from single-copy and multicopy plasmids, in the conditions indicated was determined as described in methods (section 3.2.18). Data represent the mean ± s.e.m. of duplicates of 3 independent clones (***p< 0.001, **p< 0.01, *p< 0.05 one-way Anova post Dunnett's multiple comparison test with CI 95% relative to pRS315 or pRS425 strain).

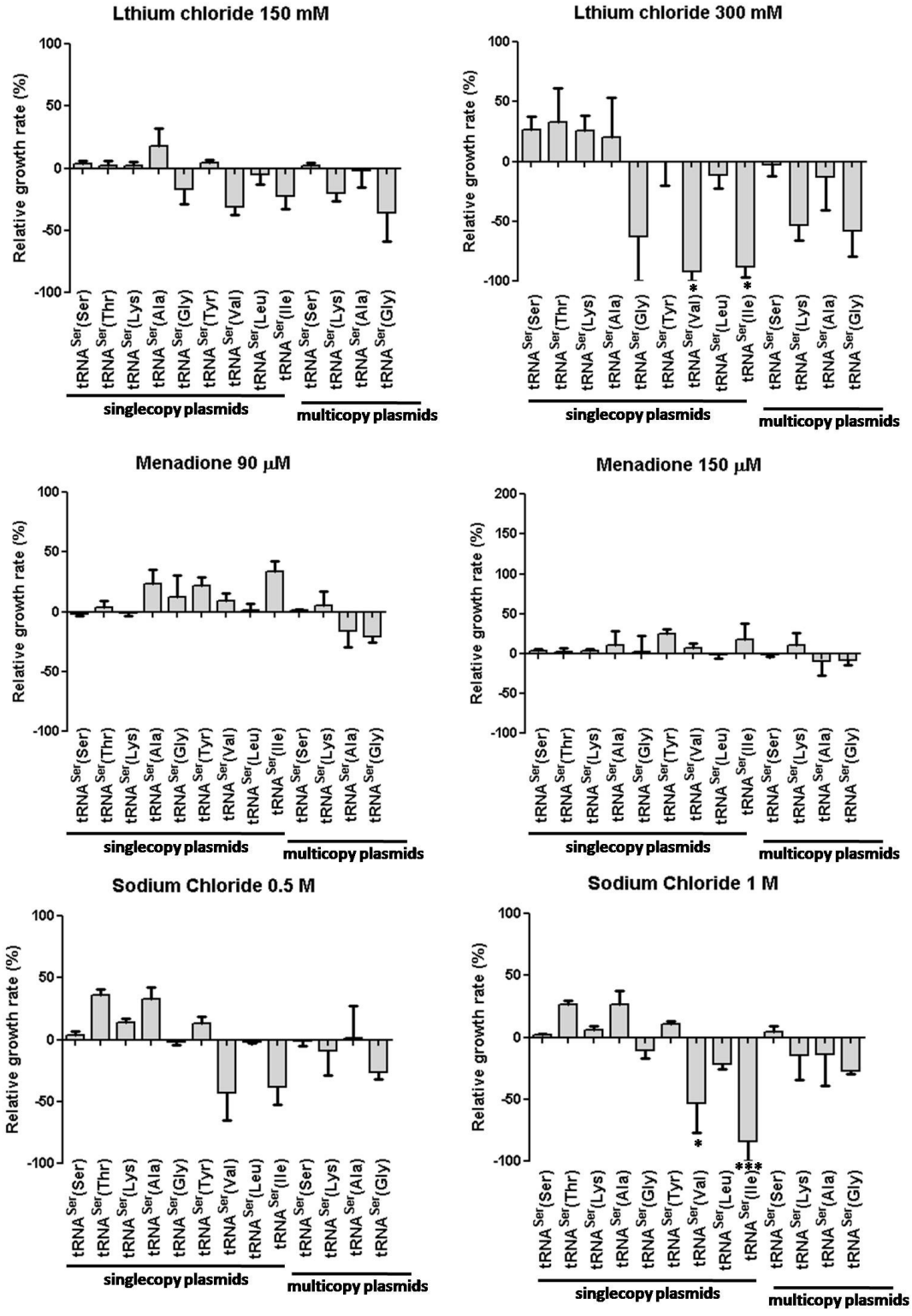

Figure 8A: Phenomics of yeast mistranslating strains. The growth performance of yeast cells, transformed with $tRNA^{Ser}$(Ser) and mistranslating $tRNA^{Ser}$ expressed from single-copy and multicopy plasmids, in the conditions indicated was determined as described in methods (section 3.2.18). Data represent the mean ± s.e.m. of duplicates of 3 independent clones (***p< 0.001, **p< 0.01, *p< 0.05 one-way Anova post Dunnett's multiple comparison test with CI 95% relative to pRS315 or pRS425 strain).

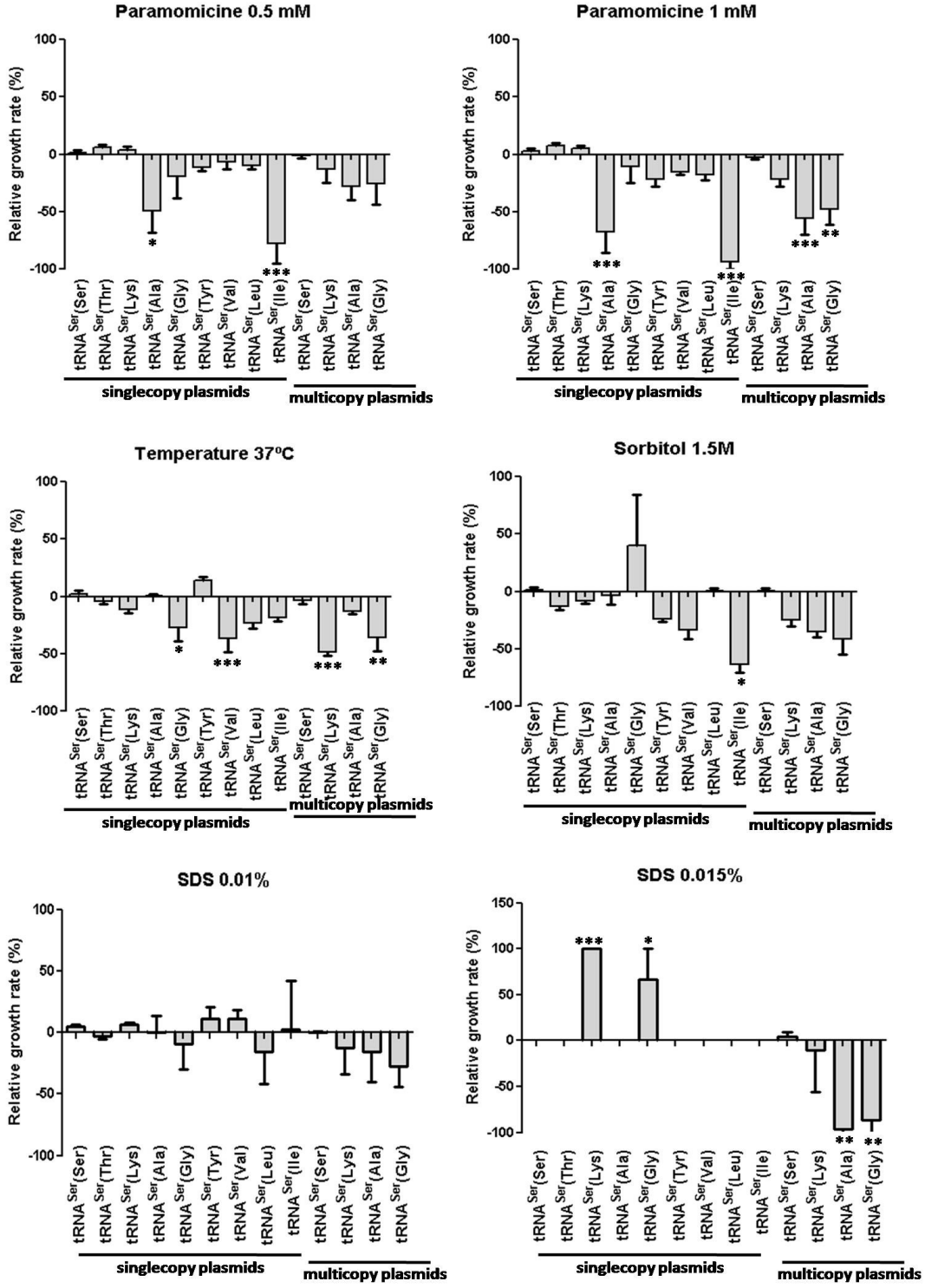

Figure 9A: Phenomics of yeast mistranslating strains. The growth performance of yeast cells, transformed with $tRNA^{Ser}$(Ser) and mistranslating $tRNA^{Ser}$ expressed from single-copy and multicopy plasmids, in the conditions indicated was determined as described in methods (section 3.2.18). Data represent the mean ± s.e.m. of duplicates of 3 independent clones (***p< 0.001, **p< 0.01, *p< 0.05 one-way Anova post Dunnett's multiple comparison test with CI 95% relative to pRS315 or pRS425 strain).